# Supporting Information

## *Ammonia activation using a heteroleptic stannylene and lithium stannylenoid formation facilitated by hemilabile iminophosphorane-based ligands*

David M. J. Krengel,[a] Nico Graw,[a] Regine Herbst-Irmer,[a] Dietmar Stalke,[a] Oliver P. E. Townrow,*[b] Malte Fischer*[a]

[a] Institut für Anorganische Chemie, Georg-August-Universität Göttingen, Tammannstraße 4, D-37077 Göttingen (Germany)
email: malte.fischer@uni-goettingen.de
[b] Inorganic and Organometallic Chemistry, Friedrich-Alexander-Universität Erlangen-Nürnberg, Egerlandstraße 1, D-91058 Erlangen (Germany)
email: oliver.townrow@fau.de

## Table of Contents

## General Considerations

### Materials and Synthetic Methods

All manipulations of air- and moisture-sensitive materials were carried out using standard Schlenk-line and glovebox techniques (with oxygen and water concentrations below 0.1 ppm, as monitored by an $O_2/H_2O$ Combi-Analyzer) under an inert atmosphere of argon or dinitrogen. Solvents were purified using a Solvent Purification System, degassed by sparging with argon, and stored over 3 Å molecular sieves. $^{Mes}$TerSn{N(SiMe$_3$)$_2$} (**1**), 1,3,4,5-tetramethylimidazol-2-ylidene ($IMe_4$), 2,6-diisopropylphenyl azide ($N_3$Dipp), and 3,5-dimethylphenyl azide ($N_3$Xyl) were synthesized according to literature procedures.[S1-S3] Trimethyl phosphine ($P(CH_3)_3$) was purchased from a commercial supplier, transferred into the glovebox, and stored in the glovebox freezer prior to use. 1-Azidoadamantane ($N_3$Ad) and lithium bis(trimethylsilyl)amide (Li{N(Si(CH$_3$)$_3$)$_2$}) were purchased from commercial suppliers and transferred into the glovebox prior to use.

### Analytical Methods

NMR spectra were measured in benzene-$d_6$ ($C_6D_6$), toluene-$d_8$ ($C_7D_8$) or tetrahydrofuran-$d_8$ ($C_4D_8O$) (dried over $CaH_2$, distilled by trap-to-trap transfer in vacuo, degassed by three freeze-pump-thaw cycles and transferred to the glovebox prior to use). NMR samples were prepared under argon in NMR tubes with J. Young Teflon valves. NMR spectra were measured on Bruker Avance 300 MHz, 400 MHz, 500 MHz, and 600 MHz spectrometers. $^1$H and $^{13}$C NMR spectra were referenced internally to residual protio-solvent ($^1$H) or solvent ($^{13}$C) resonances ($C_6D_6$: $\delta_H$ = 7.16 ppm; $\delta_C$ = 128.06 ppm; $C_7D_8$: $\delta_H$ = 2.08 ppm; $\delta_C$ = 20.43 ppm; $C_4D_8O$: $\delta_H$ = 3.58 ppm; $\delta_C$ = 67.21 ppm). $^{119}$Sn{$^1$H} NMR spectra were referenced with respect to $SnMe_4$. $^7$Li{$^1$H} NMR spectra were referenced with respect to lithium chloride (9.7 M in $D_2O$). The given chemical shifts of $^{15}$N NMR spectra are obtained from $^{15}$N/$^1$H HSCQ and $^{15}$N/$^1$H HMBC experiments with nitromethane as external standard. LIFDI-MS (JEOL AccuTOF JMS-T100GCV; inert conditions) were measured by the Zentrale Massenabteilung (Fakultät für Chemie, Georg-August-Universität Göttingen). Elemental analyses were obtained from the Analytische Labor (Georg-August-Universität Göttingen) using an Elementar Vario EL 3 analyzer.

## Synthesis and Characterization of Compounds

### Synthesis of DippNP(CH$_3$)$_3$ (2a)

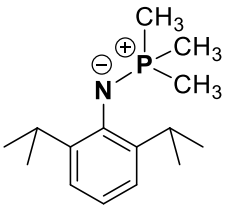

$N_3$Dipp (0.700 g, 3.44 mmol) was dissolved in 6 mL of *n*-hexane. $P(CH_3)_3$ (0.288 g, 3.44 mmol), precooled to -30 °C in 2 mL of *n*-hexane, was slowly added dropwise via syringe, resulting in immediate gas evolution. The solution was stirred for 30 minutes at room temperature, followed by removal of all volatile components under vacuum, yielding $DippNP(CH_3)_3$ (**2a**) as a slightly yellow solid. Crystals of **2a** suitable for single crystal X-ray diffraction were obtained from a saturated *n*-hexane solution of **2a** stored at -4 °C. NMR data of **2a** were recollected in $C_6D_6$ for the purpose of comparison.[S4]

**Yield**: 0.802 g (3.19 mmol; 93%).
**$^1$H NMR** (500 MHz, $C_6D_6$, 298 K): $\delta$ = 0.93 (d, $^2J_{P,H}$ = 12.0 Hz, 9H, $P(CH_3)_3$), 1.34 (d, $^3J_{H,H}$ = 7.0 Hz, 12H, $CH(CH_3)_2$), 3.58 (hept, $^3J_{H,H}$ = 6.9 Hz, 2H, $CH(CH_3)_2$), 7.04-7.09 (m, 1H, $CH_{Aryl}$), 7.22-7.24 (m, 2H, $CH_{Aryl}$) ppm.
**$^1$H NMR** (500 MHz, THF-$d_8$, 298 K): $\delta$ = 1.12 (d, $^3J_{H,H}$ = 6.9 Hz, $CH(CH_3)_2$), 1.50 (d, $^2J_{P,H}$ = 12.3 Hz, 9H, $P(CH_3)_3$), 3.43 (hept, $^3J_{H,H}$ = 6.9 Hz, 2H, $CH(CH_3)_2$), 6.56-6.62 (m, 1H, $CH_{Aryl}$), 6.83-6.86 (m, 2H, $CH_{Aryl}$) ppm.
**$^{13}$C{$^1$H} NMR** (126 MHz, $C_6D_6$, 298 K): $\delta$ = 17.7 (d, $^1J_{P,C}$ = 69.3 Hz, $P(CH_3)_3$), 24.2 ($CH(\underline{C}H_3)_2$), 28.7 (d, $J_{P,C}$ = 1.6 Hz, $\underline{C}H(CH_3)_2$), 119.6 (d, $J_{P,C}$ = 3.8 Hz, $CH_{Aryl}$), 123.0 (d, $J_{P,C}$ = 3.2 Hz, $CH_{Aryl}$), 142.5 (d, $J_{P,C}$ = 7.3 Hz, $C_{q,Aryl}$), 145.7 (d, $J_{P,C}$ = 3.0 Hz, $C_{q,Aryl}N$) ppm.
**$^{31}$P{$^1$H} NMR** (203 MHz, $C_6D_6$, 298 K): $\delta$ = -8.2 ppm.
**$^{31}$P NMR** (203 MHz, $C_6D_6$, 298 K): $\delta$ = -8.2 (m) ppm.
**$^{31}$P{$^1$H} NMR** (203 MHz, THF-$d_8$, 298 K): $\delta$ = -6.7 ppm.
**$^{31}$P NMR** (203 MHz, THF-$d_8$, 298 K): $\delta$ = -6.7 (m) ppm.
**EA**: Anal. calcd. for $C_{15}H_{26}NP$: C, 71.68; H, 10.43; N, 5.57; Found: C, 71.52; H, 10.40; N, 5.52.

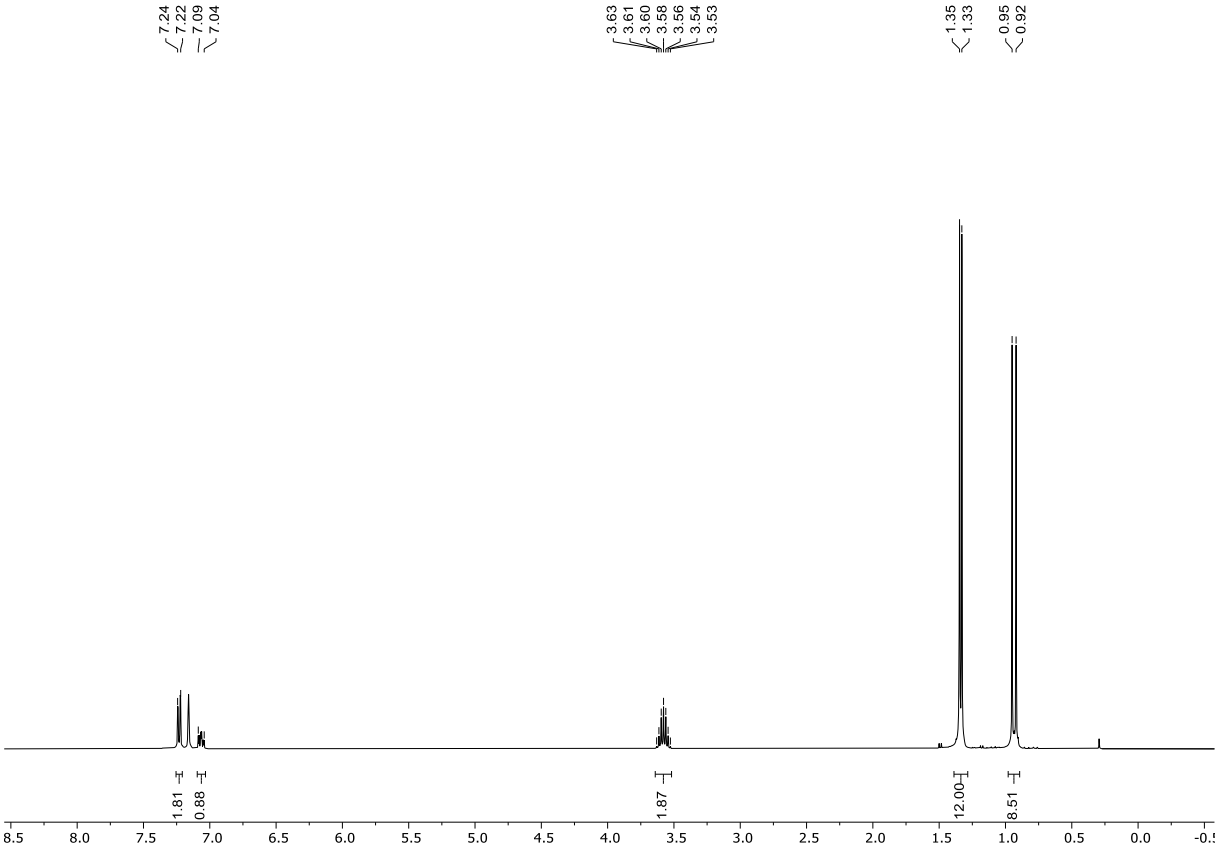


**Figure S1**. $^{1}H$ NMR spectrum of DippNP($CH_3$)$_3$ (**2a**) (500 MHz, $C_6D_6$, 298 K).

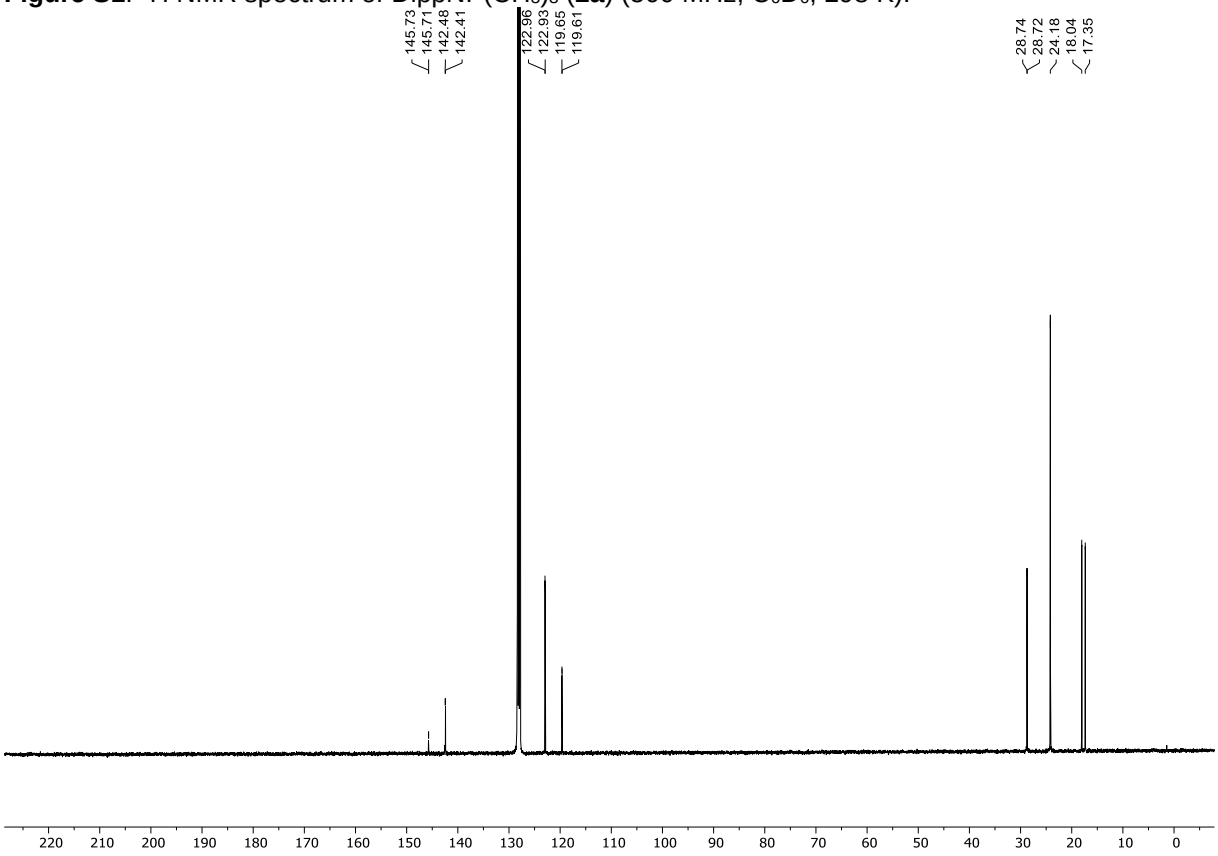


**Figure S2**. $^{13}C\{^{1}H\}$ NMR spectrum of DippNP($CH_3$)$_3$ (**2a**) (126 MHz, $C_6D_6$, 298 K).

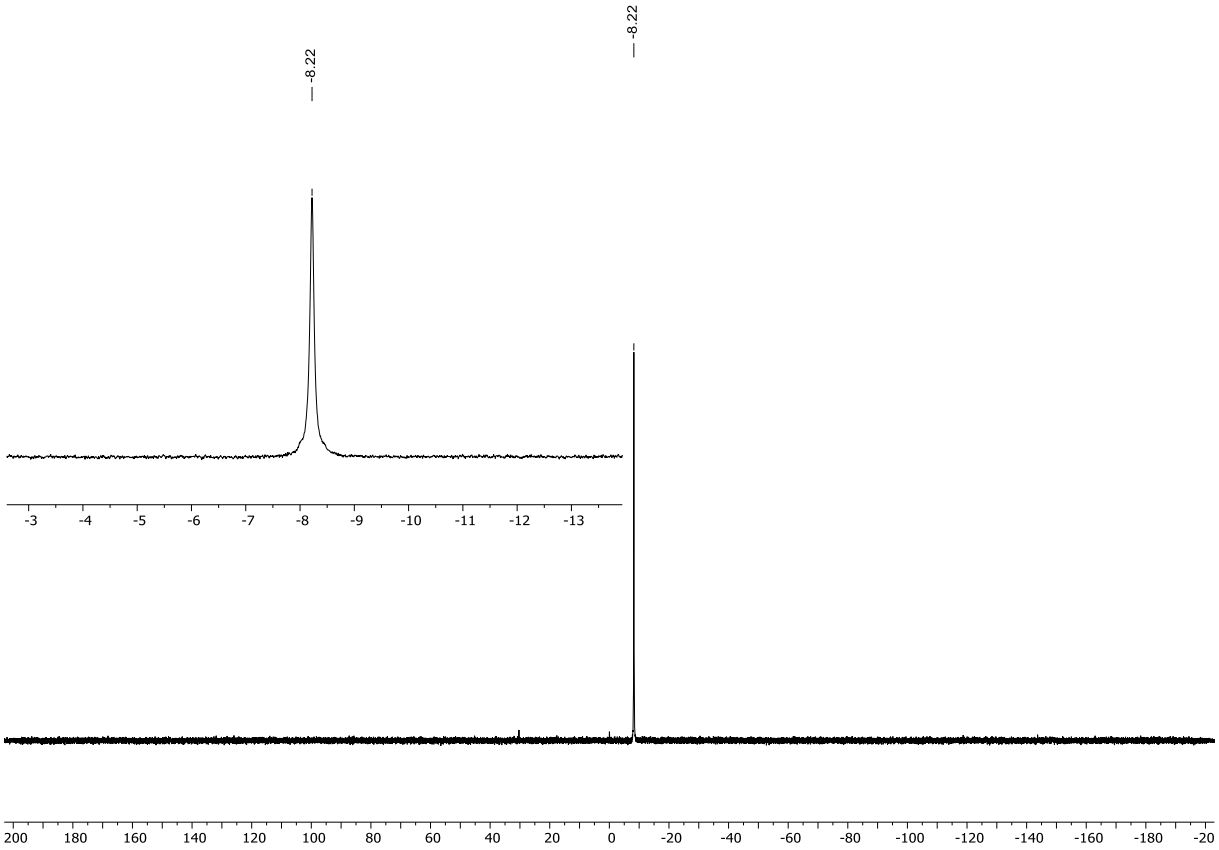


**Figure S3**. $^{31}P\{^{1}H\}$ NMR spectrum of $DippNP(CH_3)_3$ (**2a**) (203 MHz, $C_6D_6$, 298 K).

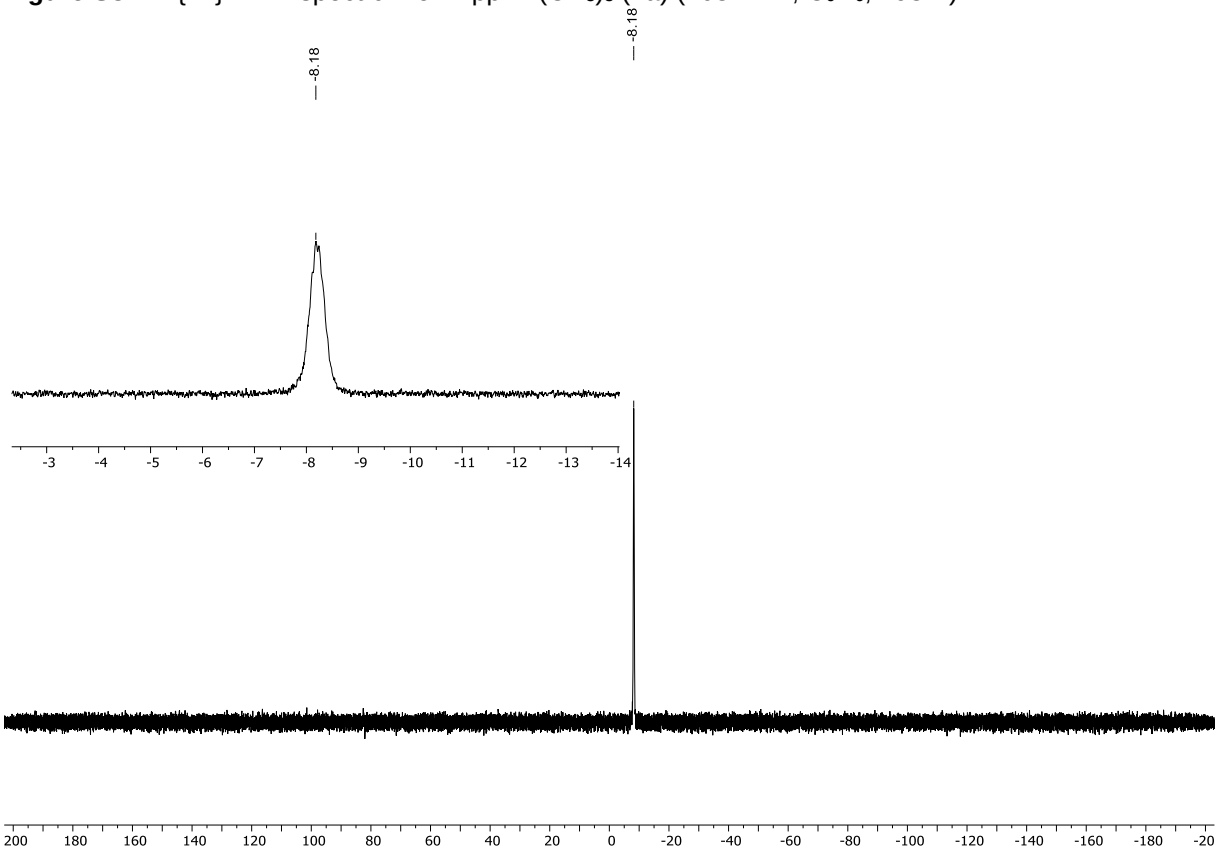


**Figure S4**. $^{31}P$ NMR spectrum of $DippNP(CH_3)_3$ (**2a**) (203 MHz, $C_6D_6$, 298 K).

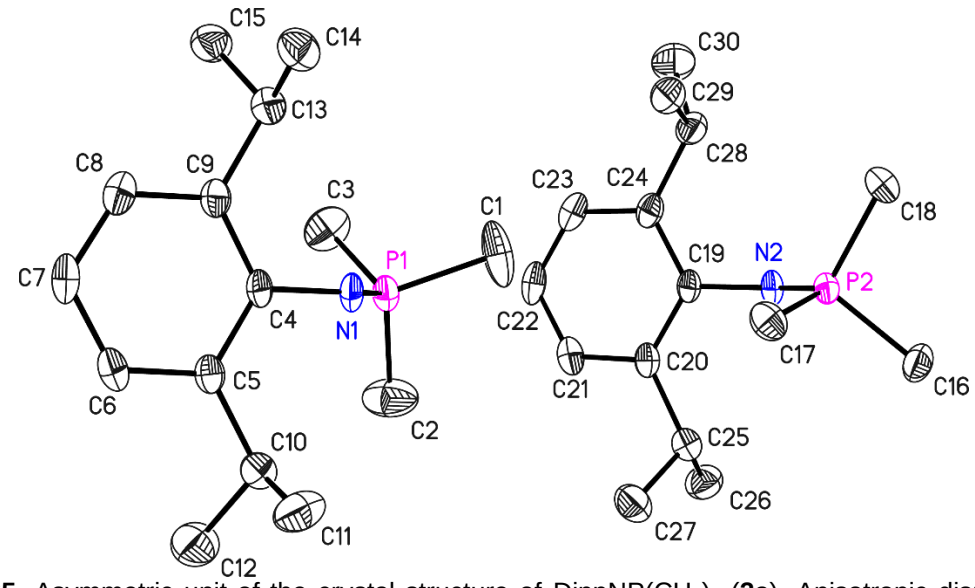


**Figure S5**. Asymmetric unit of the crystal structure of DippNP($CH_3$)$_3$ (**2a**). Anisotropic displacement parameters are drawn at the 50% probability level. Hydrogen atoms have been omitted for clarity. Selected bond lengths (Å) and angles (deg): N1–P1 1.5597(17), P1–C1 1.788(2), P1–C2 1.805(3), P1–C3 1.797(2), N1–C4 1.397(2), C4–N1–P1 131.34(13).

The data were collected on a non-merohedral twin with the twin law −0.90 0 0.19 0 −1 0 0.95 0 −0.90. The fractional contribution of the minor component refined to 0.4755(15).

**Table S1**. Bond lengths [Å] and angles [°] for **2a**.

| | | | |
|---|---|---|---|
| N(2)-C(19) | 1.388(2) | C(13)-C(15) | 1.531(3) |
| N(2)-P(2) | 1.5540(16) | C(13)-C(14) | 1.537(3) |
| P(1)-N(1) | 1.5597(17) | C(19)-C(20) | 1.413(3) |
| P(1)-C(1) | 1.788(2) | C(19)-C(24) | 1.417(3) |
| P(1)-C(3) | 1.797(2) | C(20)-C(21) | 1.394(3) |
| P(1)-C(2) | 1.805(3) | C(20)-C(25) | 1.519(3) |
| P(2)-C(16) | 1.798(2) | C(21)-C(22) | 1.389(3) |
| P(2)-C(17) | 1.802(2) | C(22)-C(23) | 1.387(3) |
| P(2)-C(18) | 1.803(2) | C(23)-C(24) | 1.396(3) |
| N(1)-C(4) | 1.397(2) | C(24)-C(28) | 1.517(3) |
| C(4)-C(5) | 1.415(3) | C(25)-C(27) | 1.523(3) |
| C(4)-C(9) | 1.415(3) | C(25)-C(26) | 1.536(3) |
| C(5)-C(6) | 1.399(3) | C(28)-C(30) | 1.522(3) |
| C(5)-C(10) | 1.516(3) | C(28)-C(29) | 1.533(3) |
| C(6)-C(7) | 1.386(3) | | |
| C(7)-C(8) | 1.387(3) | C(19)-N(2)-P(2) | 137.85(13) |
| C(8)-C(9) | 1.398(3) | N(1)-P(1)-C(1) | 107.78(10) |
| C(9)-C(13) | 1.521(3) | N(1)-P(1)-C(3) | 117.34(10) |
| C(10)-C(12) | 1.520(3) | C(1)-P(1)-C(3) | 106.50(14) |
| C(10)-C(11) | 1.529(3) | N(1)-P(1)-C(2) | 116.83(11) |

| | | | |
|---|---|---|---|
| C(1)-P(1)-C(2) | 104.68(15) | C(12)-C(10)-C(11) | 110.32(19) |
| C(3)-P(1)-C(2) | 102.61(13) | C(9)-C(13)-C(15) | 112.50(17) |
| N(2)-P(2)-C(16) | 110.57(9) | C(9)-C(13)-C(14) | 110.13(17) |
| N(2)-P(2)-C(17) | 116.73(9) | C(15)-C(13)-C(14) | 111.15(18) |
| C(16)-P(2)-C(17) | 105.52(11) | N(2)-C(19)-C(20) | 120.15(17) |
| N(2)-P(2)-C(18) | 114.61(10) | N(2)-C(19)-C(24) | 120.39(17) |
| C(16)-P(2)-C(18) | 101.96(10) | C(20)-C(19)-C(24) | 119.21(17) |
| C(17)-P(2)-C(18) | 106.07(10) | C(21)-C(20)-C(19) | 119.32(19) |
| C(4)-N(1)-P(1) | 131.34(13) | C(21)-C(20)-C(25) | 119.09(18) |
| N(1)-C(4)-C(5) | 120.48(17) | C(19)-C(20)-C(25) | 121.58(17) |
| N(1)-C(4)-C(9) | 119.95(17) | C(22)-C(21)-C(20) | 121.7(2) |
| C(5)-C(4)-C(9) | 119.23(17) | C(23)-C(22)-C(21) | 118.94(19) |
| C(6)-C(5)-C(4) | 119.32(18) | C(22)-C(23)-C(24) | 121.4(2) |
| C(6)-C(5)-C(10) | 119.73(18) | C(23)-C(24)-C(19) | 119.43(19) |
| C(4)-C(5)-C(10) | 120.82(17) | C(23)-C(24)-C(28) | 120.16(18) |
| C(7)-C(6)-C(5) | 121.59(19) | C(19)-C(24)-C(28) | 120.33(17) |
| C(6)-C(7)-C(8) | 118.87(18) | C(20)-C(25)-C(27) | 111.93(17) |
| C(7)-C(8)-C(9) | 121.72(19) | C(20)-C(25)-C(26) | 110.68(17) |
| C(8)-C(9)-C(4) | 119.20(18) | C(27)-C(25)-C(26) | 111.34(18) |
| C(8)-C(9)-C(13) | 118.97(18) | C(24)-C(28)-C(30) | 115.3(2) |
| C(4)-C(9)-C(13) | 121.76(17) | C(24)-C(28)-C(29) | 109.86(17) |
| C(5)-C(10)-C(12) | 113.84(18) | C(30)-C(28)-C(29) | 109.08(19) |
| C(5)-C(10)-C(11) | 109.81(17) | | |

**Synthesis of XylNP(CH$_3$)$_3$ (2b)**

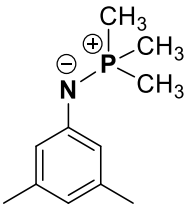

$N_3$Xyl (0.500 g, 3.40 mmol) was dissolved in 6 mL of *n*-hexane. P(CH$_3$)$_3$ (0.258 g, 3.40 mmol), precooled to -30 °C in 2 mL of *n*-hexane, was slowly added dropwise via syringe, resulting in immediate gas evolution. The solution was stirred for 30 minutes at room temperature, followed by removal of all volatile components under vacuum, yielding XylNP(CH$_3$)$_3$ (**2b**) as a yellow solid. NMR data of **2b** were recollected in $C_6D_6$ for the purpose of comparison.[S5]

**Yield**: 0.632 g (3.24 mmol; 95%).
**$^1$H NMR** (500 MHz, $C_6D_6$, 298 K): $\delta$ = 0.95 (d, $^2J_{P,H}$ = 12.4 Hz, 9H, P(CH$_3$)$_3$), 2.31 (s, 6H, CH$_3$), 6.52-6.54 (m, 1H, CH$_{Aryl}$), 6.70-6.71 (m, 2H, CH$_{Aryl}$) ppm.
**$^{13}$C{$^1$H} NMR** (126 MHz, $C_6D_6$, 298 K): $\delta$ = 16.0 (d, $^1J_{P,C}$ = 67.2 Hz, P(CH$_3$)$_3$), 21.9 (CH$_3$), 119.2 (CH$_{Aryl}$), 121.2 (d, $J_{P,C}$ = 18.9 Hz, CH$_{Aryl}$), 138.1 ($C_{q,Aryl}$CH$_3$), 153.4 (d, $^2J_{P,C}$ = 3.7 Hz, $C_{q,Aryl}$N) ppm.
**$^{31}$P{$^1$H} NMR** (203 MHz, $C_6D_6$, 298 K): $\delta$ = 1.4 ppm.
**$^{31}$P NMR** (203 MHz, $C_6D_6$, 298 K): $\delta$ = 1.4 (m) ppm.
**EA**: Anal. calcd. for $C_{11}H_{18}NP$: C, 67.67; H, 9.29; N, 7.17; Found: C, 67.46; H, 9.31; N, 7.24.

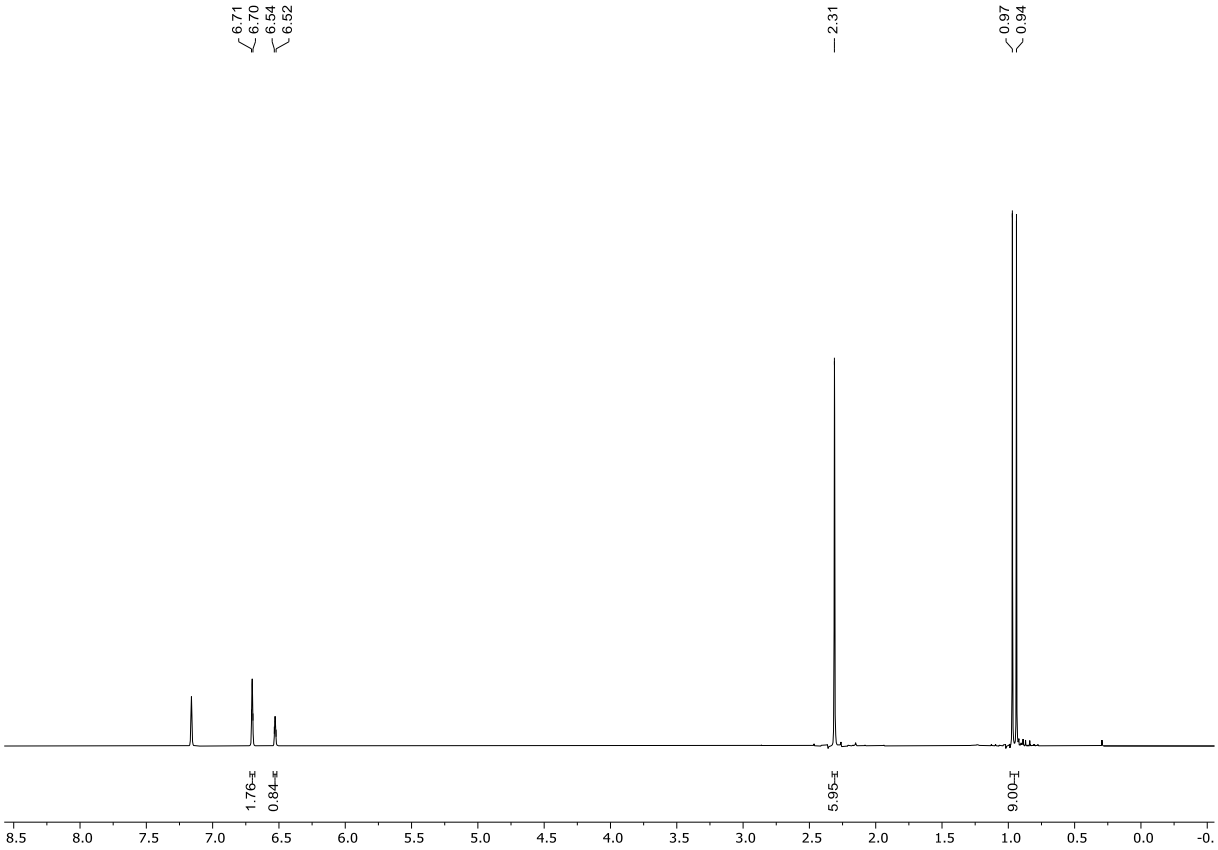


**Figure S6**. $^{1}H$ NMR spectrum of XylNP$(CH_3)_3$ (**2b**) (500 MHz, $C_6D_6$, 298 K).

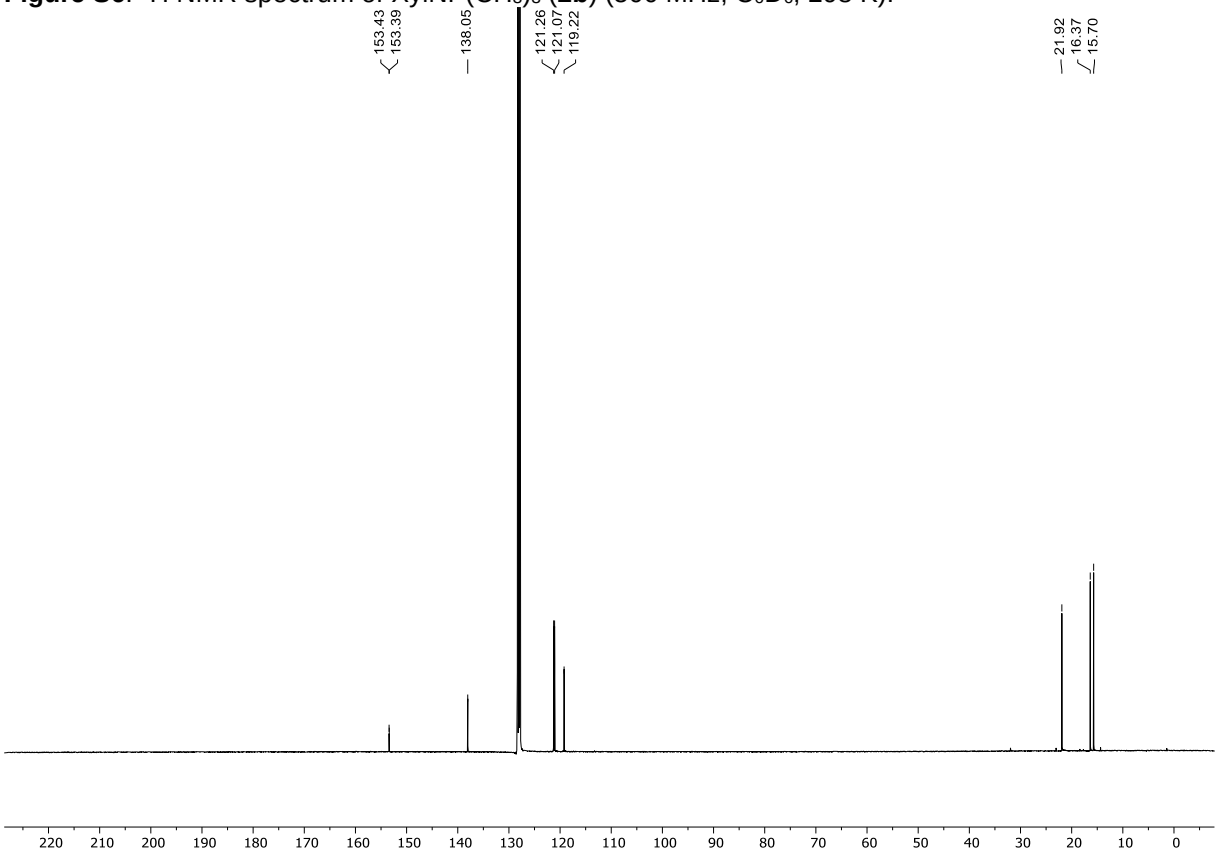


**Figure S7**. $^{13}C\{^{1}H\}$ NMR spectrum of XylNP$(CH_3)_3$ (**2b**) (126 MHz, $C_6D_6$, 298 K).

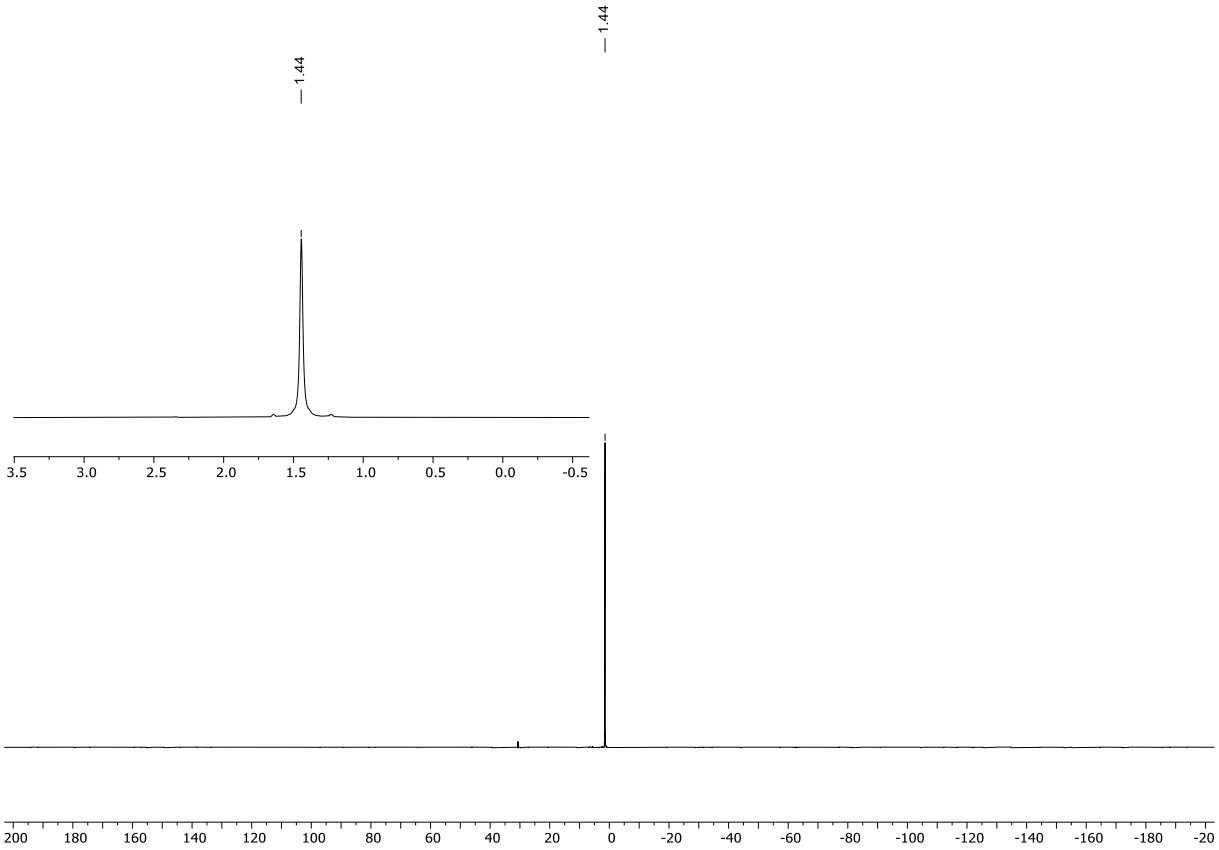


**Figure S8**. $^{31}P\{^{1}H\}$ NMR spectrum of XylNP$(CH_3)_3$ (**2b**) (203 MHz, $C_6D_6$, 298 K).

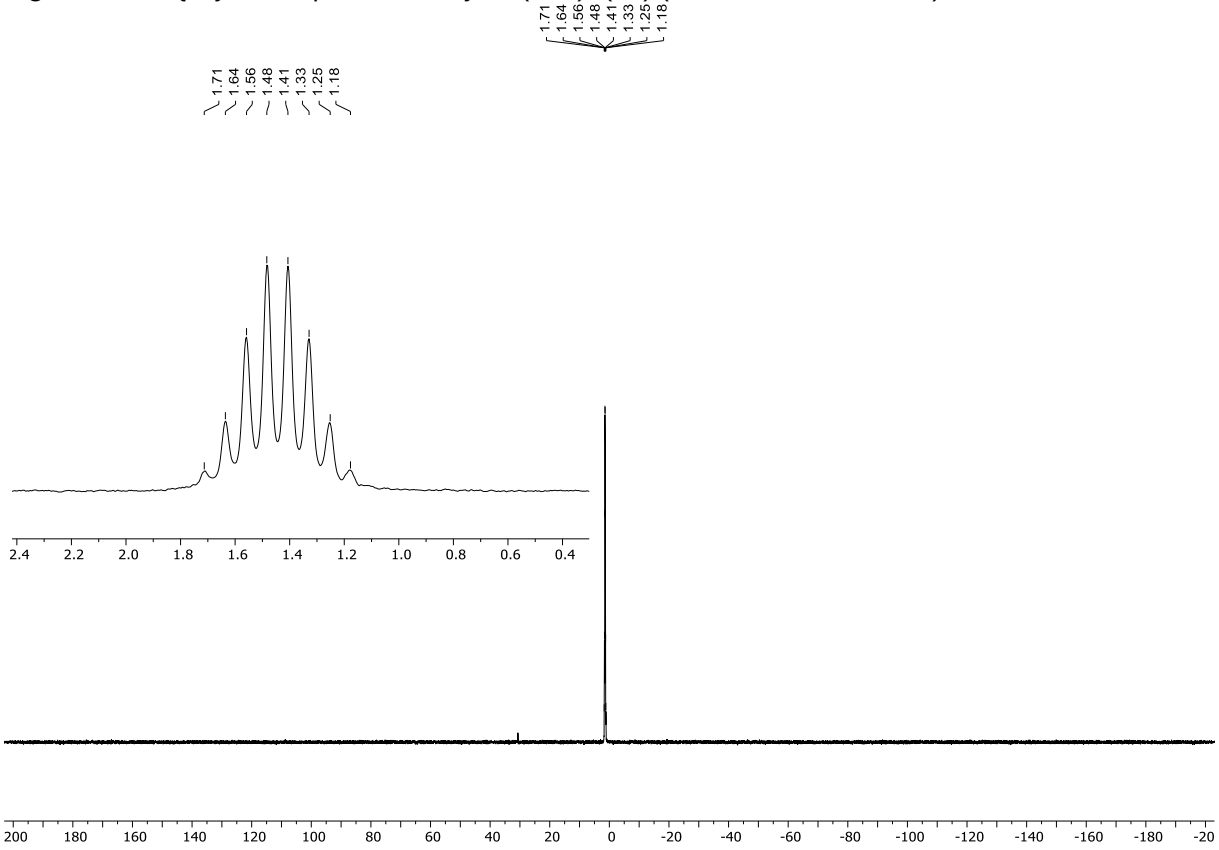


**Figure S9**. $^{31}P$ NMR spectrum of XylNP$(CH_3)_3$ (**2b**) (203 MHz, $C_6D_6$, 298 K).

**Synthesis of AdNP(CH$_3$)$_3$ (2c)**

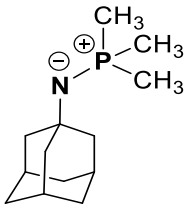

$N_3$Ad (0.700 g, 2.82 mmol) was dissolved in 6 mL of *n*-hexane. P(CH$_3$)$_3$ (0.215 g, 2.82 mmol), precooled to -30 °C in 2 mL of *n*-hexane, was slowly added dropwise via syringe. The solution was stirred for 1 h at room temperature which results in slow gas evolution, followed by removal of all volatile components under vacuum, yielding AdNP(CH$_3$)$_3$ (**2c**) as a colourless solid. Crystals of **2c** suitable for single crystal X-ray diffraction were obtained from a saturated *n*-hexane solution of **2c** stored at -4 °C. NMR data of **2c** were recollected in $C_6D_6$ for the purpose of comparison.[S6]

**Yield**: 0.802 g (3.19 mmol; 93%).
**$^1$H NMR** (500 MHz, $C_6D_6$, 298 K): $\delta$ = 1.00 (d, $^2J_{P,H}$ = 11.8 Hz, 9H, P(CH$_3$)$_3$), 1.68-1.76 (m, 6H, CH$_2$), 1.93-1.94 (m, 6H, CH$_2$), 2.12-2.15 (m, 3H, CH) ppm.
**$^{13}$C{$^1$H} NMR** (126 MHz, $C_6D_6$, 298 K): $\delta$ = 20.5 (d, $^1J_{P,C}$ = 64.9 Hz, P(CH$_3$)$_3$), 30.8 (d, $J_{P,C}$ = 2.1 Hz, CH), 37.1 (CH$_2$), 50.0 (d, $J_{P,C}$ = 11.9 Hz, CH$_2$), 51.5 (d, $^2J_{P,C}$ = 5.5 Hz, $C_q$N) ppm.
**$^{31}$P{$^1$H} NMR** (203 MHz, $C_6D_6$, 298 K): $\delta$ = -14.5 ppm.
**$^{31}$P NMR** (203 MHz, $C_6D_6$, 298 K): $\delta$ = -14.5 (m) ppm.
**EA**: Anal. calcd. for $C_{13}H_{24}NP$: C, 69.30; H, 10.74; N, 6.22; Found: C, 69.23; H, 10.81; N, 6.19.

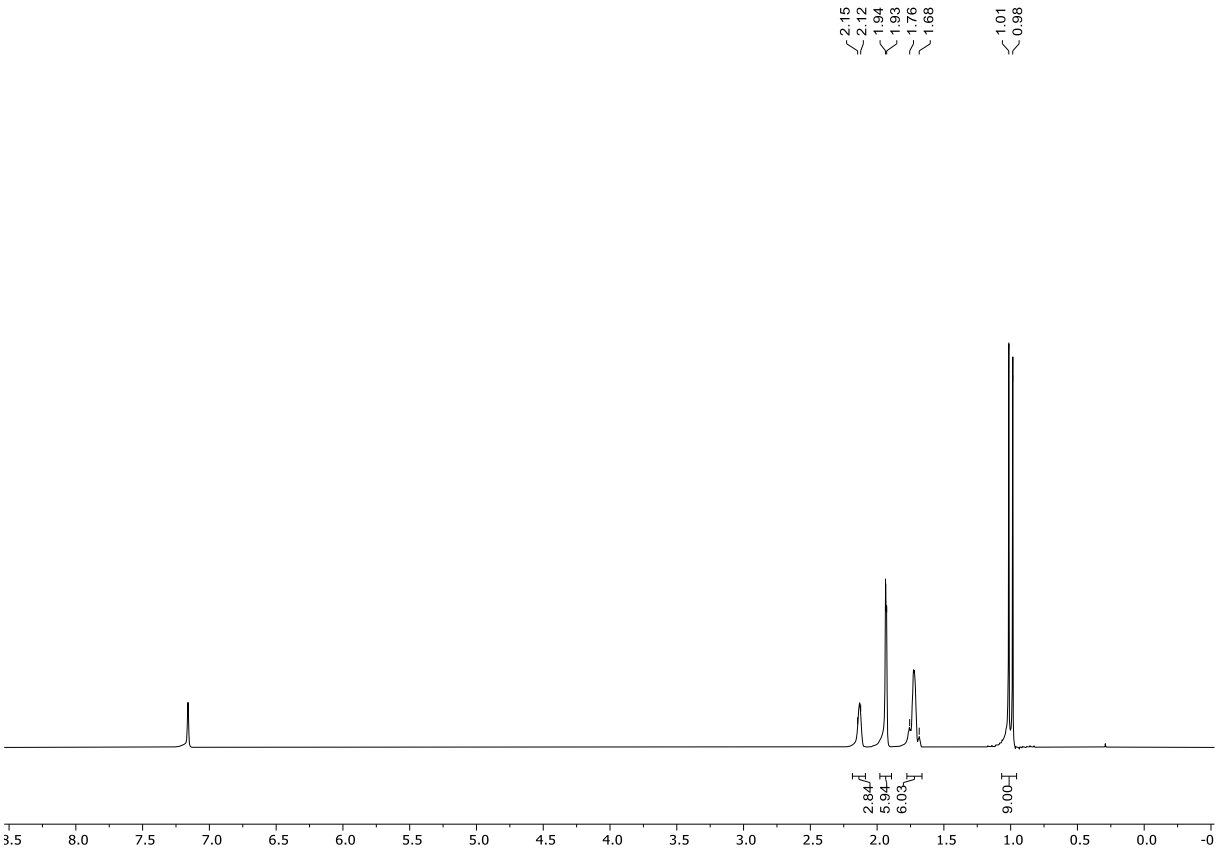


**Figure S10**. $^{1}H$ NMR spectrum of $AdNP(CH_3)_3$ (**2c**) (400 MHz, $C_6D_6$, 298 K).

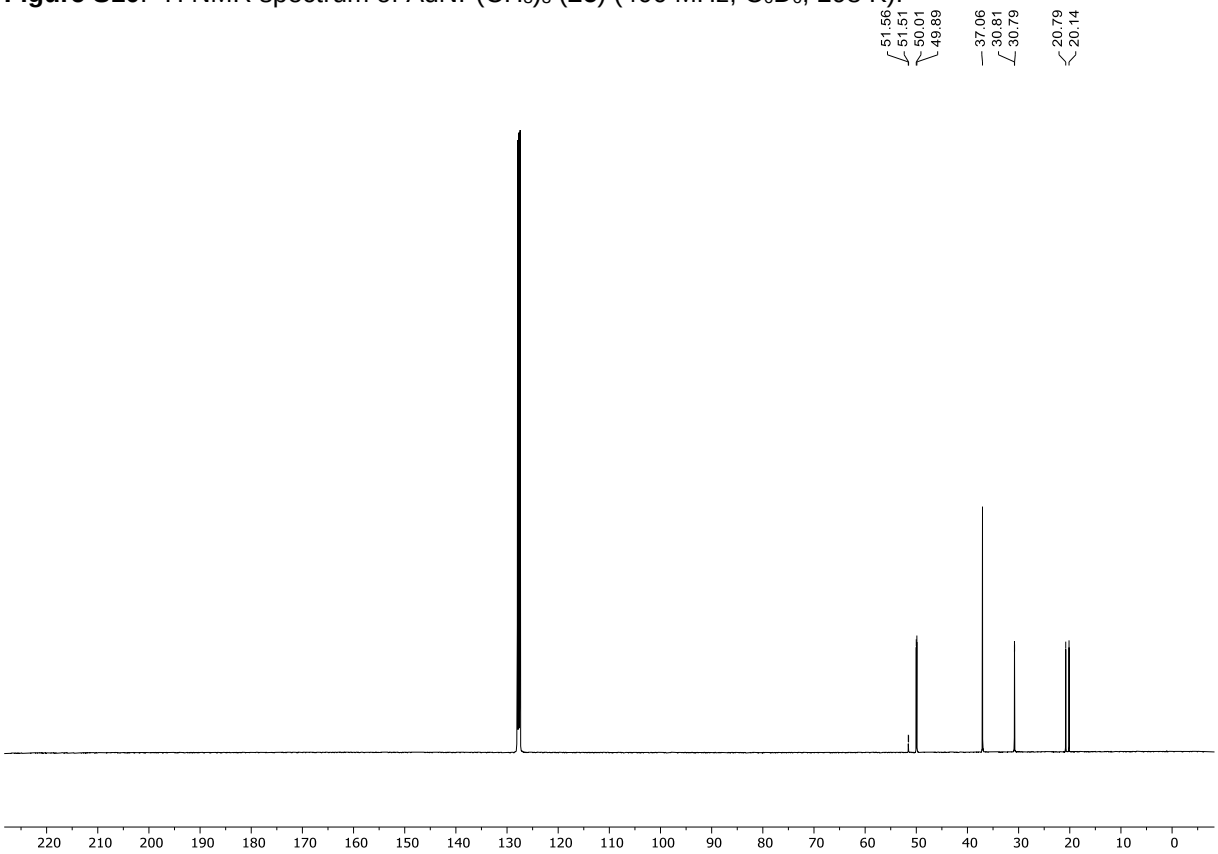


**Figure S11**. $^{13}C\{^{1}H\}$ NMR spectrum of $AdNP(CH_3)_3$ (**2c**) (126 MHz, $C_6D_6$, 298 K).

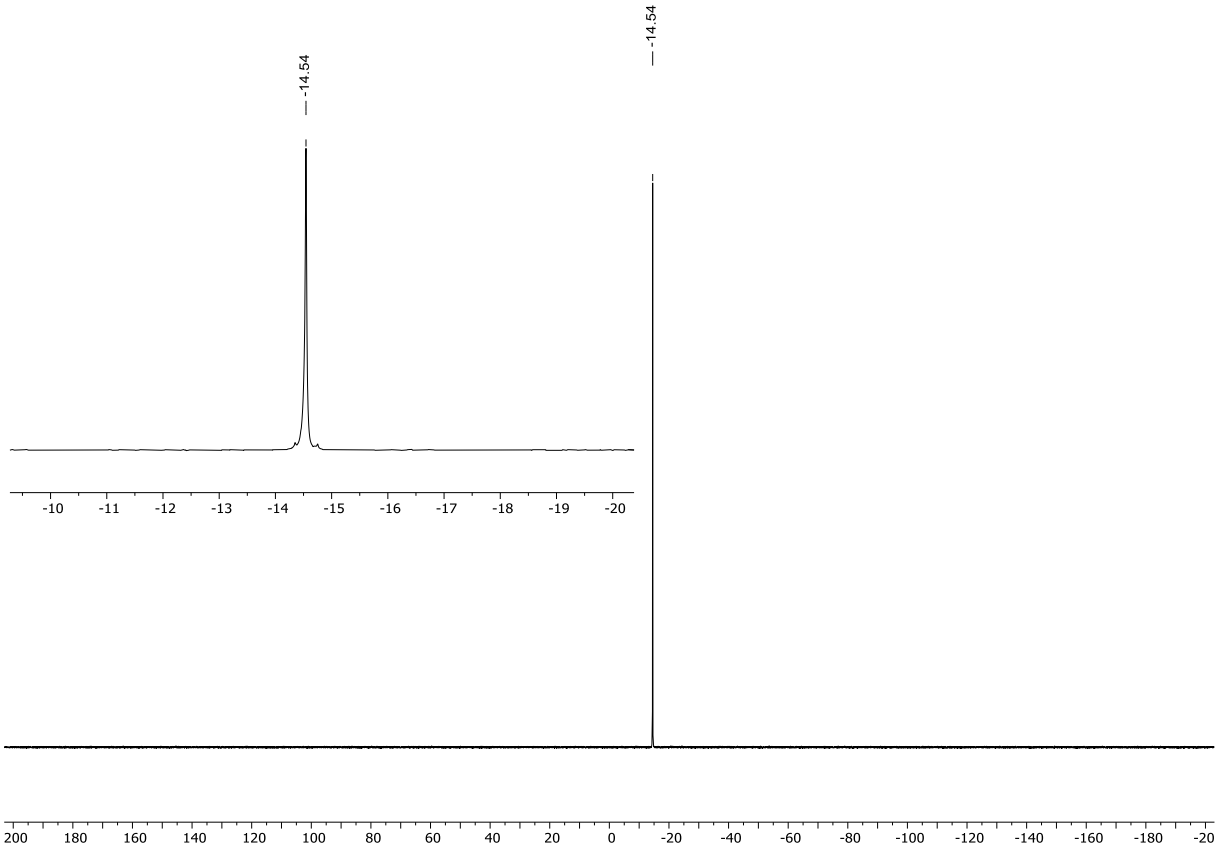


**Figure S12**. $^{31}P\{^{1}H\}$ NMR spectrum of $AdNP(CH_3)_3$ (**2c**) (203 MHz, $C_6D_6$, 298 K).

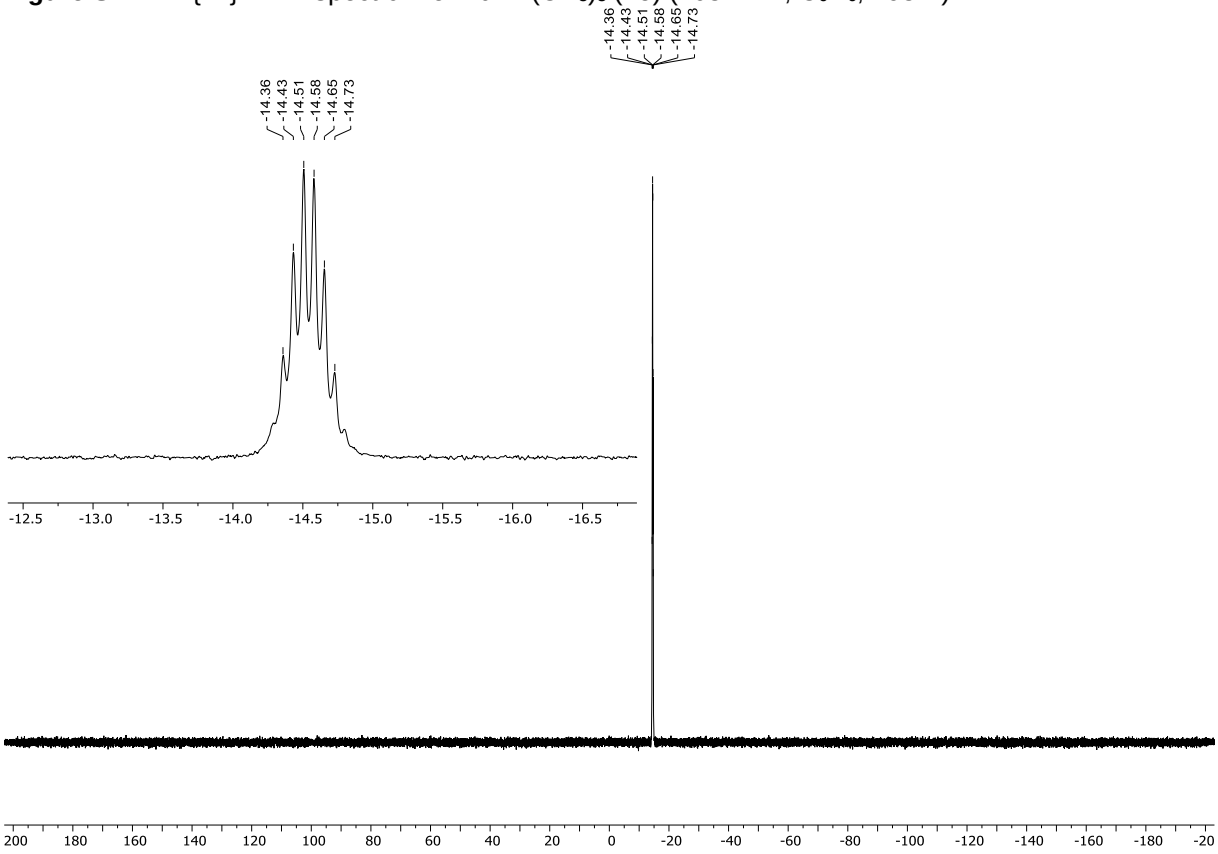


**Figure S13**. $^{31}P\{^{1}H\}$ NMR spectrum of $AdNP(CH_3)_3$ (**2c**) (203 MHz, $C_6D_6$, 298 K).

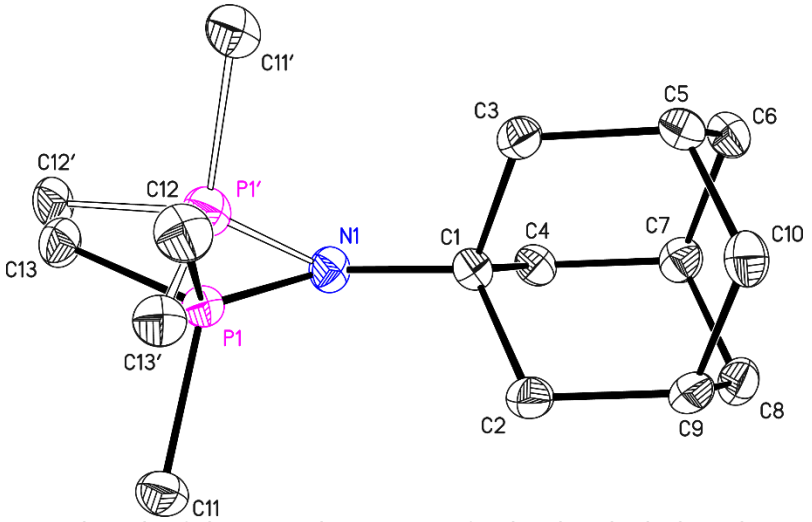


**Figure S14**. Asymmetric unit of the crystal structure of AdNP$(CH_3)_3$ (**2c**). Anisotropic displacement parameters are drawn at the 50% probability level (hydrogen atoms have been omitted for clarity). Selected bond lengths (Å) and angles (deg): N1–P1 1.558(4), N1–C1 1.461(5), P1–C11 1.828(4), P1–C12 1.825(4), P1–C13 1.791(4), C1–N1–P1 129.6(3). The $PMe_3$ group is disordered over two positions and was refined with distance restraints and restraints for the anisotropic displacement parameters. The occupancy of the minor domain refined to 0.029(3).

**Table S2**. Bond lengths [Å] and angles [°] for **2c**.

| | | | |
|---|---|---|---|
| P(1)-N(1) | 1.558(4) | N(1)-P(1)-C(13) | 107.8(2) |
| P(1)-C(13) | 1.791(4) | N(1)-P(1)-C(12) | 118.9(2) |
| P(1)-C(12) | 1.825(4) | C(13)-P(1)-C(12) | 104.8(2) |
| P(1)-C(11) | 1.828(4) | N(1)-P(1)-C(11) | 117.6(2) |
| P(1')-N(1) | 1.579(17) | C(13)-P(1)-C(11) | 103.7(2) |
| P(1')-C(12') | 1.804(15) | C(12)-P(1)-C(11) | 102.2(2) |
| P(1')-C(11') | 1.808(16) | N(1)-P(1')-C(12') | 114.8(19) |
| P(1')-C(13') | 1.812(16) | N(1)-P(1')-C(11') | 114.4(18) |
| N(1)-C(1) | 1.461(5) | C(12')-P(1')-C(11') | 104.7(17) |
| C(1)-C(4) | 1.536(6) | N(1)-P(1')-C(13') | 112.9(18) |
| C(1)-C(2) | 1.542(6) | C(12')-P(1')-C(13') | 104.8(17) |
| C(1)-C(3) | 1.543(6) | C(11')-P(1')-C(13') | 104.3(17) |
| C(2)-C(9) | 1.532(6) | C(1)-N(1)-P(1) | 129.6(3) |
| C(3)-C(5) | 1.540(6) | C(1)-N(1)-P(1') | 127.5(12) |
| C(4)-C(7) | 1.532(6) | N(1)-C(1)-C(4) | 107.5(3) |
| C(5)-C(10) | 1.524(6) | N(1)-C(1)-C(2) | 114.8(3) |
| C(5)-C(6) | 1.537(6) | C(4)-C(1)-C(2) | 107.8(3) |
| C(6)-C(7) | 1.536(6) | N(1)-C(1)-C(3) | 111.3(3) |
| C(7)-C(8) | 1.532(6) | C(4)-C(1)-C(3) | 107.6(3) |
| C(8)-C(9) | 1.527(6) | C(2)-C(1)-C(3) | 107.6(3) |
| C(9)-C(10) | 1.539(6) | C(9)-C(2)-C(1) | 111.2(3) |
| | | C(5)-C(3)-C(1) | 111.7(3) |

| | | | |
|---|---|---|---|
| C(7)-C(4)-C(1) | 111.5(3) | C(4)-C(7)-C(6) | 109.3(3) |
| C(10)-C(5)-C(6) | 109.2(3) | C(9)-C(8)-C(7) | 108.9(3) |
| C(10)-C(5)-C(3) | 109.6(3) | C(8)-C(9)-C(2) | 109.8(4) |
| C(6)-C(5)-C(3) | 109.0(4) | C(8)-C(9)-C(10) | 109.4(4) |
| C(7)-C(6)-C(5) | 109.2(3) | C(2)-C(9)-C(10) | 109.7(3) |
| C(8)-C(7)-C(4) | 109.7(3) | C(5)-C(10)-C(9) | 109.5(3) |
| C(8)-C(7)-C(6) | 109.8(4) | | |

**Reaction of $^{Mes}$TerSn{N(Si(CH$_3$)$_3$)$_2$} (1) and DippNP(CH$_3$)$_3$ (2a) – Synthesis of $^{Mes}$TerSnCH$_2$P(CH$_3$)$_2$NDipp (3a)**

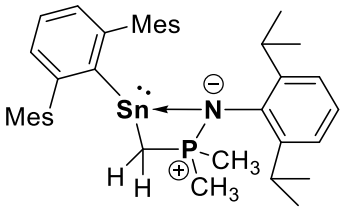


DippNP(CH$_3$)$_3$ (**2a**) (0.021 g, 0.084 mmol) in 0.2 mL of $C_6D_6$ was added to a solution of $^{Mes}$TerSn{N(Si(CH$_3$)$_3$)$_2$} (**1**) (0.050 g, 0.084 mmol) in 0.3 mL of $C_6D_6$. The reaction progress was monitored by $^1$H and $^{31}$P{$^1$H} NMR spectroscopy. The reaction slowly starts at room temperature. Therefore, the reaction mixture was heated to 70 °C which results in a colour change from orange-red to yellow-orange over time and heating was continued till all starting materials were consumed. All volatile components were removed under vacuum. The yellow amorphous material was dissolved in 1 mL of *n*-hexane, filtered and stored at -30 °C to give $^{Mes}$TerSnCH$_2$P(CH$_3$)$_2$NDipp (**3a**) as a yellow crystalline material. In certain instances, the solvent was gradually allowed to evaporate at -30 °C, resulting in the achievement of identical results. Crystals obtained through this method were suitable for single crystal X-ray diffraction.

**Yield**: 0.049 g (0.072 mmol; 86%).
**$^1$H NMR** (400 MHz, $C_6D_6$, 298 K): δ = 0.24 (d, $^2J_{P,H}$ = 6.5 Hz, 2H, CH$_2$), 0.72 (d, $^2J_{P,H}$ = 11.9 Hz, 6H, P(CH$_3$)$_2$), 0.95 (m(br), 12H, CH(C*H*$_3$)$_2$)*, 2.07 (s, 12H, CH$_3$)**, 2.24 (s, 6H, CH$_3$), 3.39 (hept, $^3J_{H,H}$ = 6.8 Hz, C*H*(CH$_3$)$_2$), 6.78 (m, 4H, CH$_{Aryl}$), 6.95-7.01 (m, 5H, CH$_{Aryl}$)**, 7.19-7.23 (m, 1H, CH$_{Aryl}$) ppm.
**$^1$H NMR** (400 MHz, $C_7D_8$, 243 K): 0.14 (d, $^2J_{P,H}$ = 11.3 Hz, 1H, CH$_2$), 0.28 (d, $^2J_{P,H}$ = 12.5 Hz, 1H, CH$_2$), 0.58 (d, $^2J_{P,H}$ = 12.1 Hz, 6H, P(CH$_3$)$_2$), 0.81 (d, $^3J_{H,H}$ = 6.5 Hz, 3H, CH(C*H*$_3$)$_2$), 0.88 (m, 3H, CH(C*H*$_3$)$_2$), 1.07-1.10 (m, 6H, CH(C*H*$_3$)$_2$), 1.86 (s, 6H, CH$_3$), 2.28 (s, 6H, CH$_3$), 2.41 (s, 6H, CH$_3$), 3.34 (hept, $^3J_{H,H}$ = 6.4 Hz, 1H, C*H*(CH$_3$)$_2$), 3.42 (hept, $^3J_{H,H}$ = 6.4 Hz, 1H, C*H*(CH$_3$)$_2$), 6.74 (m, 2H, CH$_{Aryl}$), 6.86 (m, 2H, CH$_{Aryl}$), 6.92-6.93 (m, 1H, CH$_{Aryl}$), 6.98-7.01 (m, 2H, CH$_{Aryl}$)**, 7.05-7.07 (m, 2H, CH$_{Aryl}$)**, 7.23-7.25 (m, 1H, CH$_{Aryl}$) ppm.
* = overlap with signal of residual *n*-hexane
** = overlap with $C_7D_7H$ signal(s)
**$^{13}$C{$^1$H} NMR** (126 MHz, $C_6D_6$, 298 K): δ = 8.5 (d, $^1J_{P,C}$ = 74.2 Hz, CH$_2$), 20.3 (P(CH$_3$)$_2$)***, 21.2 (CH$_3$), 22.0 (CH$_3$), 25.2 (br, CH(C̲H$_3$)$_2$), 27.3 (C̲H(CH$_3$)$_2$), 124.0 (d, $J_{P,C}$ = 3.9 Hz, CH$_{Aryl}$), 124.2 (d, $J_{P,C}$ = 3.5 Hz, CH$_{Aryl}$), 127.5 (CH$_{Aryl}$)***, 128.1 (CH$_{Aryl}$)***, 128.2 (CH$_{Aryl}$)***, 135.7 (C$_{q,Aryl}$), 136.7 (C$_{q,Aryl}$), 140.2 (d, $J_{P,C}$ = 9.1 Hz, C$_{q,Aryl}$), 142.9 (C$_{q,Aryl}$), 146.3 (d, $J_{P,C}$ = 6.1 Hz, C$_{q,Aryl}$), 139.0 (C$_{q,Aryl}$), 172.9 (C$_{q,Aryl}$Sn) ppm.
*** = overlap with $C_7D_8$ signal(s) and assigned by $^1$H/$^{13}$C HMBC
**$^1$H/$^{15}$N HMBC NMR** (51 MHz, $C_6D_6$, 298 K): δ = -354.5 ppm.
**$^{31}$P{$^1$H} NMR** (203 MHz, $C_6D_6$, 298 K): δ = 40.4 (Sn satellites: $J_{119/117Sn,P}$ = 163.6 Hz (average value)) ppm.
**$^{31}$P NMR** (203 MHz, $C_6D_6$, 298 K): δ = 40.4 (m) ppm.
**$^{119}$Sn{$^1$H} NMR** (187 MHz, $C_6D_6$, 298 K): δ = 422.0 (d, $^2J_{119Sn,P}$ = 165.9 Hz) ppm.
**MS (LIFDI)**: m/z calcd. for $C_{39}H_{50}NPSn$: 683.2703; found: 683.3.
**EA**: Anal. calcd. for $C_{39}H_{50}NPSn$: C, 68.63; H, 7.38; N, 2.05; Found: C, 68.09; H, 7.37; N, 2.02.

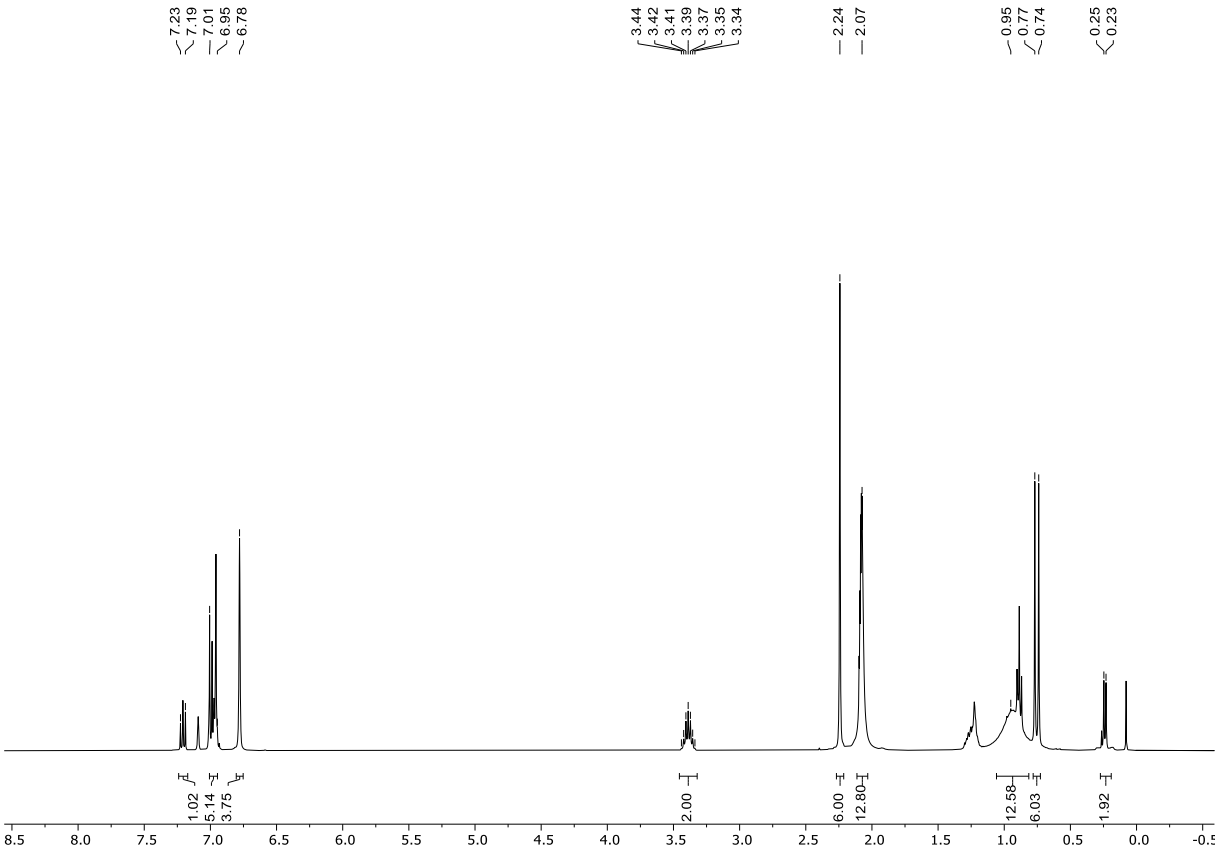


**Figure S15**. $^{1}H$ NMR spectrum of $^{Mes}TerSnCH_2P(CH_3)_2NDipp$ (**3a**) (400 MHz, $C_6D_6$, 298 K); 0.89, 1.24 ppm: *n*-hexane, 0.10 ppm: $HN(Si(CH_3)_3)_2$.

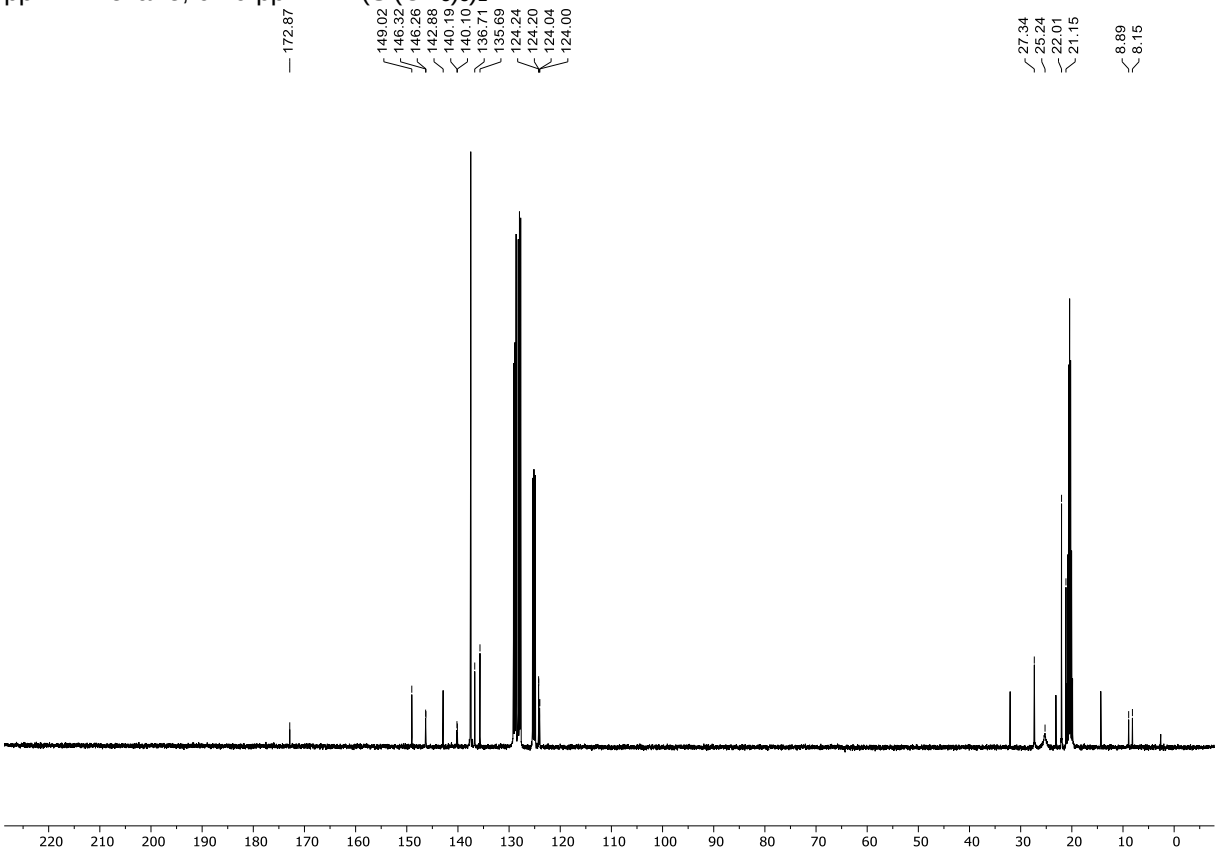


**Figure S16**. $^{13}C\{^{1}H\}$ NMR spectrum of $^{Mes}TerSnCH_2P(CH_3)_2NDipp$ (**3a**) (126 MHz, $C_6D_6$, 298 K); 14.3, 23.0, 32.0 ppm: *n*-hexane.

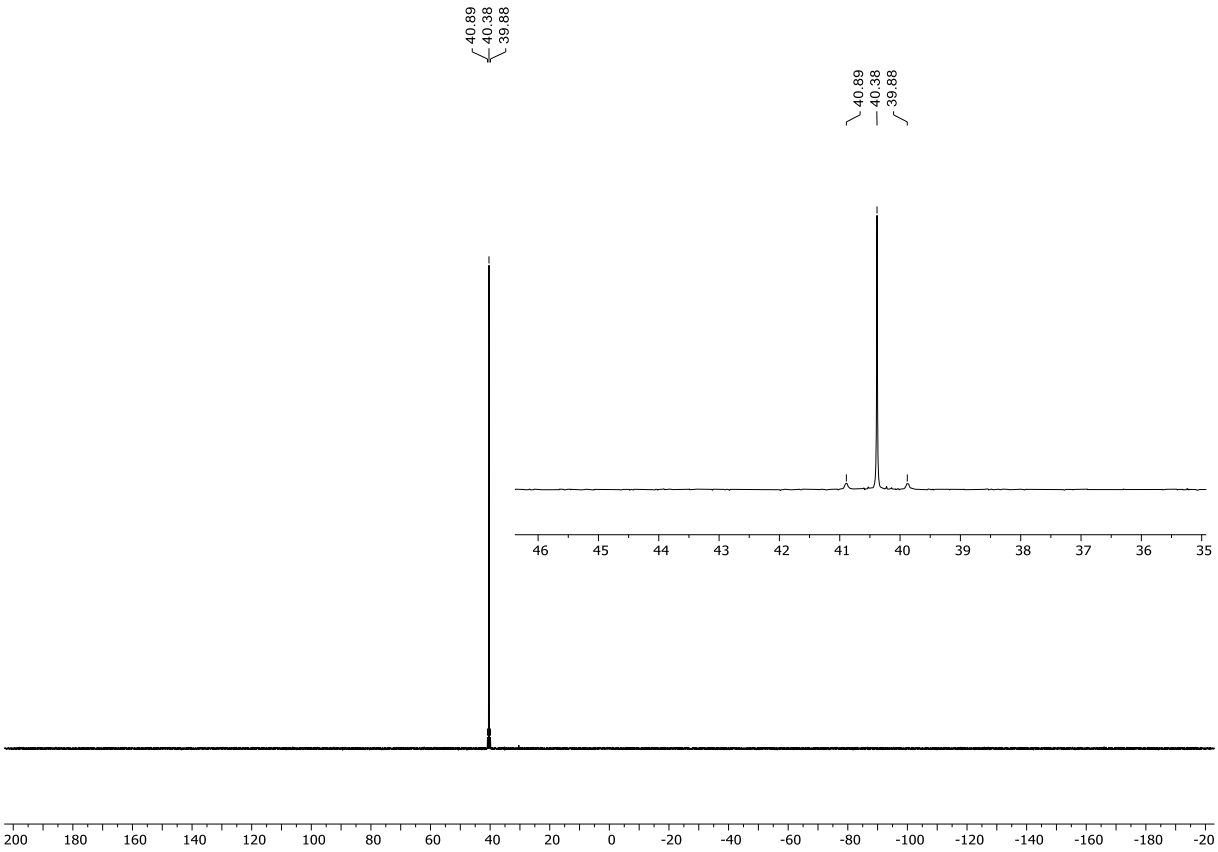


**Figure S17**. $^{31}P\{^{1}H\}$ NMR spectrum of $^{Mes}TerSnCH_2P(CH_3)_2NDipp$ (**3a**) (203 MHz, $C_6D_6$, 298 K).

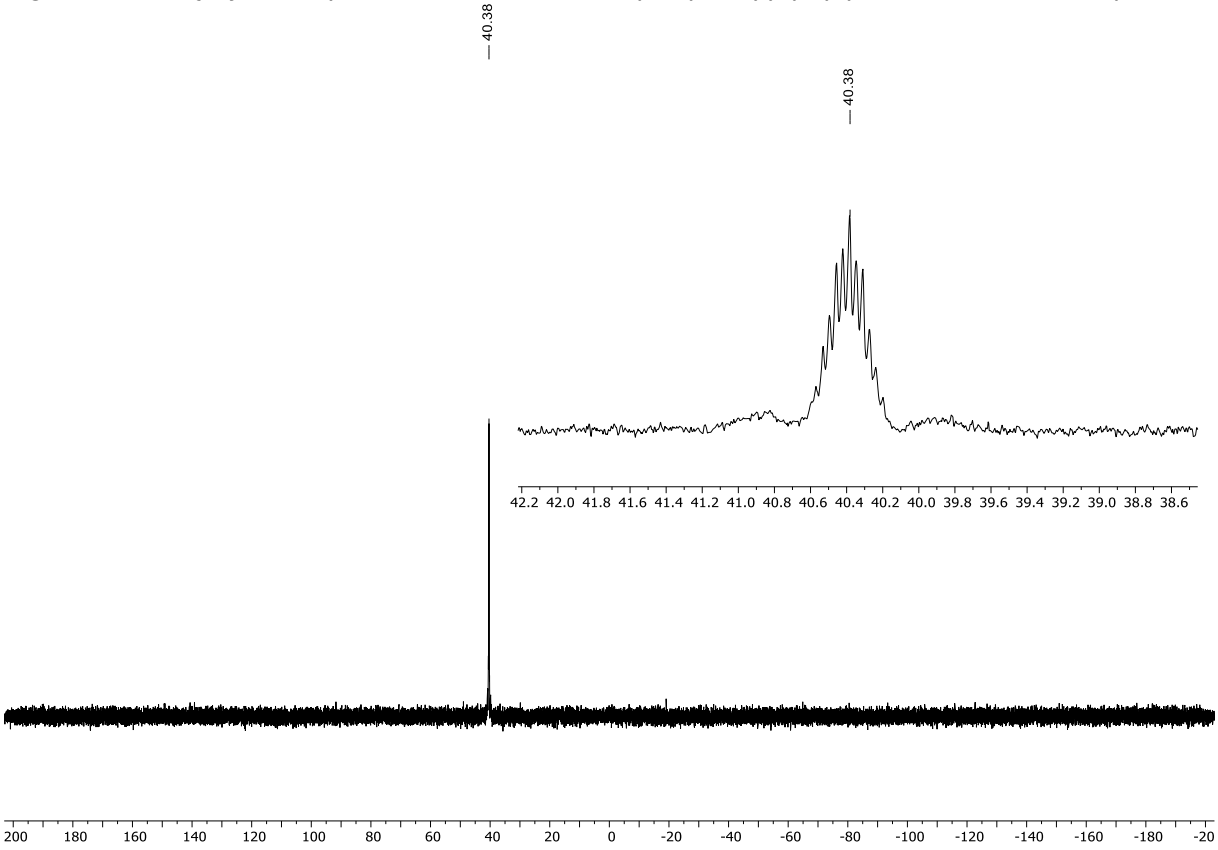


**Figure S18**. $^{31}P$ NMR spectrum of $^{Mes}TerSnCH_2P(CH_3)_2NDipp$ (**3a**) (203 MHz, $C_6D_6$, 298 K).

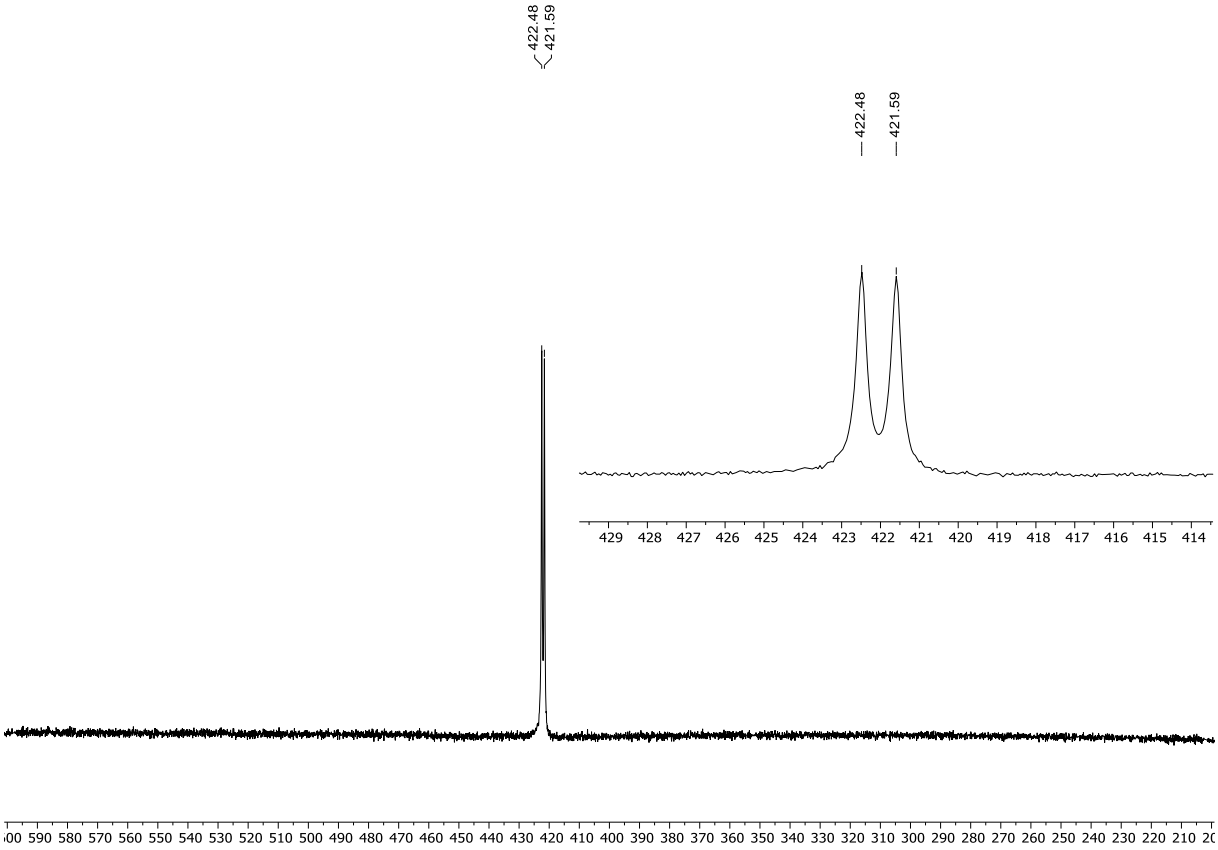


**Figure S19**. $^{119}Sn\{^{1}H\}$ NMR spectrum of $^{Mes}TerSnCH_2P(CH_3)_2NDipp$ (**3a**) (187 MHz, $C_6D_6$, 298 K).

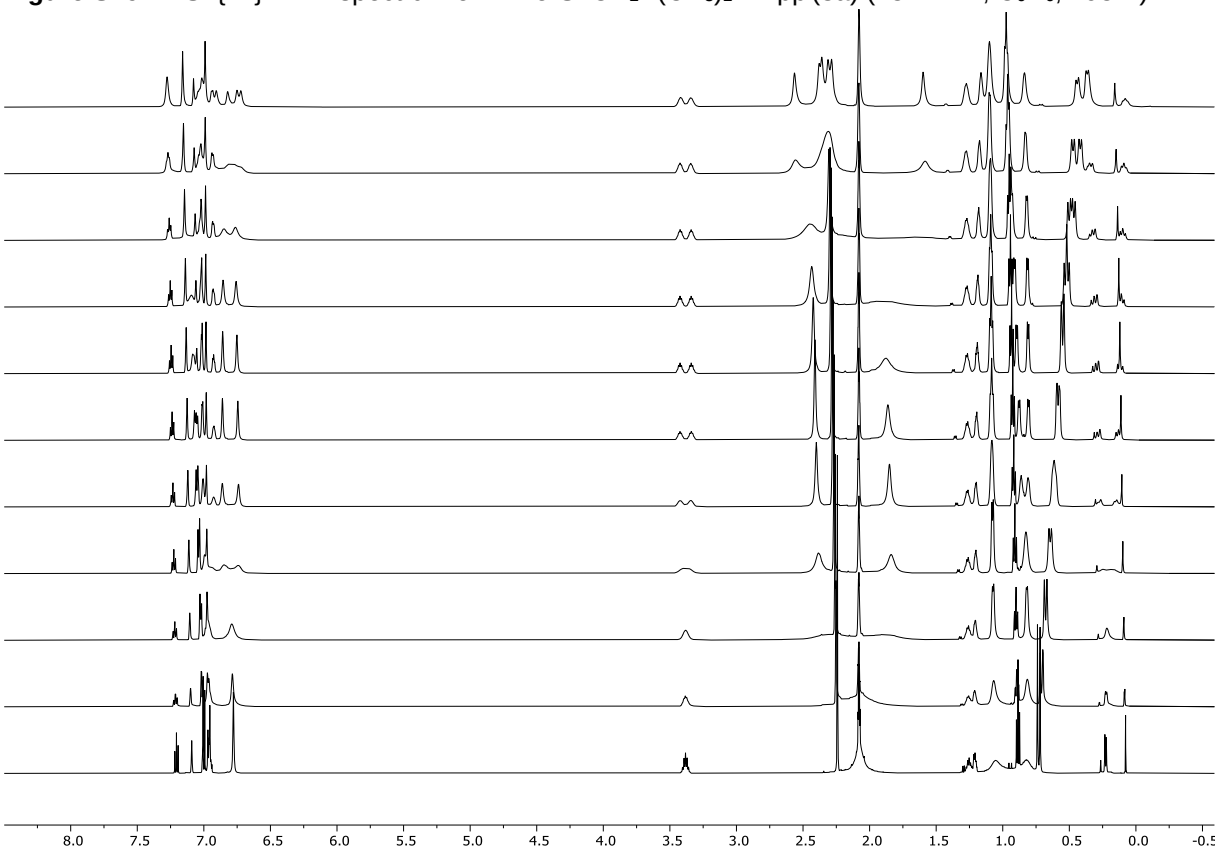


**Figure S20**. VT $^{1}H$ NMR spectrum of $^{Mes}TerSnCH_2P(CH_3)_2NDipp$ (**3a**) from 193 K (top) to 293 K (bottom) in steps of 10 K (600 MHz, $C_7D_8$); 0.88, 1.22 ppm: *n*-hexane, 0.10 ppm: $HN(SiMe_3)_2$.

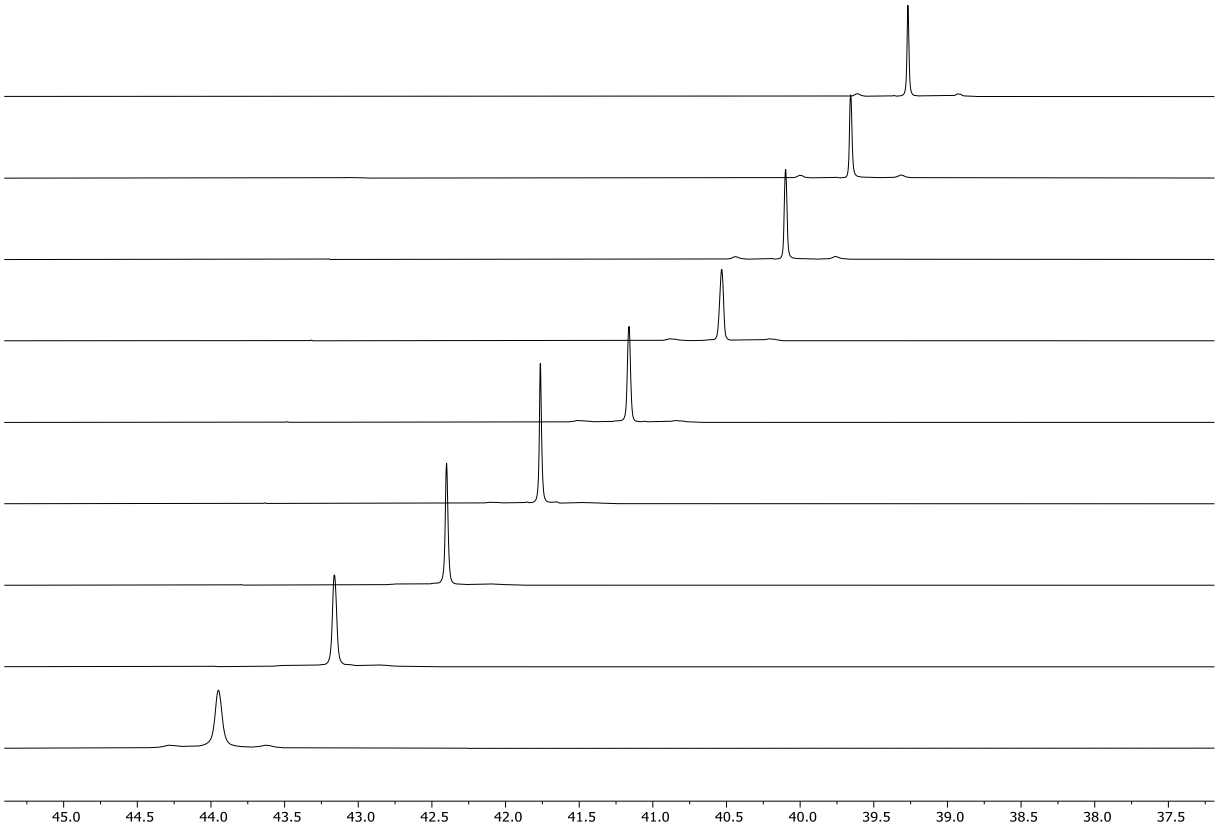


**Figure S21**. VT $^{31}P\{^{1}H\}$ NMR spectrum of $^{Mes}TerSnCH_2P(CH_3)_2NDipp$ (**3a**) from 193 K (bottom) to 353 K (top) in steps of 20 K (203 MHz, $C_7D_8$).

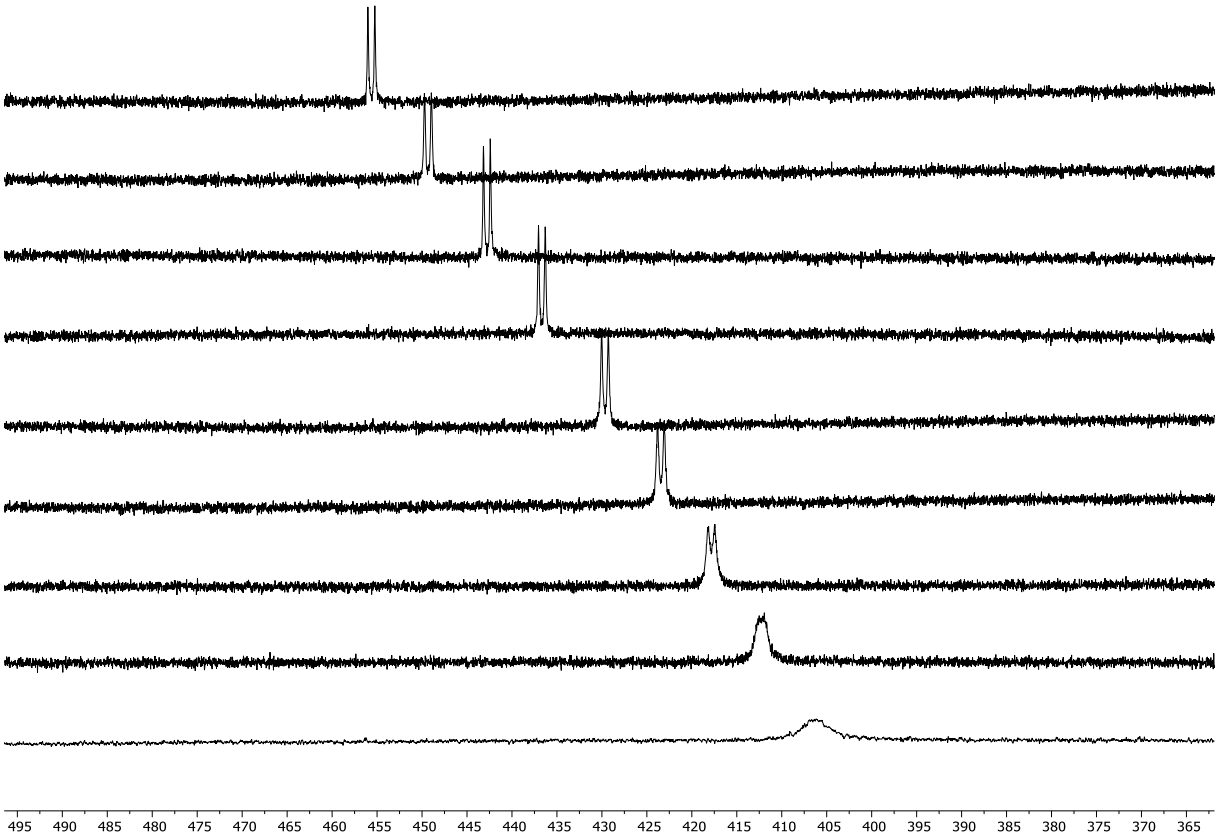


**Figure S22**. VT $^{119}Sn\{^{1}H\}$ NMR spectrum of $^{Mes}TerSnCH_2P(CH_3)_2NDipp$ (**3a**) from 193 K (bottom) to 353 K (top) in steps of 20 K (187 MHz, $C_7D_8$).

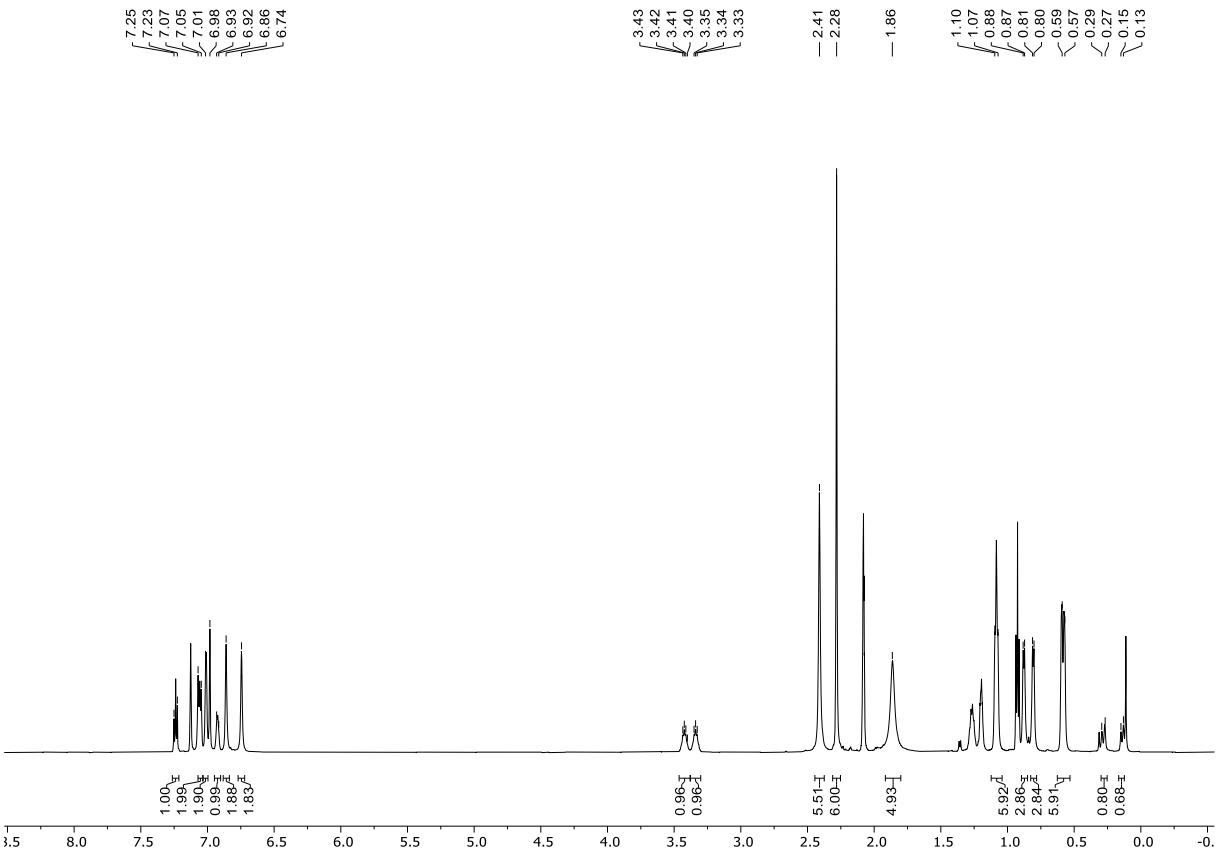


**Figure S23**. $^{1}H$ NMR spectrum of $^{Mes}TerSnCH_2P(CH_3)_2NDipp$ (**3a**) (600 MHz, $C_7D_8$, 243 K); 0.88, 1.22 ppm: *n*-hexane, 0.10 ppm: $HN(SiMe_3)_2$.

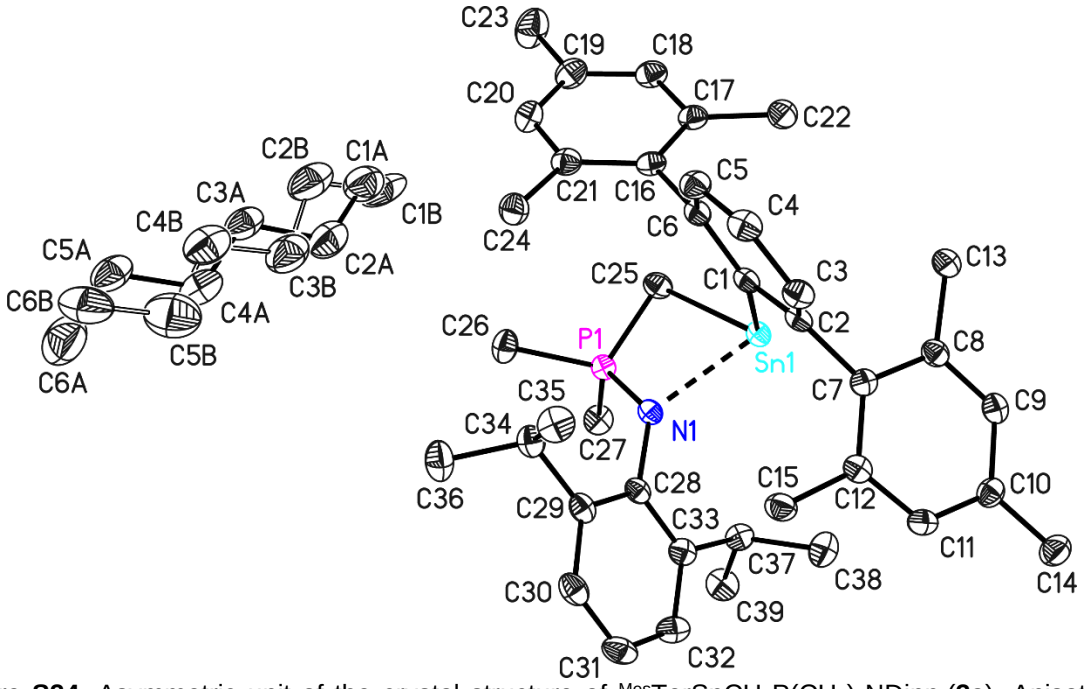


**Figure S24**. Asymmetric unit of the crystal structure of $^{Mes}$TerSnCH$_2$P(CH$_3$)$_2$NDipp (**3a**). Anisotropic displacement parameters are drawn at the 50% probability level. Hydrogen atoms have been omitted for clarity. Selected bond lengths (Å) and angles (deg): Sn1–C1 2.2527(16), Sn1•••N1 2.2877(14), P1–N1 1.6143(13), Sn1–C25 2.3220(17), P1–C25 1.7503(17), P1–C26 1.8001(17), P1–C27 1.8050(17), N1–C28 1.426(2), C1–Sn1–C25 106.05(6), P1–C25–Sn1 91.90(7), C25–P1–N1 100.92(7), P1–N1–C28 127.42(11).

The data were collected on a split crystal. The integration was performed with two orientation matrices. The data were detwinned using a fractional contribution of the minor domain of 0.4159. The asymmetric unit contains one molecule of hexane disordered over two positions. The disorder was treated with distance restraints and restraints for the anisotropic displacement parameters. The occupancy of the minor component refined to 0.206(5). Two methyl groups (C15 and C23) showed rotational disorder over two positions. Occupations of the minor components refined to 0.48(2) and 0.45(3), respectively.

**Table S3**. Bond lengths [Å] and angles [°] for **3a**.

| | | | |
|---|---|---|---|
| Sn(1)-C(1) | 2.2527(16) | C(3)-C(4) | 1.383(2) |
| Sn(1)-N(1) | 2.2876(14) | C(4)-C(5) | 1.383(2) |
| Sn(1)-C(25) | 2.3220(17) | C(5)-C(6) | 1.400(2) |
| Sn(1)-P(1) | 2.9537(8) | C(6)-C(16) | 1.501(2) |
| P(1)-N(1) | 1.6143(13) | C(7)-C(12) | 1.406(2) |
| P(1)-C(25) | 1.7503(17) | C(7)-C(8) | 1.410(2) |
| P(1)-C(26) | 1.8001(17) | C(8)-C(9) | 1.389(2) |
| P(1)-C(27) | 1.8050(17) | C(8)-C(13) | 1.507(2) |
| N(1)-C(28) | 1.426(2) | C(9)-C(10) | 1.390(2) |
| C(1)-C(6) | 1.412(2) | C(10)-C(11) | 1.387(2) |
| C(1)-C(2) | 1.413(2) | C(10)-C(14) | 1.508(2) |
| C(2)-C(3) | 1.398(2) | C(11)-C(12) | 1.395(2) |
| C(2)-C(7) | 1.506(2) | C(12)-C(15) | 1.506(2) |

| | | | |
|---|---|---|---|
| C(16)-C(21) | 1.406(2) | N(1)-P(1)-C(25) | 100.92(7) |
| C(16)-C(17) | 1.407(2) | N(1)-P(1)-C(26) | 115.94(8) |
| C(17)-C(18) | 1.392(2) | C(25)-P(1)-C(26) | 112.17(9) |
| C(17)-C(22) | 1.511(2) | N(1)-P(1)-C(27) | 113.00(8) |
| C(18)-C(19) | 1.388(3) | C(25)-P(1)-C(27) | 112.69(8) |
| C(19)-C(20) | 1.389(2) | C(26)-P(1)-C(27) | 102.58(9) |
| C(19)-C(23) | 1.512(2) | N(1)-P(1)-Sn(1) | 50.26(5) |
| C(20)-C(21) | 1.392(2) | C(25)-P(1)-Sn(1) | 51.79(6) |
| C(21)-C(24) | 1.512(2) | C(26)-P(1)-Sn(1) | 138.65(6) |
| C(28)-C(33) | 1.414(2) | C(27)-P(1)-Sn(1) | 118.74(6) |
| C(28)-C(29) | 1.415(2) | C(28)-N(1)-P(1) | 127.42(11) |
| C(29)-C(30) | 1.395(2) | C(28)-N(1)-Sn(1) | 132.24(10) |
| C(29)-C(34) | 1.517(2) | P(1)-N(1)-Sn(1) | 96.88(6) |
| C(30)-C(31) | 1.379(3) | C(6)-C(1)-C(2) | 117.39(14) |
| C(31)-C(32) | 1.386(2) | C(6)-C(1)-Sn(1) | 129.55(11) |
| C(32)-C(33) | 1.394(2) | C(2)-C(1)-Sn(1) | 113.05(11) |
| C(33)-C(37) | 1.519(2) | C(3)-C(2)-C(1) | 120.95(14) |
| C(34)-C(36) | 1.531(2) | C(3)-C(2)-C(7) | 116.85(14) |
| C(34)-C(35) | 1.533(2) | C(1)-C(2)-C(7) | 121.94(13) |
| C(37)-C(39) | 1.528(2) | C(4)-C(3)-C(2) | 120.70(15) |
| C(37)-C(38) | 1.530(2) | C(3)-C(4)-C(5) | 119.23(15) |
| C(1A)-C(2A) | 1.511(6) | C(4)-C(5)-C(6) | 121.16(15) |
| C(2A)-C(3A) | 1.501(4) | C(5)-C(6)-C(1) | 120.46(15) |
| C(3A)-C(4A) | 1.527(5) | C(5)-C(6)-C(16) | 117.04(14) |
| C(4A)-C(5A) | 1.509(4) | C(1)-C(6)-C(16) | 122.36(14) |
| C(5A)-C(6A) | 1.504(5) | C(12)-C(7)-C(8) | 119.13(14) |
| C(1B)-C(2B) | 1.504(13) | C(12)-C(7)-C(2) | 122.33(14) |
| C(2B)-C(3B) | 1.516(13) | C(8)-C(7)-C(2) | 118.32(14) |
| C(3B)-C(4B) | 1.513(14) | C(9)-C(8)-C(7) | 119.53(14) |
| C(4B)-C(5B) | 1.478(13) | C(9)-C(8)-C(13) | 119.10(14) |
| C(5B)-C(6B) | 1.513(15) | C(7)-C(8)-C(13) | 121.37(14) |
| | | C(8)-C(9)-C(10) | 121.92(15) |
| C(1)-Sn(1)-N(1) | 95.43(5) | C(11)-C(10)-C(9) | 117.98(15) |
| C(1)-Sn(1)-C(25) | 106.05(6) | C(11)-C(10)-C(14) | 121.18(15) |
| N(1)-Sn(1)-C(25) | 68.55(5) | C(9)-C(10)-C(14) | 120.83(15) |
| C(1)-Sn(1)-P(1) | 107.55(4) | C(10)-C(11)-C(12) | 122.08(15) |
| N(1)-Sn(1)-P(1) | 32.86(3) | C(11)-C(12)-C(7) | 119.28(14) |
| C(25)-Sn(1)-P(1) | 36.32(4) | C(11)-C(12)-C(15) | 118.70(14) |

| | | | |
|---|---|---|---|
| C(7)-C(12)-C(15) | 122.02(14) | C(28)-C(29)-C(34) | 122.12(14) |
| C(21)-C(16)-C(17) | 119.02(15) | C(31)-C(30)-C(29) | 121.45(15) |
| C(21)-C(16)-C(6) | 120.99(14) | C(30)-C(31)-C(32) | 119.38(16) |
| C(17)-C(16)-C(6) | 119.91(14) | C(31)-C(32)-C(33) | 121.61(16) |
| C(18)-C(17)-C(16) | 119.33(15) | C(32)-C(33)-C(28) | 118.78(15) |
| C(18)-C(17)-C(22) | 118.73(15) | C(32)-C(33)-C(37) | 118.34(15) |
| C(16)-C(17)-C(22) | 121.93(15) | C(28)-C(33)-C(37) | 122.88(14) |
| C(19)-C(18)-C(17) | 122.20(16) | C(29)-C(34)-C(36) | 111.65(14) |
| C(18)-C(19)-C(20) | 117.90(16) | C(29)-C(34)-C(35) | 111.47(14) |
| C(18)-C(19)-C(23) | 120.69(17) | C(36)-C(34)-C(35) | 110.37(14) |
| C(20)-C(19)-C(23) | 121.39(17) | C(33)-C(37)-C(39) | 112.09(14) |
| C(19)-C(20)-C(21) | 121.70(16) | C(33)-C(37)-C(38) | 111.69(14) |
| C(20)-C(21)-C(16) | 119.81(15) | C(39)-C(37)-C(38) | 110.47(14) |
| C(20)-C(21)-C(24) | 118.77(15) | C(3A)-C(2A)-C(1A) | 113.4(3) |
| C(16)-C(21)-C(24) | 121.41(15) | C(2A)-C(3A)-C(4A) | 114.0(3) |
| P(1)-C(25)-Sn(1) | 91.90(7) | C(5A)-C(4A)-C(3A) | 113.4(3) |
| C(33)-C(28)-C(29) | 119.77(14) | C(6A)-C(5A)-C(4A) | 113.7(3) |
| C(33)-C(28)-N(1) | 119.87(14) | C(1B)-C(2B)-C(3B) | 112.6(12) |
| C(29)-C(28)-N(1) | 120.22(14) | C(4B)-C(3B)-C(2B) | 110.5(12) |
| C(30)-C(29)-C(28) | 119.02(15) | C(5B)-C(4B)-C(3B) | 116.7(12) |
| C(30)-C(29)-C(34) | 118.84(14) | C(4B)-C(5B)-C(6B) | 114.7(14) |

**UV-vis spectrum and extinction coefficient of 3a**

The UV-vis spectrum of **3a** was recorded in benzene. The UV-vis cuvette was filled in the glovebox and sealed with a PTFE cap. Saturation below 350 nm was reached even at low concentrations. Therefore, we focused on characteristic absorptions in the visible region and observed a maximum at 387 nm (Figure S25).

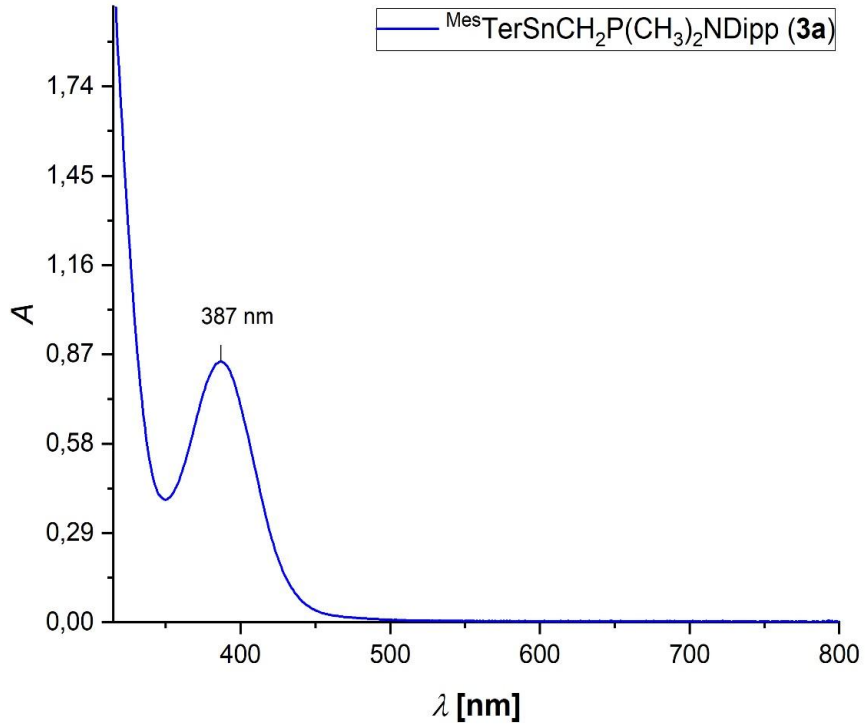


**Figure S25**. UV-vis spectrum of **3a** (c = 0.33 mg/mL) in benzene at room temperature with $\varepsilon = 17 \cdot 10^2$ $L \cdot mol^{-1} \cdot cm^{-1}$ at $\lambda_{max} = 387$ nm.

**Reaction of $^{Mes}$TerSn{N(Si(CH$_3$)$_3$)$_2$} (1) and XylNP(CH$_3$)$_3$ (2b) – Synthesis of $^{Mes}$TerSnCH$_2$P(CH$_3$)$_2$NXyl (3b)**

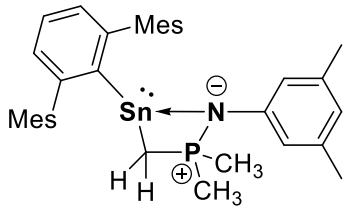


XylNP(CH$_3$)$_3$ (**2b**) (0.013 g, 0.068 mmol) in 0.2 mL of $C_6D_6$ was added to a solution of $^{Mes}$TerSn{N(Si(CH$_3$)$_3$)$_2$} (**1**) (0.040 g, 0.068 mmol) in 0.3 mL of $C_6D_6$. The reaction progress was monitored by $^1$H and $^{31}$P{$^1$H} NMR spectroscopy, revealing the clean formation of $^{Mes}$TerSnCH$_2$P(CH$_3$)$_2$NXyl (**3b**) over the course of a couple of hours. All volatile components were removed under vacuum. The remaining solid was dissolved in 0.5 mL of *n*-hexane, filtered, and stored at -30 °C to give **3b** as a slightly orange microcrystalline solid.

**Yield**: 0.031 g (0.049 mmol; 74%).
**$^1$H NMR** (500 MHz, $C_7D_8$, 298 K): $\delta$ = 0.39 (dd, $^2J_{H,H}$ = 12.7 Hz, $^2J_{P,H}$ = 4.7 Hz, 1H, CH$_2$), 0.47 (dd, $^2J_{H,H}$ = 12.7 Hz, $^2J_{P,H}$ = 6.2 Hz, 1H, CH$_2$), 0.63 (d, $^2J_{P,H}$ = 12.0 Hz, 3H, P(CH$_3$)$_2$), 1.00 (d, $^2J_{P,H}$ = 12.5 Hz, 3H, P(CH$_3$)$_2$), 2.14 (s, 6H, CH$_{3,Xyl}$), 2.15 (s, 6H, CH$_3$), 2.32 (s, 6H, CH$_3$), 2.42 (s, 6H, CH$_3$), 5.99 (s, 2H, *o*-CH$_{Aryl}$N), 6.38 (s, 1H, *p*-CH$_{Aryl}$N), 6.56 (s, 2H, CH$_{Aryl}$), 6.86 (s, 2H, CH$_{Aryl}$), 7.04-7.06 (m, 2H, CH$_{Aryl}$), 7.29-7.31 (m, 1H, CH$_{Aryl}$) ppm.
**$^{13}$C{$^1$H} NMR** (126 MHz, $C_6D_6$, 298 K): $\delta$ = 3.7 (d, $^1J_{P,C}$ = 74.4 Hz, CH$_2$), 15.4 (d, $^1J_{P,C}$ = 47.8 Hz, P(CH$_3$)$_2$), 21.3 (CH$_3$), 21.6 (CH$_{3,Xyl}$), 21.7 (d, $^1J_{P,C}$ = 50.9 Hz, P(CH$_3$)$_2$), 22.0 (CH$_3$), 22.1 (CH$_3$), 119.2 (d, $^{TS}J_{P,C}$ = 12.3 Hz, *o*-CH$_{Aryl}$N), 121.7 (*p*-CH$_{Aryl}$N), 127.2 (CH$_{Aryl}$), 128.4 (CH$_{Aryl}$), 128.5 (CH$_{Aryl}$), 129.1 (CH$_{Aryl}$), 135.2 (C$_{q,Aryl}$), 135.8 (C$_{q,Aryl}$), 135.9 (C$_{q,Aryl}$), 137.4 (*m*-C$_{q,Aryl}$N), 141.3 (C$_{q,Aryl}$), 146.7 (d, $^2J_{P,C}$ = 4.8 Hz, NC$_{q,Aryl}$), 148.5 (C$_{q,Aryl}$), 169.2 (C$_{q,Aryl}$Sn) ppm.
**$^1$H/$^{15}$N HMBC NMR** (51 MHz, $C_6D_6$, 298 K): $\delta$ = -318.7 ppm.
**$^{31}$P{$^1$H} NMR** (203 MHz, $C_6D_6$, 298 K): $\delta$ = 42.1 (Sn satellites: $J_{119/117Sn,P}$ = 142.3 Hz (average value)) ppm.
**$^{31}$P NMR** (203 MHz, $C_6D_6$, 298 K): $\delta$ = 42.1 (m) ppm.
**$^{119}$Sn{$^1$H} NMR** (187 MHz, $C_6D_6$, 298 K): $\delta$ = 217.6 (d, $^2J_{119Sn,P}$ = 145.7 Hz) ppm.
**EA**: Anal. calcd. for $C_{35}H_{42}NPSn$•0.5 $C_6H_{14}$: C, 67.11; H, 6.76; N, 2.24; Found: C, 66.45; H, 6.34; N, 2.11.

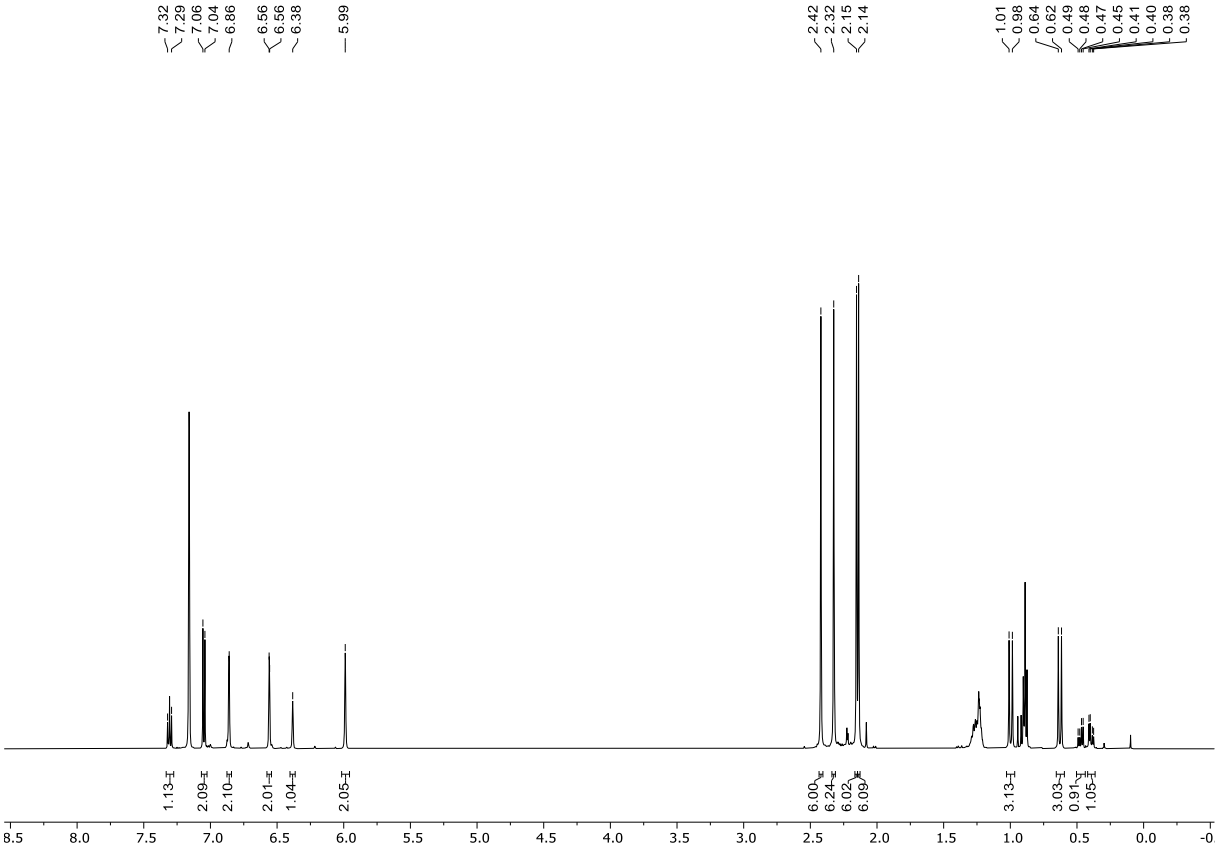


**Figure S26**. $^{1}H$ NMR spectrum of $^{Mes}TerSnCH_2P(CH_3)_2NXyl$ (**3b**) (500 MHz, $C_6D_6$, 298 K); 0.89, 1.24 ppm: *n*-hexane.

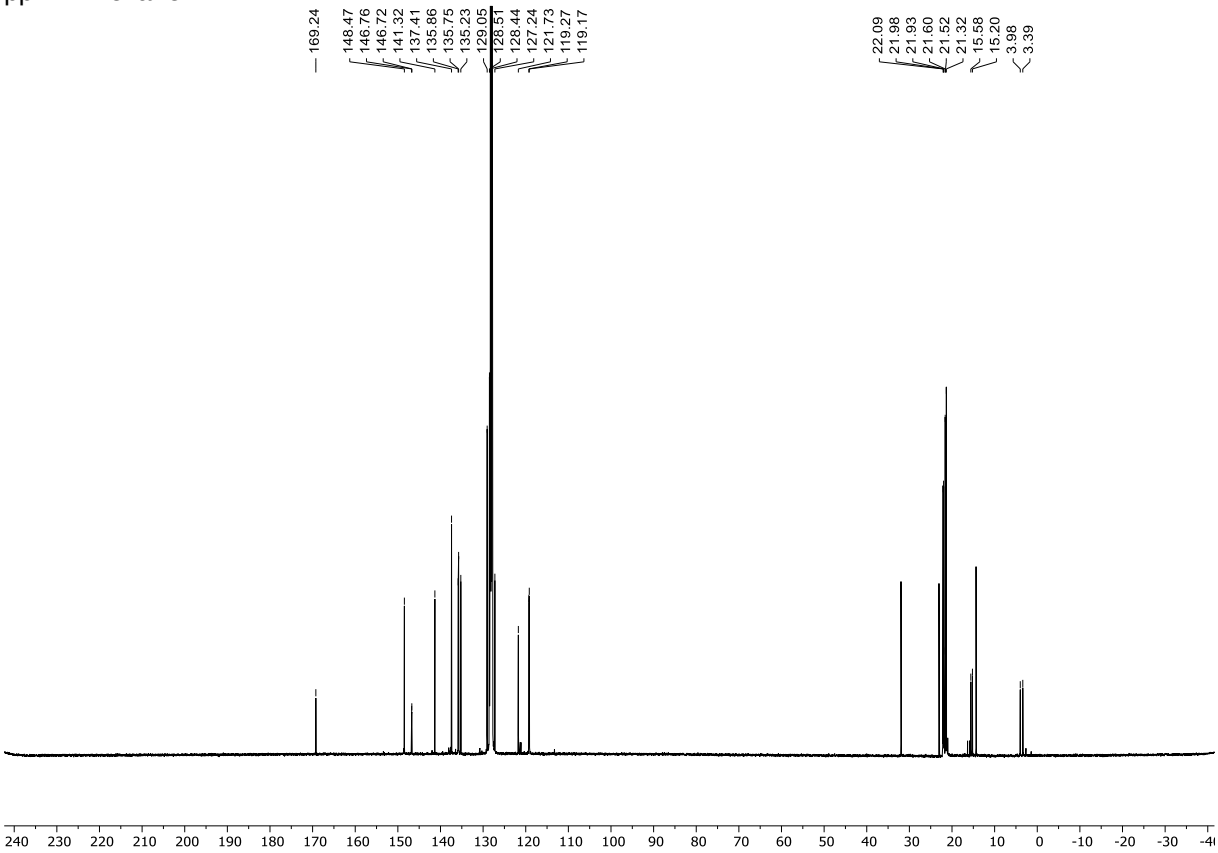


**Figure S27**. $^{13}C\{^{1}H\}$ NMR spectrum of $^{Mes}TerSnCH_2P(CH_3)_2NXyl$ (**3b**) (126 MHz, $C_6D_6$, 298 K); 14.3, 23.0, 32.0 ppm: *n*-hexane.

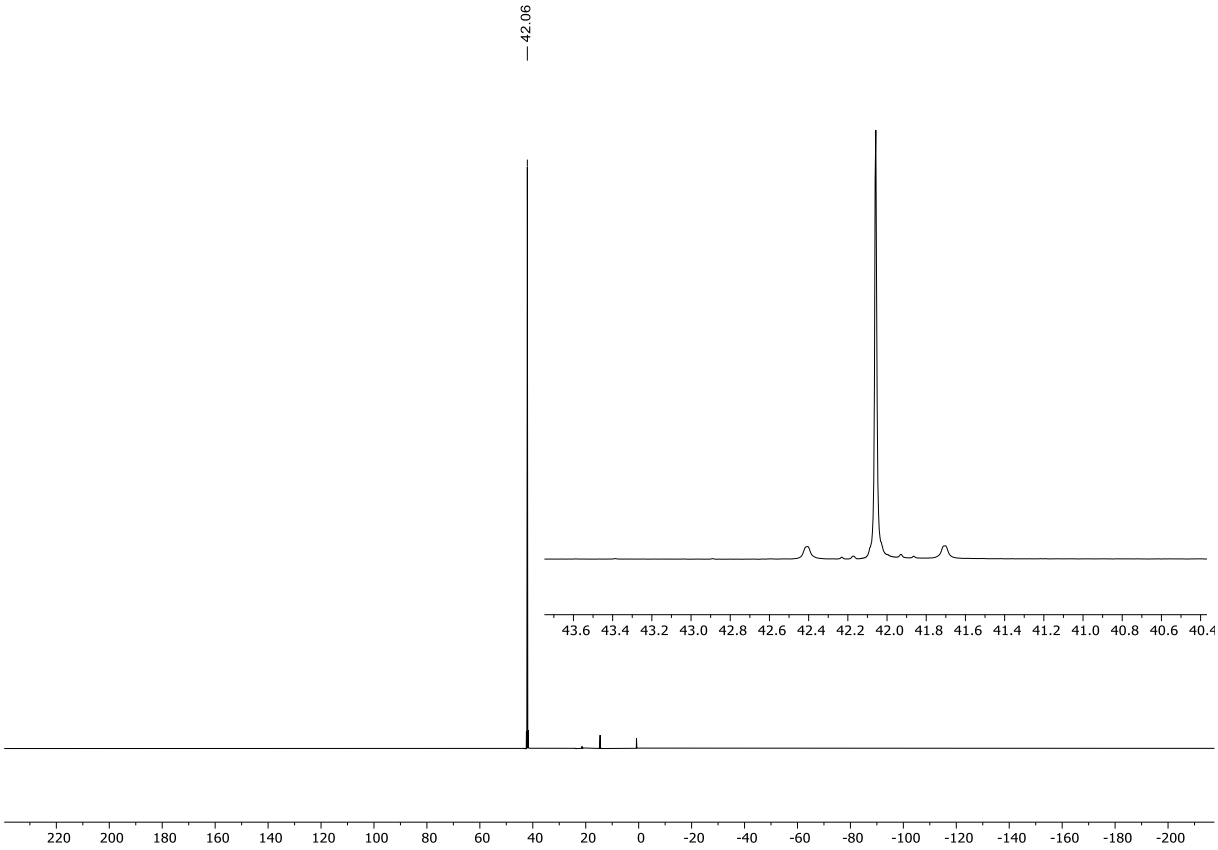


**Figure S28**. $^{31}P\{^{1}H\}$ NMR spectrum of $^{Mes}TerSnCH_2P(CH_3)_2NXyl$ (**3b**) (203 MHz, $C_6D_6$, 298 K).

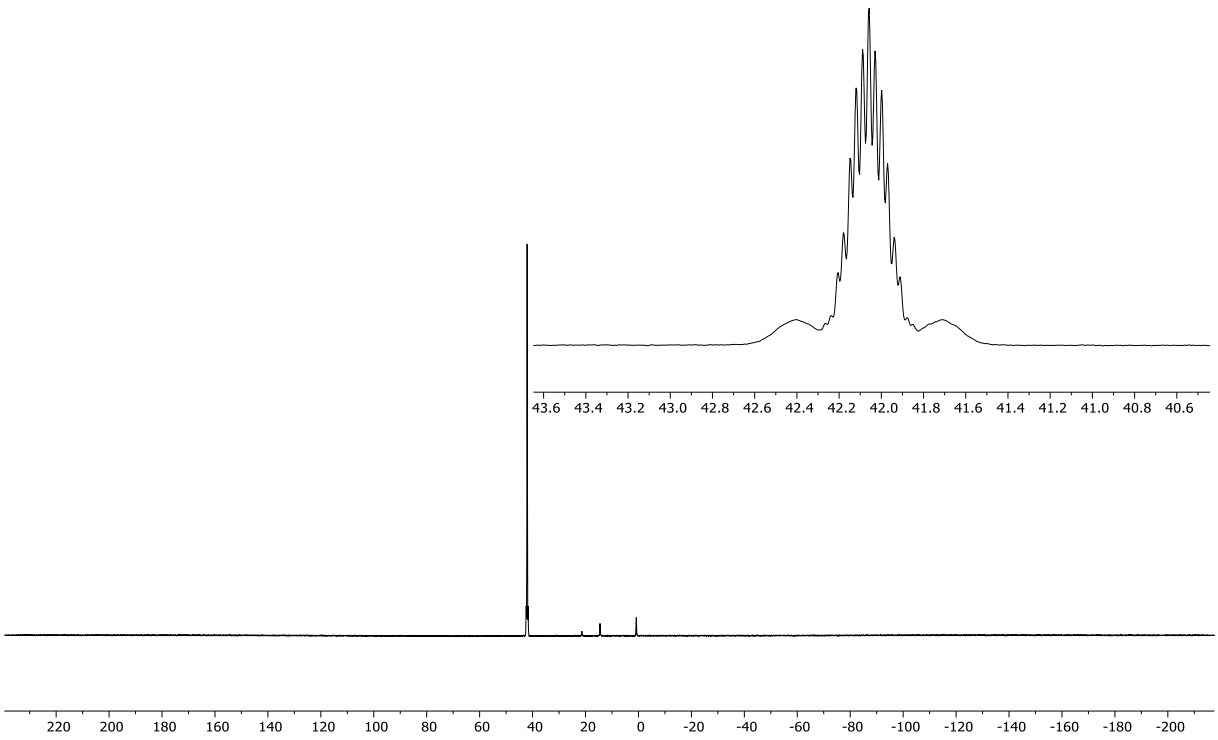


**Figure S29**. $^{31}P$ NMR spectrum of $^{Mes}TerSnCH_2P(CH_3)_2NXyl$ (**3b**) (203 MHz, $C_6D_6$, 298 K).

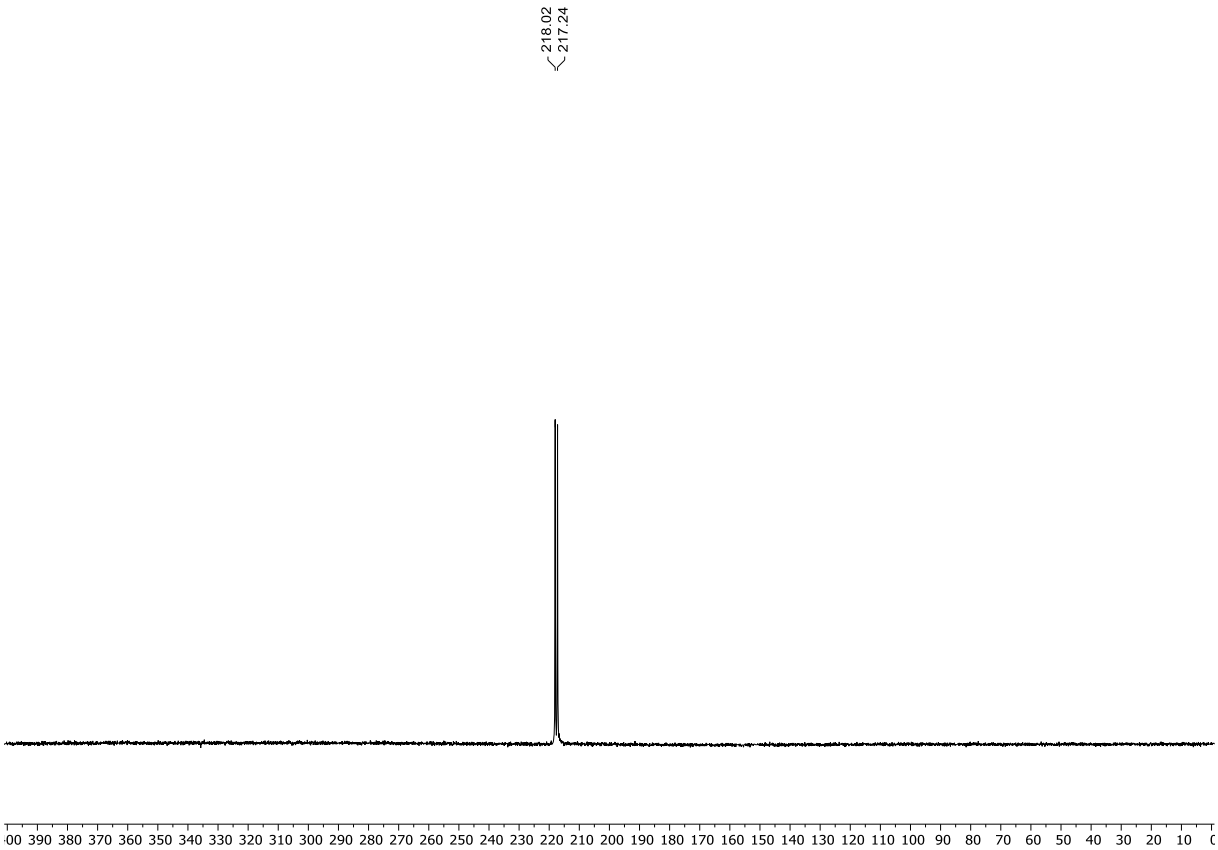


**Figure S30**. $^{119}Sn\{^{1}H\}$ NMR spectrum of $^{Mes}TerSnCH_2P(CH_3)_2NXyl$ (**3b**) (187 MHz, $C_6D_6$, 298 K).

**Reaction of $^{Mes}$TerSn{N(Si(CH$_3$)$_3$)$_2$} (1) and AdNP(CH$_3$)$_3$ (2c) – Synthesis of $^{Mes}$TerSnCH$_2$P(CH$_3$)$_2$NAd (3c)**

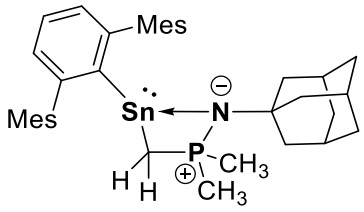


AdNP(CH$_3$)$_3$ (**2c**) (0.015 g, 0.068 mmol) in 0.2 mL of $C_6D_6$ was added to a solution of $^{Mes}$TerSn{N(Si(CH$_3$)$_3$)$_2$} (**1**) (0.040 g, 0.068 mmol) in 0.3 mL of $C_6D_6$. The reaction progress was monitored by $^1$H and $^{31}$P{$^1$H} NMR spectroscopy, revealing the clean formation of $^{Mes}$TerSnCH$_2$P(CH$_3$)$_2$NAd (**3c**) over the course of a couple of hours. All volatile components were removed under vacuum, the colourless solid was dissolved in 0.5 mL of *n*-hexane, filtered, and stored at -30 °C to give **3c** as a colourless crystalline material. Crystals obtained through this method were suitable for single crystal X-ray diffraction.

**Yield**: 0.028 g (0.043 mmol; 63%).
**$^1$H NMR** (400 MHz, $C_6D_6$, 298 K): $\delta$ = 0.39 (dd, *J* = 12.3 Hz, *J* = 4.3 Hz, 1H, PCH$_2$), 0.62 (dd, *J* = 12.3 Hz, *J* = 6.4 Hz, 1H, PCH$_2$), 0.74 (d, $^2J_{P,H}$ = 11.8 Hz, 3H, P(CH$_3$)$_2$), 0.86-0.88 (m, 3H, CH$_{2,Ad}$), 0.89 (d, $^2J_{P,H}$ = 12.4 Hz, 3H, P(CH$_3$)$_2$), 1.21-1.25 (m, 3H, CH$_{2,Ad}$), 1.43-1.51 (m, 6H, CH$_{2,Ad}$), 1.81-1.84 (m, 3H, CH$_{Ad}$), 2.25 (s, 6H, CH$_3$), 2.39 (s, 6H, CH$_3$), 2.41 (s, 6H, CH$_3$), 6.89 (s, 4H, CH$_{Ary}$), 6.99-7.01 (m, 2H, CH$_{Aryl}$), 7.28-7.31 (m, 1H, CH$_{Aryl}$) ppm.
**$^{13}$C{$^1$H} NMR** (126 MHz, $C_6D_6$, 298 K): $\delta$ = 6.9 (d, $^1J_{P,C}$ = 76.2 Hz, PCH$_2$), 21.3 (CH$_3$), 22.16 (CH$_3$), 22.22 (CH$_3$), 23.2 (d, $^1J_{P,C}$ = 41.2 Hz, P(CH$_3$)$_2$), 24.0 (d, $^1J_{P,C}$ = 50.0 Hz, P(CH$_3$)$_2$), 30.4 (CH$_{Ad}$), 36.4 (CH$_{2,Ad}$), 45.8 (d, $^3J_{P,C}$ = 8.2 Hz, CH$_{2,Ad}$), 50.7 (d, $^2J_{P,C}$ = 5.9 Hz, NC$_q$) 126.9 (CH$_{Aryl}$), 128.8 (CH$_{Aryl}$), 128.9 (CH$_{Aryl}$), 135.8 (C$_{q,Aryl}$), 136.5 (C$_{q,Aryl}$), 136.7 (C$_{q,Aryl}$), 142.4 (C$_{q,Aryl}$), 148.4 (C$_{q,Aryl}$), 171.6 (C$_{q,Aryl}$Sn) ppm.
**$^1$H/$^{15}$N HMBC NMR** (51 MHz, $C_6D_6$, 298 K): $\delta$ = -308.8 ppm.
**$^{31}$P{$^1$H} NMR** (203 MHz, $C_6D_6$, 298 K): $\delta$ = 33.8 (Sn satellites: $J_{119/117Sn,P}$ = 137.6 Hz (average value)) ppm.
**$^{31}$P NMR** (203 MHz, $C_6D_6$, 298 K): $\delta$ = 33.8 (m) ppm.
**$^{119}$Sn{$^1$H} NMR** (187 MHz, $C_6D_6$, 298 K): $\delta$ = 213.3 (d, $^2J_{119Sn,P}$ = 138.6 Hz) ppm.
**EA**: Anal. calcd. for $C_{37}H_{48}NPSn$: C, 67.70; H, 7.37; N, 2.13; Found: C, 67.35; H, 7.33; N, 2.14.

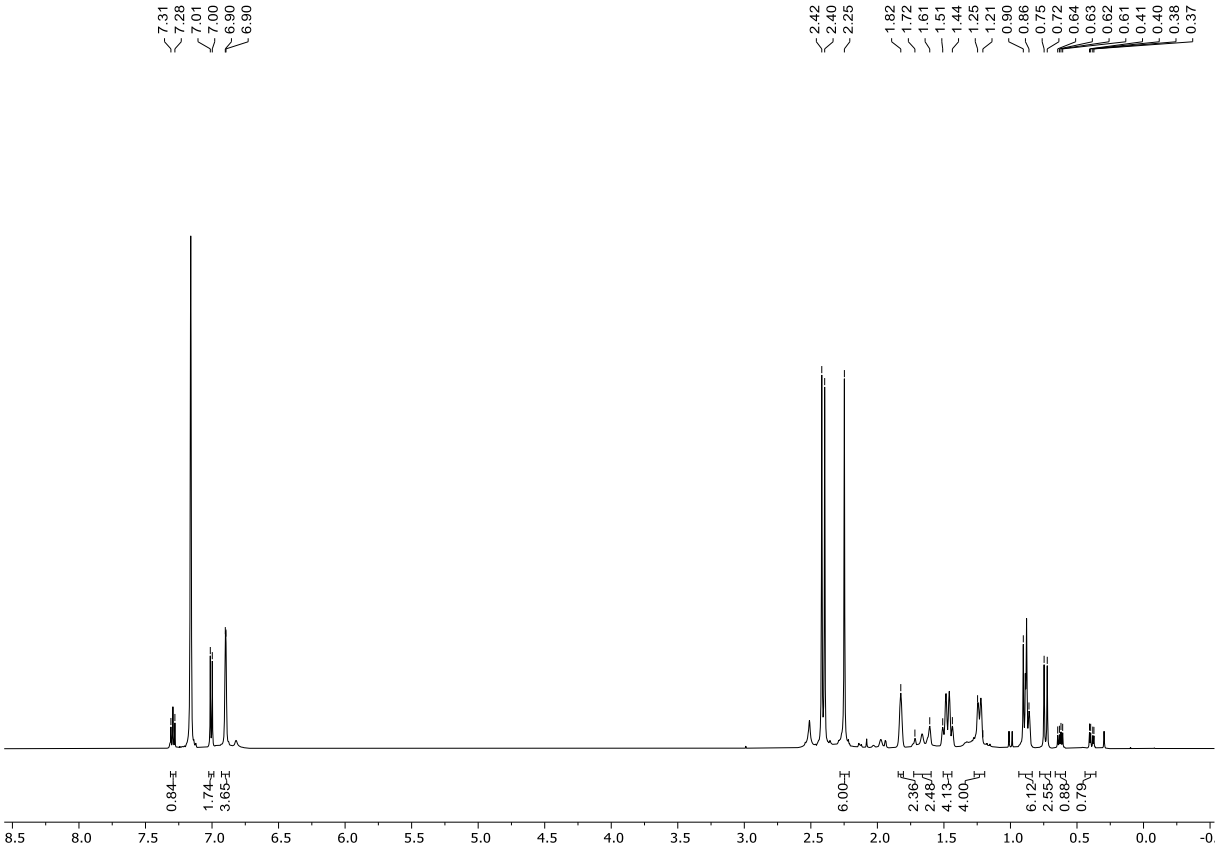


**Figure S31**. $^{1}H$ NMR spectrum of $^{Mes}TerSnCH_2P(CH_3)_2NAd$ (**3c**) (400 MHz, $C_6D_6$, 298 K); 0.89, 1.24 ppm: *n*-hexane.

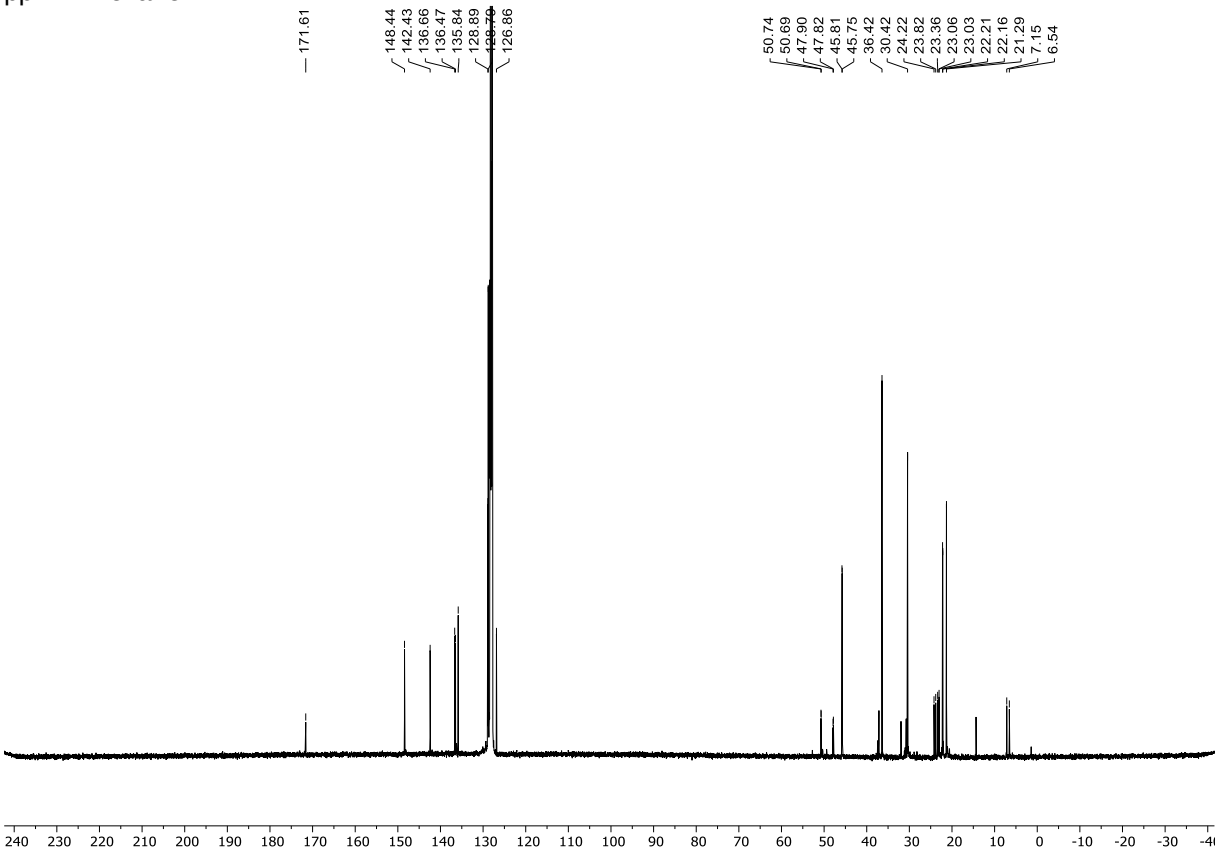


**Figure S32**. $^{13}C\{^{1}H\}$ NMR spectrum of $^{Mes}TerSnCH_2P(CH_3)_2NAd$ (**3c**) (126 MHz, $C_6D_6$, 298 K); 14.3, 23.0, 32.0 ppm: *n*-hexane.

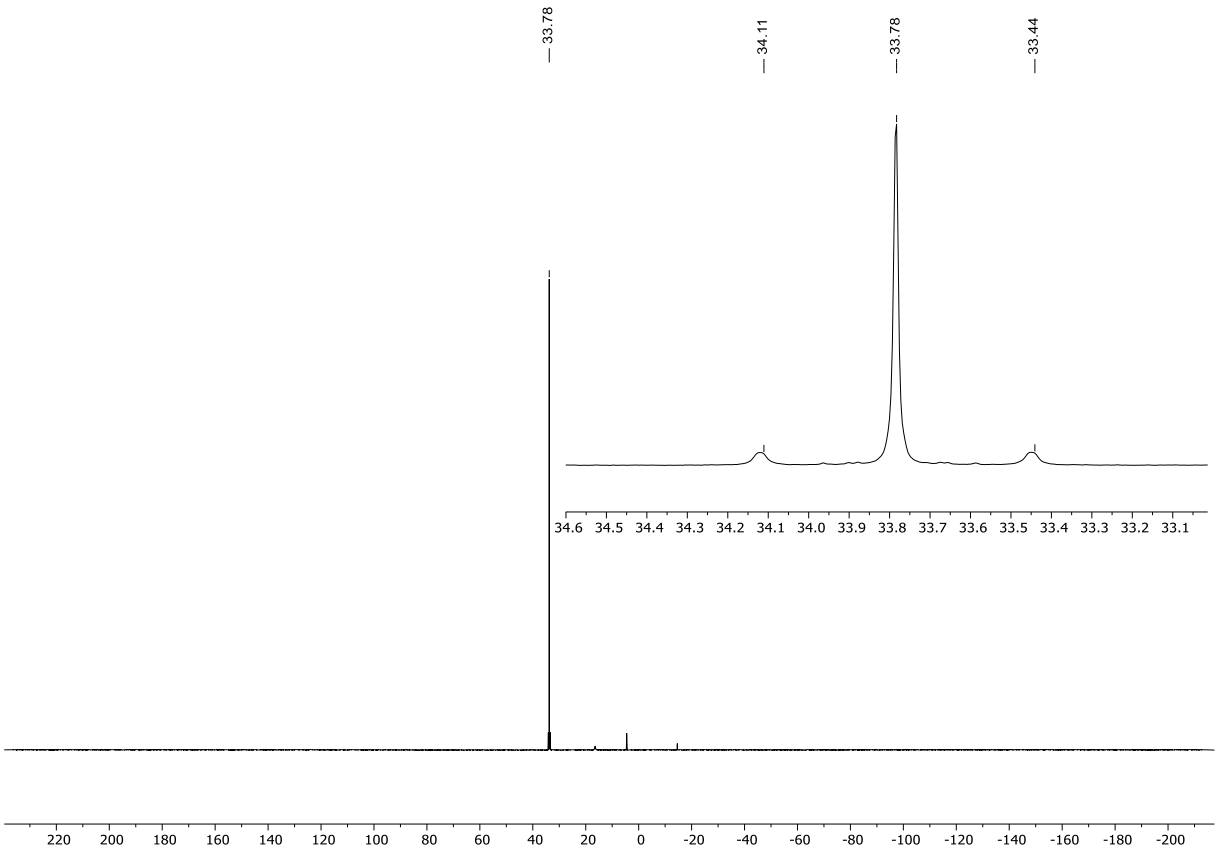


**Figure S33**. $^{31}P\{^{1}H\}$ NMR spectrum of $^{Mes}TerSnCH_2P(CH_3)_2NAd$ (**3c**) (203 MHz, $C_6D_6$, 298 K).

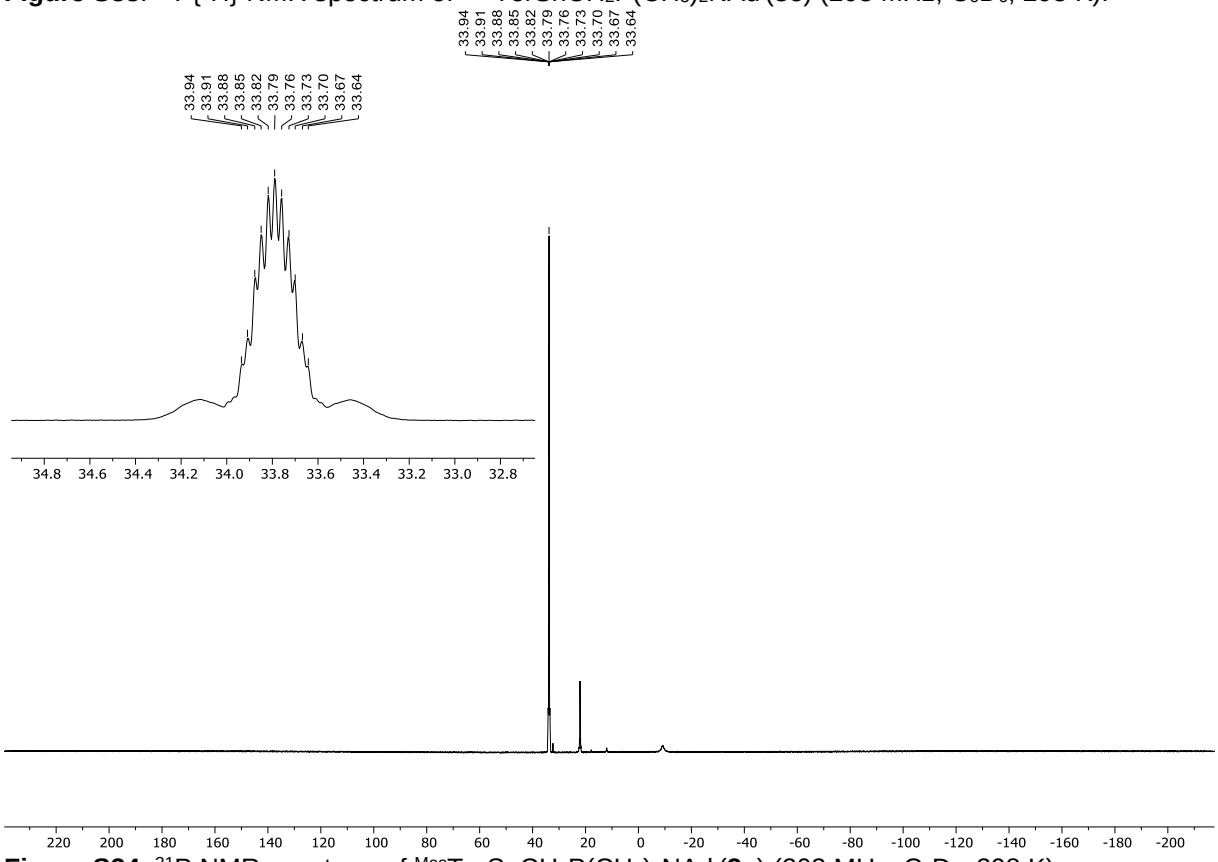


**Figure S34**. $^{31}P$ NMR spectrum of $^{Mes}TerSnCH_2P(CH_3)_2NAd$ (**3c**) (203 MHz, $C_6D_6$, 298 K).

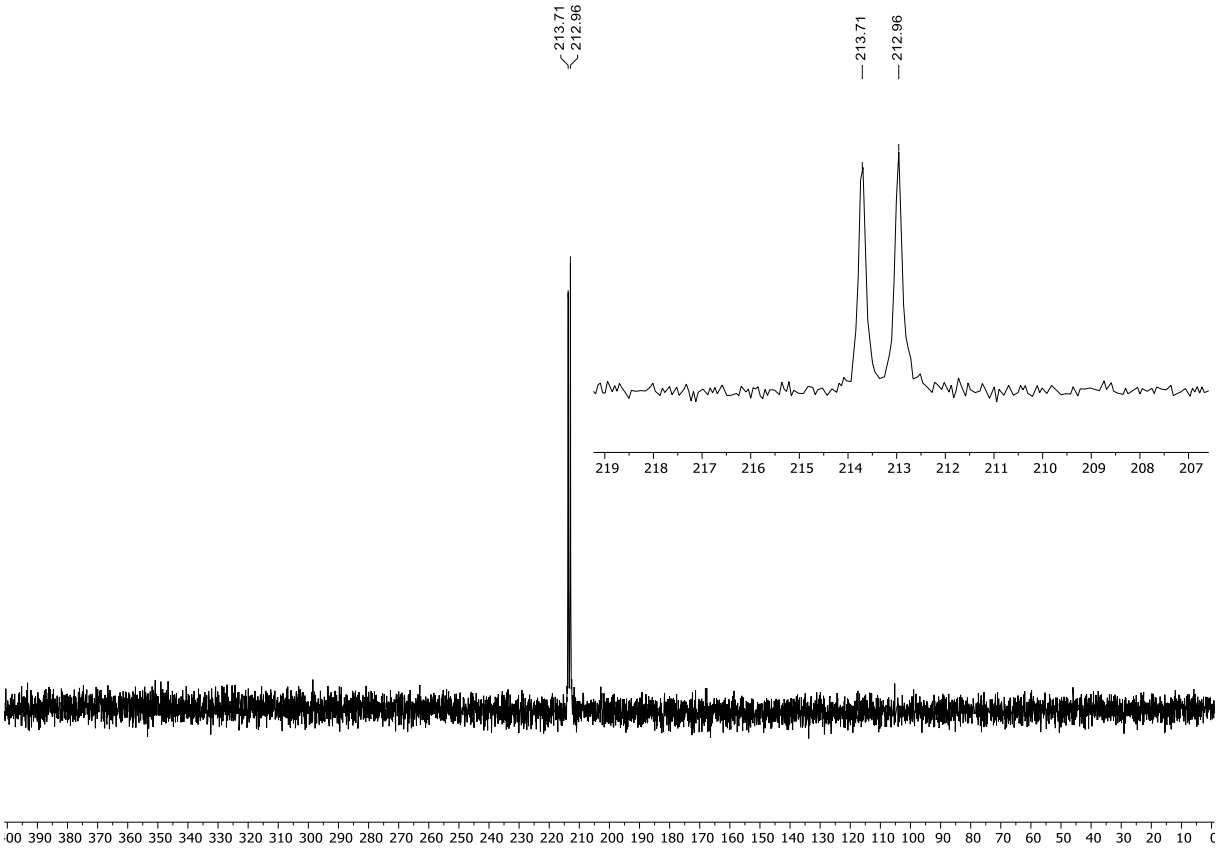


**Figure S35**. $^{119}Sn\{^{1}H\}$ NMR spectrum of $^{Mes}TerSnCH_2P(CH_3)_2NAd$ (**3c**) (187 MHz, $C_6D_6$, 298 K).

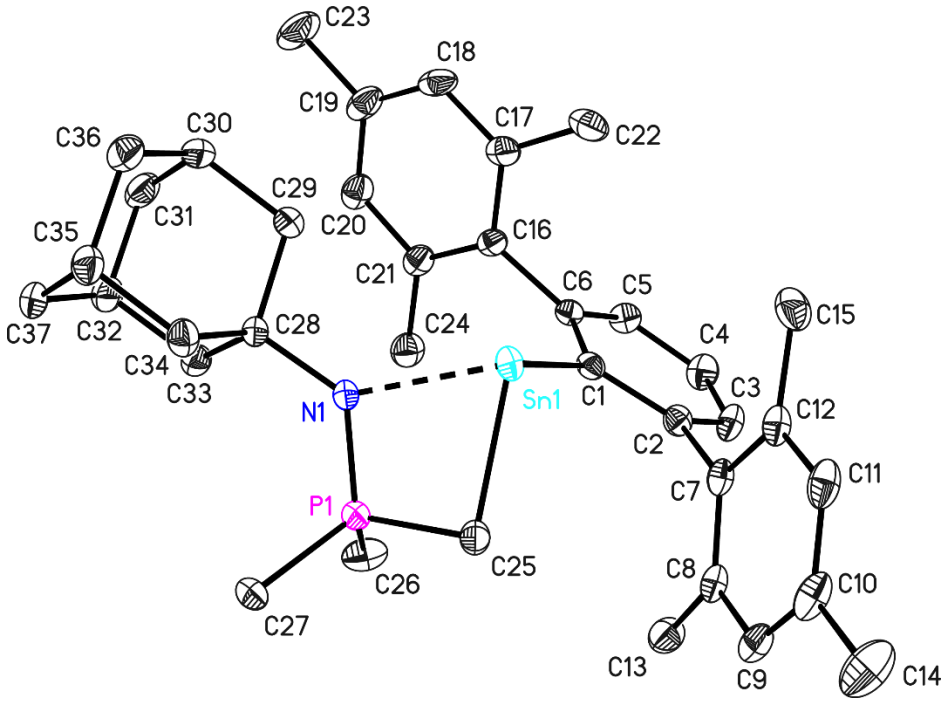


**Figure S36**. Asymmetric unit of the crystal structure of $^{Mes}$TerSnCH$_2$P(CH$_3$)$_2$NAd (**3c**). Anisotropic displacement parameters are drawn at the 50% probability level (hydrogen atoms have been omitted for clarity). Selected bond lengths (Å) and angles (deg): Sn1–C1 2.284(2), Sn1•••N1 2.269(2), P1–N1 1.6116(17), Sn1–C25 2.303(2), Sn1–N1–P1 32.94(4), C25–P1–N1 100.15(9), C25–Sn1–N1 68.84(6), P1–C25–Sn1 91.87(9).

**Table S4**. Bond lengths [Å] and angles [°] for **3c**.

| | | | |
|---|---|---|---|
| Sn(1)-N(1) | 2.269(2) | C(8)-C(9) | 1.395(3) |
| Sn(1)-C(1) | 2.284(2) | C(8)-C(13) | 1.510(3) |
| Sn(1)-C(25) | 2.303(2) | C(9)-C(10) | 1.391(3) |
| Sn(1)-P(1) | 2.9414(14) | C(10)-C(11) | 1.389(3) |
| P(1)-N(1) | 1.6116(17) | C(10)-C(14) | 1.511(3) |
| P(1)-C(25) | 1.756(2) | C(11)-C(12) | 1.393(3) |
| P(1)-C(26) | 1.809(2) | C(12)-C(15) | 1.517(3) |
| P(1)-C(27) | 1.811(2) | C(16)-C(21) | 1.403(3) |
| N(1)-C(28) | 1.476(2) | C(16)-C(17) | 1.411(3) |
| C(1)-C(6) | 1.416(3) | C(17)-C(18) | 1.398(3) |
| C(1)-C(2) | 1.418(3) | C(17)-C(22) | 1.503(3) |
| C(2)-C(3) | 1.396(3) | C(18)-C(19) | 1.389(3) |
| C(2)-C(7) | 1.502(3) | C(19)-C(20) | 1.387(3) |
| C(3)-C(4) | 1.382(3) | C(19)-C(23) | 1.517(3) |
| C(4)-C(5) | 1.390(3) | C(20)-C(21) | 1.404(3) |
| C(5)-C(6) | 1.400(3) | C(21)-C(24) | 1.510(3) |
| C(6)-C(16) | 1.503(3) | C(28)-C(33) | 1.534(3) |
| C(7)-C(12) | 1.407(3) | C(28)-C(29) | 1.537(3) |
| C(7)-C(8) | 1.408(3) | C(28)-C(34) | 1.546(3) |

| | | | |
|---|---|---|---|
| C(29)-C(30) | 1.540(3) | C(5)-C(6)-C(1) | 120.98(16) |
| C(30)-C(36) | 1.532(3) | C(5)-C(6)-C(16) | 114.49(16) |
| C(30)-C(31) | 1.534(3) | C(1)-C(6)-C(16) | 124.31(16) |
| C(31)-C(32) | 1.530(3) | C(12)-C(7)-C(8) | 119.46(17) |
| C(32)-C(37) | 1.533(3) | C(12)-C(7)-C(2) | 119.90(17) |
| C(32)-C(33) | 1.538(3) | C(8)-C(7)-C(2) | 120.50(16) |
| C(34)-C(35) | 1.542(3) | C(9)-C(8)-C(7) | 119.49(18) |
| C(35)-C(37) | 1.533(3) | C(9)-C(8)-C(13) | 119.32(18) |
| C(35)-C(36) | 1.535(3) | C(7)-C(8)-C(13) | 121.19(17) |
| | | C(10)-C(9)-C(8) | 121.44(19) |
| N(1)-Sn(1)-C(1) | 105.96(7) | C(11)-C(10)-C(9) | 118.27(18) |
| N(1)-Sn(1)-C(25) | 68.84(6) | C(11)-C(10)-C(14) | 121.3(2) |
| C(1)-Sn(1)-C(25) | 96.62(7) | C(9)-C(10)-C(14) | 120.4(2) |
| N(1)-Sn(1)-P(1) | 32.94(4) | C(10)-C(11)-C(12) | 122.12(18) |
| C(1)-Sn(1)-P(1) | 98.61(6) | C(11)-C(12)-C(7) | 119.03(18) |
| C(25)-Sn(1)-P(1) | 36.64(5) | C(11)-C(12)-C(15) | 119.37(18) |
| N(1)-P(1)-C(25) | 100.15(9) | C(7)-C(12)-C(15) | 121.59(17) |
| N(1)-P(1)-C(26) | 115.17(10) | C(21)-C(16)-C(17) | 119.41(17) |
| C(25)-P(1)-C(26) | 108.41(10) | C(21)-C(16)-C(6) | 121.04(16) |
| N(1)-P(1)-C(27) | 116.22(9) | C(17)-C(16)-C(6) | 118.93(16) |
| C(25)-P(1)-C(27) | 113.63(10) | C(18)-C(17)-C(16) | 119.25(19) |
| C(26)-P(1)-C(27) | 103.42(11) | C(18)-C(17)-C(22) | 120.09(18) |
| N(1)-P(1)-Sn(1) | 49.96(6) | C(16)-C(17)-C(22) | 120.64(17) |
| C(25)-P(1)-Sn(1) | 51.49(7) | C(19)-C(18)-C(17) | 122.07(19) |
| C(26)-P(1)-Sn(1) | 115.90(8) | C(20)-C(19)-C(18) | 117.98(18) |
| C(27)-P(1)-Sn(1) | 140.52(8) | C(20)-C(19)-C(23) | 120.9(2) |
| C(28)-N(1)-P(1) | 129.07(12) | C(18)-C(19)-C(23) | 121.1(2) |
| C(28)-N(1)-Sn(1) | 133.31(11) | C(19)-C(20)-C(21) | 122.03(19) |
| P(1)-N(1)-Sn(1) | 97.11(7) | C(16)-C(21)-C(20) | 119.25(18) |
| C(6)-C(1)-C(2) | 116.15(16) | C(16)-C(21)-C(24) | 121.57(17) |
| C(6)-C(1)-Sn(1) | 128.06(13) | C(20)-C(21)-C(24) | 119.17(18) |
| C(2)-C(1)-Sn(1) | 115.30(13) | P(1)-C(25)-Sn(1) | 91.87(9) |
| C(3)-C(2)-C(1) | 121.85(17) | N(1)-C(28)-C(33) | 112.10(15) |
| C(3)-C(2)-C(7) | 116.54(16) | N(1)-C(28)-C(29) | 108.39(14) |
| C(1)-C(2)-C(7) | 121.54(16) | C(33)-C(28)-C(29) | 108.35(15) |
| C(4)-C(3)-C(2) | 120.84(17) | N(1)-C(28)-C(34) | 111.23(15) |
| C(3)-C(4)-C(5) | 118.60(17) | C(33)-C(28)-C(34) | 108.83(15) |
| C(4)-C(5)-C(6) | 121.44(18) | C(29)-C(28)-C(34) | 107.79(15) |

| | | | |
|---|---|---|---|
| C(28)-C(29)-C(30) | 110.80(15) | C(28)-C(33)-C(32) | 110.67(15) |
| C(36)-C(30)-C(31) | 109.13(17) | C(35)-C(34)-C(28) | 110.82(16) |
| C(36)-C(30)-C(29) | 109.54(17) | C(37)-C(35)-C(36) | 109.48(17) |
| C(31)-C(30)-C(29) | 109.59(16) | C(37)-C(35)-C(34) | 109.02(16) |
| C(32)-C(31)-C(30) | 109.50(17) | C(36)-C(35)-C(34) | 109.50(16) |
| C(31)-C(32)-C(37) | 109.45(17) | C(30)-C(36)-C(35) | 109.40(16) |
| C(31)-C(32)-C(33) | 109.06(16) | C(35)-C(37)-C(32) | 109.49(16) |
| C(37)-C(32)-C(33) | 109.96(16) | | |

**Reaction of $^{Mes}$TerSnCH$_2$P(CH$_3$)$_2$NDipp (3a) and IMe$_4$ – Synthesis of $^{Mes}$TerSn(IMe$_4$)CH$_2$P(CH$_3$)$_2$NDipp (4a)**

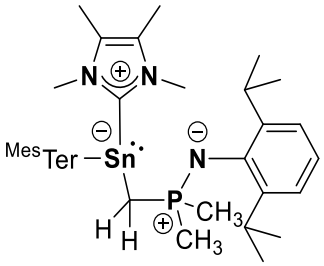

To a solution of $^{Mes}$TerSnCH$_2$PNDipp (**3a**) (0.030 g, 0.044 mmol) in 0.3 mL of $C_6D_6$ was added a solution of IMe$_4$ (0.005 g, 0.044 mmol) in 0.3 mL of $C_6D_6$, leading to an immediate but slight observable colour change. Subsequent analysis by $^1$H NMR spectroscopy reveals complete consumption of **3a** and formation of $^{Mes}$TerSn(IMe$_4$)CH$_2$PNDipp (**4a**). All volatiles were removed under vacuum to yield **4a** as a colourless solid. Crystal suitable for single crystal X-ray diffraction were obtained by slow diffusion of *n*-hexane into a solution of **4a** in toluene at -30 °C.

**Yield**: 0.031 g (0.038 mmol; 86%).
**$^1$H NMR** (500 MHz, $C_6D_6$, 298 K): $\delta$ = -0.45 (dd, $^2J_{H,H}$ = 12.4 Hz, $^2J_{P,H}$ = 7.7 Hz, 1H, CH$_2$), 0.93 (d, $^2J_{H,H}$ = 12.0 Hz, 1H, CH$_2$), 1.07-1.10 (m, 9H, P(CH$_3$)$_2$, CH(C*H*$_3$)$_2$), 1.24 (d, $^3J_{H,H}$ = 6.9 Hz, 6H, CH(C*H*$_3$)$_2$), 1.31-1.33 (m, 9H, P(CH$_3$)$_2$, NC$_q$CH$_3$), 1.99 (s, 6H, CH$_3$), 2.15 (s, 6H, CH$_3$), 2.43 (s, 6H, CH$_3$), 3.48 (hept, $^3J_{H,H}$ = 7.0 Hz, 2H, C*H*(CH$_3$)$_2$), 6.55 (m, 2H, CH$_{Aryl}$), 6.84 (m, 2H, CH$_{Aryl}$), 6.88-6.92 (m, 1H, CH$_{Aryl}$), 6.98-6.99 (m, 2H, CH$_{Aryl}$), 7.08-7.10 (m, 2H, CH$_{Aryl}$), 7.24-7.27 (m, 1H, CH$_{Aryl}$) ppm.
**$^{13}$C{$^1$H} NMR** (126 MHz, $C_6D_6$, 298 K): $\delta$ = 8.4 (NC$_q$CH$_3$), 16.2 (d, $^1J_{P,C}$ = 75.0 Hz, CH$_2$), 19.2 (d, $^1J_{P,C}$ = 56.2 Hz, P(CH$_3$)$_2$), 19.5 (d, $^1J_{P,C}$ = 64.6 Hz, P(CH$_3$)$_2$), 21.1 (CH$_3$), 21.2 (CH$_3$), 21.9 (CH$_3$), 24.28 (CH(CH$_3$)$_2$), 24.31 (CH(CH$_3$)$_2$), 28.1 (CH(CH$_3$)$_2$), 35.4 (NCH$_3$), 117.8 (d, $J_{P,C}$ = 3.9 Hz, CH$_{Aryl}$), 122.5 (d, $J_{P,C}$ = 3.9 Hz, CH$_{Aryl}$), 124.3 (NC$_q$CH$_3$), 126.4 (CH$_{Aryl}$), 127.8 (CH$_{Aryl}$)*, 127.9 (CH$_{Aryl}$)*, 128.6 (CH$_{Aryl}$), 135.2 (C$_{q,Aryl}$), 136.1 (C$_{q,Aryl}$), 136.5 (C$_{q,Aryl}$), 142.35 (C$_{q,Aryl}$), 142.40 (C$_{q,Aryl}$), 143.3 (C$_{q,Aryl}$), 147.9 (d, $J_{P,C}$ = 3.6 Hz, C$_{q,Aryl}$), 149.5 (C$_{q,Aryl}$), 161.2 (d, $^3J_{P,C}$ = 7.6 Hz, C$_{q,Aryl}$Sn) 173.6 (C$_{NHC}$) ppm.
* = overlap with $C_6D_6$ signal(s) and assigned by $^1$H/$^{13}$C HMBC
**$^1$H/$^{15}$N HMBC NMR** (51 MHz, $C_6D_6$, 298 K): $\delta$ = -303.3 (PN), -201.6 (NHC) ppm.
**$^{31}$P{$^1$H} NMR** (203 MHz, $C_6D_6$, 298 K): $\delta$ = 5.6 (Sn satellites: $J_{119/117Sn,P}$ = 129.1 Hz (average value)) ppm.
**$^{31}$P NMR** (203 MHz, $C_6D_6$, 298 K): $\delta$ = 5.6 (m) ppm.
**$^{119}$Sn{$^1$H} NMR** (187 MHz, $C_6D_6$, 298 K): $\delta$ = -175.1 (d, $^2J_{119Sn,P}$ = 131.9 Hz) ppm.
**MS (LIFDI)**: m/z calcd. for $C_{46}H_{62}N_3PSn$: 807.3703; found: 807.3.
**EA**: Anal. calcd. for $C_{46}H_{62}N_3PSn$: C, 68.49; H, 7.75; N, 5.21; Found: C, 69.21; H, 7.92; N, 5.43.

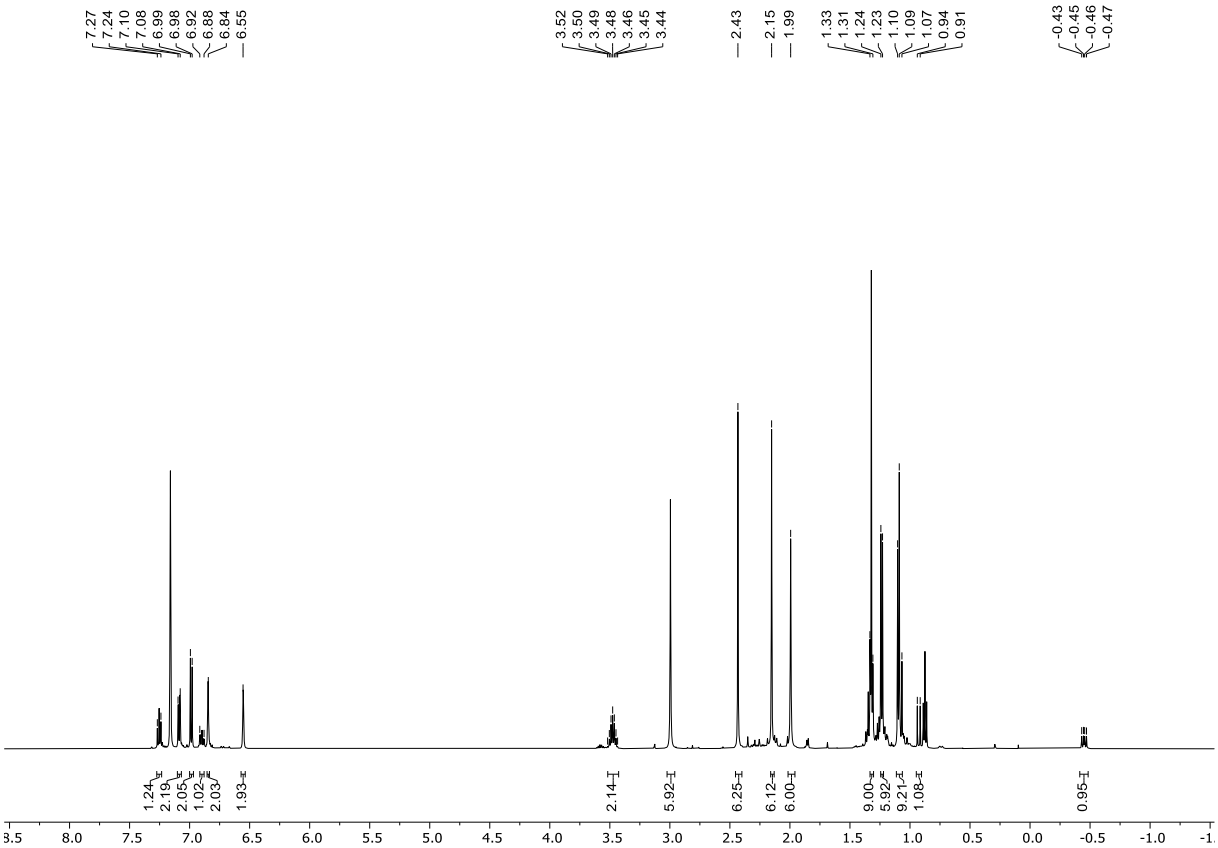

**Figure S37**. $^{1}H$ NMR spectrum of $^{Mes}$TerSn(IMe$_4$)CH$_2$PNDipp (**4a**) (500 MHz, $C_6D_6$, 298 K); 0.89, 1.24 ppm: *n*-hexane.

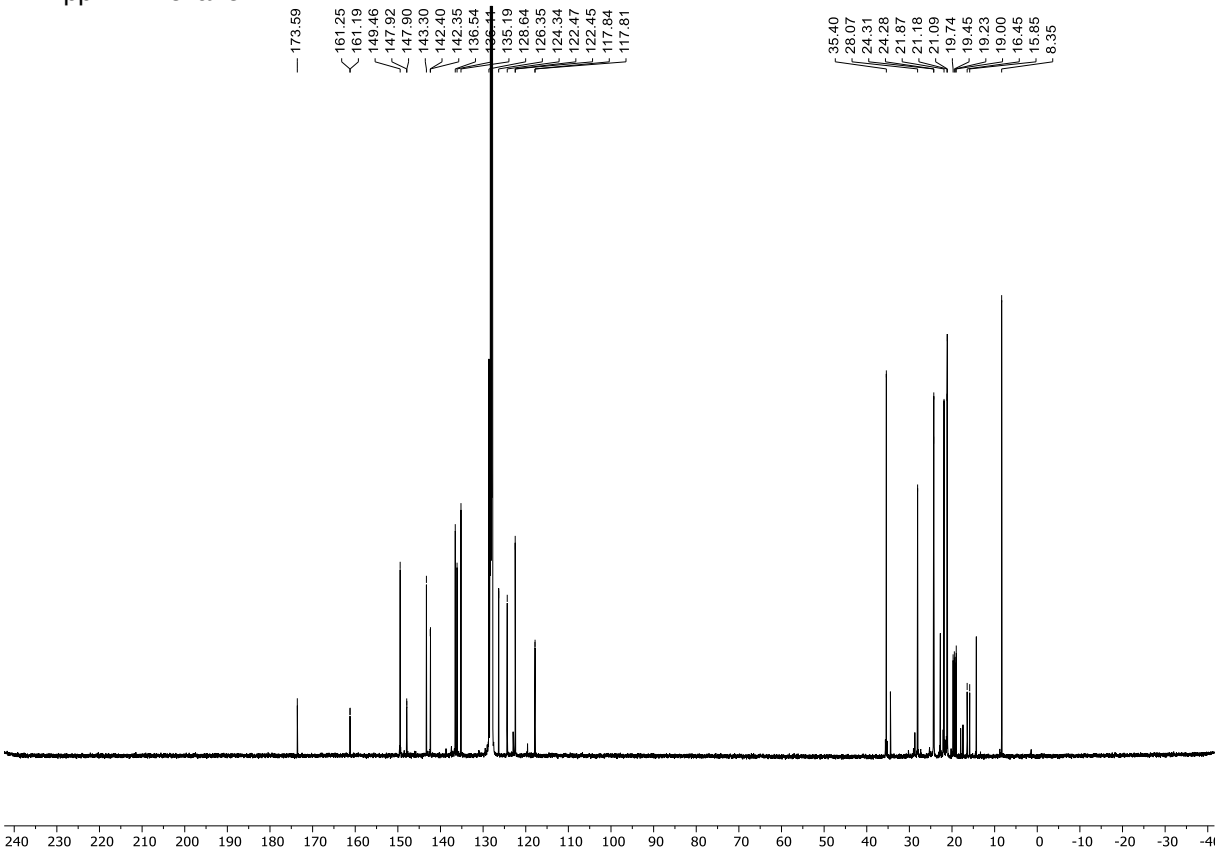

**Figure S38**. $^{13}C\{^{1}H\}$ NMR spectrum of $^{Mes}$TerSn(IMe$_4$)CH$_2$PNDipp (**4a**) (126 MHz, $C_6D_6$, 298 K); 14.3, 23.0, 32.0 ppm: *n*-hexane.

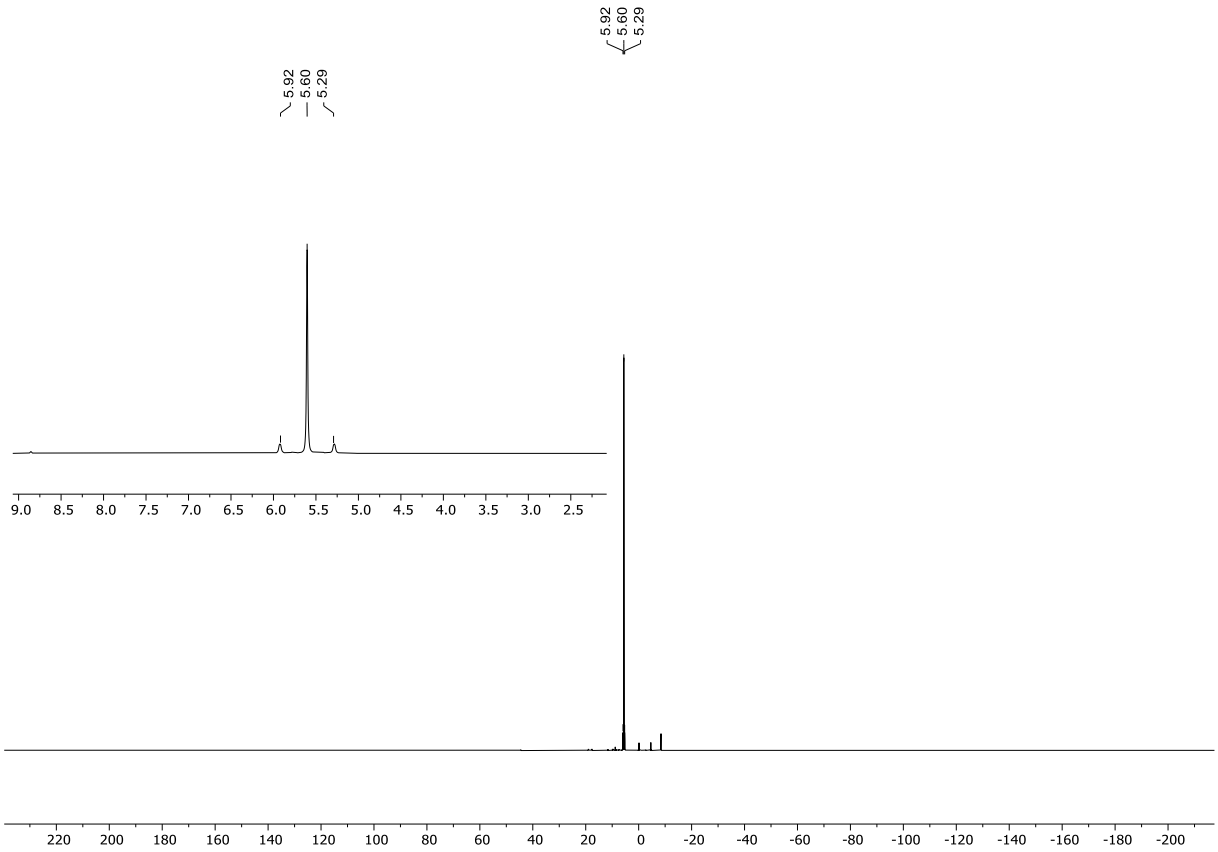


**Figure S39**. $^{31}P\{^{1}H\}$ NMR spectrum of $^{Mes}$TerSn(IMe$_4$)CH$_2$PNDipp (**4a**) (203 MHz, $C_6D_6$, 298 K).

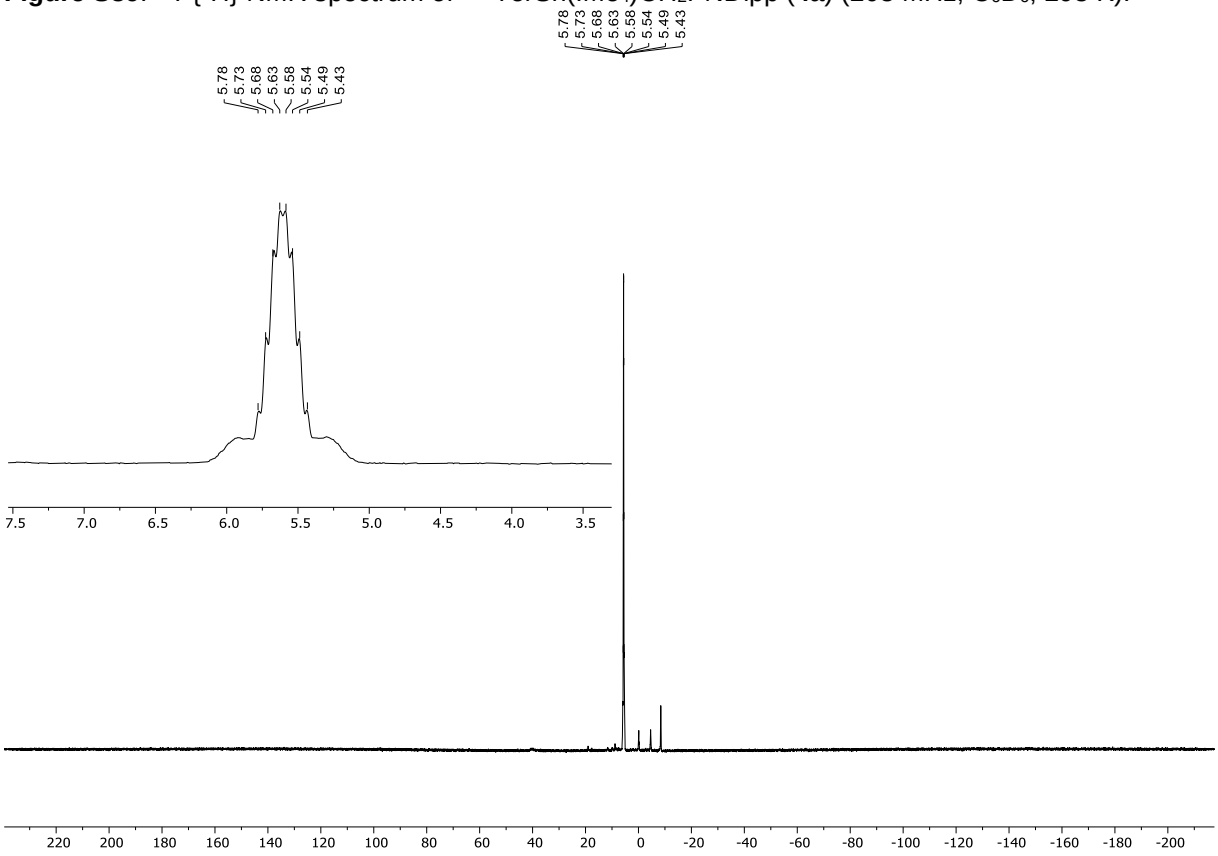


**Figure S40**. $^{31}P$ NMR spectrum of $^{Mes}$TerSn(IMe$_4$)CH$_2$PNDipp (**4a**) (203 MHz, $C_6D_6$, 298 K).

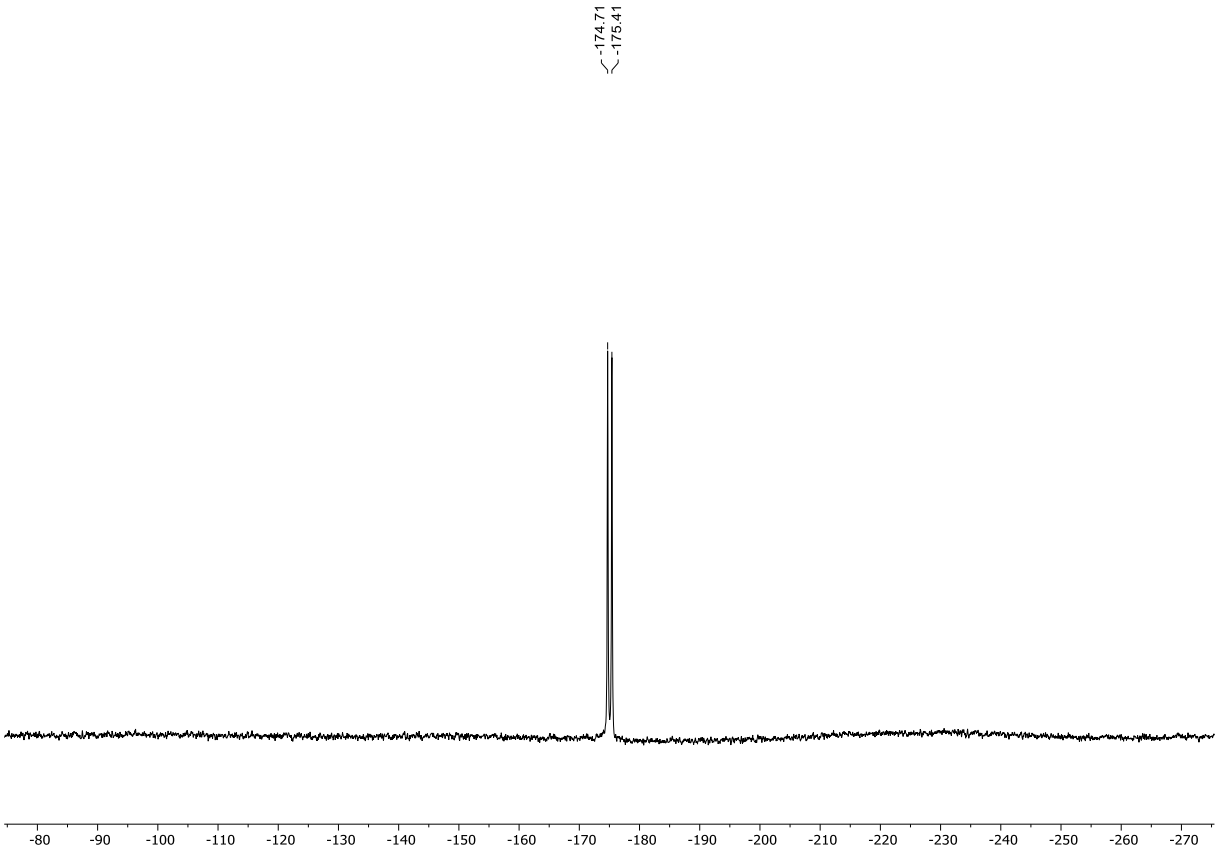


**Figure S41**. $^{119}Sn\{^{1}H\}$ NMR spectrum of $^{Mes}$TerSn(IMe$_4$)CH$_2$PNDipp (**4a**) (187 MHz, $C_6D_6$, 298 K).

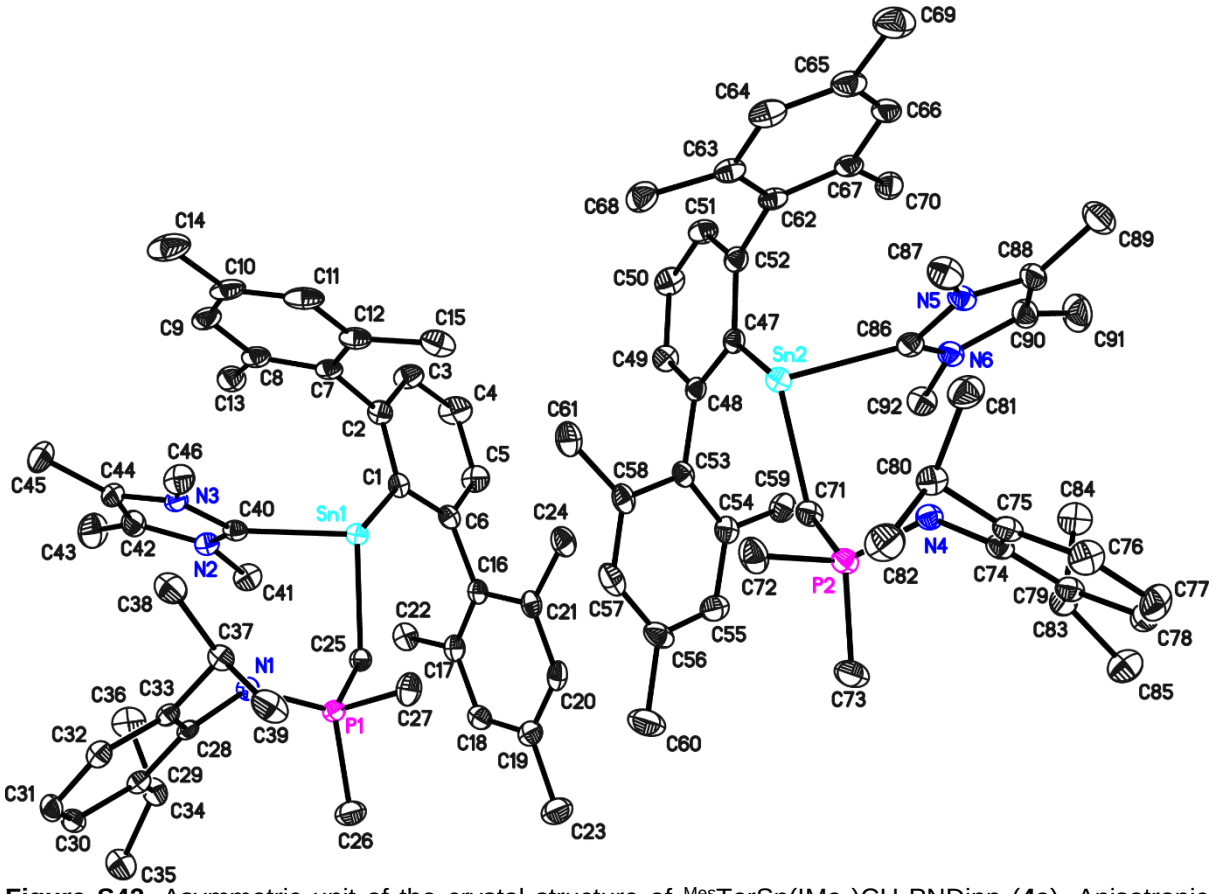


**Figure S42**. Asymmetric unit of the crystal structure of $^{Mes}$TerSn(IMe$_4$)CH$_2$PNDipp (**4a**). Anisotropic displacement parameters are drawn at the 50% probability level (hydrogen atoms have been omitted for clarity). Selected bond lengths (Å) and angles (deg): Sn1•••N1 3.571(3), Sn1–C1 2.269(3), Sn1–C25 2.263(3), Sn1–C40 2.287(3), N1–P1 1.573(3), P1–C25 1.766(3), C1–Sn1–C25 104.10(11), C1–Sn1–C40 92.65(11), C25–Sn1–C40 90.49(11).

**Table S5**. Bond lengths [Å] and angles [°] for **4a**.

| | | | |
|---|---|---|---|
| C(2)-C(3) | 1.396(4) | P(2)-C(73) | 1.819(3) |
| C(2)-C(1) | 1.410(4) | P(2)-C(72) | 1.824(3) |
| C(2)-C(7) | 1.505(4) | N(3)-C(40) | 1.353(4) |
| C(1)-C(6) | 1.415(4) | N(3)-C(44) | 1.386(4) |
| C(1)-Sn(1) | 2.269(3) | N(3)-C(46) | 1.459(4) |
| N(1)-C(28) | 1.388(4) | N(4)-C(74) | 1.403(4) |
| N(1)-P(1) | 1.573(3) | N(5)-C(86) | 1.345(4) |
| P(1)-C(25) | 1.766(3) | N(5)-C(88) | 1.389(4) |
| P(1)-C(27) | 1.813(3) | N(5)-C(87) | 1.461(4) |
| P(1)-C(26) | 1.816(3) | N(6)-C(86) | 1.343(4) |
| N(2)-C(40) | 1.346(4) | N(6)-C(90) | 1.397(4) |
| N(2)-C(42) | 1.385(4) | N(6)-C(92) | 1.463(4) |
| N(2)-C(41) | 1.456(4) | Sn(1)-C(25) | 2.263(3) |
| P(2)-N(4) | 1.564(3) | Sn(1)-C(40) | 2.287(3) |
| P(2)-C(71) | 1.769(3) | Sn(2)-C(71) | 2.261(3) |

| | | | |
|---|---|---|---|
| Sn(2)-C(47) | 2.267(3) | C(44)-C(45) | 1.486(5) |
| Sn(2)-C(86) | 2.282(3) | C(47)-C(48) | 1.411(4) |
| C(3)-C(4) | 1.384(5) | C(47)-C(52) | 1.413(4) |
| C(4)-C(5) | 1.378(5) | C(48)-C(49) | 1.397(4) |
| C(5)-C(6) | 1.398(4) | C(48)-C(53) | 1.498(4) |
| C(6)-C(16) | 1.502(4) | C(49)-C(50) | 1.389(5) |
| C(7)-C(8) | 1.405(5) | C(50)-C(51) | 1.383(5) |
| C(7)-C(12) | 1.406(5) | C(51)-C(52) | 1.402(4) |
| C(8)-C(9) | 1.395(5) | C(52)-C(62) | 1.503(4) |
| C(8)-C(13) | 1.507(5) | C(53)-C(54) | 1.403(4) |
| C(9)-C(10) | 1.379(5) | C(53)-C(58) | 1.406(4) |
| C(10)-C(11) | 1.387(5) | C(54)-C(55) | 1.394(5) |
| C(10)-C(14) | 1.516(5) | C(54)-C(59) | 1.512(4) |
| C(11)-C(12) | 1.395(5) | C(55)-C(56) | 1.390(5) |
| C(12)-C(15) | 1.506(5) | C(56)-C(57) | 1.382(5) |
| C(16)-C(17) | 1.396(4) | C(56)-C(60) | 1.509(5) |
| C(16)-C(21) | 1.407(4) | C(57)-C(58) | 1.392(5) |
| C(17)-C(18) | 1.399(5) | C(58)-C(61) | 1.506(5) |
| C(17)-C(22) | 1.512(4) | C(62)-C(67) | 1.405(5) |
| C(18)-C(19) | 1.389(5) | C(62)-C(63) | 1.406(5) |
| C(19)-C(20) | 1.390(5) | C(63)-C(64) | 1.393(5) |
| C(19)-C(23) | 1.514(5) | C(63)-C(68) | 1.503(5) |
| C(20)-C(21) | 1.397(5) | C(64)-C(65) | 1.394(5) |
| C(21)-C(24) | 1.504(4) | C(65)-C(66) | 1.383(5) |
| C(28)-C(29) | 1.419(4) | C(65)-C(69) | 1.509(5) |
| C(28)-C(33) | 1.424(4) | C(66)-C(67) | 1.391(5) |
| C(29)-C(30) | 1.396(4) | C(67)-C(70) | 1.511(5) |
| C(29)-C(34) | 1.523(4) | C(74)-C(75) | 1.413(4) |
| C(30)-C(31) | 1.384(4) | C(74)-C(79) | 1.422(4) |
| C(31)-C(32) | 1.381(4) | C(75)-C(76) | 1.394(5) |
| C(32)-C(33) | 1.394(4) | C(75)-C(80) | 1.519(4) |
| C(33)-C(37) | 1.513(4) | C(76)-C(77) | 1.385(5) |
| C(34)-C(36) | 1.525(5) | C(77)-C(78) | 1.391(5) |
| C(34)-C(35) | 1.528(4) | C(78)-C(79) | 1.390(4) |
| C(37)-C(38) | 1.528(4) | C(79)-C(83) | 1.526(4) |
| C(37)-C(39) | 1.534(4) | C(80)-C(82) | 1.528(5) |
| C(42)-C(44) | 1.354(5) | C(80)-C(81) | 1.531(4) |
| C(42)-C(43) | 1.488(5) | C(83)-C(84) | 1.532(5) |

| | | | |
|---|---|---|---|
| C(83)-C(85) | 1.532(4) | C(25)-Sn(1)-C(40) | 90.49(11) |
| C(88)-C(90) | 1.347(5) | C(1)-Sn(1)-C(40) | 92.65(11) |
| C(88)-C(89) | 1.483(5) | C(71)-Sn(2)-C(47) | 103.93(11) |
| C(90)-C(91) | 1.476(5) | C(71)-Sn(2)-C(86) | 90.28(11) |
| | | C(47)-Sn(2)-C(86) | 92.33(11) |
| C(3)-C(2)-C(1) | 121.3(3) | C(4)-C(3)-C(2) | 120.3(3) |
| C(3)-C(2)-C(7) | 117.1(3) | C(5)-C(4)-C(3) | 119.7(3) |
| C(1)-C(2)-C(7) | 121.6(3) | C(4)-C(5)-C(6) | 120.8(3) |
| C(2)-C(1)-C(6) | 117.1(3) | C(5)-C(6)-C(1) | 120.8(3) |
| C(2)-C(1)-Sn(1) | 115.7(2) | C(5)-C(6)-C(16) | 118.0(3) |
| C(6)-C(1)-Sn(1) | 126.4(2) | C(1)-C(6)-C(16) | 121.1(3) |
| C(28)-N(1)-P(1) | 131.7(2) | C(8)-C(7)-C(12) | 119.7(3) |
| N(1)-P(1)-C(25) | 108.87(14) | C(8)-C(7)-C(2) | 120.4(3) |
| N(1)-P(1)-C(27) | 115.86(15) | C(12)-C(7)-C(2) | 119.9(3) |
| C(25)-P(1)-C(27) | 105.69(16) | C(9)-C(8)-C(7) | 119.1(3) |
| N(1)-P(1)-C(26) | 115.36(15) | C(9)-C(8)-C(13) | 119.2(3) |
| C(25)-P(1)-C(26) | 109.53(15) | C(7)-C(8)-C(13) | 121.6(3) |
| C(27)-P(1)-C(26) | 100.91(16) | C(10)-C(9)-C(8) | 121.9(3) |
| C(40)-N(2)-C(42) | 111.6(3) | C(9)-C(10)-C(11) | 118.3(3) |
| C(40)-N(2)-C(41) | 123.9(3) | C(9)-C(10)-C(14) | 120.6(4) |
| C(42)-N(2)-C(41) | 124.5(3) | C(11)-C(10)-C(14) | 121.1(4) |
| N(4)-P(2)-C(71) | 109.58(14) | C(10)-C(11)-C(12) | 122.1(3) |
| N(4)-P(2)-C(73) | 115.77(15) | C(11)-C(12)-C(7) | 118.7(3) |
| C(71)-P(2)-C(73) | 108.80(16) | C(11)-C(12)-C(15) | 119.7(3) |
| N(4)-P(2)-C(72) | 116.01(16) | C(7)-C(12)-C(15) | 121.5(3) |
| C(71)-P(2)-C(72) | 104.78(16) | C(17)-C(16)-C(21) | 119.6(3) |
| C(73)-P(2)-C(72) | 101.04(17) | C(17)-C(16)-C(6) | 121.7(3) |
| C(40)-N(3)-C(44) | 111.7(3) | C(21)-C(16)-C(6) | 118.8(3) |
| C(40)-N(3)-C(46) | 123.6(3) | C(16)-C(17)-C(18) | 119.4(3) |
| C(44)-N(3)-C(46) | 124.7(3) | C(16)-C(17)-C(22) | 122.2(3) |
| C(74)-N(4)-P(2) | 131.4(2) | C(18)-C(17)-C(22) | 118.4(3) |
| C(86)-N(5)-C(88) | 112.0(3) | C(19)-C(18)-C(17) | 121.8(3) |
| C(86)-N(5)-C(87) | 123.8(3) | C(18)-C(19)-C(20) | 118.1(3) |
| C(88)-N(5)-C(87) | 124.2(3) | C(18)-C(19)-C(23) | 120.9(3) |
| C(86)-N(6)-C(90) | 111.8(3) | C(20)-C(19)-C(23) | 121.0(3) |
| C(86)-N(6)-C(92) | 124.2(3) | C(19)-C(20)-C(21) | 121.7(3) |
| C(90)-N(6)-C(92) | 123.9(3) | C(20)-C(21)-C(16) | 119.3(3) |
| C(25)-Sn(1)-C(1) | 104.10(11) | C(20)-C(21)-C(24) | 119.3(3) |

| | | | |
|---|---|---|---|
| C(16)-C(21)-C(24) | 121.3(3) | C(51)-C(52)-C(47) | 121.1(3) |
| P(1)-C(25)-Sn(1) | 108.54(14) | C(51)-C(52)-C(62) | 117.5(3) |
| N(1)-C(28)-C(29) | 120.6(3) | C(47)-C(52)-C(62) | 121.3(3) |
| N(1)-C(28)-C(33) | 120.9(3) | C(54)-C(53)-C(58) | 119.3(3) |
| C(29)-C(28)-C(33) | 118.3(3) | C(54)-C(53)-C(48) | 121.9(3) |
| C(30)-C(29)-C(28) | 119.8(3) | C(58)-C(53)-C(48) | 118.8(3) |
| C(30)-C(29)-C(34) | 120.8(3) | C(55)-C(54)-C(53) | 119.3(3) |
| C(28)-C(29)-C(34) | 119.3(3) | C(55)-C(54)-C(59) | 118.8(3) |
| C(31)-C(30)-C(29) | 121.5(3) | C(53)-C(54)-C(59) | 121.8(3) |
| C(32)-C(31)-C(30) | 119.1(3) | C(56)-C(55)-C(54) | 121.8(3) |
| C(31)-C(32)-C(33) | 121.8(3) | C(57)-C(56)-C(55) | 118.0(3) |
| C(32)-C(33)-C(28) | 119.6(3) | C(57)-C(56)-C(60) | 121.0(3) |
| C(32)-C(33)-C(37) | 119.6(3) | C(55)-C(56)-C(60) | 120.9(3) |
| C(28)-C(33)-C(37) | 120.8(3) | C(56)-C(57)-C(58) | 122.1(3) |
| C(29)-C(34)-C(36) | 110.6(3) | C(57)-C(58)-C(53) | 119.3(3) |
| C(29)-C(34)-C(35) | 114.2(3) | C(57)-C(58)-C(61) | 119.5(3) |
| C(36)-C(34)-C(35) | 110.9(3) | C(53)-C(58)-C(61) | 121.1(3) |
| C(33)-C(37)-C(38) | 112.6(3) | C(67)-C(62)-C(63) | 119.1(3) |
| C(33)-C(37)-C(39) | 110.6(3) | C(67)-C(62)-C(52) | 120.9(3) |
| C(38)-C(37)-C(39) | 109.5(3) | C(63)-C(62)-C(52) | 119.9(3) |
| N(2)-C(40)-N(3) | 104.2(3) | C(64)-C(63)-C(62) | 119.2(3) |
| N(2)-C(40)-Sn(1) | 131.7(2) | C(64)-C(63)-C(68) | 119.4(3) |
| N(3)-C(40)-Sn(1) | 123.4(2) | C(62)-C(63)-C(68) | 121.3(3) |
| C(44)-C(42)-N(2) | 106.5(3) | C(63)-C(64)-C(65) | 121.9(3) |
| C(44)-C(42)-C(43) | 131.1(3) | C(66)-C(65)-C(64) | 117.9(3) |
| N(2)-C(42)-C(43) | 122.3(3) | C(66)-C(65)-C(69) | 121.1(3) |
| C(42)-C(44)-N(3) | 106.0(3) | C(64)-C(65)-C(69) | 121.0(3) |
| C(42)-C(44)-C(45) | 130.6(3) | C(65)-C(66)-C(67) | 121.9(3) |
| N(3)-C(44)-C(45) | 123.2(3) | C(66)-C(67)-C(62) | 119.6(3) |
| C(48)-C(47)-C(52) | 117.0(3) | C(66)-C(67)-C(70) | 119.3(3) |
| C(48)-C(47)-Sn(2) | 125.7(2) | C(62)-C(67)-C(70) | 121.1(3) |
| C(52)-C(47)-Sn(2) | 116.6(2) | P(2)-C(71)-Sn(2) | 109.63(15) |
| C(49)-C(48)-C(47) | 121.2(3) | N(4)-C(74)-C(75) | 121.4(3) |
| C(49)-C(48)-C(53) | 117.9(3) | N(4)-C(74)-C(79) | 119.6(3) |
| C(47)-C(48)-C(53) | 120.8(3) | C(75)-C(74)-C(79) | 118.8(3) |
| C(50)-C(49)-C(48) | 120.7(3) | C(76)-C(75)-C(74) | 119.5(3) |
| C(51)-C(50)-C(49) | 119.3(3) | C(76)-C(75)-C(80) | 119.1(3) |
| C(50)-C(51)-C(52) | 120.6(3) | C(74)-C(75)-C(80) | 121.4(3) |

| | | | |
|---|---|---|---|
| C(77)-C(76)-C(75) | 121.5(3) | C(84)-C(83)-C(85) | 110.1(3) |
| C(76)-C(77)-C(78) | 119.4(3) | N(6)-C(86)-N(5) | 104.0(3) |
| C(79)-C(78)-C(77) | 121.0(3) | N(6)-C(86)-Sn(2) | 131.6(2) |
| C(78)-C(79)-C(74) | 119.8(3) | N(5)-C(86)-Sn(2) | 124.0(2) |
| C(78)-C(79)-C(83) | 120.5(3) | C(90)-C(88)-N(5) | 106.2(3) |
| C(74)-C(79)-C(83) | 119.6(3) | C(90)-C(88)-C(89) | 130.7(3) |
| C(75)-C(80)-C(82) | 111.9(3) | N(5)-C(88)-C(89) | 123.0(3) |
| C(75)-C(80)-C(81) | 112.1(3) | C(88)-C(90)-N(6) | 105.9(3) |
| C(82)-C(80)-C(81) | 109.3(3) | C(88)-C(90)-C(91) | 131.3(3) |
| C(79)-C(83)-C(84) | 110.4(3) | N(6)-C(90)-C(91) | 122.7(3) |
| C(79)-C(83)-C(85) | 114.1(3) | | |

**Reaction of $^{Mes}$TerSnCH$_2$P(CH$_3$)$_2$NXyl (3b) and IMe$_4$ – Synthesis of $^{Mes}$TerSn(IMe$_4$)CH$_2$P(CH$_3$)$_2$NXyl (4b)**

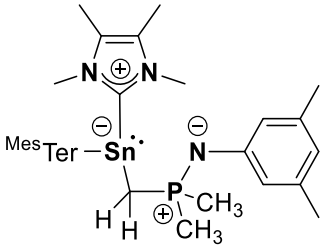

To a solution of $^{Mes}$TerSnCH$_2$PNXyl (**3b**) (0.030 g, 0.048 mmol) in 0.3 mL of $C_6D_6$ was added a solution of IMe$_4$ (0.006 g, 0.048 mmol) in 0.3 mL of $C_6D_6$, leading to an immediate but slight observable colour change. Subsequent analysis by $^1$H NMR spectroscopy reveals complete consumption of **3b** and formation of $^{Mes}$TerSn(IMe$_4$)CH$_2$PNXyl (**4b**). Multinuclear NMR data was collected at that point. All volatiles were removed under vacuum to yield **4b** as a slightly orange solid.

**Yield**: 0.032 g (0.043 mmol; 90%).
**$^1$H NMR** (500 MHz, $C_6D_6$, 298 K): $\delta$ = -0.77 (dd, $^2J_{H,H}$ = 12.7 Hz, $^2J_{P,H}$ = 9.2 Hz, 1H, CH$_2$), 1.20 (d, $^2J_{P,H}$ = 11.2 Hz, 3H, P(CH$_3$)$_2$), 1.37 (s, 6H, NC$_q$CH$_3$), 1.40 (d, $^2J_{P,H}$ = 12.4 Hz, 3H, P(CH$_3$)$_2$), 1.48-1.53 (m, 1H, CH$_2$), 2.00 (s, 6H, CH$_{3,Ter}$), 2.10 (s, 6H, *m*-CH$_3$N), 2.15 (s, 6H, CH$_{3,Ter}$), 2.45 (s, 6H, CH$_{3,Ter}$), 3.04 (s, 6H, NCH$_3$), 6.03 (s, 2H, *o*-CH$_{Aryl}$N), 6.09 (s, 1H, *p*-CH$_{Aryl}$N), 6.54 (s, 2H, *m*-C*H*$_{Aryl}$C$_6$H$_3$), 6.85 (s, 2H, *m*-C*H*$_{Aryl}$C$_6$H$_3$), 7.01 (d, $^3J_{H,H}$ = 7.5 Hz, 2H, *m*-CH$_{Aryl}$Sn), 7.27 (t, $^3J_{H,H}$ = 7.5 Hz, 1H, *p*-CH$_{Aryl}$Sn) ppm.
**$^{13}$C{$^1$H} NMR** (126 MHz, $C_6D_6$, 298 K): $\delta$ = 8.4 (NC$_q$CH$_3$), 14.9 (d, $^1J_{P,C}$ = 55.2 Hz, PCH$_2$), 17.7 (d, $^1J_{P,C}$ = 49.5 Hz, P(CH$_3$)$_2$), 17.8 (d, $^1J_{P,C}$ = 84.0 Hz, P(CH$_3$)$_2$), 21.1 (CH$_{3,Ter}$), 21.2 (CH$_{3,Ter}$), 21.8 (CH$_{3,Ter}$), 22.1 (*m*-CH$_3$N), 35.3 (NCH$_3$), 115.8 (*p*-CH$_{Aryl}$N), 119.3 (*m*-CH$_{Aryl}$C$_6$H$_3$), 119.5 (*o*-CH$_{Aryl}$N), 124.1 (NC$_q$CH$_3$), 126.4 (*p*-CH$_{Aryl}$Sn), 128.0 (*m*-CH$_{Aryl}$Sn)*, 128.6 (*m*-CH$_{Aryl}$C$_6$H$_3$), 135.2 (C$_{q,Aryl}$), 136.2 (C$_{q,Aryl}$), 136.6 (d, $J_{P,C}$ = 2.2 Hz, C$_{q,Aryl}$), 136.7 (C$_{q,Aryl}$), 143.2 (C$_{q,Aryl}$), 149.5 (C$_{q,Aryl}$), 155.3 (d, $J_{P,C}$ = 3.2 Hz, C$_{q,Aryl}$), 161.2 (d, $^3J_{P,C}$ = 8.1 Hz, C$_{q,Aryl}$Sn) 172.4 (C$_{NHC}$) ppm.
* = overlap with $C_6D_6$ signal(s) and assigned by $^1$H/$^{13}$C HMBC
**$^1$H/$^{15}$N HMBC NMR** (51 MHz, $C_6D_6$, 298 K): $\delta$ = -282.9 (PN), -201.8 (NHC) ppm.
**$^{31}$P{$^1$H} NMR** (203 MHz, $C_6D_6$, 298 K): $\delta$ = 17.4 (Sn satellites: $J_{119/117Sn,P}$ = 123.7 Hz (average value)) ppm.
**$^{31}$P NMR** (203 MHz, $C_6D_6$, 298 K): $\delta$ = 17.4 (m) ppm.
**$^{119}$Sn{$^1$H} NMR** (187 MHz, $C_6D_6$, 298 K): $\delta$ = -184.8 (d, $^2J_{119Sn,P}$ = 128.2 Hz) ppm.
**EA**: Anal. calcd. for $C_{42}H_{54}N_3PSn$: C, 67.21; H, 7.25; N, 5.60; Found: C, 66.30; H, 6.92; N, 4.80.

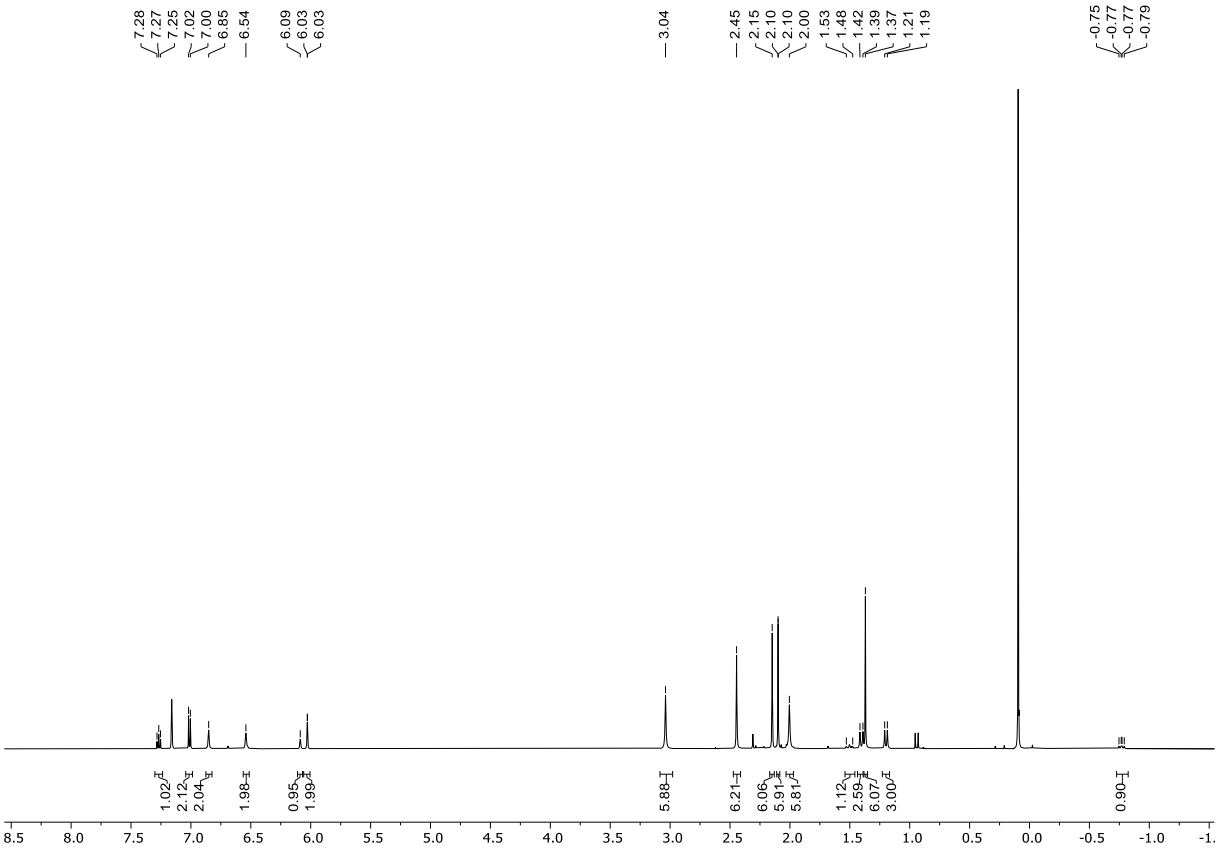

**Figure S43**. $^{1}H$ NMR spectrum of $^{Mes}TerSn(IMe_4)CH_2PNXyl$ (**4b**) (500 MHz, $C_6D_6$, 298 K); 0.10 ppm: $HN(Si(CH_3)_3)_2$.

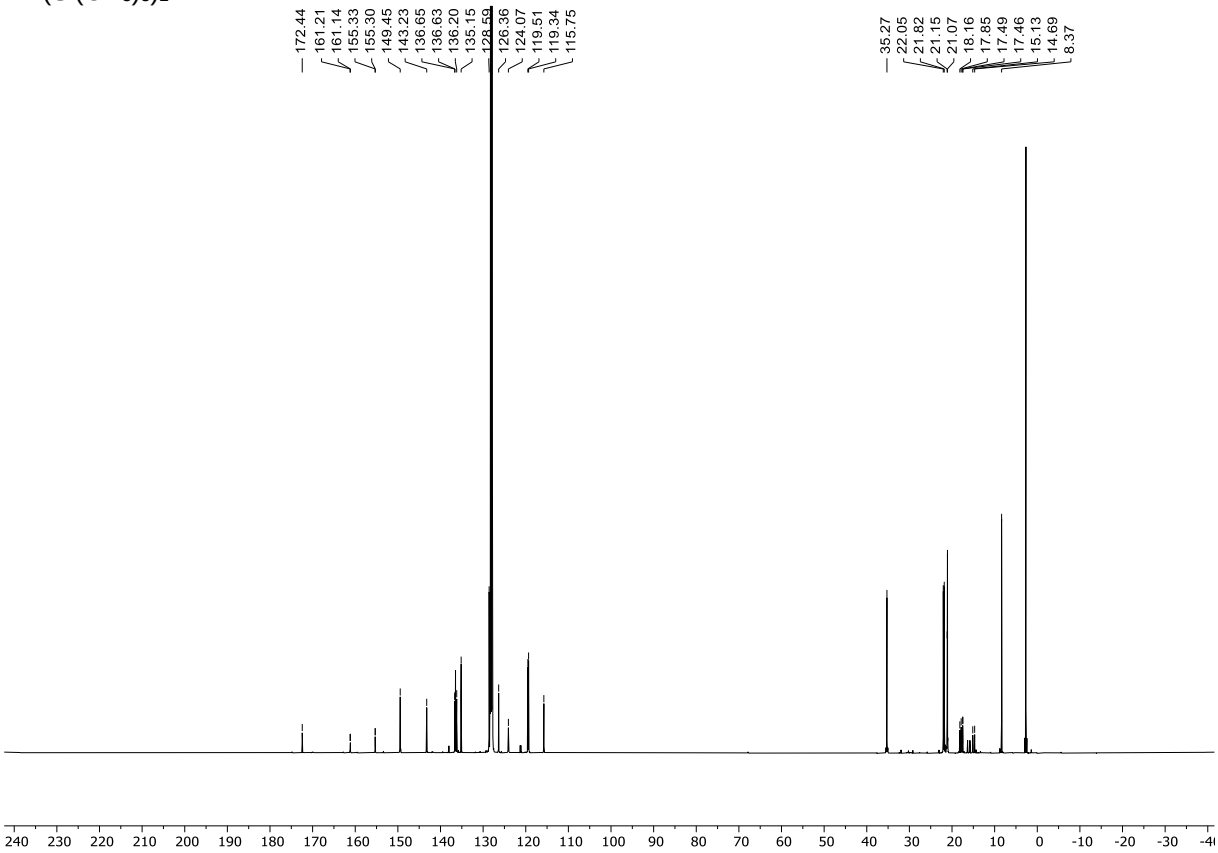

**Figure S44**. $^{13}C\{^{1}H\}$ NMR spectrum of $^{Mes}TerSn(IMe_4)CH_2PNXyl$ (**4b**) (126 MHz, $C_6D_6$, 298 K); 2.7 ppm: $HN(Si(CH_3)_3)_2$.

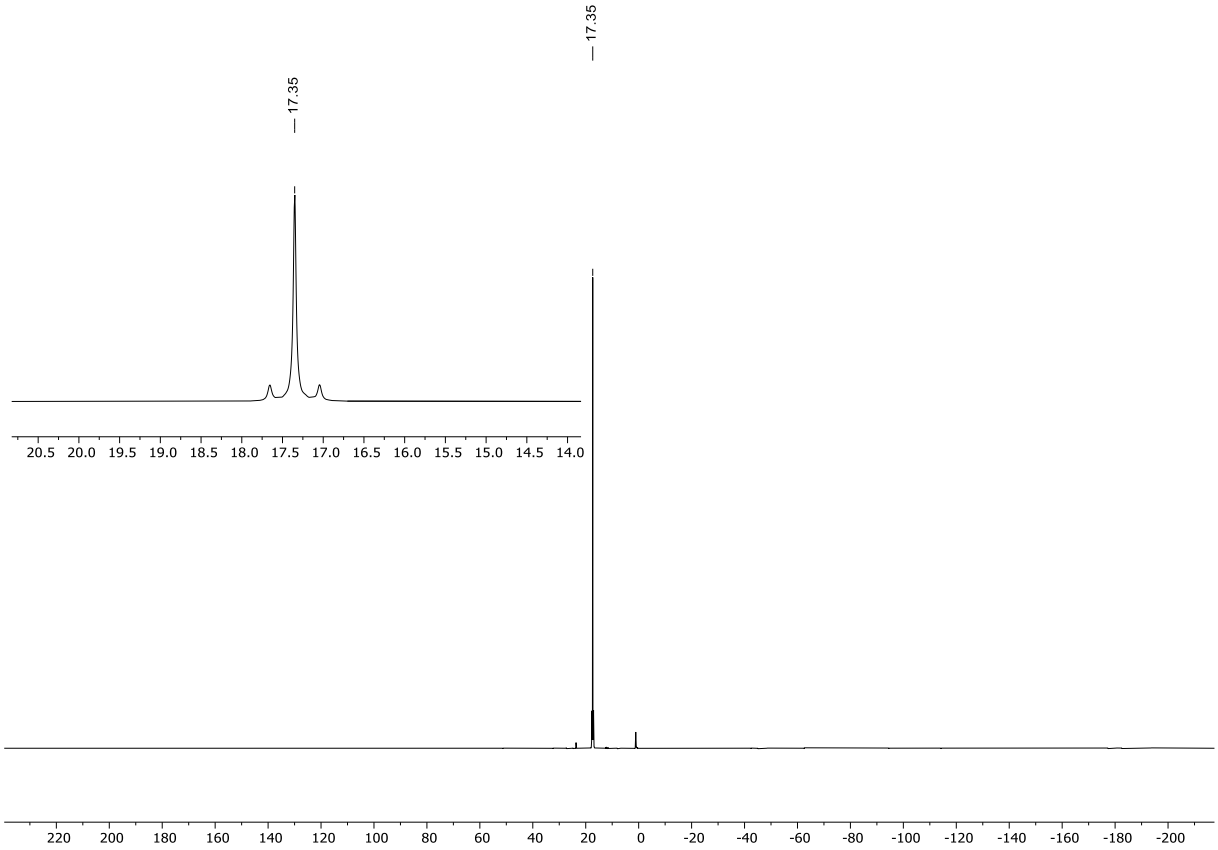


**Figure S45**. $^{31}P\{^{1}H\}$ NMR spectrum of $^{Mes}$TerSn(IMe$_4$)CH$_2$PNXyl (**4b**) (203 MHz, $C_6D_6$, 298 K).

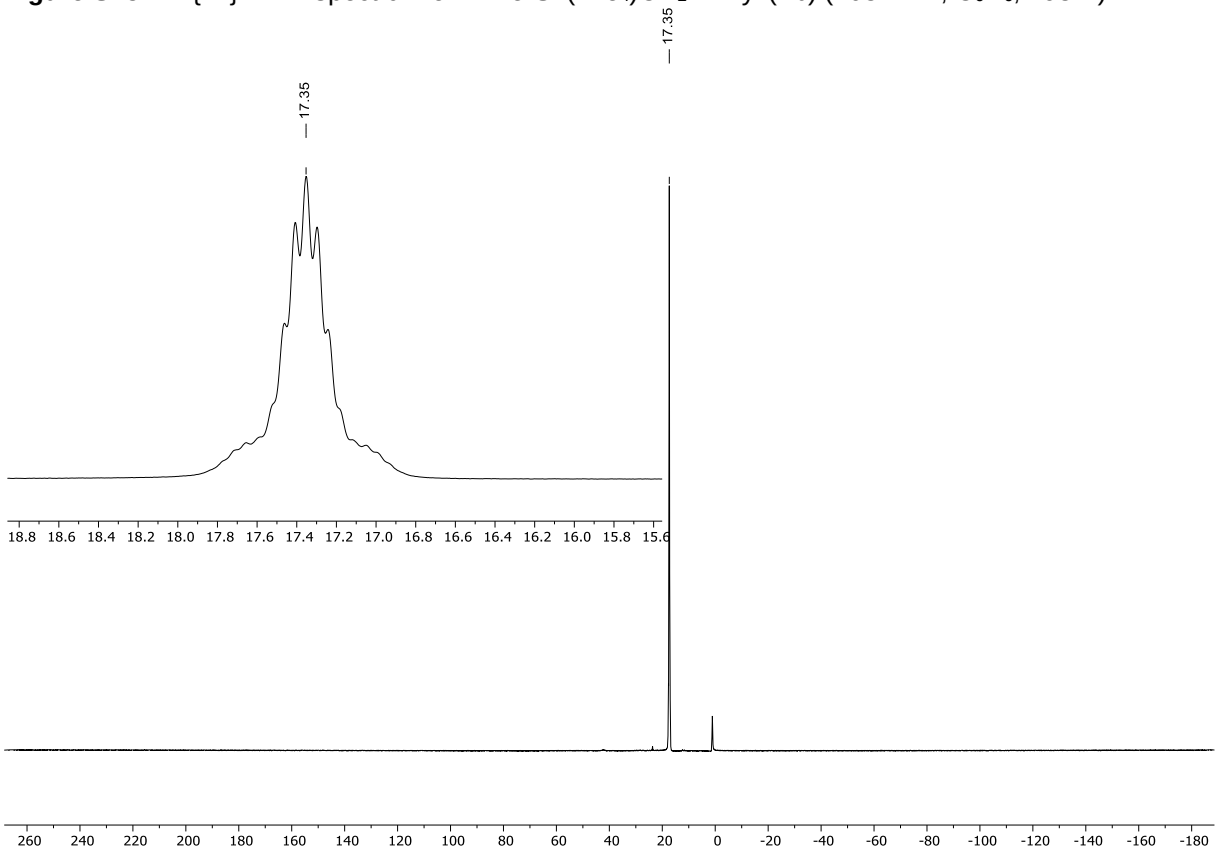


**Figure S46**. $^{31}P$ NMR spectrum of $^{Mes}$TerSn(IMe$_4$)CH$_2$PNXyl (**4b**) (203 MHz, $C_6D_6$, 298 K).

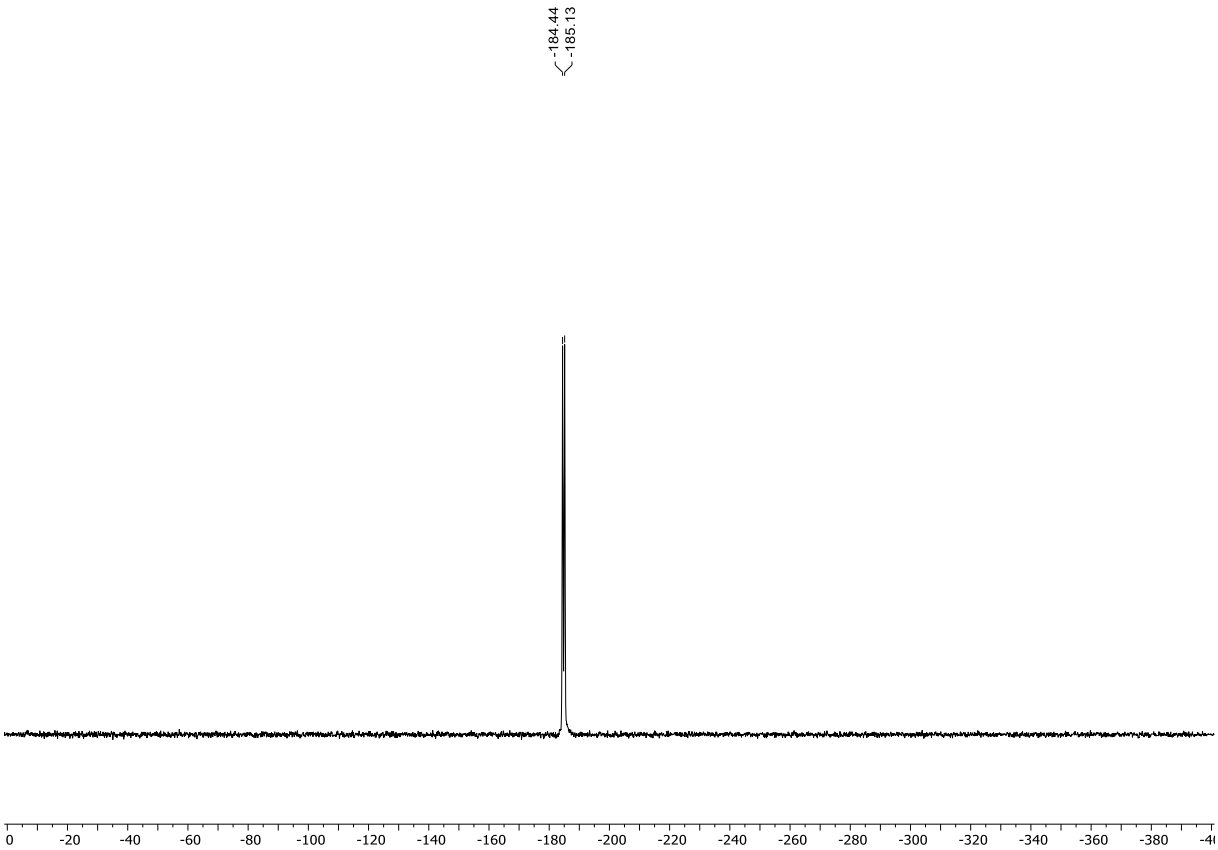


**Figure S47**. $^{119}Sn\{^{1}H\}$ NMR spectrum of $^{Mes}TerSn(IMe_4)CH_2PNXyl$ (**4b**) (187 MHz, $C_6D_6$, 298 K).

**Reaction of $^{Mes}$TerSnCH$_2$P(CH$_3$)$_2$NAd (3c) and IMe$_4$ – Synthesis of $^{Mes}$TerSn(IMe$_4$)CH$_2$P(CH$_3$)$_2$NAd (4c)**

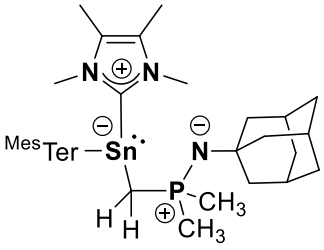

To a solution of $^{Mes}$TerSnCH$_2$PNAd (**3c**) (0.010 g, 0.015 mmol) in 0.3 mL of $C_6D_6$ was added a solution of IMe$_4$ (0.002 g, 0.015 mmol) in 0.3 mL of $C_6D_6$, leading to an immediate but slight observable colour change. Subsequent analysis by $^1$H NMR spectroscopy reveals complete consumption of **3c** and formation of $^{Mes}$TerSn(IMe$_4$)CH$_2$PNAd (**4c**). Multinuclear NMR data was collected at that point.

**$^1$H NMR** (500 MHz, $C_6D_6$, 298 K): $\delta$ = 1.00 (d, $^2J_{P,H}$ = 12.0 Hz, PCH$_2$), 1.18-1.33 (m, 7H, P(CH$_3$)$_2$, PCH$_2$)*, 1.44 (s, 6H, NC$_q$CH$_3$), 1.48 (s, 6H, CH$_{2,Ad}$), 1.62-1.73 (m, 6H, CH$_{2,Ad}$), 2.04 (s, 3H, CH$_{Ad}$), 2.08 (s, 6H, CH$_3$), 2.21 (s, 6H, CH$_3$), 2.48 (s, 6H, CH$_3$), 3.16 (s, 6H, NCH$_3$), 6.62 (s, 2H, CH$_{Aryl}$), 6.88 (s, 2H, CH$_{Aryl}$), 6.99-7.01 (m, 2H, CH$_{Aryl}$), 7.25-7.28 (m, 1H, CH$_{Aryl}$) ppm.
* = overlap with *n*-hexane signal
**$^{13}$C{$^1$H} NMR** (126 MHz, $C_6D_6$, 298 K): $\delta$ = 8.5 (NC$_q$CH$_3$), 20.9 (d, $^1J_{P,C}$ = 65.3 Hz, PCH$_2$), 21.2 (CH$_3$), 21.4 (CH$_3$), 22.0 (CH$_3$), 24.3 (d, $^1J_{P,C}$ = 43.4 Hz, P(CH$_3$)$_2$), 31.2 (CH$_{Ad}$), 35.6 (NCH$_3$), 37.6 (CH$_{2,Ad}$), 49.9 (CH$_{2,Ad}$), 51.2 (d, $^2J_{P,C}$ = 6.7 Hz, NC$_{q,Ad}$), 123.9 (NC$_q$CH$_3$), 126.3 (CH$_{Aryl}$), 127.7 (CH$_{Aryl}$)*, 127.8 (CH$_{Aryl}$)*, 128.7 (CH$_{Aryl}$), 135.1 (C$_{q,Aryl}$), 136.2 (C$_{q,Aryl}$), 136.6 (C$_{q,Aryl}$), 143.6 (C$_{q,Aryl}$), 149.5 (C$_{q,Aryl}$) ppm.
Note: The signal of the C$_{NHC}$ was not observed.
* = overlap with $C_6D_6$ signal
**$^{31}$P NMR** (203 MHz, $C_6D_6$, 298 K): $\delta$ = -0.2 (m) ppm.
**$^{119}$Sn{$^1$H} NMR** (187 MHz, $C_6D_6$, 298 K): $\delta$ = -169.4 ppm.

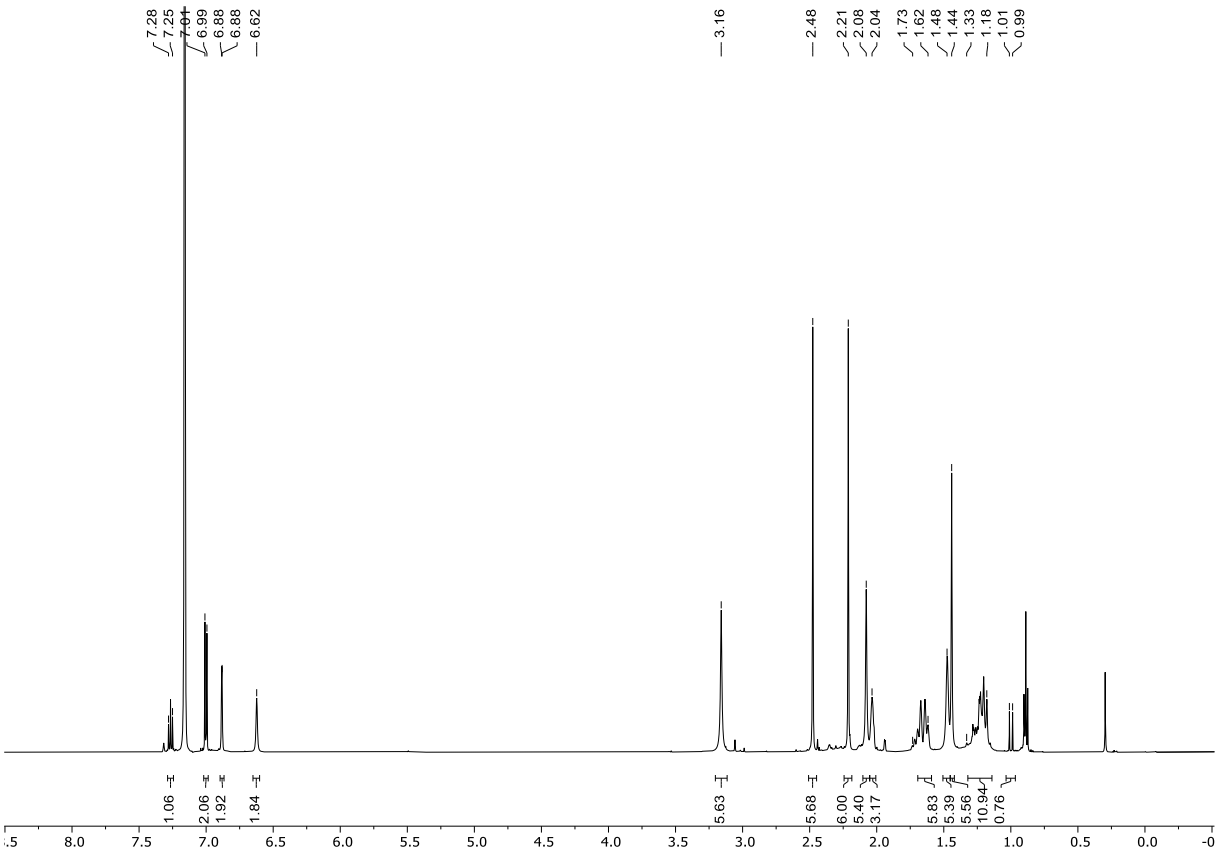


**Figure S48**. $^{1}H$ NMR spectrum of $^{Mes}$TerSn(IMe$_4$)CH$_2$PNAd (**4c**) (500 MHz, $C_6D_6$, 298 K); 0.29 ppm: silicon grease, 0.89, 1.24 ppm: *n*-hexane.

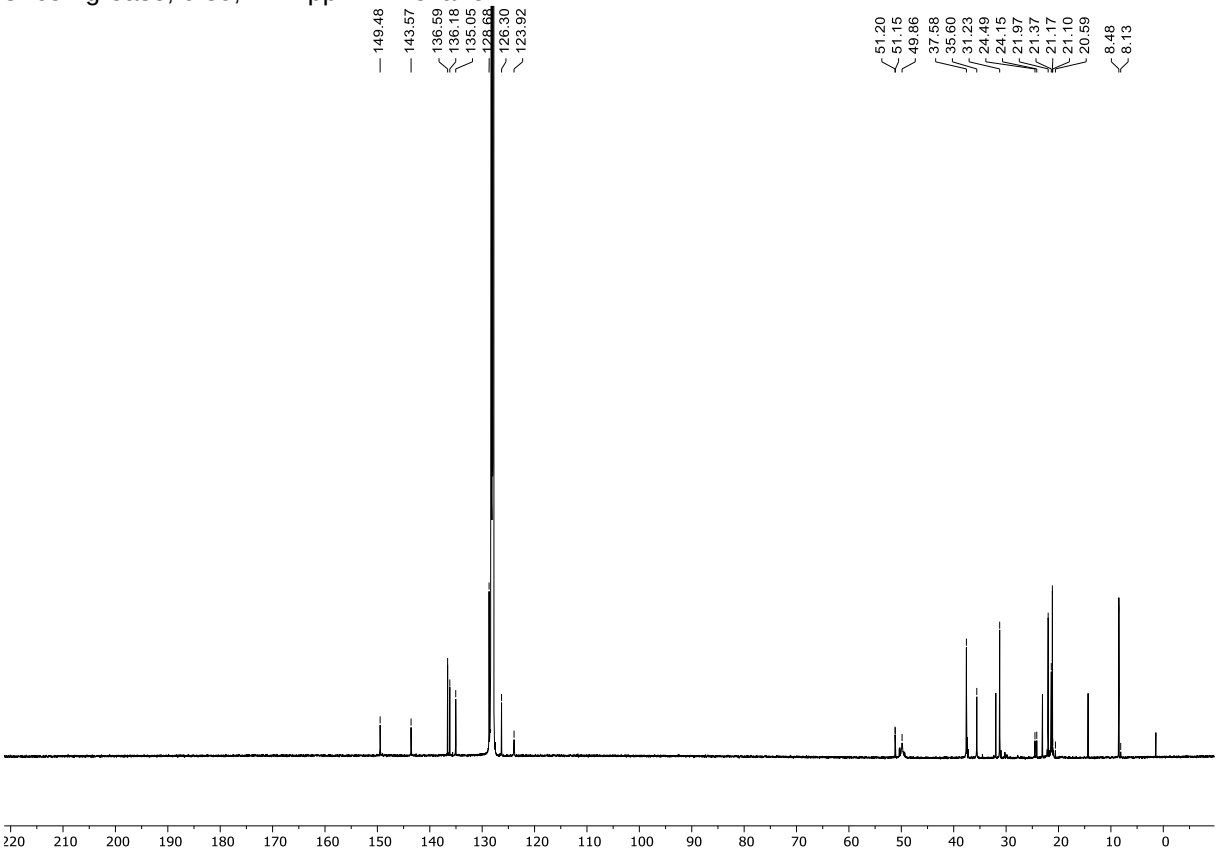


**Figure S49**. $^{13}C\{^{1}H\}$ NMR spectrum of $^{Mes}$TerSn(IMe$_4$)CH$_2$PNAd (**4c**) (126 MHz, $C_6D_6$, 298 K); 1.4 ppm: silicon grease, 14.3, 23.0, 32.0 ppm: *n*-hexane.

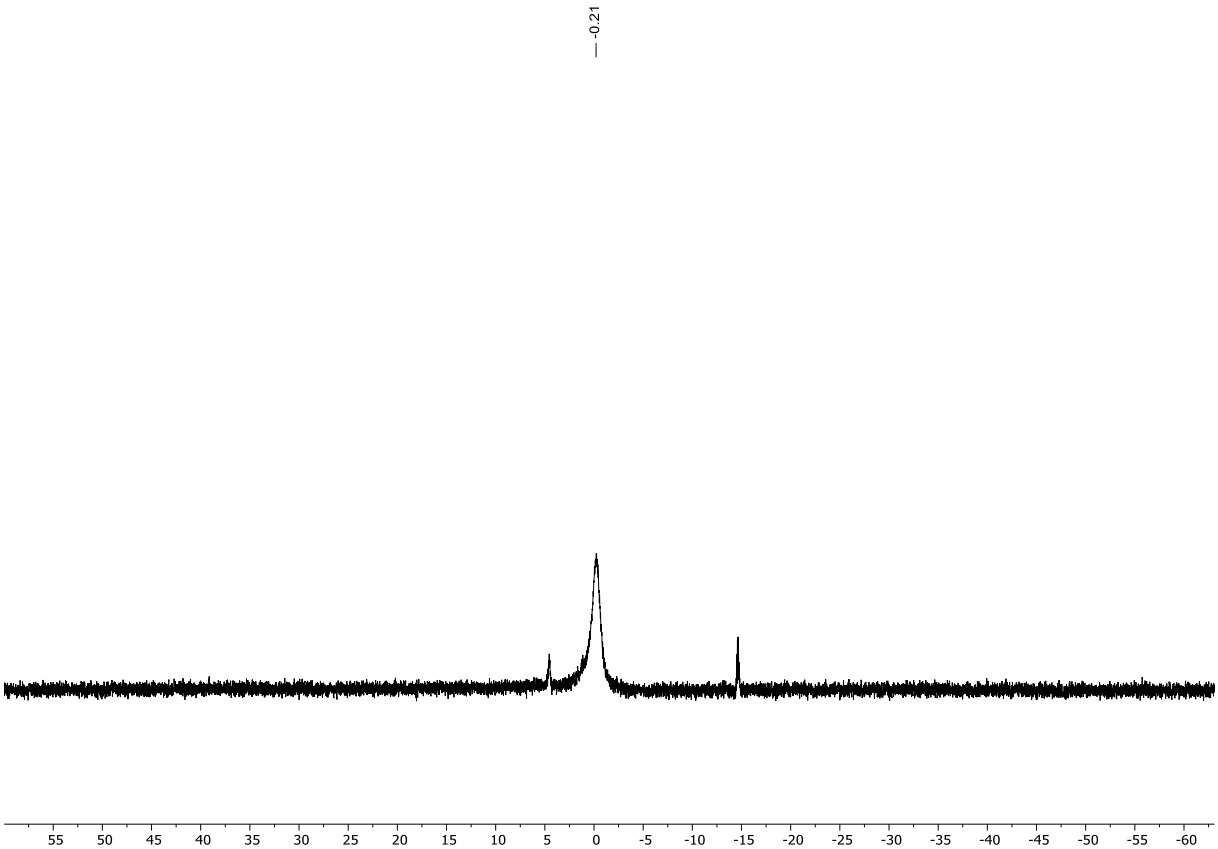


**Figure S50**. $^{31}P$ NMR spectrum of $^{Mes}TerSn(IMe_4)CH_2PNAd$ (**4c**) (203 MHz, $C_6D_6$, 298 K).

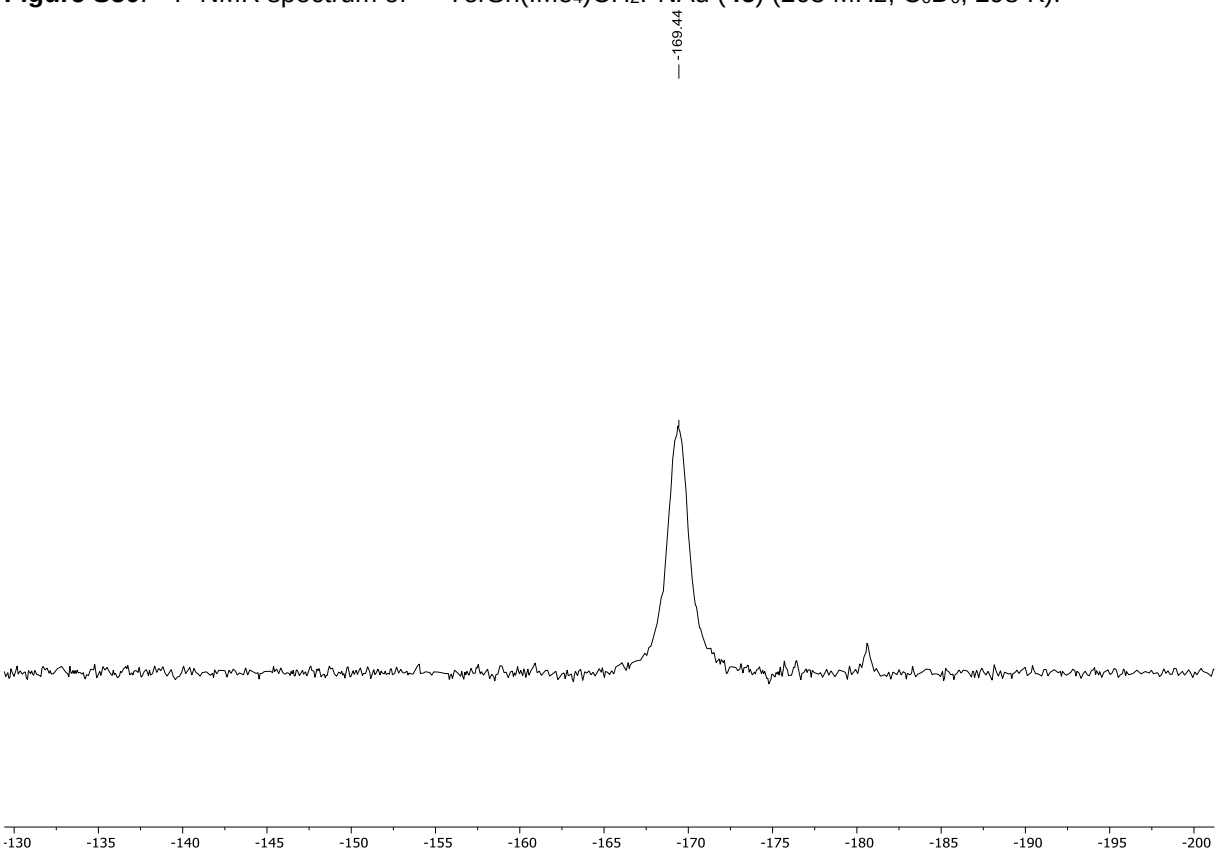


**Figure S51**. $^{119}Sn\{^1H\}$ NMR spectrum of $^{Mes}TerSn(IMe_4)CH_2PNAd$ (**4c**) (187 MHz, $C_6D_6$, 298 K).

**Reaction of DippNP(CH$_3$)$_3$ (2a) with Li{N(Si(CH$_3$)$_3$)$_2$} – Synthesis of the "LiCH$_2$P(CH$_3$)$_2$NDipp source 6"**

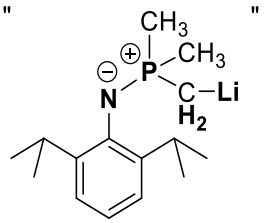

DippNP(CH$_3$)$_3$ (**2a**) (0.020 g, 0.080 mmol) was dissolved in either 0.3 mL of benzene or $C_6D_6$, followed by the addition of Li{N(Si(CH$_3$)$_3$)$_2$} (0.017 g, 0.080 mmol) in 0.3 mL of benzene or $C_6D_6$. Subsequent analysis by $^1$H NMR spectroscopy revealed complete consumption of **2a**. Attempts to perform the reaction in THF-$d_8$ as a solvent did not yield any reaction, even when heated to 90 °C for 8 hours (Figure S52). Adamantane (0.005 g, 0.037 mmol) was added as an internal standard for ECC-$^1$H-DOSY NMR spectroscopy (Figure S53 and details on page S59). The sample was further analyzed by multinuclear NMR spectroscopy, which showed that **2a** is converted to an approximately 3:1 mixture of seemingly two species. The minor component was assigned to be "LiCH$_2$P(CH$_3$)$_2$NDipp" with equimolar amounts of HN(Si(CH$_3$)$_3$)$_2$ observed in the $^1$H NMR spectrum (Figure S53), and the other initially as a "DippNP(CH$_3$)$_3$•Li{N(Si(CH$_3$)$_3$)$_2$} adduct" (Figure S54). At lower temperatures, the broad signals initially assigned to the above-mentioned, initially assigned, adduct split into separate signals, overall showing the same integral ratios of the respective signals when assuming adduct formation (Figure S58-S60). Despite multiple attempts, crystalline material suitable for single crystal X-ray diffraction could not be obtained, and all attempts to separate the species by washing or recrystallization failed. Nevertheless, the obtained mixture perfectly converts to **7** using both synthetic protocols reported herein, thus can be regarded as a source of "LiCH$_2$P(CH$_3$)$_2$NDipp" (**6**).

**Characteristic NMR chemical shift of "LiCH$_2$P(CH$_3$)$_2$NDipp":**
**$^1$H NMR** (400 MHz, $C_6D_6$, 298 K): $\delta$ = -0.76 (d, $^2J_{P,H}$ = 11.9 Hz, 2H, CH$_2$), 0.98 (d, $^2J_{P,H}$ = 11.1 Hz, 6H, P(CH$_3$)$_2$), 1.31 (d, $^3J_{H,H}$ = 6.9 Hz, 12H, CH(C*H*$_3$)$_2$), 3.82 (hept, $^3J_{H,H}$ = 6.9 Hz, 2H, C*H*(CH$_3$)$_2$), 7.00-7.07 (m, 1H, CH$_{Aryl}$)*, 7.17-7.18 (m, 2H, CH$_{Aryl}$)** ppm.
* = overlap with CH$_{Aryl}$ signal of the other species
** = overlap with $C_6D_5H$ signal
**$^{13}$C{$^1$H} NMR** (126 MHz, $C_6D_6$, 298 K): $\delta$ = 6.7 (CH$_2$)***, 20.1 (d, $^1J_{P,C}$ = 50.4 Hz, P(CH$_3$)$_2$), 24.1 (br, CH(CH$_3$)$_2$), 27.3 (br, CH(C̲H$_3$)$_2$), 28.3 (C̲H(CH$_3$)$_2$), 121.7 (d, $J_{P,C}$ = 4.4 Hz, CH$_{Aryl}$), 122.9 (br, CH$_{Aryl}$), 145.1 (d, $J_{P,C}$ = 6.9 Hz, C$_{q,Aryl}$), 146.7 (d, $J_{P,C}$ = 9.4 Hz, C$_{q,Aryl}$) ppm.
*** = overlap with Si(CH$_3$)$_3$ signal of the other species
**$^7$Li{$^1$H} NMR** (140 MHz, $C_6D_6$, 298 K): $\delta$ = 2.5 ppm.
**$^{31}$P{$^1$H} NMR** (203 MHz, $C_6D_6$, 298 K): $\delta$ = 25.9 ppm.

**Characteristic NMR chemical shift of the remaining signals at 298 K:**
**$^1$H NMR** (400 MHz, $C_6D_6$, 298 K): $\delta$ = 0.30-0.36 (m, 18H, Si(CH$_3$)$_3$), 0.91 (d, $^2J_{P,H}$ = 12.1 Hz, 6H, P(CH$_3$)$_2$), 1.23 (d, $^3J_{H,H}$ = 6.9 Hz, 12H, CH(C*H*$_3$)$_2$), 3.35-3.42 (hept, $^3J_{H,H}$ = 6.8 Hz, 2H, C*H*(CH$_3$)$_2$), 7.00-7.07 (m, 1H, CH$_{Aryl}$)****, 7.09-7.10 (m, 2H, CH$_{Aryl}$) ppm.
**** = overlap with CH$_{Aryl}$ signal of "LiCH$_2$NP(CH$_3$)$_2$NDipp
**$^{13}$C{$^1$H} NMR** (126 MHz, $C_6D_6$, 298 K): $\delta$ = 6.8 (Si(CH$_3$)$_3$), 17.1 (d, $^1J_{P,C}$ = 68.1 Hz, P(CH$_3$)$_2$), 25.4 (CH(C̲H$_3$)$_2$), 28.7 (C̲H(CH$_3$)$_2$), 123.7 (d, $J_{P,C}$ = 4.0 Hz, CH$_{Aryl}$), 124.3 (d, $J_{P,C}$ = 4.1 Hz, CH$_{Aryl}$), 143.8 (br, C$_{q,Aryl}$), 144.7 (br d, $J_{P,C}$ = 7.3 Hz, C$_{q,Aryl}$) ppm.
**$^7$Li{$^1$H} NMR** (140 MHz, $C_6D_6$, 298 K): $\delta$ = 1.5 ppm.
**$^{31}$P{$^1$H} NMR** (203 MHz, $C_6D_6$, 298 K): $\delta$ = 11.3 (br) ppm.

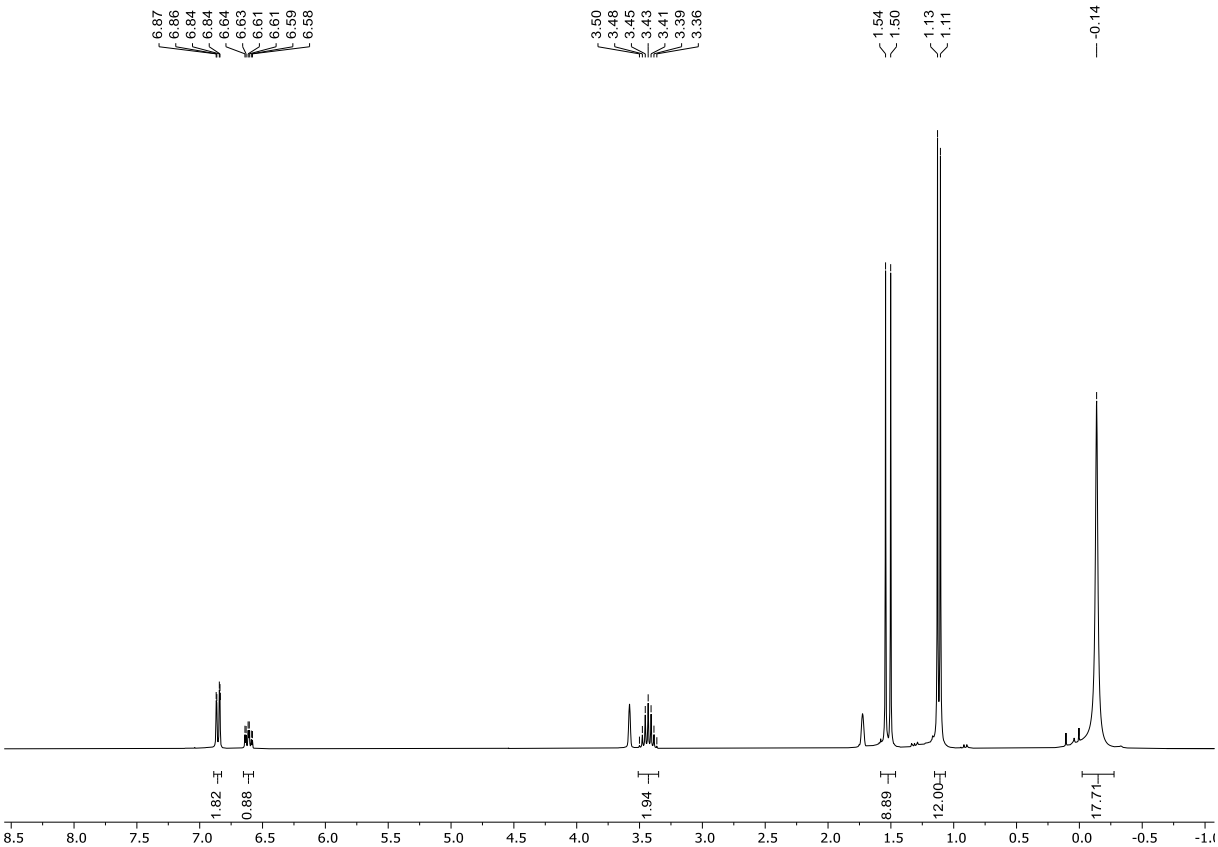


**Figure S52**. $^{1}$H NMR spectrum of DippNP(CH$_3$)$_3$ (**2a**) and LiN(SiMe$_3$)$_2$ after 8 h at 90 °C (400 MHz, THF-$d_8$, 298 K).

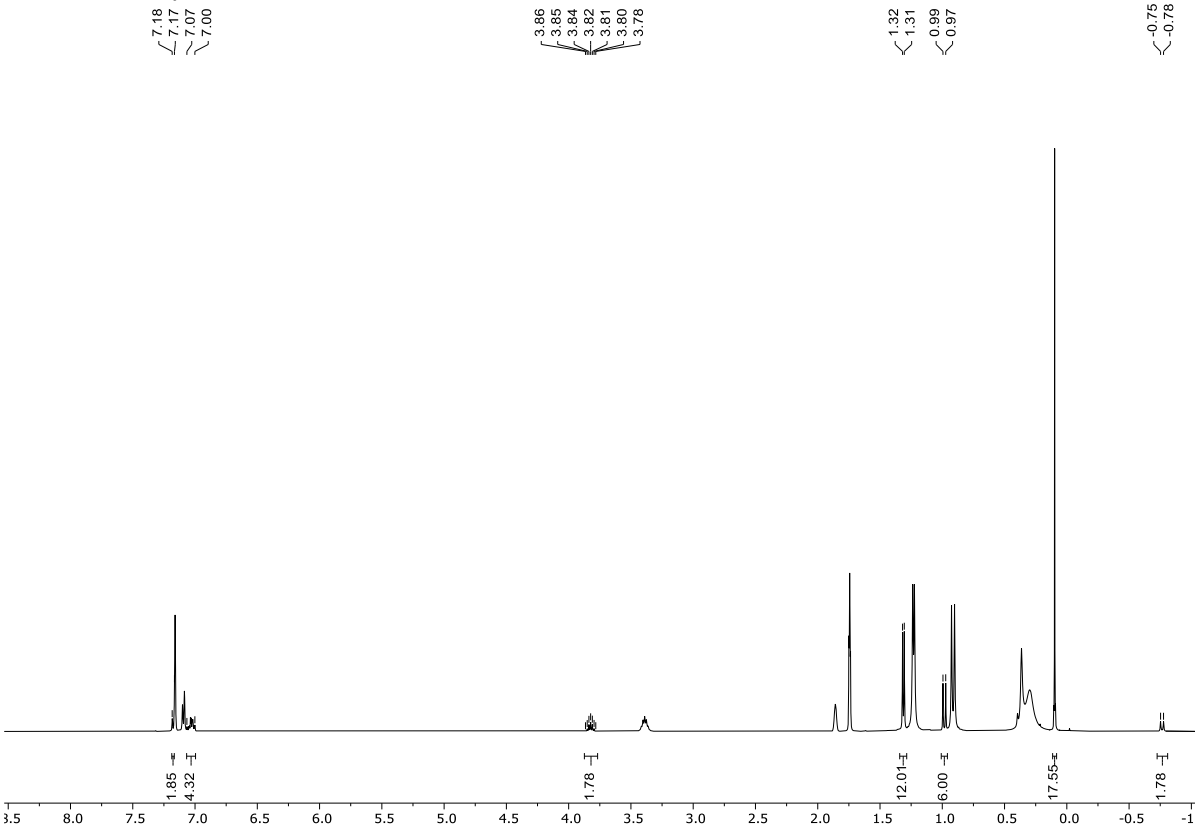


**Figure S53**. $^{1}$H NMR spectrum of the "LiCH$_2$P(CH$_3$)$_2$NDipp source" **6** with only the signals of **"**LiCH$_2$P(CH$_3$)$_2$NDipp" being picked (400 MHz, C$_6$D$_6$, 298 K); 0.10 ppm: HN(SiMe$_3$)$_2$; 1.74 and 1.86 ppm: adamantane.

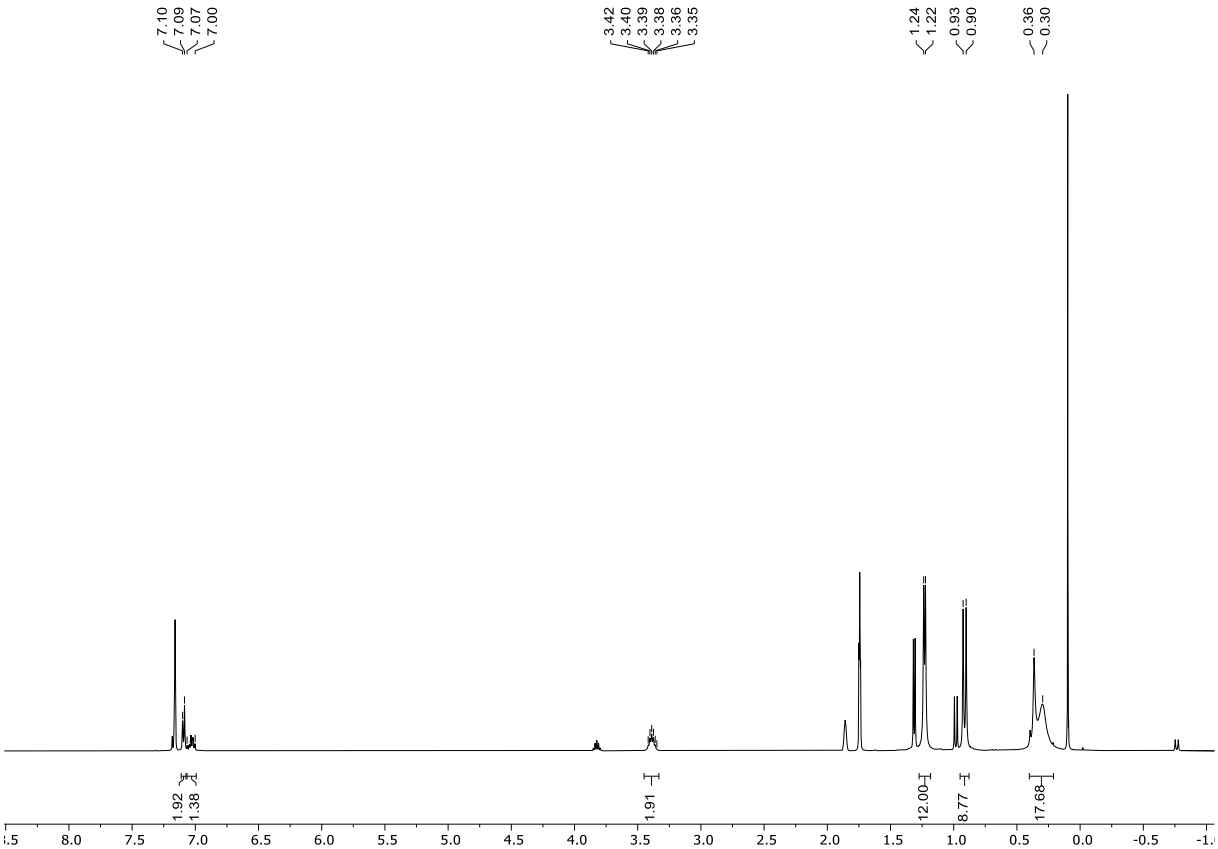


**Figure S54**. $^{1}H$ NMR spectrum of the "$LiCH_2P(CH_3)_2NDipp$ source" **6** with only the signals of the other species being picked (400 MHz, $C_6D_6$, 298 K); 0.10 ppm: $HN(SiMe_3)_2$; 1.74 and 1.86 ppm: adamantane.

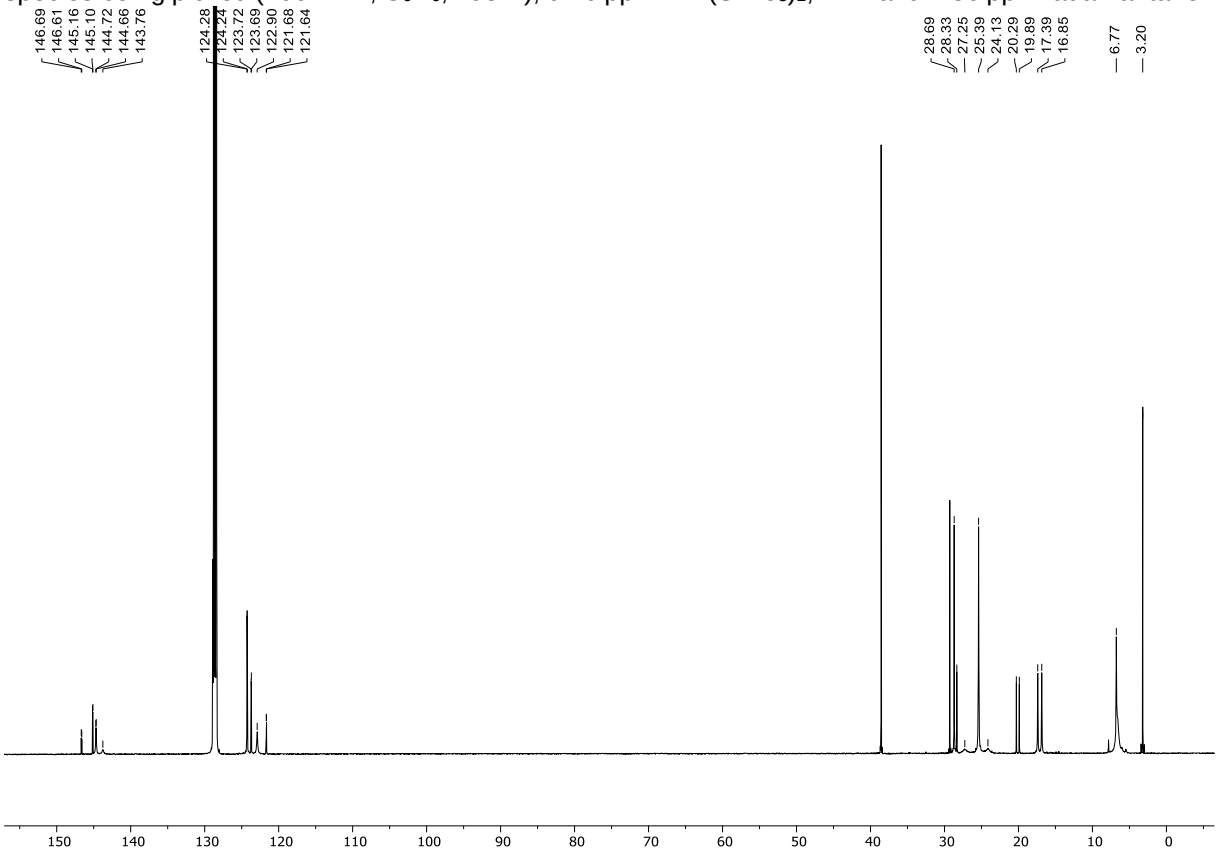


**Figure S55**. $^{13}C\{^{1}H\}$ NMR spectrum of of the "$LiCH_2P(CH_3)_2NDipp$ source" **6** (126 MHz, $C_6D_6$, 298 K); 3.2 ppm: $H(NSiMe_3)_2$; 29.3 and 38.6 ppm: adamantane.

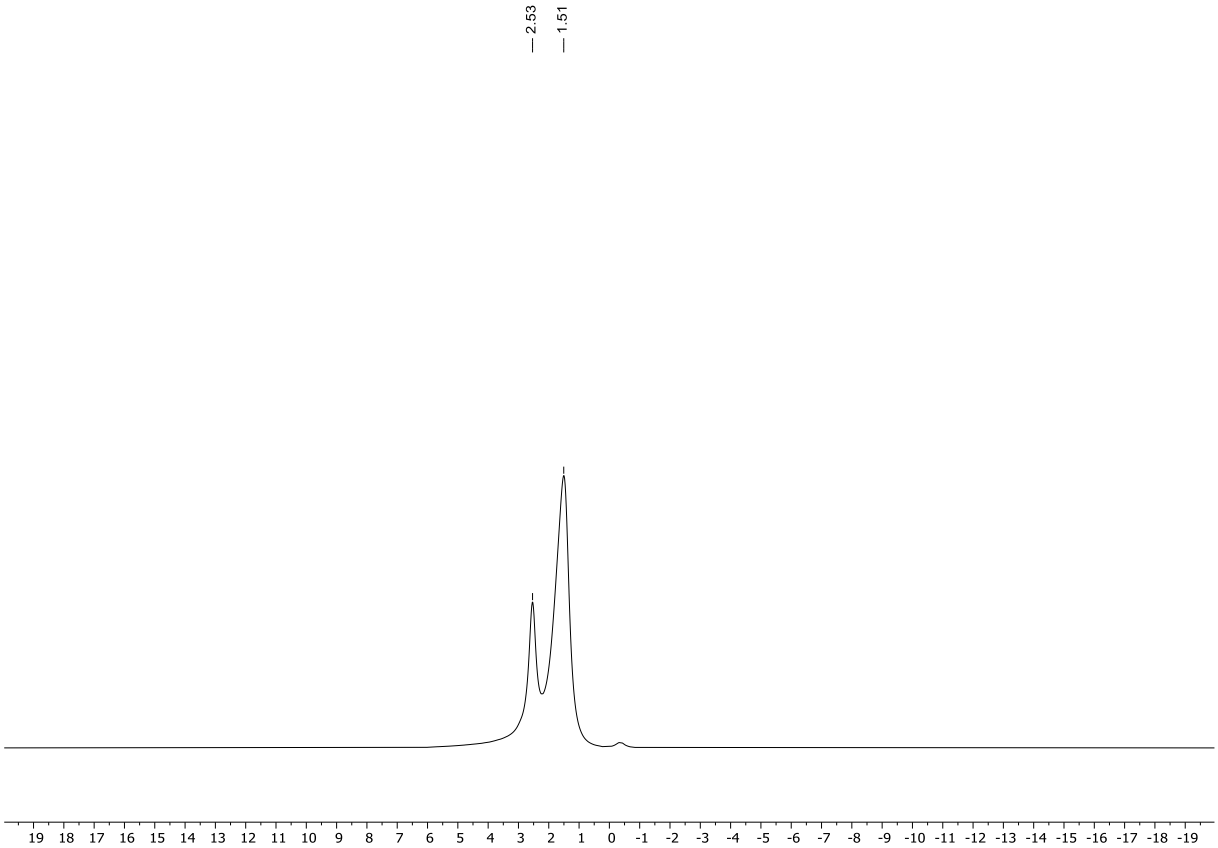


**Figure S56**. $^{7}Li\{^{1}H\}$ NMR spectrum of of the "$LiCH_2P(CH_3)_2NDipp$ source" **6** (140 MHz, $C_6D_6$, 298 K).

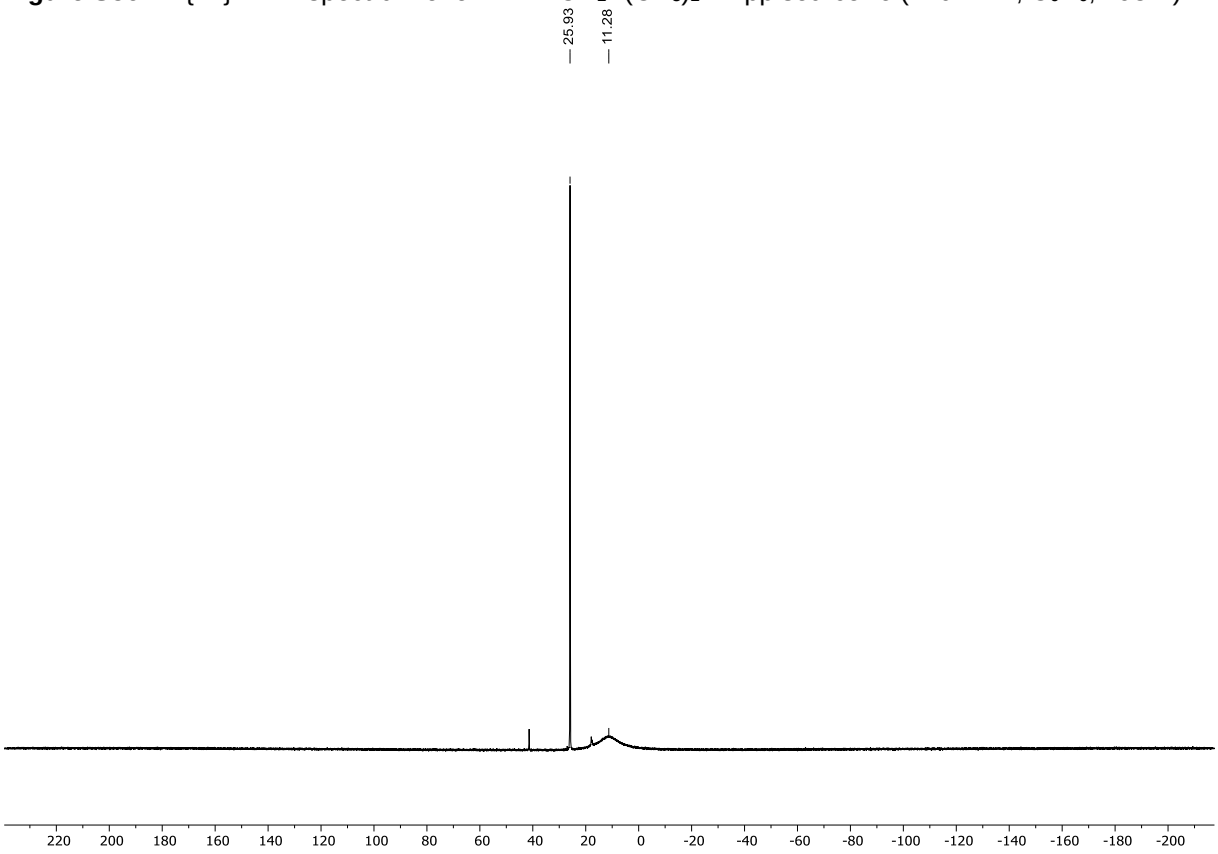


**Figure S57**. $^{31}P\{^{1}H\}$ NMR spectrum of the "$LiCH_2P(CH_3)_2NDipp$ source" **6** (203 MHz, $C_6D_6$, 298 K).

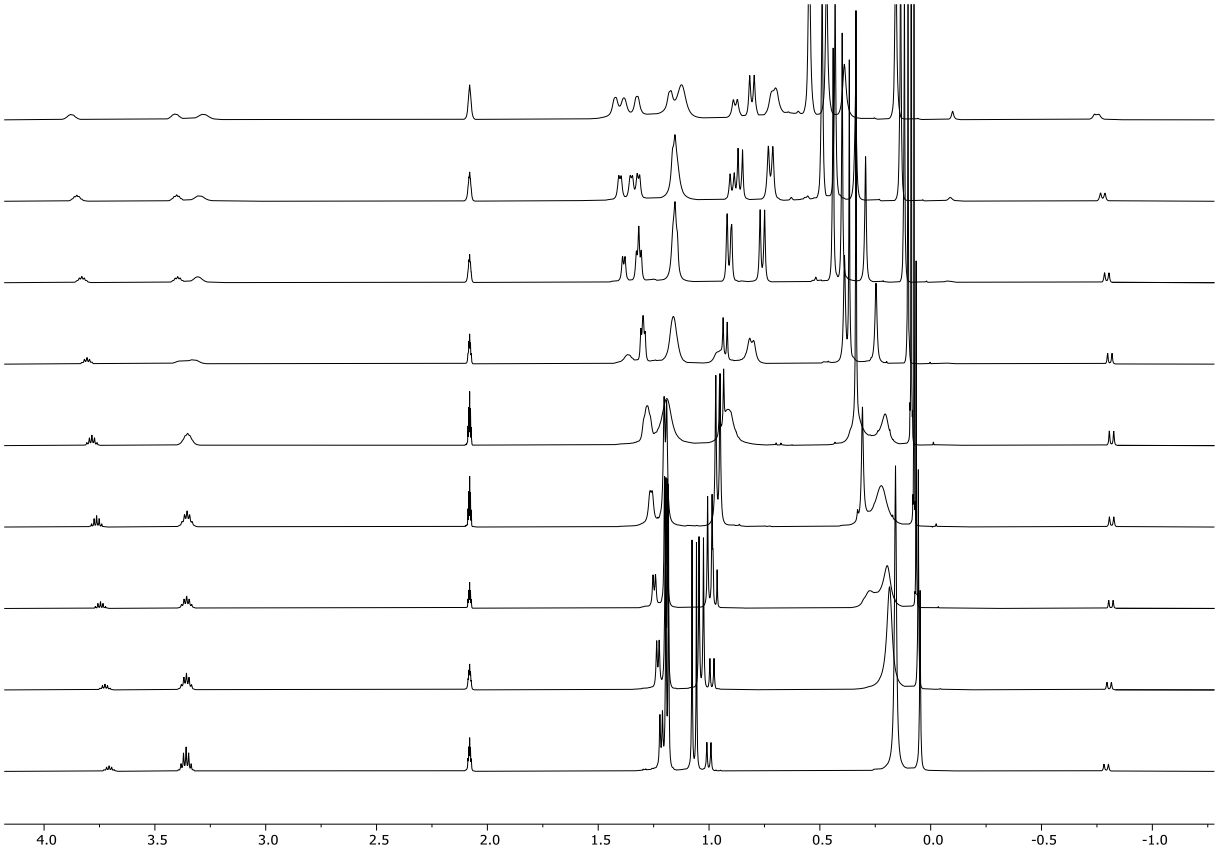


**Figure S58**. Excerpt of the VT $^{1}H$ NMR spectrum after the reaction of $DippNP(CH_3)_3$ (**2a**) and $LiN(SiMe_3)_2$ from 193 K (top) to 353 K (bottom) in steps of 20 K (600 MHz, toluene-$d_8$).

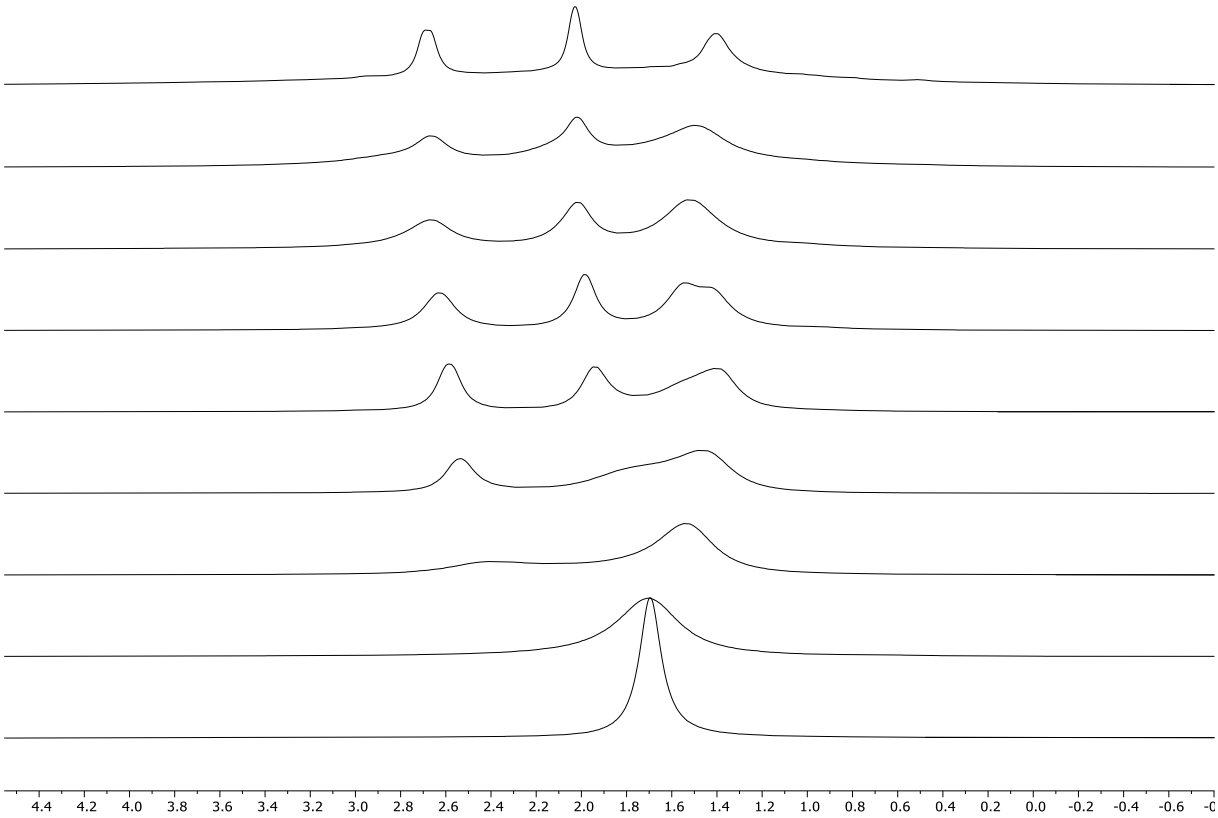


**Figure S59**. Excerpt of the VT $^{7}Li\{^{1}H\}$ NMR spectrum after the reaction of $DippNP(CH_3)_3$ (**2a**) and $LiN(SiMe_3)_2$ from 193 K (top) to 353 K (bottom) in steps of 20 K (140 MHz, toluene-$d_8$).

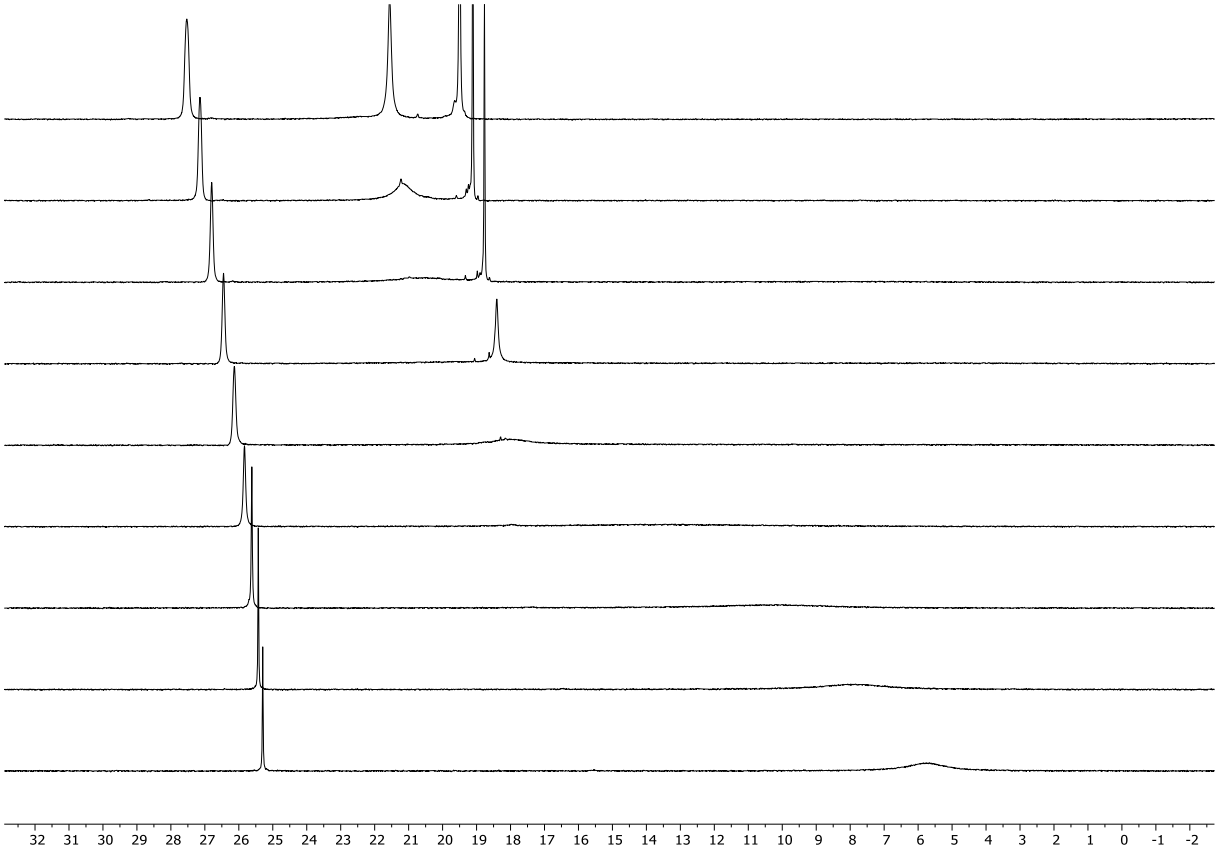


**Figure S60**. Excerpt of the VT $^{31}P\{^{1}H\}$ NMR spectrum after the reaction of DippNP$(CH_3)_3$ (**2a**) and LiN$(SiMe_3)_2$ from 193 K (top) to 353 K (bottom) in steps of 20 K (203 MHz, toluene-$d_8$).

## ECC-$^1$H-DOSY NMR experiment

The experiment was conducted using the pulse program *dstebpgp3s* at ambient temperature (298 K) on a *Bruker Avance III* HD 500 MHz spectrometer. Gradient pulses ranging from 0.65 ms to 1.0 ms were applied with a diffusion time of 0.075 s. Phases and baselines were corrected, and the *T1/T2* software on *Topspin 4.4.0* was utilized to derive the diffusion coefficients. These coefficients were then correlated to molecular weights (MW) using an external calibration curve (ECC) with shape optimization for dissipated spheres and ellipsoids (DSE).
For the experiment, DippNP($CH_3$)$_3$ (**2a**) (0.020 g, 0.080 mmol) and Li{N($Si(CH_3)_3$)$_2$} (0.017 g, 0.080 mmol) were dissolved in 0.4 mL of $C_6D_6$, and 1H-DOSY NMR experiments were performed. The $^1$H-DOSY NMR spectrum with adamantane as the internal standard is depicted in Figure S59.
The correlation of the results from the $^1$H-DOSY NMR experiment with the molecular weights of the proposed products "$LiCH_2P(CH_3)_2NDipp$" and "DippNP($CH_3$)$_3$•Li{N($Si(CH_3)_3$)$_2$}" shows overall good agreement and suggests a dimeric structure in solution for "$LiCH_2P(CH_3)_2NDipp$" (Table S1). Despite the product mixture being more complex, it can still be utilized quantitatively for the formation of the stannylenoid **7** reported herein, thus serving as a clean source of "$LiCH_2P(CH_3)_2NDipp$".

**Table S6**. Measured logarithmic diffusion coefficients Log($D_x$) from the $^1$H-DOSY NMR experiment and their normalized logarithmic diffusion coefficient log($D_{x,norm}$) by normalization with adamantane as internal standard with an experimental logarithmic diffusion coefficient of log($D_{ref}$) = -8.8854. Molecular weights $MW_{det}$ were determined with an external calibration curve (ECC), with shape optimization for dissipated spheres and ellipsoids (DSE).[S7] Aggregation tendencies were proposed based on the deviation in molecular weight, expressed as a percentage ($MW_{diff}$), between the determined molecular weight $MW_{det}$ and the theoretical molecular weight.

| Aggregate | log($D_x$) | log($D_{x,norm}$) | $MW_{det}$ [g•mol$^{-1}$] | Proposed Aggregation | $MW_{diff}$ [%] |
|---|---|---|---|---|---|
| HN{$Si(CH_3)_3$}$_2$ | -8.8976 | -8.8147 | 154 | HN{$Si(CH_3)_3$}$_2$ | 10 |
| **1** | -9.2635 | -9.1806 | 563 | [$LiCH_2P(CH_3)_2NDipp$]$_2$ | -9 |
| **2** | -9.1672 | -9.0843 | 394 | DippNP($CH_3$)$_3$•Li{N($Si(CH_3)_3$)$_2$} | 6 |

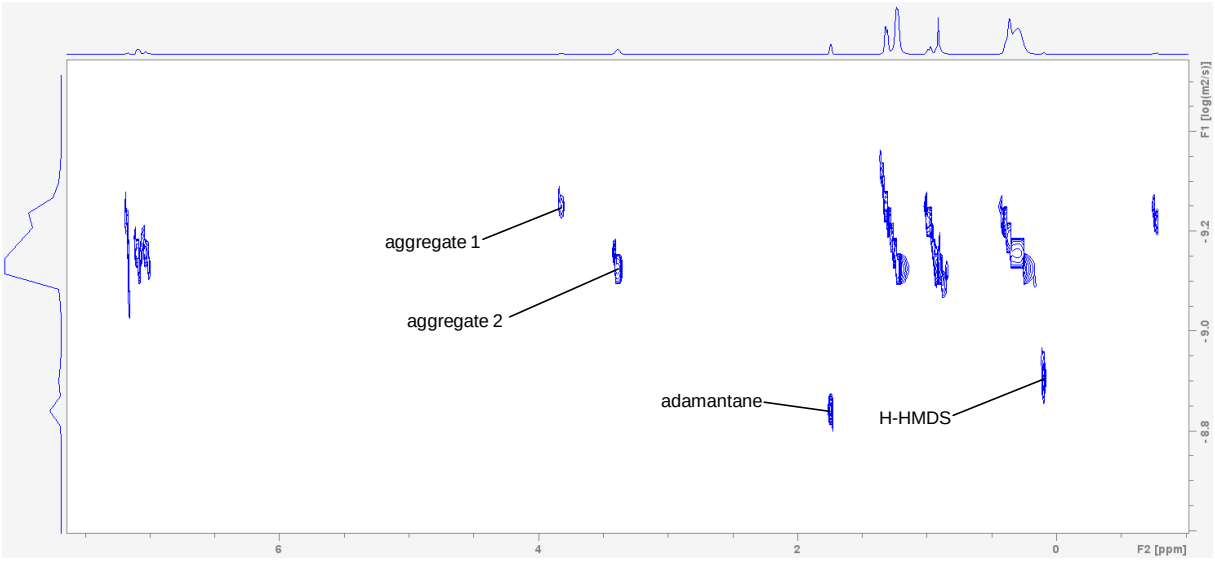


**Figure S61**. $^1$H-DOSY NMR spectrum of the obtained product mixture from the reaction of DippNP($CH_3$)$_3$ (**2a**) with Li{N($Si(CH_3)_3$)$_2$}.

**Reaction of $^{Mes}$TerSn{N(Si(CH$_3$)$_3$)$_2$} (1), LiN(Si(CH$_3$)$_3$)$_2$ and DippNP(CH$_3$)$_3$ (2a) / Reaction of $^{Mes}$TerSnCH$_2$P(CH$_3$)$_2$NDipp, LiN(Si(CH$_3$)$_3$)$_2$ and DippNP(CH$_3$)$_3$ (2a) – Synthesis of $^{Mes}$TerSn(CH$_2$P(CH$_3$)$_2$NDipp)$_2$Li (7)**

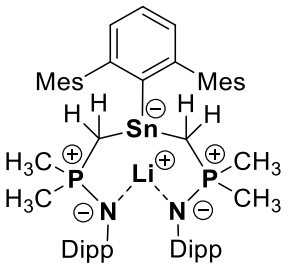


**A**) DippNP(CH$_3$)$_3$ (**2a**) (0.025 g, 0.099 mmol) and LiN(Si(CH$_3$)$_3$)$_2$ (0.017 g, 0.099 mmol) were dissolved in 0.4 mL of $C_6D_6$, leading to the immediate formation of the "LiCH$_2$P(CH$_3$)$_2$NDipp source" described on page 41 as verified by $^1$H NMR spectroscopy. $^{Mes}$TerSn{N(Si(CH$_3$)$_3$)$_2$} (**1**) (0.029 g, 0.050 mmol) in 0.2 mL of $C_6D_6$ was added which results in a clear yellow solution and the corresponding $^{31}$P NMR indicates full consumption of the starting material and formation of one main product. All volatiles were removed from the reaction mixture, the bright yellow residue was suspended in 1 mL of *n*-hexane, filtered and stored at -30 °C to give $^{Mes}$TerSn(CH$_2$P(CH$_3$)$_2$NDipp)$_2$Li (**7**) as colourless crystals. These crystals were suitable for single crystal X-ray diffraction.
**B**) DippNP(CH$_3$)$_3$ (**2a**) (0.011 g, 0.044 mmol) and LiN(Si(CH$_3$)$_3$)$_2$ (0.007 g, 0.044 mmol) were dissolved in 0.3 mL of $C_6D_6$, leading to the immediate formation of the mixture described on page 41 as verified by $^1$H NMR spectroscopy. $^{Mes}$TerSnCH$_2$P(CH$_3$)$_2$NDipp (**3a**) (0.030 g, 0.044 mmol) in 0.3 mL of $C_6D_6$ was added and subsequent analysis by $^{31}$P NMR spectroscopy reveals full consumption of the starting material and formation of $^{Mes}$TerSn(CH$_2$P(CH$_3$)$_2$NDipp)$_2$Li (**7**). All volatile components were removed under vacuum to give crude $^{Mes}$TerSn(CH$_2$P(CH$_3$)$_2$NDipp)$_2$Li (**7**) as a colourless solid.

**Yield**: 0.028 g (0.030 mmol; 60% (**A**)); 0.037 g (0.039 mmol; 89% (**B**)).
**$^1$H NMR** (500 MHz, $C_6D_6$, 298 K): $\delta$ = 0.43 (dd, $^2J_{P,H}$ = 12.4 Hz, $J$ = 5.0 Hz, 2H, CH$_2$), 0.75 (d, $^3J_{H,H}$ = 6.7 Hz, 6H, CH(C*H*$_3$)$_2$), 0.85-0.89 (m, 12H, P(CH$_3$)$_2$, CH(C*H*$_3$)$_2$), 0.93-1.03 (m, 2H, CH$_2$), 1.04 (d, $^2J_{P,H}$ = 11.8 Hz, 6H, PCH$_3$), 1.18 (d, $^3J_{H,H}$ = 6.9 Hz, 6H, CH(C*H*$_3$)$_2$), 1.22 (d, $^3J_{H,H}$ = 7.0 Hz, 6H, CH(C*H*$_3$)$_2$), 2.23 (s, 6H, CH$_3$), 2.30 (s, 12H, CH$_3$), 3.36 (hept, $^3J_{H,H}$ = 6.9 Hz, 2H, C*H*(CH$_3$)$_2$), 3.69 (hept, $^3J_{H,H}$ = 6.8 Hz, 2H, C*H*(CH$_3$)$_2$), 6.85 (m, 4H, CH$_{Aryl}$), 6.91-6.95 (m, 2H, CH$_{Aryl}$), 6.99-7.01 (m, 4H, CH$_{Aryl}$), 7.03-7.04 (m, 2H, CH$_{Aryl}$), 7.31-7.34 (m, 1H, CH$_{Aryl}$) ppm.
**$^{13}$C{$^1$H} NMR** (126 MHz, $C_6D_6$, 298 K): $\delta$ = 14.9 (dd, $^1J_{P,C}$ = 80.5 Hz, $J$ = 4.4 Hz, CH$_2$), 16.2 (d, $^1J_{P,C}$ = 62.3 Hz, P(CH$_3$)$_2$), 17.0 (d, $^1J_{P,C}$ = 52.4 Hz, P(CH$_3$)$_2$), 21.2 (CH$_3$), 22.1 (CH$_3$), 22.7 (CH(C̲H$_3$)$_2$), 23.4 (CH(C̲H$_3$)$_2$), 25.4 (CH(C̲H$_3$)$_2$), 26.1 (CH(C̲H$_3$)$_2$), 27.4 (C̲H(CH$_3$)$_2$), 27.9 (C̲H(CH$_3$)$_2$), 122.5 (d, $J_{P,C}$ = 4.3 Hz, CH$_{Aryl}$), 123.5 (dd, $J$ = 8.2 Hz, $J$ = 3.8 Hz, CH$_{Aryl}$), 127.3 (CH$_{Aryl}$), 127.9 (CH$_{Aryl}$)*, 128.4 (CH$_{Aryl}$)*, 135.7 (C$_{q,Aryl}$), 136.6 (C$_{q,Aryl}$), 143.1 (d, $J_{P,C}$ = 9.4 Hz, C$_{q,Aryl}$), 143.9 (C$_{q,Aryl}$), 143.9 (C$_{q,Aryl}$), 145.0 (dd, $J$ = 23.7 Hz, $J$ = 6.6 Hz, C$_{q,Aryl}$), 150.2 (C$_{q,Aryl}$) 157.6 (pt, $J$ = 8.3 Hz, C$_{q,Aryl}$) ppm.
* = overlap with $C_6D_6$ signal and assigned by $^1$H/$^{13}$C HMBC
**$^7$Li{$^1$H} NMR** (140 MHz, $C_6D_6$, 298 K): $\delta$ = 1.3 ppm.
**$^1$H/$^{15}$N HMBC NMR** (51 MHz, $C_6D_6$, 298 K): $\delta$ = -322.8 ppm.
**$^{31}$P{$^1$H} NMR** (203 MHz, $C_6D_6$, 298 K): $\delta$ = 30.5 (Sn satellites: $J_{119Sn,P}$ = 182.7 Hz, $J_{117Sn,P}$ = 173.7 Hz) ppm.
**$^{31}$P NMR** (203 MHz, $C_6D_6$, 298 K): $\delta$ = 30.5 (m) ppm.
**$^{119}$Sn{$^1$H} NMR** (187 MHz, $C_6D_6$, 298 K): $\delta$ = 437.9 (d, $^2J_{119Sn,P}$ = 167.0 Hz) ppm.
**EA**: Anal. calcd. for $C_{54}H_{75}LiN_2P_2Sn$: C, 69.01; H, 8.04; N, 2.98; Found: C, 68.77; H, 8.18; N, 2.87.

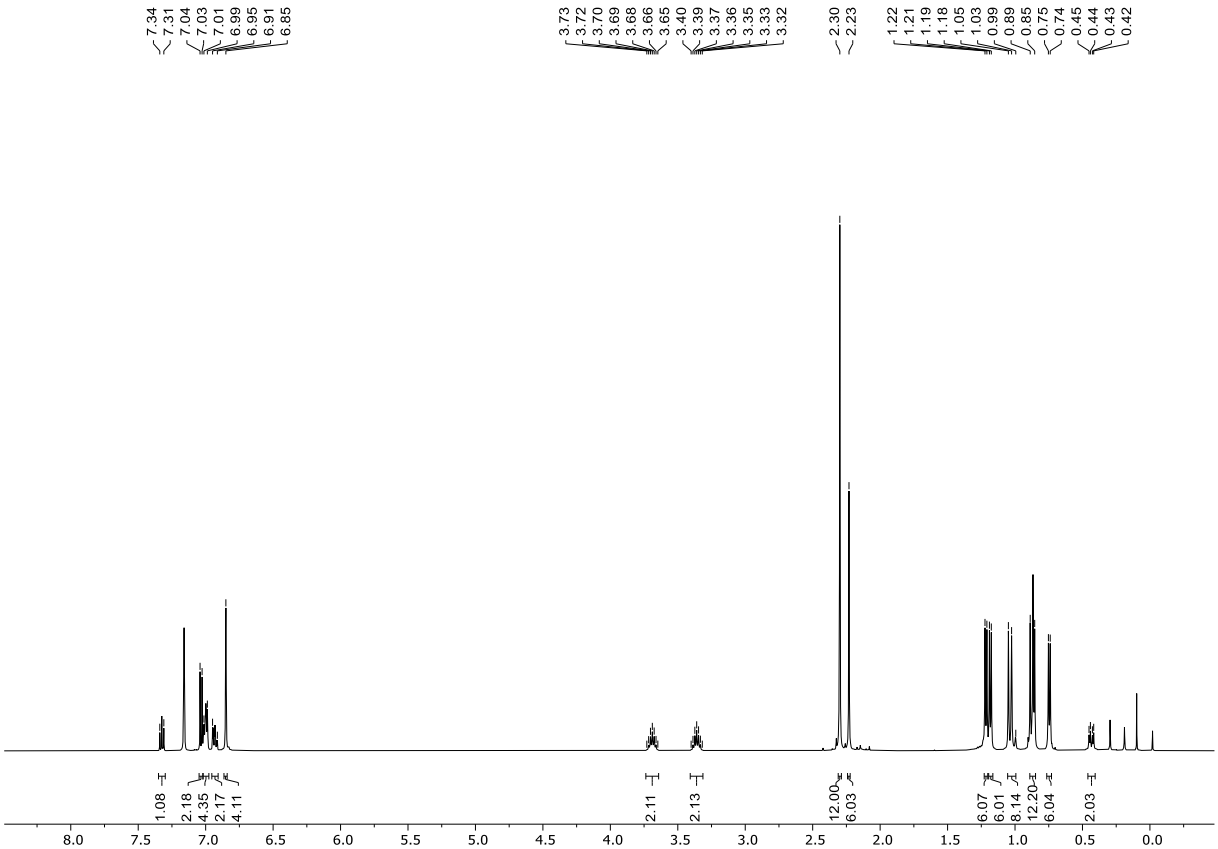

**Figure S62**. $^{1}H$ NMR spectrum of $^{Mes}TerSn(CH_2P(CH_3)_2NDipp)_2Li$ (**7**) (500 MHz, $C_6D_6$, 298 K); -0.02 ppm: $MesTerSn\{N(Si(CH_3)_3)_2\}$; 0.10 ppm: 0.10 ppm: $HN(Si(CH_3)_3)_2$; 0.19 ppm: $LiN(Si(CH_3)_3)_2$; 0.29 ppm: silicon grease.

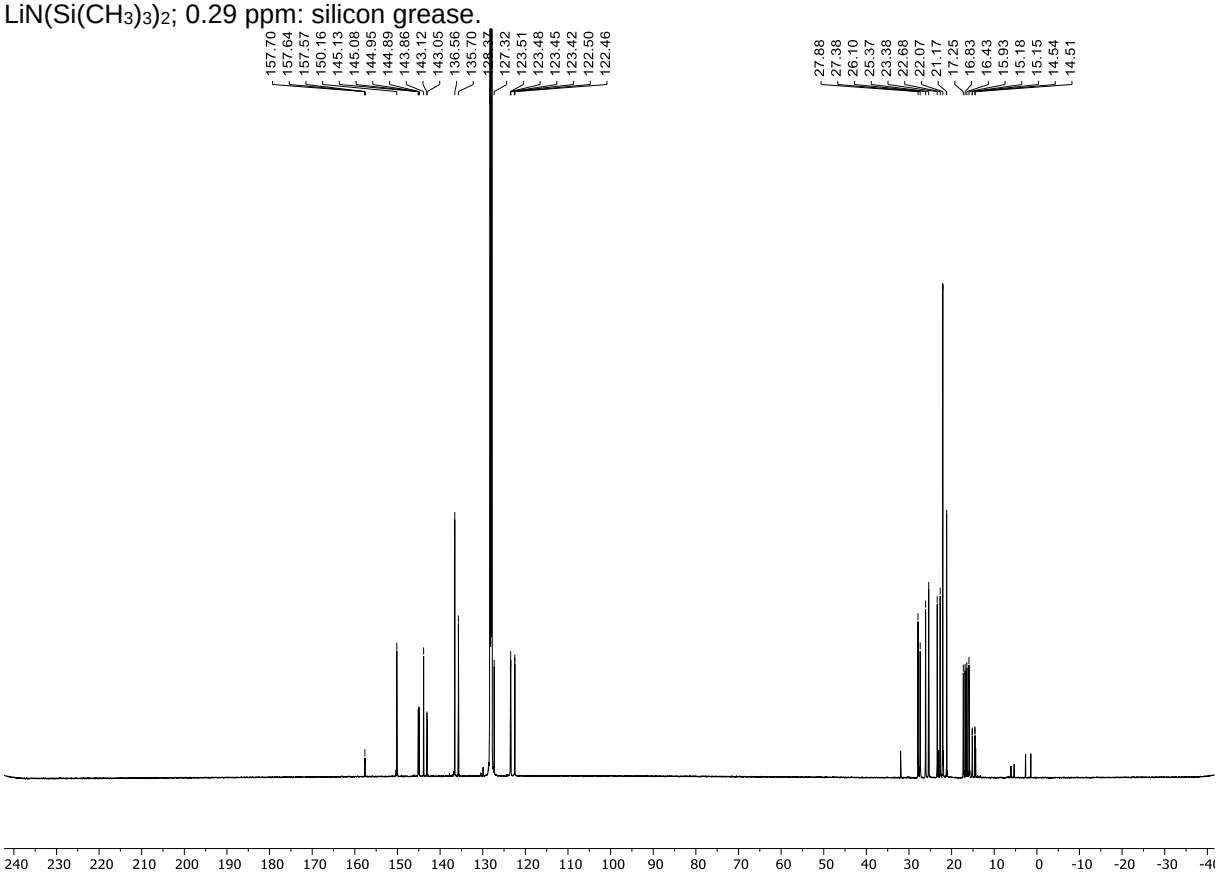

**Figure S63**. $^{13}C\{^{1}H\}$ NMR spectrum of $^{Mes}TerSn(CH_2P(CH_3)_2NDipp)_2Li$ (**7**) (126 MHz, $C_6D_6$, 298 K).

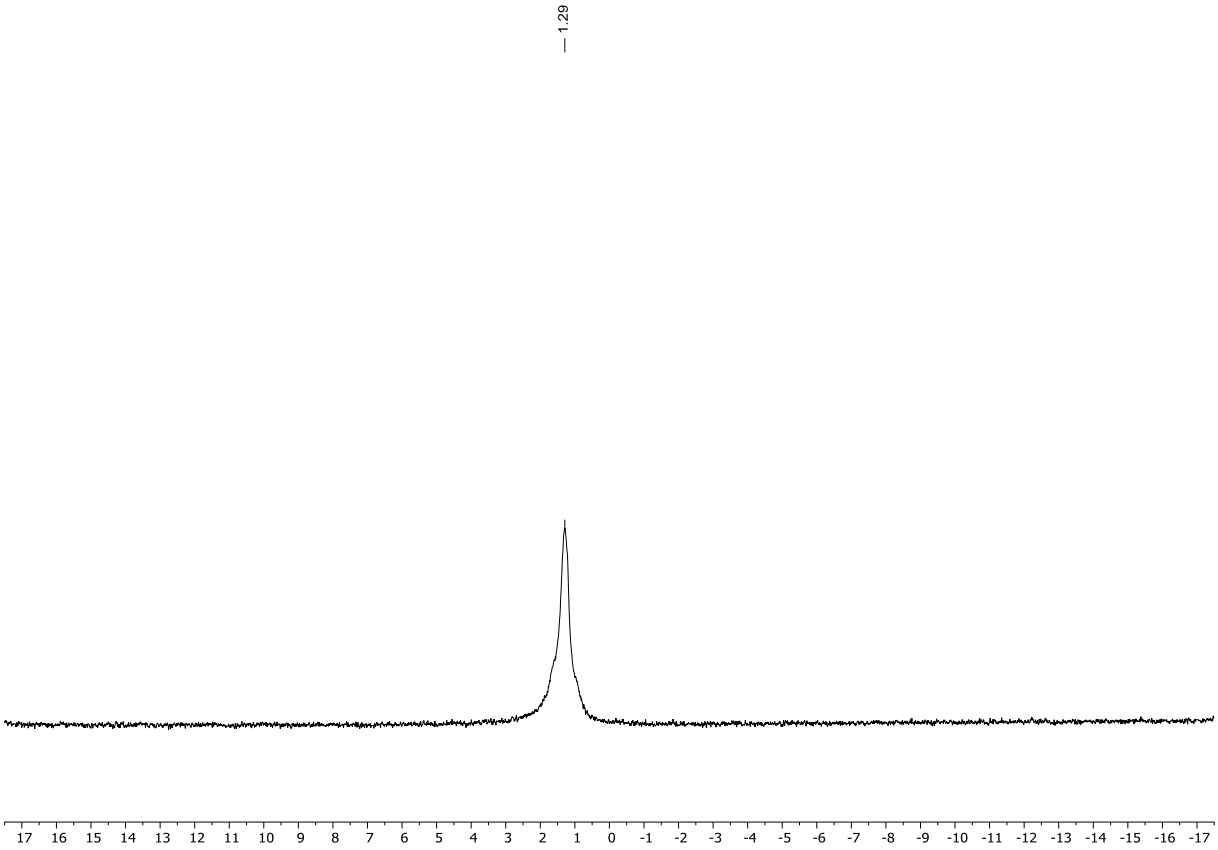


**Figure S64**. $^{7}Li\{^{1}H\}$ NMR spectrum of $^{Mes}TerSn(CH_2P(CH_3)_2NDipp)_2Li$ (**7**) (140 MHz, $C_6D_6$, 298 K).

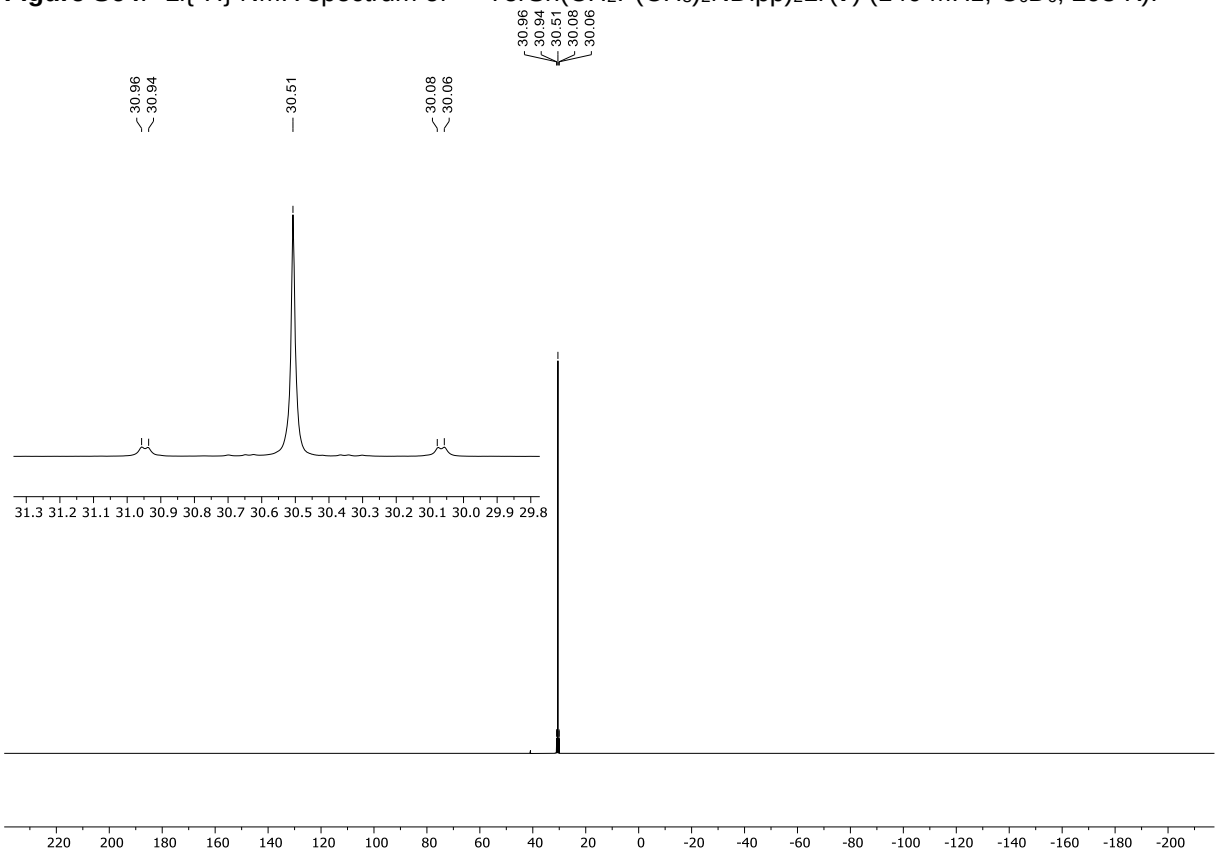


**Figure S65**. $^{31}P\{^{1}H\}$ NMR spectrum of $^{Mes}TerSn(CH_2P(CH_3)_2NDipp)_2Li$ (**7**) (203 MHz, $C_6D_6$, 298 K).

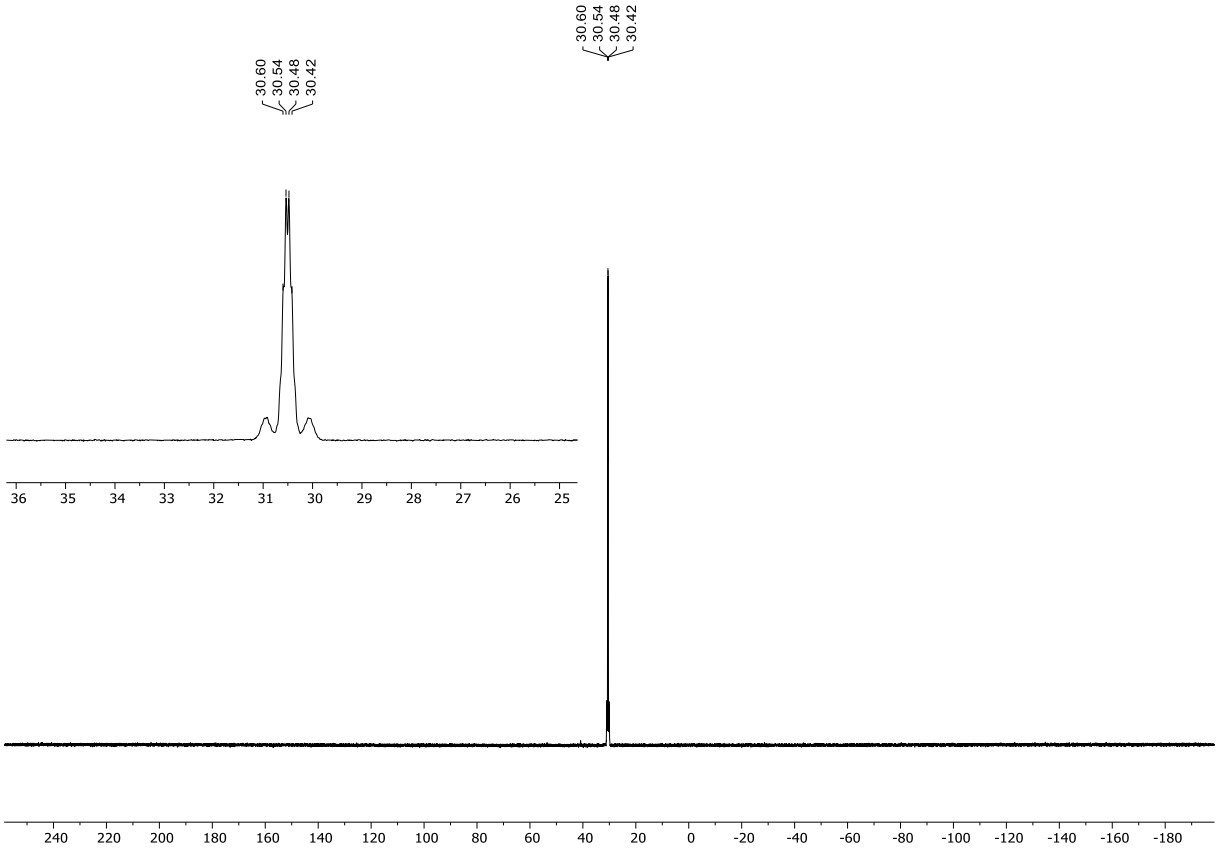


**Figure S66**. $^{31}$P NMR spectrum of $^{Mes}$TerSn(CH$_2$P(CH$_3$)$_2$NDipp)$_2$Li (**5a**) (203 MHz, C$_6$D$_6$, 298 K).

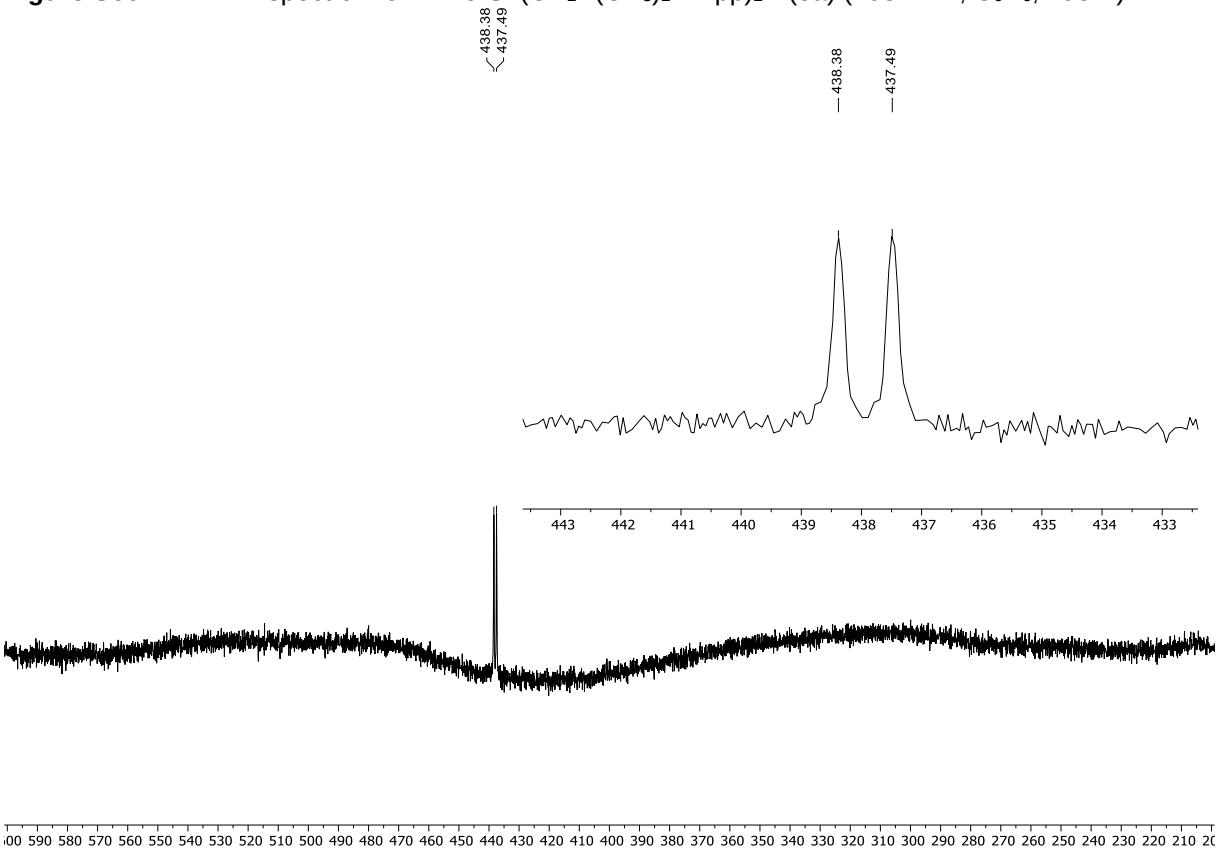


**Figure S67**. $^{119}$Sn{$^1$H} NMR spectrum of $^{Mes}$TerSn(CH$_2$P(CH$_3$)$_2$NDipp)$_2$Li (**5a**) (187 MHz, C$_6$D$_6$, 298 K).

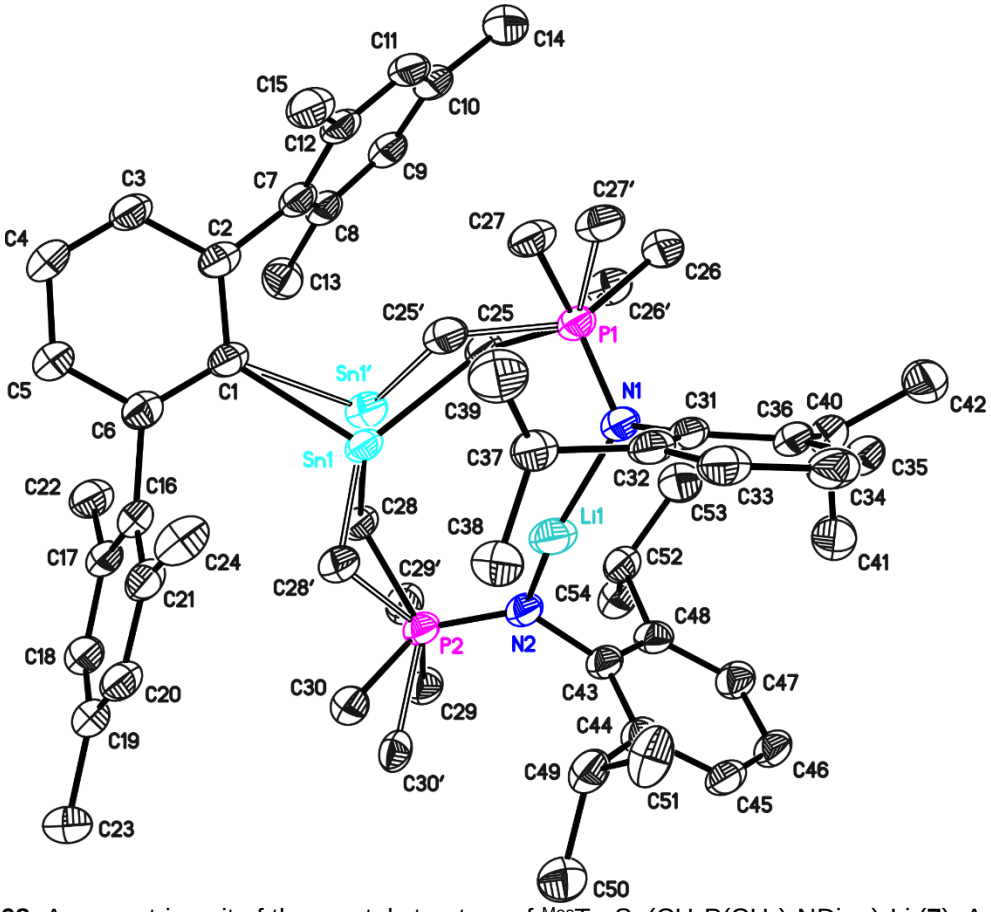


**Figure S68**. Asymmetric unit of the crystal structure of $^{Mes}$TerSn($CH_2$P($CH_3$)$_2$NDipp)$_2$Li (**7**). Anisotropic displacement parameters are drawn at the 50% probability level (hydrogen atoms have been omitted for clarity). Selected bond lengths (Å) and angles (deg): Sn1–C1 2.242(3), Sn1–C25 2.293(3), Sn1–C28 2.288(3), N1–P1 1.598(2), N2–P2 1.596(2), Sn1•••Li1 2.913(5), Li1–N1 1.921(5), Li1–N2 1.924(6), P1–C25 1.766(3), P2–C28 1.773(3), P1–C26 1.822(3), P1–C27 1.800(3), P2–C29 1.807(3), P2–C30 1.804(3), N1–C31 1.429(4), N2–C43 1.428(3), C1–Sn1–C25 106.51(10), C1–Sn1–C28 100.13(10), C25–Sn1–C28 91.72(11), N1–P1–C25 108.65(13), N2–P2–C28 109.55(13), N1–Li1–N2 147.1(3).

The data were collected on a non-merohedral twin with the twin law −0.67 0.64 0.00 0.87 0.66 0 0.44 0.84 −1.00. The fractional contribution of the minor component refined to 0.4996(15). The difference density maps showed signs of positional disorder involving Sn1. The disorder was modelled involving only Sn1 and the neighboring methyl and methylene groups, because the occupancy of the minor component refined to only 0.0483(9). The disorder was treated with distance restraints and restraints for the anisotropic displacement parameters.

**Table S7**. Bond lengths [Å] and angles [°] for **7**.

| | | | |
|---|---|---|---|
| Sn(1)-C(1) | 2.242(3) | Li(1)-N(2) | 1.924(6) |
| Sn(1)-C(28) | 2.288(3) | Li(1)-C(43) | 2.735(6) |
| Sn(1)-C(25) | 2.293(3) | Li(1)-P(1) | 2.962(5) |
| Sn(1)-Li(1) | 2.913(5) | Li(1)-P(2) | 3.097(5) |
| Sn(1')-C(25') | 2.264(17) | C(1)-C(6) | 1.412(4) |
| Sn(1')-C(28') | 2.274(17) | C(1)-C(2) | 1.417(4) |
| Sn(1')-C(1) | 2.361(5) | C(2)-C(3) | 1.400(4) |
| Li(1)-N(1) | 1.921(5) | C(2)-C(7) | 1.493(4) |

| | | | |
|---|---|---|---|
| C(3)-C(4) | 1.373(4) | C(31)-C(32) | 1.411(4) |
| C(4)-C(5) | 1.387(4) | C(31)-C(36) | 1.414(4) |
| C(5)-C(6) | 1.399(4) | C(32)-C(33) | 1.393(4) |
| C(6)-C(16) | 1.502(4) | C(32)-C(37) | 1.523(4) |
| C(7)-C(8) | 1.403(4) | C(33)-C(34) | 1.382(5) |
| C(7)-C(12) | 1.413(4) | C(34)-C(35) | 1.377(5) |
| C(8)-C(9) | 1.381(4) | C(35)-C(36) | 1.390(4) |
| C(8)-C(13) | 1.507(4) | C(36)-C(40) | 1.517(5) |
| C(9)-C(10) | 1.389(4) | C(37)-C(38) | 1.523(4) |
| C(10)-C(11) | 1.389(5) | C(37)-C(39) | 1.525(4) |
| C(10)-C(14) | 1.510(5) | C(40)-C(42) | 1.523(4) |
| C(11)-C(12) | 1.386(4) | C(40)-C(41) | 1.540(4) |
| C(12)-C(15) | 1.503(4) | C(43)-C(48) | 1.409(4) |
| C(16)-C(21) | 1.403(4) | C(43)-C(44) | 1.416(4) |
| C(16)-C(17) | 1.411(4) | C(44)-C(45) | 1.393(4) |
| C(17)-C(18) | 1.396(4) | C(44)-C(49) | 1.508(4) |
| C(17)-C(22) | 1.498(4) | C(45)-C(46) | 1.378(4) |
| C(18)-C(19) | 1.386(5) | C(46)-C(47) | 1.382(4) |
| C(19)-C(20) | 1.381(5) | C(47)-C(48) | 1.397(4) |
| C(19)-C(23) | 1.510(4) | C(48)-C(52) | 1.513(4) |
| C(20)-C(21) | 1.398(4) | C(49)-C(51) | 1.522(5) |
| C(21)-C(24) | 1.495(5) | C(49)-C(50) | 1.532(5) |
| N(1)-C(31) | 1.429(4) | C(52)-C(53) | 1.520(4) |
| N(1)-P(1) | 1.598(2) | C(52)-C(54) | 1.532(5) |
| P(1)-C(25) | 1.766(3) | | |
| P(1)-C(26') | 1.770(14) | C(1)-Sn(1)-C(28) | 100.13(10) |
| P(1)-C(25') | 1.790(15) | C(1)-Sn(1)-C(25) | 106.51(10) |
| P(1)-C(27) | 1.800(3) | C(28)-Sn(1)-C(25) | 91.72(11) |
| P(1)-C(27') | 1.814(14) | C(1)-Sn(1)-Li(1) | 173.15(12) |
| P(1)-C(26) | 1.822(3) | C(28)-Sn(1)-Li(1) | 84.45(13) |
| N(2)-C(43) | 1.428(3) | C(25)-Sn(1)-Li(1) | 68.05(13) |
| N(2)-P(2) | 1.596(2) | C(25')-Sn(1')-C(28') | 104.2(16) |
| P(2)-C(28') | 1.772(15) | C(25')-Sn(1')-C(1) | 84.3(6) |
| P(2)-C(28) | 1.773(3) | C(28')-Sn(1')-C(1) | 93.1(5) |
| P(2)-C(29') | 1.777(14) | N(1)-Li(1)-N(2) | 147.1(3) |
| P(2)-C(30) | 1.804(3) | N(1)-Li(1)-C(43) | 131.2(3) |
| P(2)-C(29) | 1.807(3) | N(2)-Li(1)-C(43) | 29.68(12) |
| P(2)-C(30') | 1.823(15) | N(1)-Li(1)-Sn(1) | 95.7(2) |

| | | | |
|---|---|---|---|
| N(2)-Li(1)-Sn(1) | 90.7(2) | C(7)-C(12)-C(15) | 120.7(3) |
| C(43)-Li(1)-Sn(1) | 120.27(19) | C(21)-C(16)-C(17) | 119.6(3) |
| N(1)-Li(1)-P(1) | 29.44(11) | C(21)-C(16)-C(6) | 123.1(3) |
| N(2)-Li(1)-P(1) | 129.1(3) | C(17)-C(16)-C(6) | 116.7(3) |
| C(43)-Li(1)-P(1) | 133.2(2) | C(18)-C(17)-C(16) | 119.4(3) |
| Sn(1)-Li(1)-P(1) | 70.91(12) | C(18)-C(17)-C(22) | 119.8(3) |
| N(1)-Li(1)-P(2) | 152.0(3) | C(16)-C(17)-C(22) | 120.7(3) |
| N(2)-Li(1)-P(2) | 25.61(11) | C(19)-C(18)-C(17) | 121.6(3) |
| C(43)-Li(1)-P(2) | 54.62(11) | C(20)-C(19)-C(18) | 118.1(3) |
| Sn(1)-Li(1)-P(2) | 66.82(11) | C(20)-C(19)-C(23) | 121.7(3) |
| P(1)-Li(1)-P(2) | 123.28(18) | C(18)-C(19)-C(23) | 120.2(3) |
| C(6)-C(1)-C(2) | 116.9(3) | C(19)-C(20)-C(21) | 122.7(3) |
| C(6)-C(1)-Sn(1) | 113.80(19) | C(20)-C(21)-C(16) | 118.5(3) |
| C(2)-C(1)-Sn(1) | 127.8(2) | C(20)-C(21)-C(24) | 119.3(3) |
| C(6)-C(1)-Sn(1') | 131.2(2) | C(16)-C(21)-C(24) | 122.1(3) |
| C(2)-C(1)-Sn(1') | 107.7(2) | C(31)-N(1)-P(1) | 124.07(18) |
| C(3)-C(2)-C(1) | 120.6(3) | C(31)-N(1)-Li(1) | 119.6(2) |
| C(3)-C(2)-C(7) | 115.2(2) | P(1)-N(1)-Li(1) | 114.3(2) |
| C(1)-C(2)-C(7) | 124.1(3) | N(1)-P(1)-C(25) | 108.65(13) |
| C(4)-C(3)-C(2) | 121.3(3) | N(1)-P(1)-C(26') | 120.4(14) |
| C(3)-C(4)-C(5) | 119.2(3) | N(1)-P(1)-C(25') | 102.8(13) |
| C(4)-C(5)-C(6) | 120.6(3) | C(26')-P(1)-C(25') | 109.8(14) |
| C(5)-C(6)-C(1) | 121.1(3) | N(1)-P(1)-C(27) | 114.36(14) |
| C(5)-C(6)-C(16) | 114.9(3) | C(25)-P(1)-C(27) | 109.87(15) |
| C(1)-C(6)-C(16) | 123.6(2) | N(1)-P(1)-C(27') | 111.3(14) |
| C(8)-C(7)-C(12) | 118.9(3) | C(26')-P(1)-C(27') | 105.7(16) |
| C(8)-C(7)-C(2) | 120.8(3) | C(25')-P(1)-C(27') | 106.1(14) |
| C(12)-C(7)-C(2) | 120.1(3) | N(1)-P(1)-C(26) | 114.38(14) |
| C(9)-C(8)-C(7) | 119.7(3) | C(25)-P(1)-C(26) | 108.09(15) |
| C(9)-C(8)-C(13) | 119.1(3) | C(27)-P(1)-C(26) | 101.17(16) |
| C(7)-C(8)-C(13) | 121.2(3) | N(1)-P(1)-Li(1) | 36.21(13) |
| C(8)-C(9)-C(10) | 122.4(3) | C(25)-P(1)-Li(1) | 72.50(14) |
| C(11)-C(10)-C(9) | 117.5(3) | C(26')-P(1)-Li(1) | 110.4(15) |
| C(11)-C(10)-C(14) | 121.5(3) | C(25')-P(1)-Li(1) | 74.4(12) |
| C(9)-C(10)-C(14) | 121.0(3) | C(27)-P(1)-Li(1) | 126.74(16) |
| C(12)-C(11)-C(10) | 122.2(3) | C(27')-P(1)-Li(1) | 141.3(14) |
| C(11)-C(12)-C(7) | 119.4(3) | C(26)-P(1)-Li(1) | 129.59(16) |
| C(11)-C(12)-C(15) | 119.9(3) | C(43)-N(2)-P(2) | 125.94(19) |

| | | | |
|---|---|---|---|
| C(43)-N(2)-Li(1) | 108.5(2) | C(35)-C(34)-C(33) | 119.6(3) |
| P(2)-N(2)-Li(1) | 123.0(2) | C(34)-C(35)-C(36) | 121.7(3) |
| N(2)-P(2)-C(28') | 104.5(13) | C(35)-C(36)-C(31) | 118.9(3) |
| N(2)-P(2)-C(28) | 109.55(13) | C(35)-C(36)-C(40) | 120.2(3) |
| N(2)-P(2)-C(29') | 118.0(14) | C(31)-C(36)-C(40) | 120.7(3) |
| C(28')-P(2)-C(29') | 113.2(15) | C(32)-C(37)-C(38) | 110.7(3) |
| N(2)-P(2)-C(30) | 114.84(14) | C(32)-C(37)-C(39) | 113.1(3) |
| C(28)-P(2)-C(30) | 105.19(15) | C(38)-C(37)-C(39) | 110.9(3) |
| N(2)-P(2)-C(29) | 111.88(14) | C(36)-C(40)-C(42) | 113.5(3) |
| C(28)-P(2)-C(29) | 112.26(15) | C(36)-C(40)-C(41) | 109.4(3) |
| C(30)-P(2)-C(29) | 102.87(15) | C(42)-C(40)-C(41) | 111.1(3) |
| N(2)-P(2)-C(30') | 109.3(13) | C(48)-C(43)-C(44) | 119.1(3) |
| C(28')-P(2)-C(30') | 108.2(19) | C(48)-C(43)-N(2) | 120.5(3) |
| C(29')-P(2)-C(30') | 103.4(15) | C(44)-C(43)-N(2) | 120.1(3) |
| N(2)-P(2)-Li(1) | 31.41(13) | C(48)-C(43)-Li(1) | 124.2(2) |
| C(28')-P(2)-Li(1) | 73.2(13) | C(44)-C(43)-Li(1) | 97.2(2) |
| C(28)-P(2)-Li(1) | 88.40(13) | N(2)-C(43)-Li(1) | 41.84(16) |
| C(29')-P(2)-Li(1) | 134.6(14) | C(45)-C(44)-C(43) | 119.2(3) |
| C(30)-P(2)-Li(1) | 100.34(15) | C(45)-C(44)-C(49) | 118.2(3) |
| C(29)-P(2)-Li(1) | 143.14(15) | C(43)-C(44)-C(49) | 122.7(3) |
| C(30')-P(2)-Li(1) | 117.5(13) | C(46)-C(45)-C(44) | 121.9(3) |
| P(1)-C(25)-Sn(1) | 113.61(14) | C(45)-C(46)-C(47) | 118.9(3) |
| P(2)-C(28)-Sn(1) | 108.66(14) | C(46)-C(47)-C(48) | 121.6(3) |
| P(1)-C(25')-Sn(1') | 126.4(12) | C(47)-C(48)-C(43) | 119.4(3) |
| P(2)-C(28')-Sn(1') | 108.2(9) | C(47)-C(48)-C(52) | 118.3(3) |
| C(32)-C(31)-C(36) | 119.4(3) | C(43)-C(48)-C(52) | 122.3(3) |
| C(32)-C(31)-N(1) | 120.2(2) | C(44)-C(49)-C(51) | 112.3(3) |
| C(36)-C(31)-N(1) | 120.1(3) | C(44)-C(49)-C(50) | 110.5(3) |
| C(33)-C(32)-C(31) | 119.4(3) | C(51)-C(49)-C(50) | 110.1(3) |
| C(33)-C(32)-C(37) | 118.7(3) | C(48)-C(52)-C(53) | 110.7(3) |
| C(31)-C(32)-C(37) | 121.8(3) | C(48)-C(52)-C(54) | 112.1(3) |
| C(34)-C(33)-C(32) | 121.0(3) | C(53)-C(52)-C(54) | 111.3(3) |

**Reactions of $^{Mes}$TerSnCH$_2$P(CH$_3$)$_2$NR (3a-c) (R = XyDipp, Xyl, Ad) with NH$_3$ – Formation of [$^{Mes}$TerSn(μ-NH$_2$)$_2$]$_2$ (5) and the Respective Iminophosphoranes RNP(CH$_3$)$_3$ (2a-c)**

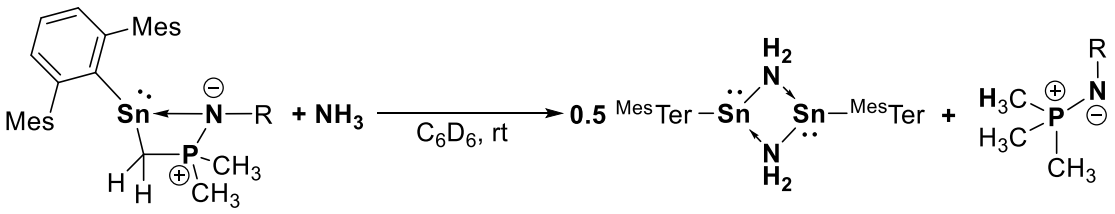


The complexes $^{Mes}$TerSnCH$_2$P(CH$_3$)$_2$NR (**3a-c**) (0.030 g) were dissolved in 0.5 mL of C$_6$D$_6$ and transferred to J-Young NMR tubes. After three freeze-pump-thaw cycles, the NMR tubes were backfilled with 1.2 bar of ammonia. The reactions were monitored by $^{31}$P NMR spectroscopy (Figures S69-S71), which initially indicated the formation of the respective free iminophosphorane **2a-c**. Depending on the substitution pattern, the reaction finished quickly for R = Ad and took longer for the aryl-substituted derivatives. Additionally, in the case of R = Dipp, an additional species was detected ($\delta^{31}$P = 16.3 ppm; Figure S70; for details see page S73). The reactions continued over time until only the signals of the free iminophosphorane **2a-c** remained. The final tin-containing product of all reactions could be identified as the NH$_2$-bridged dimeric tin complex [$^{Mes}$TerSn(μ-NH$_2$)]$_2$ (**5**) by multinuclear NMR spectroscopy. Crystals suitable for single-crystal X-ray diffraction of **5** were obtained from saturated toluene solutions of the reaction mixtures at -30 °C and match the literature data of previously reported **6**.[S8]

**NMR data of [$^{Mes}$TerSn(NH$_2$)]$_2$ (5)**:
**$^1$H NMR** (500 MHz, C$_6$D$_6$, 298 K): δ = 0.11 (s(br), 4H, NH$_2$), 2.15 (s, 24H, CH$_3$), 2.24 (s, 12H, CH$_3$), 6.79 (s, 8H, CH$_{Aryl}$), 6.94-6.96 (m, 4H, CH$_{Aryl}$), 7.22-7.25 (m, 2H, CH$_{Aryl}$) ppm.
**$^{13}$C{$^1$H} NMR** (126 MHz, C$_6$D$_6$, 298 K): δ = 21.3 (), 21.5 (), 128.0 (CH$_{Aryl}$)*, 128.2 (CH$_{Aryl}$)*, 128.7 (CH$_{Aryl}$), 136.2 (C$_{q,Aryl}$), 136.3 (C$_{q,Aryl}$), 141.0 (C$_{q,Aryl}$), 147.9 (C$_{q,Aryl}$), 165.9 (C$_{q,Aryl}$Sn) ppm.
* = overlap with C$_6$D$_6$ signal(s) and assigned by $^1$H/$^{13}$C HMBC
**$^1$H/$^{15}$N HMBC NMR** (51 MHz, C$_6$D$_6$, 298 K): δ = -375.4 ppm.
**$^{119}$Sn{$^1$H} NMR** (187 MHz, C$_6$D$_6$, 298 K): δ = 313.8 ppm.

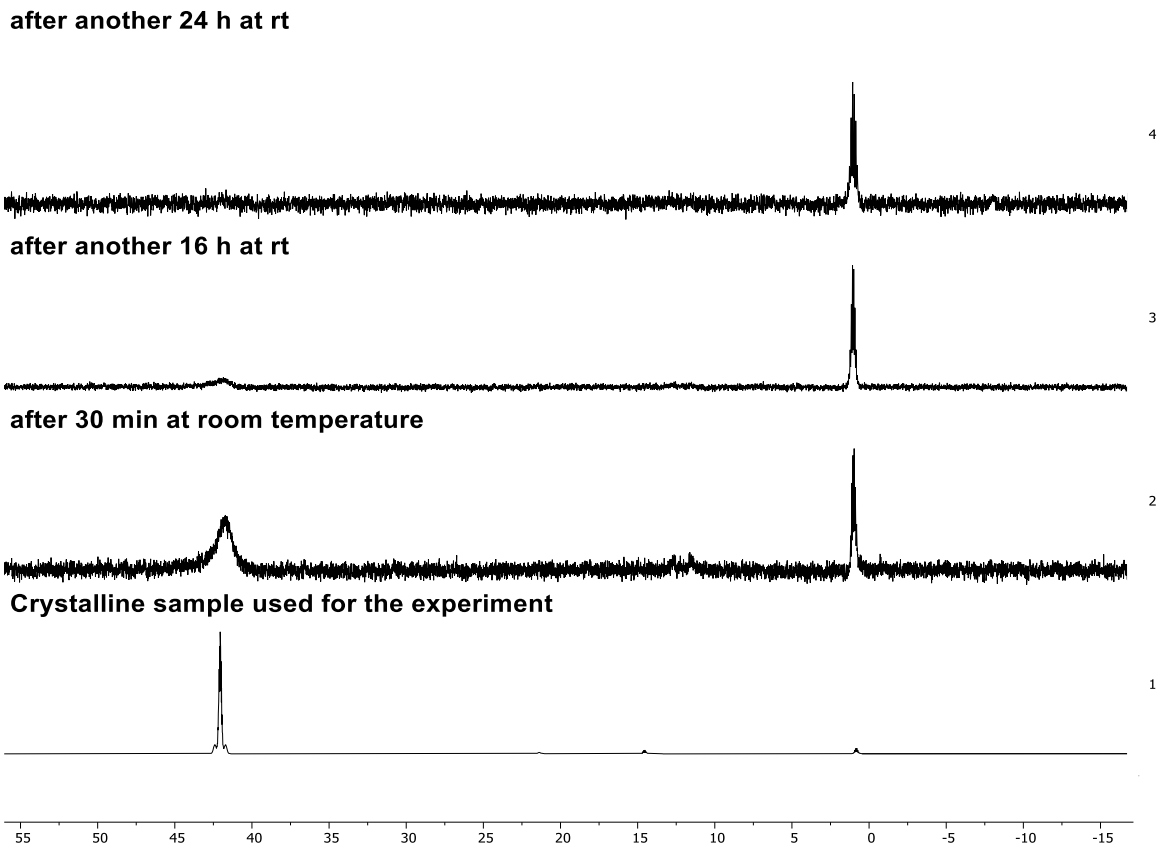


**Figure S69**. Monitoring of the reaction of $^{Mes}$TerSnCH$_2$PNXyl (**3b**) with ammonia by $^{31}$P NMR spectroscopy (203 MHz, $C_6D_6$, 298 K).

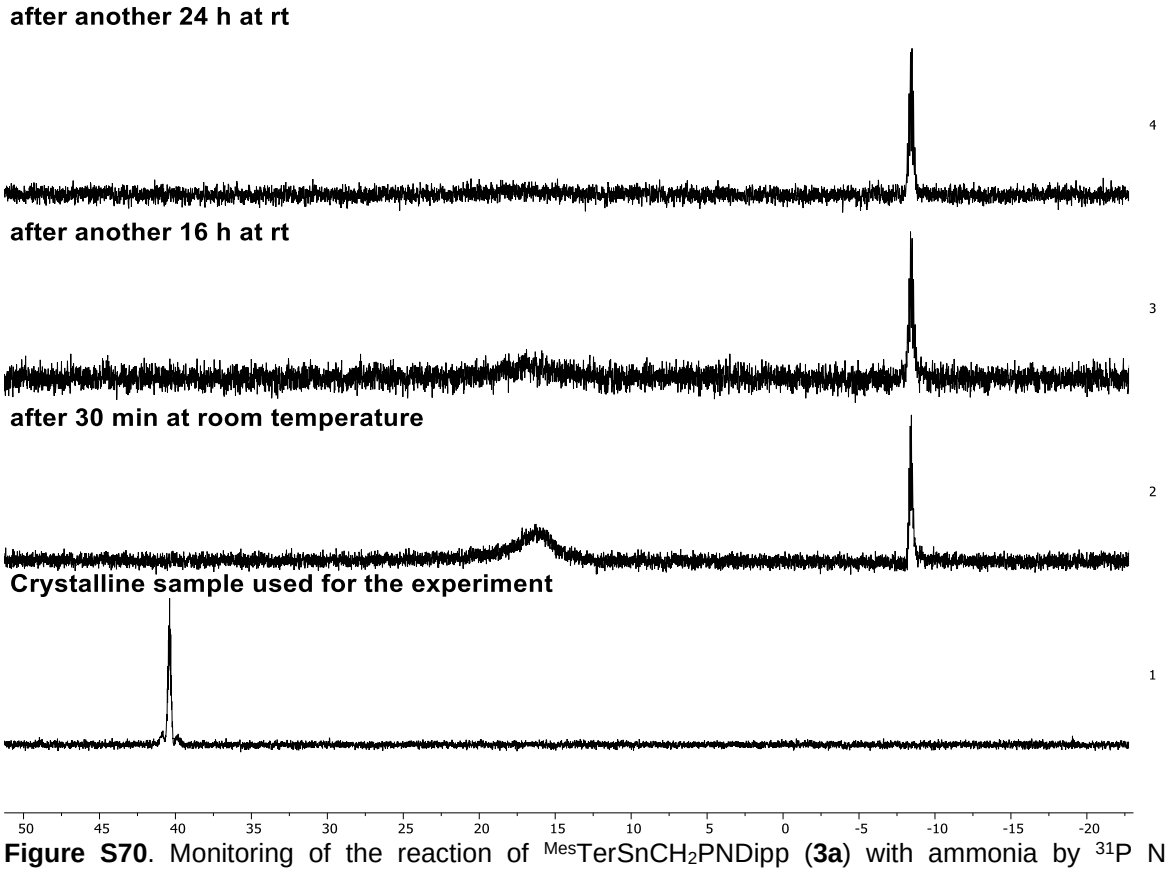


**Figure S70**. Monitoring of the reaction of $^{Mes}$TerSnCH$_2$PNDipp (**3a**) with ammonia by $^{31}$P NMR spectroscopy (203 MHz, $C_6D_6$, 298 K).

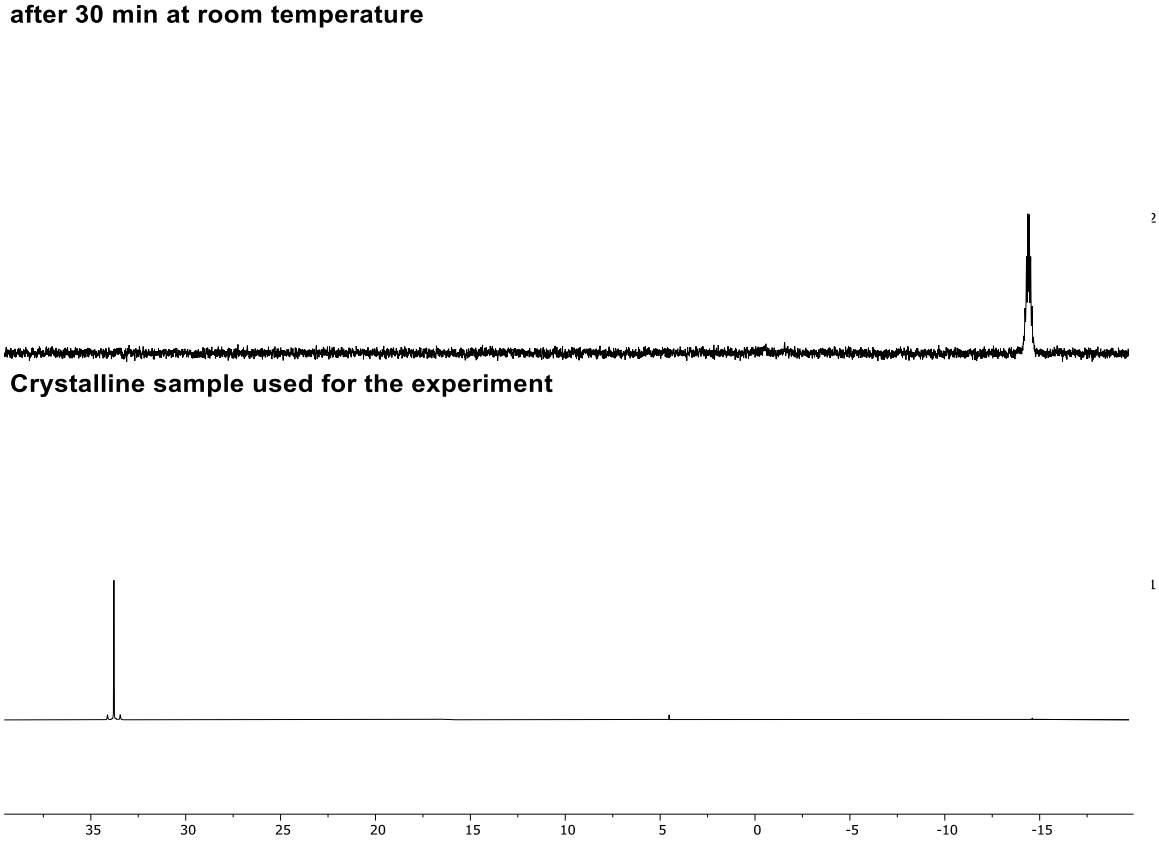


**Figure S71**. Monitoring of the reaction of $^{Mes}$TerSnCH$_2$PNAd (**3c**) with ammonia by $^{31}$P NMR spectroscopy (203 MHz, $C_6D_6$, 298 K).

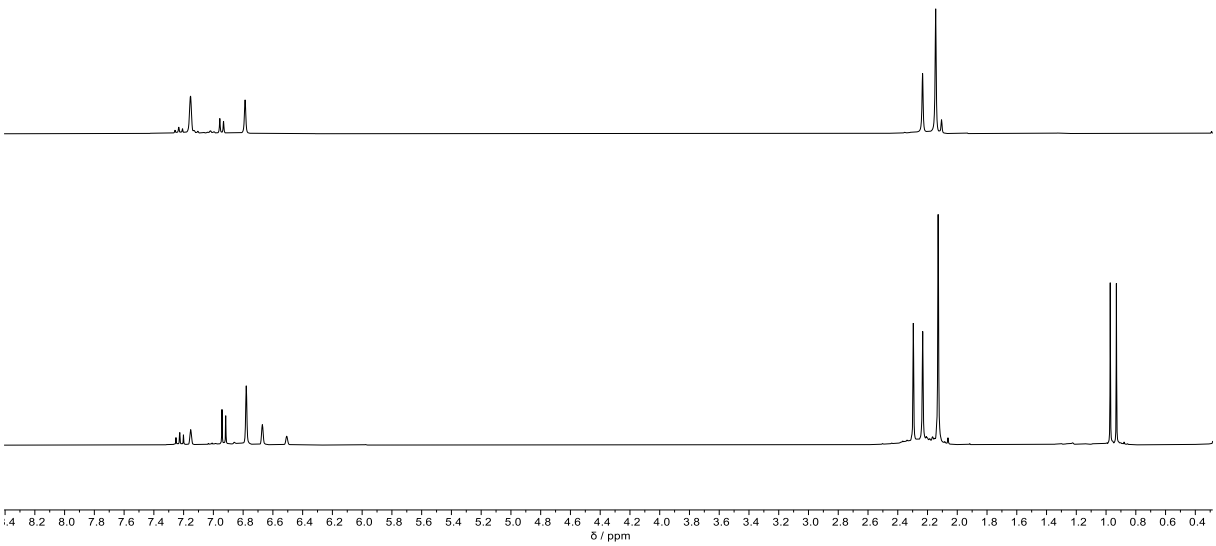


**Figure S72**. Bottom: $^1$H NMR spectrum after the reaction of $^{Mes}$TerSnCH$_2$P(CH$_3$)$_2$NXyl (**3b**) with NH$_3$ to give [$^{Mes}$TerSn(NH$_2$)]$_2$ (**6**) and XylNP(CH$_3$)$_3$ (**2b**); Top: $^1$H NMR spectrum of isolated [$^{Mes}$TerSn(μ-NH$_2$)]$_2$ (**6**) (300 MHz, $C_6D_6$, 298 K).

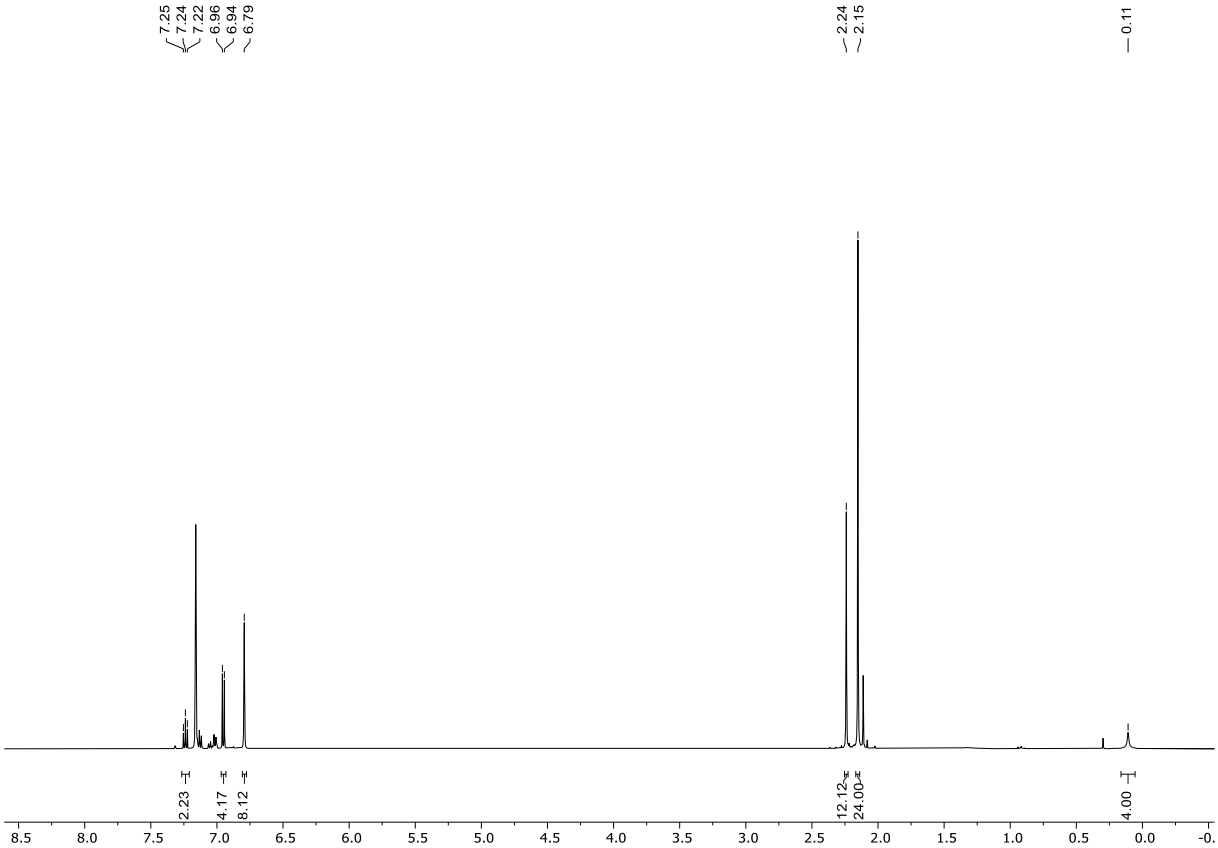


**Figure S73**. $^{1}H$ NMR spectrum of [$^{Mes}$TerSn(μ-$NH_2$)]$_2$ (**6**) (500 MHz, $C_6D_6$, 298 K); 2.11, 7.02, 7.13 ppm: toluene.

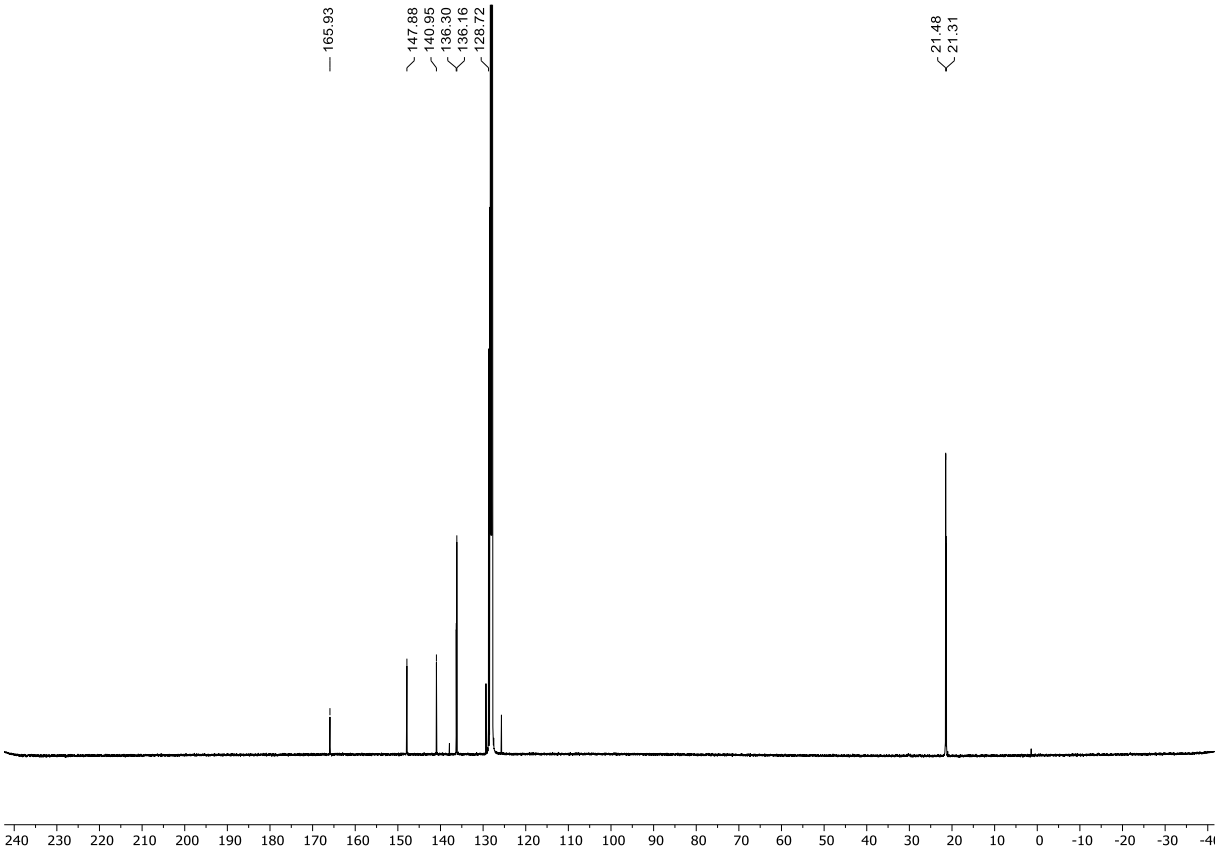


**Figure S74**. $^{13}C\{^{1}H\}$ NMR spectrum of [$^{Mes}$TerSn(μ-$NH_2$)]$_2$ (**6**) (126 MHz, $C_6D_6$, 298 K); 21.1, 125.7 , 128.3, 129.1, 137.7 ppm: toluene.

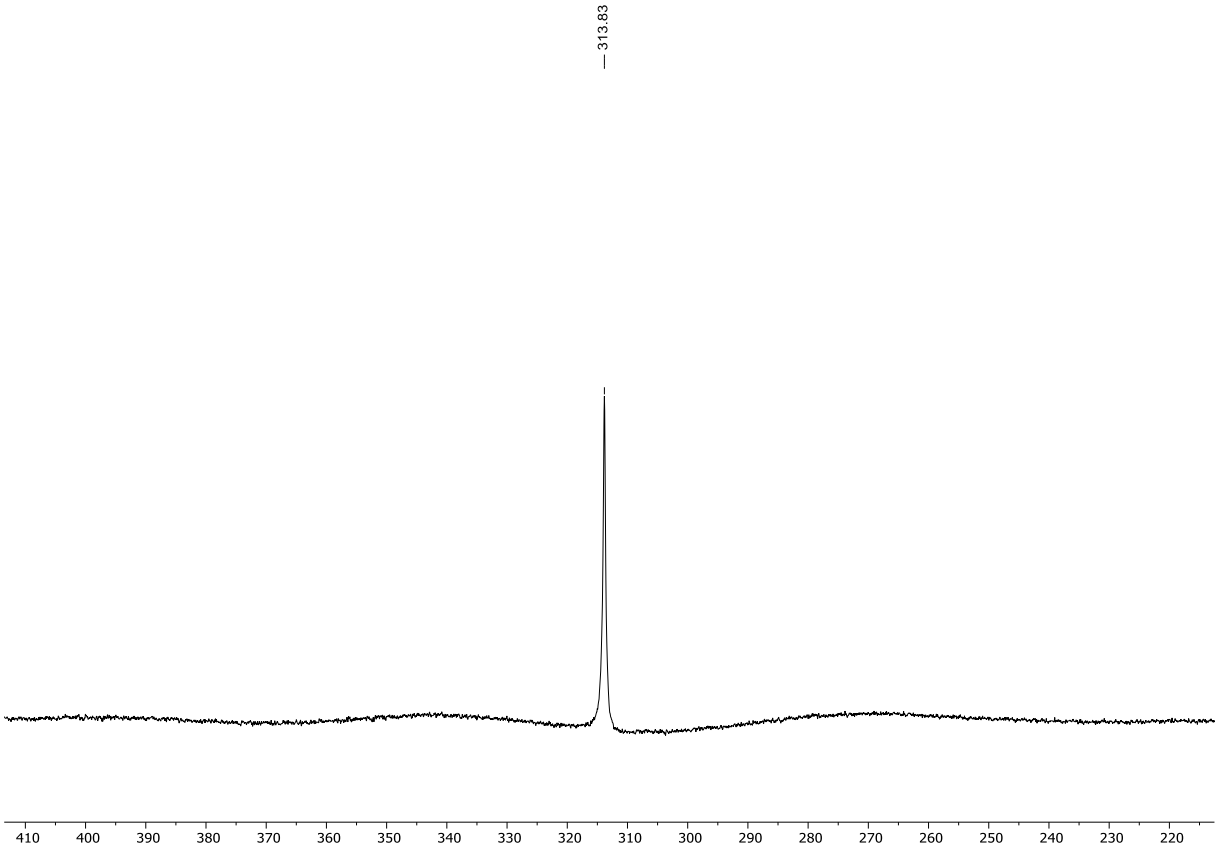


**Figure S75**. $^{119}Sn\{^{1}H\}$ NMR spectrum of [$^{Mes}$TerSn(μ-$NH_2$)]$_2$ (**6**) (187 MHz, $C_6D_6$, 298 K).

**Characterisation of the intermediate $^{Mes}$TerSn(NH$_3$)CH$_2$P(CH$_3$)NDipp (A2a) by multinuclear NMR spectroscopy**

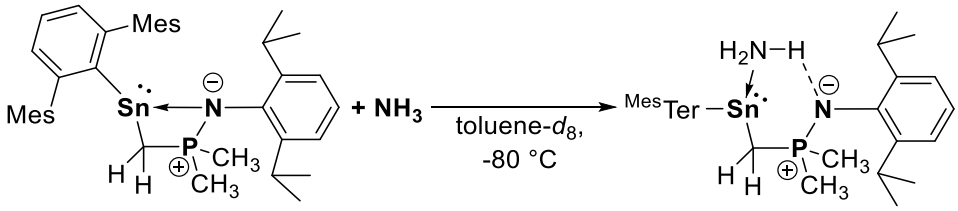


Due to the observation of an intermediate detectable via $^{31}$P NMR spectroscopy during the reaction of $^{Mes}$TerSnCH$_2$P(CH$_3$)$_2$NDipp (**3a**) with NH$_3$, **3a** (0.030 g, 0.044 mmol) was dissolved in 0.5 mL of toluene-$d_8$ and transferred to a J-Young NMR tube. After three freeze-pump-thaw cycles, the solution was kept frozen, and 1.2 bar of NH$_3$ was introduced. Subsequently, the still-frozen solution, with NH$_3$ in the headspace of the J-Young NMR tube, was allowed to equilibrate to room temperature, shaken once, resulting in a colour change to pale yellow, and then transferred to an NMR spectrometer precooled to -80 °C, allowing for the characterization of $^{Mes}$TerSn(NH$_3$)CH$_2$P(CH$_3$)$_2$NDipp (**A1a**) (see Figure S78-S82). As the sample was gradually heated to room temperature in 20 °C increments, the formation of the free iminophosphorane DippNP(CH$_3$)$_3$ (**2a**) and [$^{Mes}$TerSn(μ-NH$_2$)]$_2$ (**6**) increased (Figure S76-S77).

**$^1$H NMR** (600 MHz, C$_7$D$_8$, 193 K): δ = 0.10 (d(br), $^2J_{P,H}$ = 11.9 Hz, 1H, PCH$_2$), 0.74 (d, $^2J_{P,H}$ = 12.0 Hz, 1H, PCH$_2$), 0.80 (d, $^2J_{P,H}$ = 11.1 Hz, 3H, P(CH$_3$)$_2$), 1.02 (d, $^2J_{P,H}$ = 11.4 Hz, 3H, P(CH$_3$)$_2$), 1.18-1.36 (m(br), 12H, CH(C*H*$_3$)$_2$), 2.15 (s, 6H, CH$_3$), 2.21 (s, 6H, CH$_3$), 2.39 (s, 6H, CH$_3$), 2.74 (s(br), 3H, NH$_3$), 3.42 (m, 1H, C*H*(CH$_3$)$_2$), 3.70 (m, 1H, C*H*(CH$_3$)$_2$), 6.60 (s, 2H, CH$_{Aryl}$), 6.72 (s, 2H, CH$_{Aryl}$), 7.14-7.15 (m, 2H, CH$_{Aryl}$)*, 7.29-7.31 (m, 1H, CH$_{Aryl}$) ppm.
* = overlap with C$_7$D$_7$H signal
**$^{13}$C{$^1$H} NMR** (151 MHz, C$_7$D$_8$, 193 K): δ = 16.4 (d, $^2J$ = 68.3 Hz, PCH$_2$), 17.6 (d, $^2J$ = 47.4 Hz, P(CH$_3$)$_2$), 18.8 (d, $^2J$ = 60.1 Hz, P(CH$_3$)$_2$), 21.0 (CH$_3$), 21.7 (CH$_3$), 21.9 (CH$_3$), 120.2 (CH$_{Aryl}$), 123.0 (CH$_{Aryl}$), 127.2 (CH$_{Aryl}$), 135.9 (C$_{q,Aryl}$), 136.1 (C$_{q,Aryl}$), 136.6 (C$_{q,Aryl}$), 140.9 (C$_{q,Aryl}$), 143.0 (C$_{q,Aryl}$), 143.4 (C$_{q,Aryl}$), 145.3 (d, $J_{P,C}$ = 7.1 Hz, C$_{q,Aryl}$), 148.0 (C$_{q,Aryl}$), 162.8 (d, $J_{P,C}$ = 10.4 Hz, C$_{q,Aryl}$) ppm.
Note: Due to signal broadening, only the clearly assignable signals are listed
**$^1$H/$^{15}$N HSQC NMR** (61 MHz, C$_6$D$_6$, 298 K): δ = -375.0 (SnNH$_3$) ppm.
**$^{31}$P{$^1$H} NMR** (243 MHz, C$_7$D$_8$, 193 K): δ = 15.2 (Sn satellites: $J_{119/117Sn,P}$ = 93.2 Hz (average value)) ppm.
**$^{31}$P NMR** (243 MHz, C$_7$D$_8$, 193 K): δ = 15.2 ppm.
**$^{119}$Sn{$^1$H} NMR** (224 MHz, C$_7$D$_8$, 193 K): δ = 61.4 ppm.

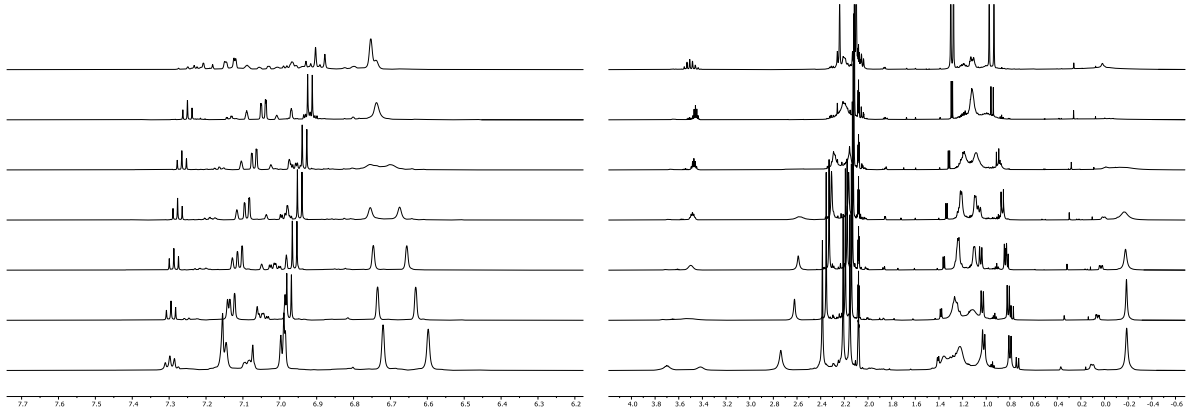

**Figure S76**. Excerpts of the VT $^{1}$H NMR spectrum of $^{Mes}$TerSn(NH$_3$)CH$_2$P(CH$_3$)$_2$NDipp (**A1a**) from 193 K (top) to 313 K (bottom) in steps of 20 K (600 MHz, toluene-$d_8$).

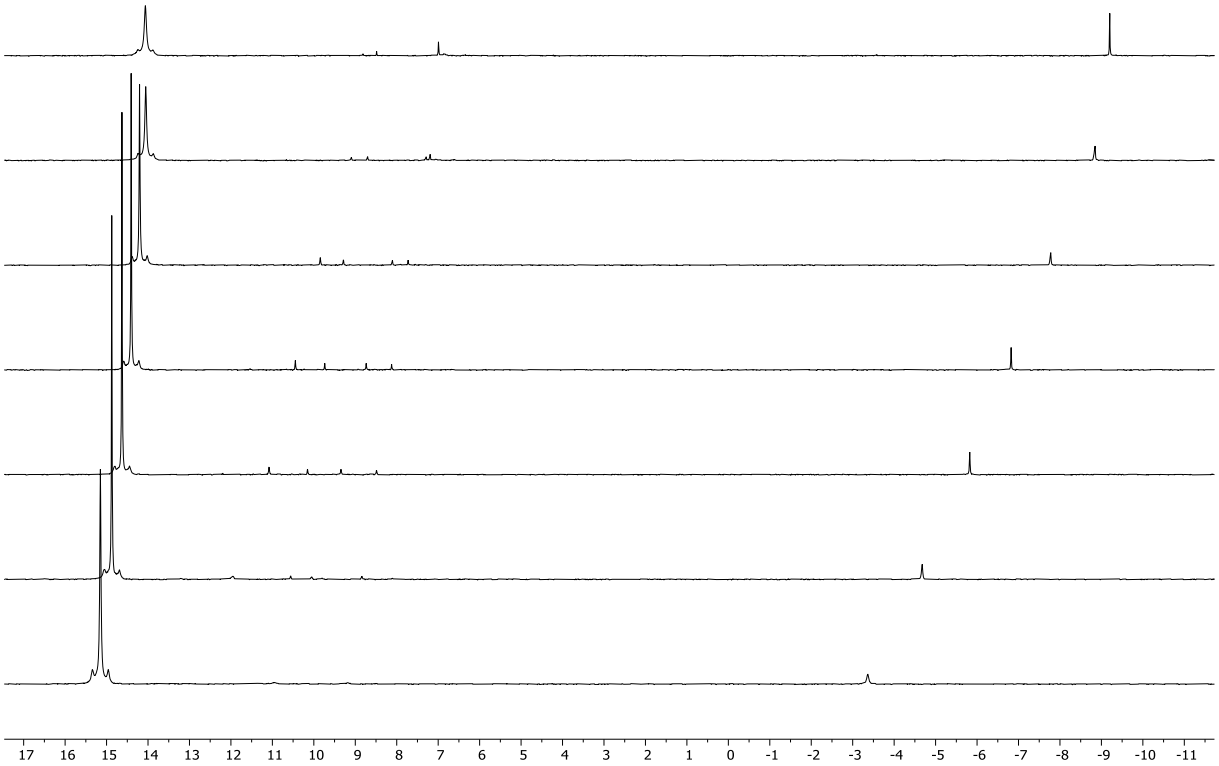


**Figure S77**. Excerpt of the VT $^{31}$P{$^{1}$H} NMR spectrum of $^{Mes}$TerSn(NH$_3$)CH$_2$P(CH$_3$)$_2$NDipp (**A1a**) from 193 K (top) to 313 K (bottom) in steps of 20 K (243 MHz, toluene-$d_8$).

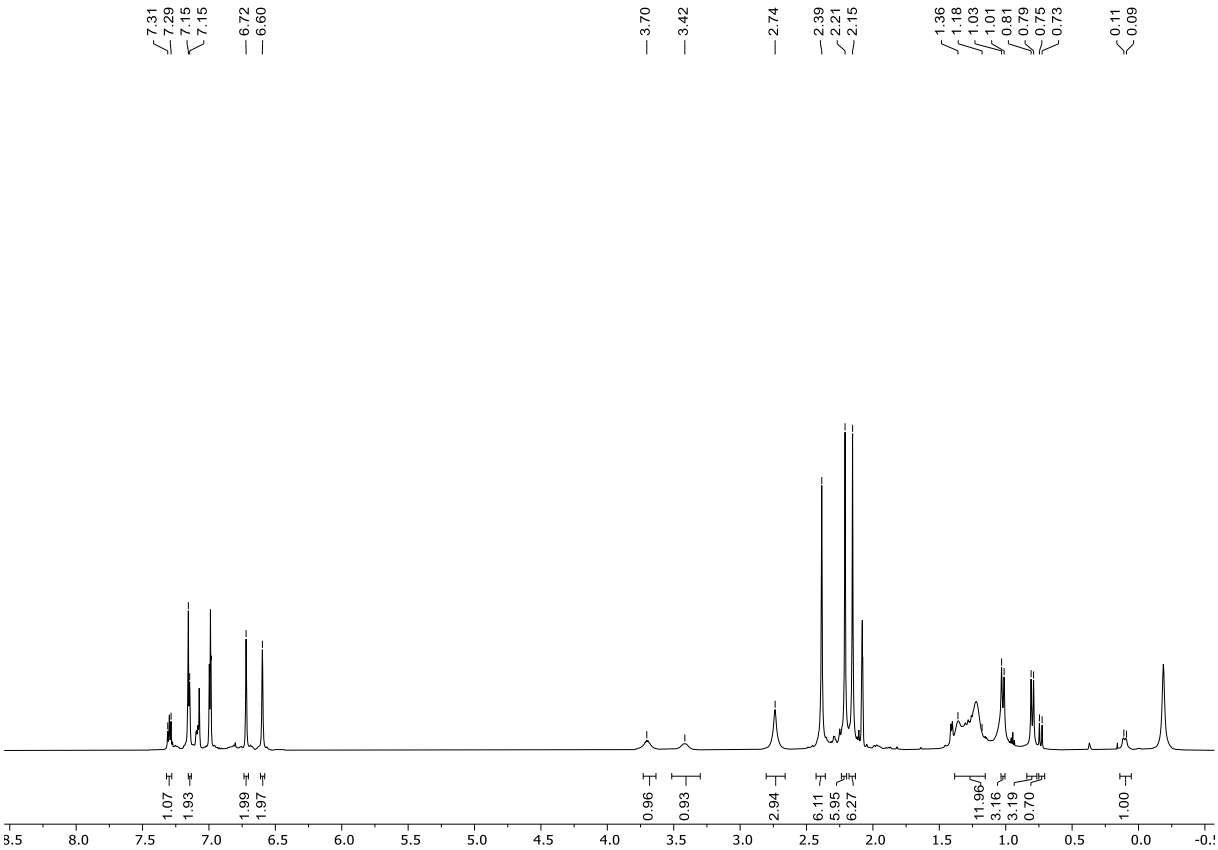


**Figure S78**. $^{1}H$ NMR spectrum of $^{Mes}TerSn(NH_3)CH_2P(CH_3)_2NDipp$ (**A2a**) (600 MHz, $C_7D_8$, 193 K); -0.19 ppm: free $NH_3$.

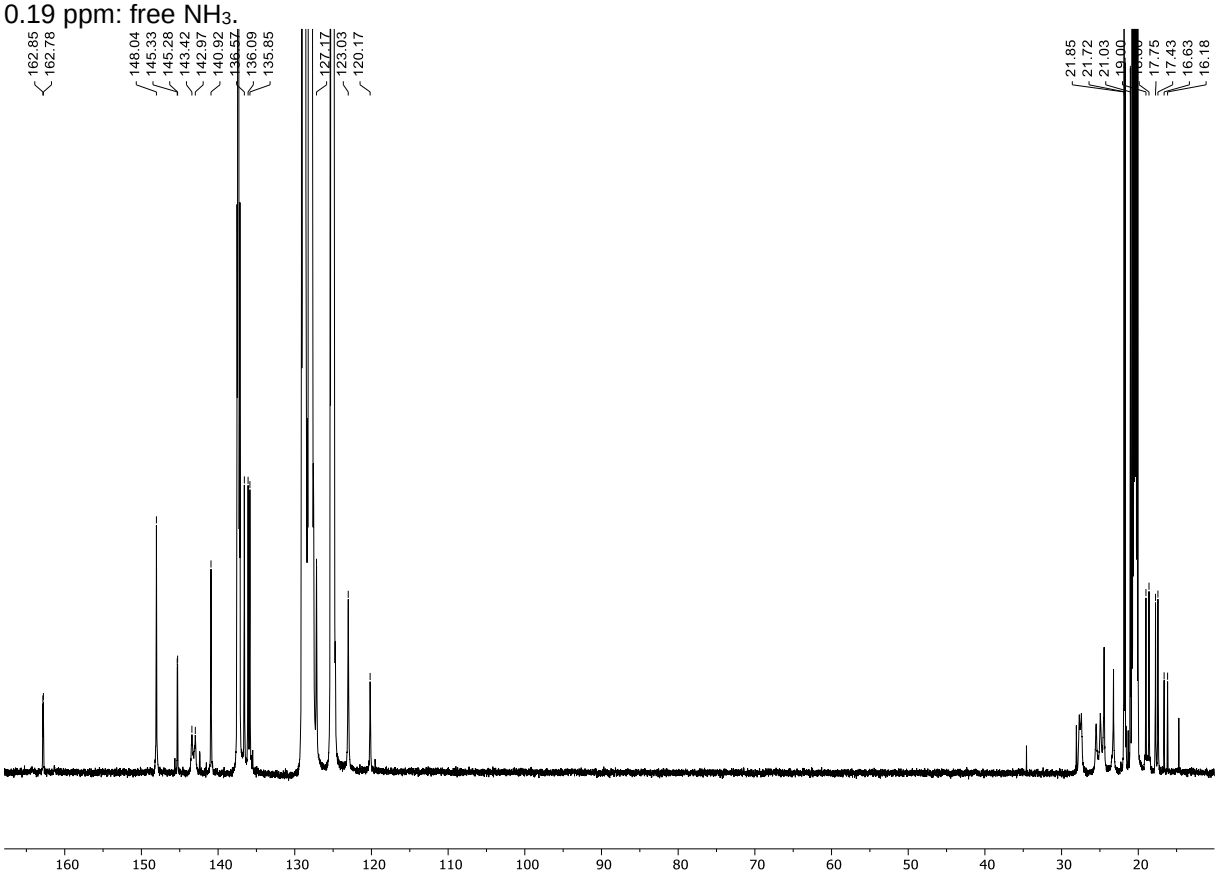


**Figure S79**. $^{13}C\{^{1}H\}$ NMR spectrum of $^{Mes}TerSn(NH_3)CH_2P(CH_3)_2NDipp$ (**A2a**) (151 MHz, $C_7D_8$, 193 K).

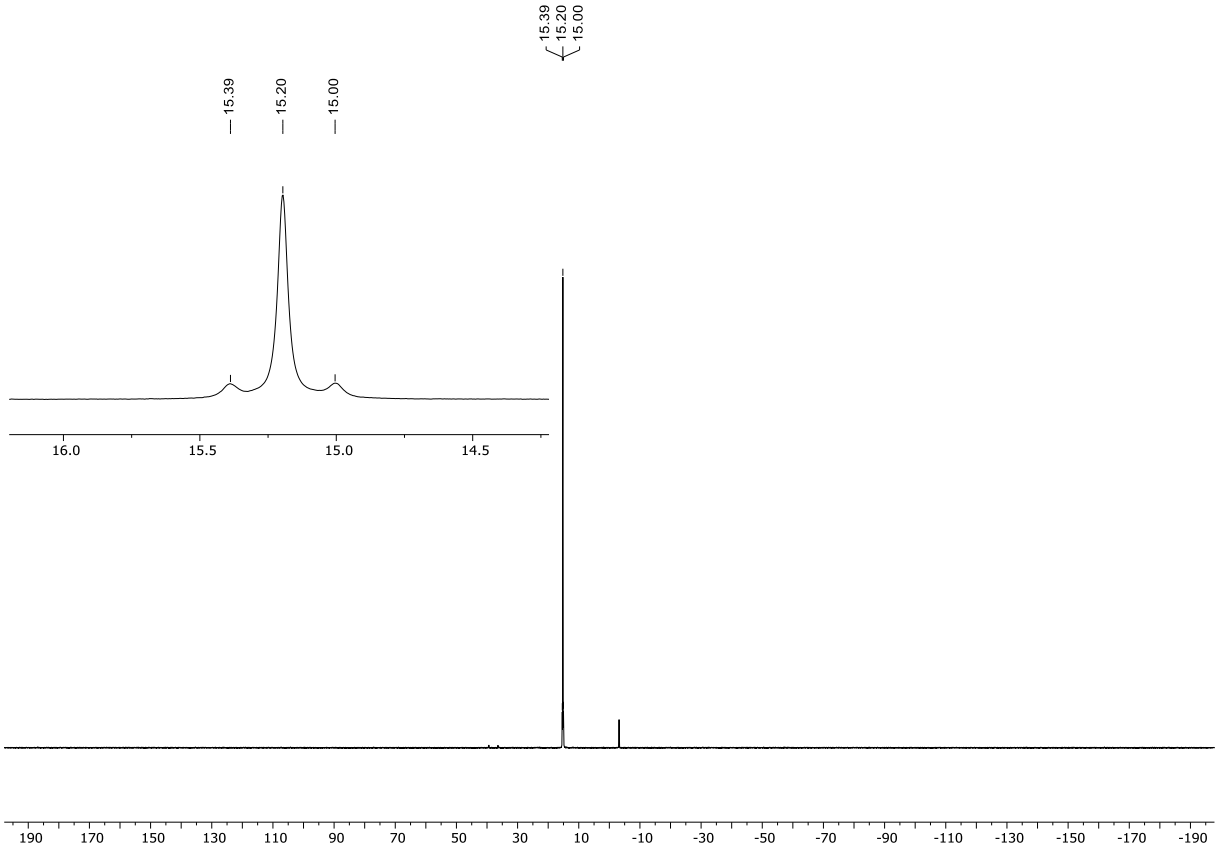


**Figure S80**. $^{31}P\{^{1}H\}$ NMR spectrum of $^{Mes}TerSn(NH_3)CH_2P(CH_3)_2NDipp$ (**A2a**) (243 MHz, $C_7D_8$, 193 K).

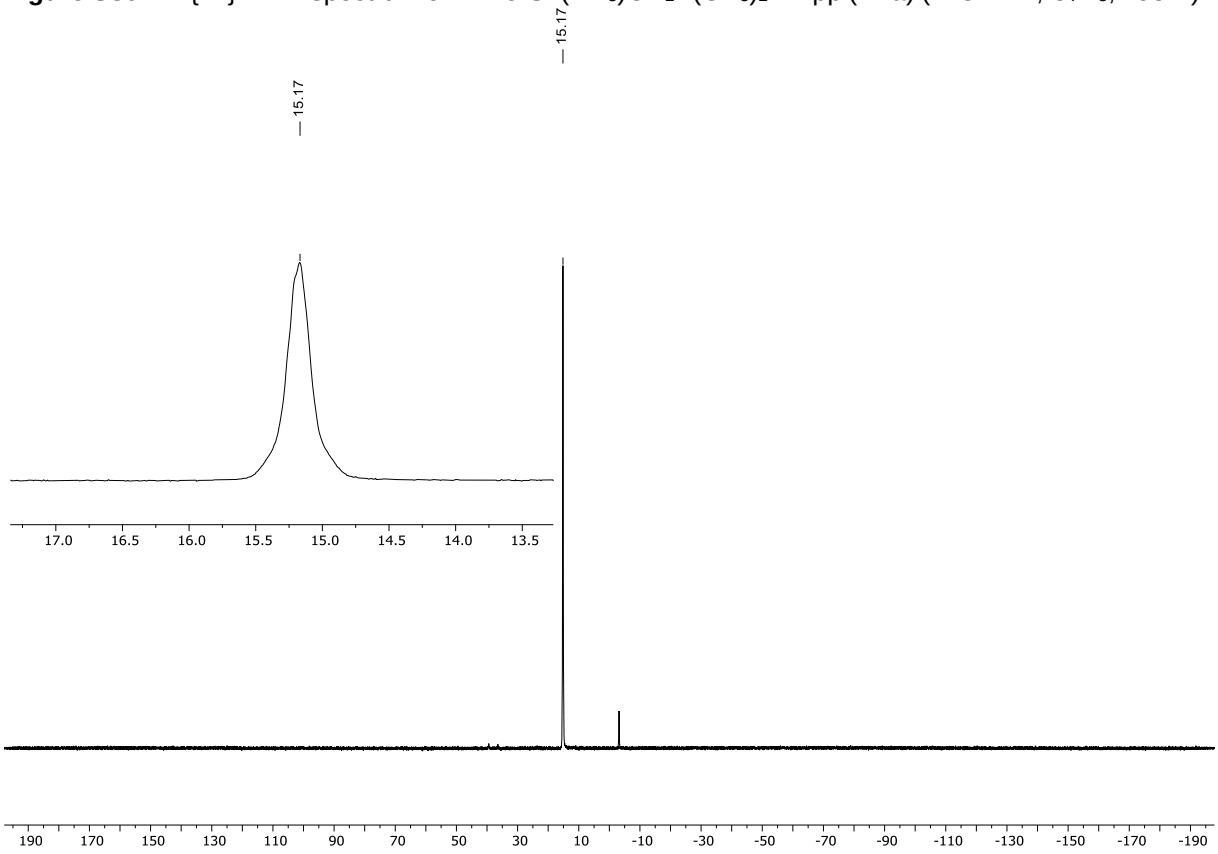


**Figure S81**. $^{31}P$ NMR spectrum of $^{Mes}TerSn(NH_3)CH_2P(CH_3)_2NDipp$ (**A2a**) (243 MHz, $C_7D_8$, 193 K).

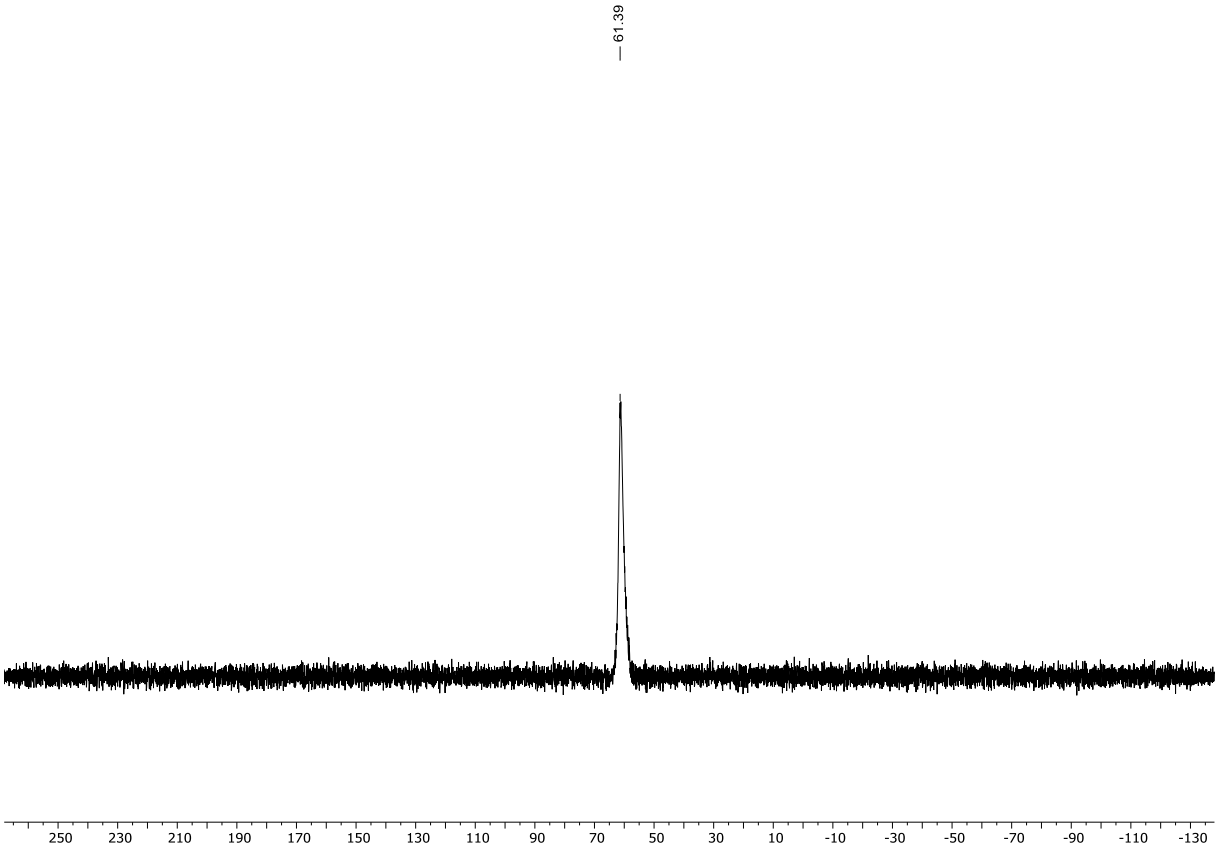


**Figure S82**. $^{119}Sn\{^{1}H\}$ NMR spectrum of $^{Mes}TerSn(NH_3)CH_2P(CH_3)_2NDipp$ (**A2a**) (224 MHz, $C_7D_8$, 193 K).

**Additional analytical data of the starting materials:**
**$^{Mes}$TerSn{N(SiMe$_3$)$_2$} (1): $^{119}$Sn{$^1$H} NMR** (149 MHz, $C_6D_6$, 298 K): $\delta$ = 1192.3 ppm.

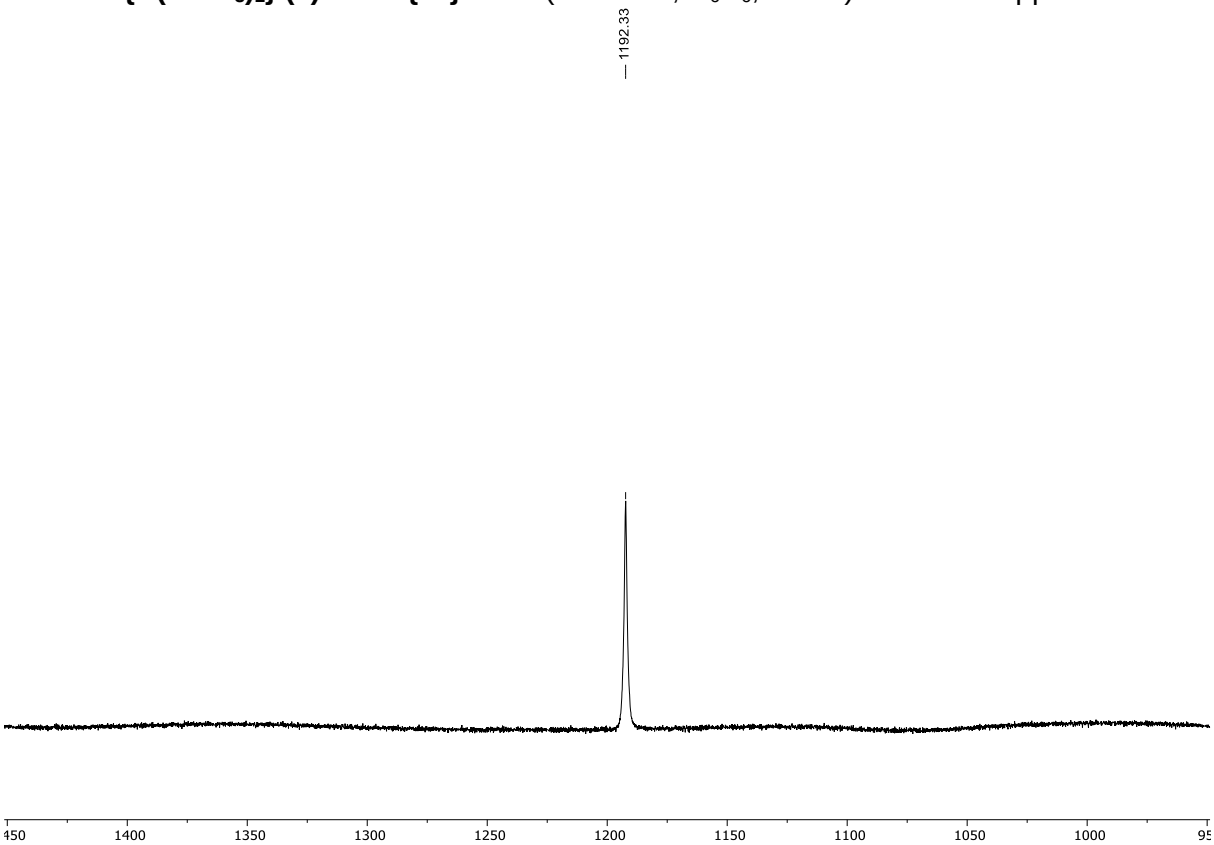


**Figure S83**. $^{119}$Sn{$^1$H} NMR spectrum of **1** (149 MHz, $C_6D_6$, 298 K).

## Crystallographic Details

Single crystal X-ray data were collected at 100(2) K using an open flow nitrogen stream on a Bruker Smart Apex diffractometer equipped with a Bruker rotating anode (Mo) Incoatec, Incoatec mirror optics and a Photon III detector (**2a**, **2c**, **3a**, **4a**, **5a**) or a Bruker Smart Apex diffractometer equipped with an Incoatec microfocus source (Ag) Incoatec, Incoatec mirror optics and an Apex II CCD detector (**3c**). The data were integrated with SAINT[S9]. A multi-scan absorption correction was applied using SADABS[S10] (**2c**, **3c**, **4a**) or TWINABS[S11] (**2a**, **3a**, **7**). All structures were solved using the dual-space algorithm in ShelXT[S12] and refined against $F^2$ with the use of SHELXL[S13] in the graphical user interface SelXle[S14]. All non-hydrogen atoms were refined using anisotropic displacement parameters. Unless noted otherwise, hydrogen atoms were refined using a riding model with their $U_{iso}$ values constrained to 1.5 $U_{eq}$ of their pivot atoms for terminal $sp^3$ carbon atoms and 1.2 times for all other carbon atoms. Crystallographic data for the structural analyses have been deposited with the Cambridge Crystallographic Data Centre under reference numbers 2356897-2356902. Copies of this information may be obtained free of charge from The Director, CCDC, 12 Union Road, Cambridge CB2 1EZ, UK (Fax: +44-1223-336033; email: deposit@ccdc.cam.ac.uk or http://www.ccdc.cam.ac.uk).

**Table S8**. Crystal structure data for compounds **2a**, **2c** and **3a**.

| | **2a** | **2c** | **3a** |
|---|---|---|---|
| CCDC | 2356897 | 2356898 | 2356899 |
| empirical formula | $C_{15}H_{26}NP$ | $C_{13}H_{24}NP$ | $C_{39}H_{50}NPSn \cdot C_6H_{14}$ |
| formula weight | 251.34 | 225.30 | 768.63 |
| colour | colourless | colourless | yellow |
| habit | block | needle | block |
| cryst. dimens, mm | 0.48 x 0.48 x 0.32 | 0.59 x 0.15 x 0.11 | 0.29 x 0.20 x 0.16 |
| $T$, K | 100(2) | 100(2) | 100(2) |
| crystal system | monoclinic | triclinic | triclinic |
| space group | $P2_1/c$ | $P\bar{1}$ | $P\bar{1}$ |
| $a$, Å | 14.148(2) | 6.537(2) | 9.615(2) |
| $b$, Å | 13.096(2) | 9.288(2) | 14.658(2) |
| $c$, Å | 17.636 (3) | 10.366(3) | 15.730(3) |
| $\alpha$, deg | | 96.41(2) | 72.09(2) |
| $\beta$, deg | 106.84(2) | 90.76(2) | 83.31(2) |
| $\gamma$, deg | | 90.69(2) | 84.26(2) |
| $V$, Å$^3$ | 3127.5(9) | 625.3(3) | 2090.3(7) |
| $Z$ | 8 | 2 | 2 |
| $D_{calc}$, g•cm$^{-3}$ | 1.068 | 1.197 | 1.221 |
| $\mu$, mm$^{-1}$ | 0.158 | 0.190 | 0.679 |
| radiation | Mo $K\alpha$ ($\lambda$ = 0.71073) | Mo $K\alpha$ ($\lambda$ = 0.71073) | Mo $K\alpha$ ($\lambda$ = 0.71073) |
| $\theta$ range, deg | 1.504 – 25.052 | 1.977 – 25.213 | 2.138 – 26.397 |
| no. of rflns collected | 202500 | 34069 | 338908 |
| no. of indep. reflns. | 5542 | 2246 | 8548 |
| $R$(int) | 0.0745 | 0.0916 | 0.0592 |
| Data / restraints / parameters | 5542 / 0 / 322 | 2246 / 149 / 176 | 8548 / 235 / 502 |
| $R$ indices ($I$>2$\sigma$($I$)) | $R$1 = 0.0474<br>w$R$2 = 0.1351 | $R$1 = 0.0746<br>w$R$2 =0.2015 | $R$1 = 0.0227<br>w$R$2 =0.0484 |
| $R$ indices (all data) | $R$1 = 0.0500<br>w$R$2 = 0.1381 | $R$1 = 0.0812<br>w$R$2 = 0.2053 | $R$1 = 0.0249<br>w$R$2 = 0.0493 |
| GOF on $F^2$ | 1.058 | 1.140 | 1.078 |
| $\Delta\rho_{max}/\Delta\rho_{min}$, e Å$^{-3}$ | 0.395/−0.432 | 0.414/−0.410 | 0.337/−0.415 |

**Table S9**. Crystal structure data for compounds **3c**, **4a** and **5a**.

| | **3c** | **4a** | **7** |
|---|---|---|---|
| CCDC | 2356900 | 2356901 | 2356902 |
| empirical formula | $C_{37}H_{48}NPSn$ | $C_{46}H_{62}N_3PSn$ | $C_{54}H_{75}LiN_2P_2Sn$ |
| formula weight | 656.42 | 806.64 | 939.73 |
| colour | yellow | colourless | colourless |
| habit | block | block | block |
| cryst. dimens, mm | 0.57 x 0.50 x 0.39 | 0.22 x 0.17 x 0.14 | 0.27 x 0.18 x 0.16 |
| *T*, K | 100(2) | 100(2) | 100(2) |
| crystal system | monoclinic | monoclinic | triclinic |
| space group | $P2_1/c$ | $P2_1/n$ | $P\bar{1}$ |
| *a*, Å | 12.065(8) | 9.354(2) | 9.533(2) |
| *b*, Å | 19.678(13) | 38.331(3) | 12.651(2) |
| *c*, Å | 14.365(9) | 23.653(2) | 21.604(3) |
| $\alpha$, deg | | | 74.71(2) |
| $\beta$, deg | 104.21(2) | 98.67(2) | 83.26(2) |
| $\gamma$, deg | | | 81.63(2) |
| *V*, Å$^3$ | 3306(4) | 8384(2) | 2478.0(8) |
| *Z* | 4 | 8 | 2 |
| $D_{calc}$, g•cm$^{-3}$ | 1.319 | 1.278 | 1.259 |
| $\mu$, mm$^{-1}$ | 0.454 | 0.682 | 0.617 |
| radiation | Ag *K*$\alpha$ ($\lambda$ = 0.56086) | Mo *K*$\alpha$ ($\lambda$ = 0.71073) | Mo *K*$\alpha$ ($\lambda$ = 0.71073) |
| $\theta$ range, deg | 1.598 – 20.727 | 1.020 – 25.042 | 2.148 – 25.062 |
| no. of rflns collected | 91982 | 363908 | 232510 |
| no. of indep. reflns. | 6823 | 14813 | 8781 |
| *R*(int) | 0.0736 | 0.0556 | 0.1081 |
| Data / restraints / parameters | 6823 / 0 / 371 | 14813 / 0 / 954 | |
| *R* indices (*I*>2$\sigma$(*I*)) | *R*1 = 0.0232<br>w*R*2 = 0.0546 | *R*1 = 0.0362<br>w*R*2 = 0.0806 | *R*1 = 0.0393<br>w*R*2 = 0.1003 |
| *R* indices (all data) | *R*1 = 0.0286<br>w*R*2 = 0.0575 | *R*1 = 0.0390<br>w*R*2 = 0.0816 | *R*1 = 0.0433<br>w*R*2 = 0.1039 |
| GOF on $F^2$ | 1.041 | 1.215 | 1.031 |
| $\Delta\rho_{max}/\Delta\rho_{min}$, e Å$^{-3}$ | 0.356/−0.302 | 1.967/−1.091 | 0.816/−0.830 |

## Computational Details

Geometry optimizations, frequency calculations and PCM solvent corrections were run with Gaussian 16 Revision A.03[S15] using the BP86[S16,S17] functional. For geometry optimisations, all atoms were described with def2-SVP basis sets of Ahlrichs and Weigand.[S18] Single point energy calculations were performed on the optimised geometries, at the BP86/def2-TZVP level of theory. Stationary points were fully characterized using analytical frequency calculations as either minima (all positive eigenvalues) or transition states (one negative eigenvalue). IRC calculations and subsequent geometry optimizations were used to confirm the minima linked by the transition states. Energies reported in the text are based on the gas-phase free energies and incorporate a correction for dispersion effects using Grimme's D3 parameter set with Becke-Johnson dampening[S19,S20] (i.e. BP86-D3BJ) as well as solvation (PCM approach) in benzene. Energies are given in atomic units (a.u.) unless otherwise stated. Natural Bond Orbital (NBO) and Natural Localised Molecular Orbital (NLMO) analysis was performed using NBO-7 using the single point calculations performed at the BP86/def2-TZVP level of theory.[S21]

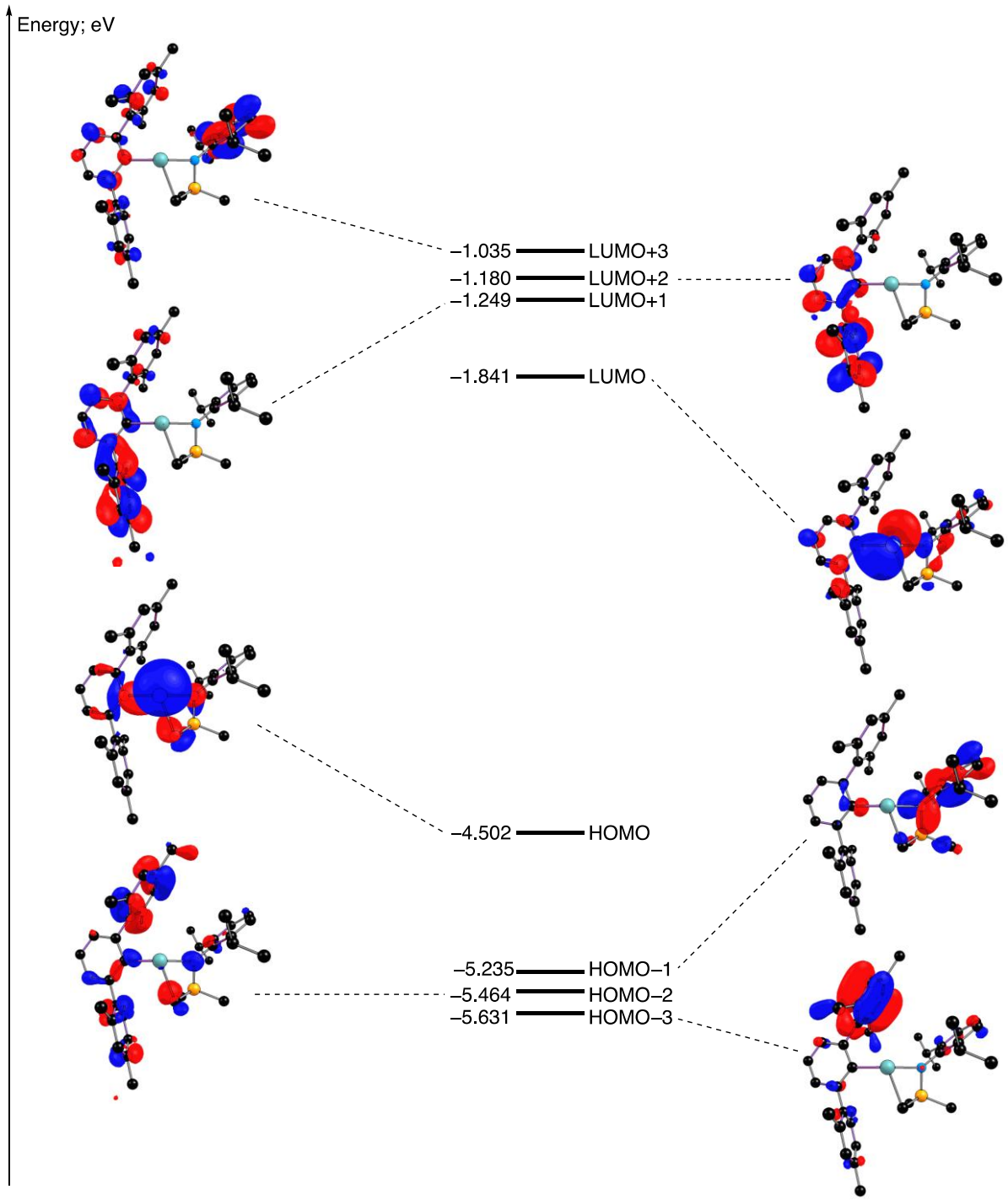


**Figure S84**. Molecular Orbital (BP86/def2-TZVP) diagram of **3a**.

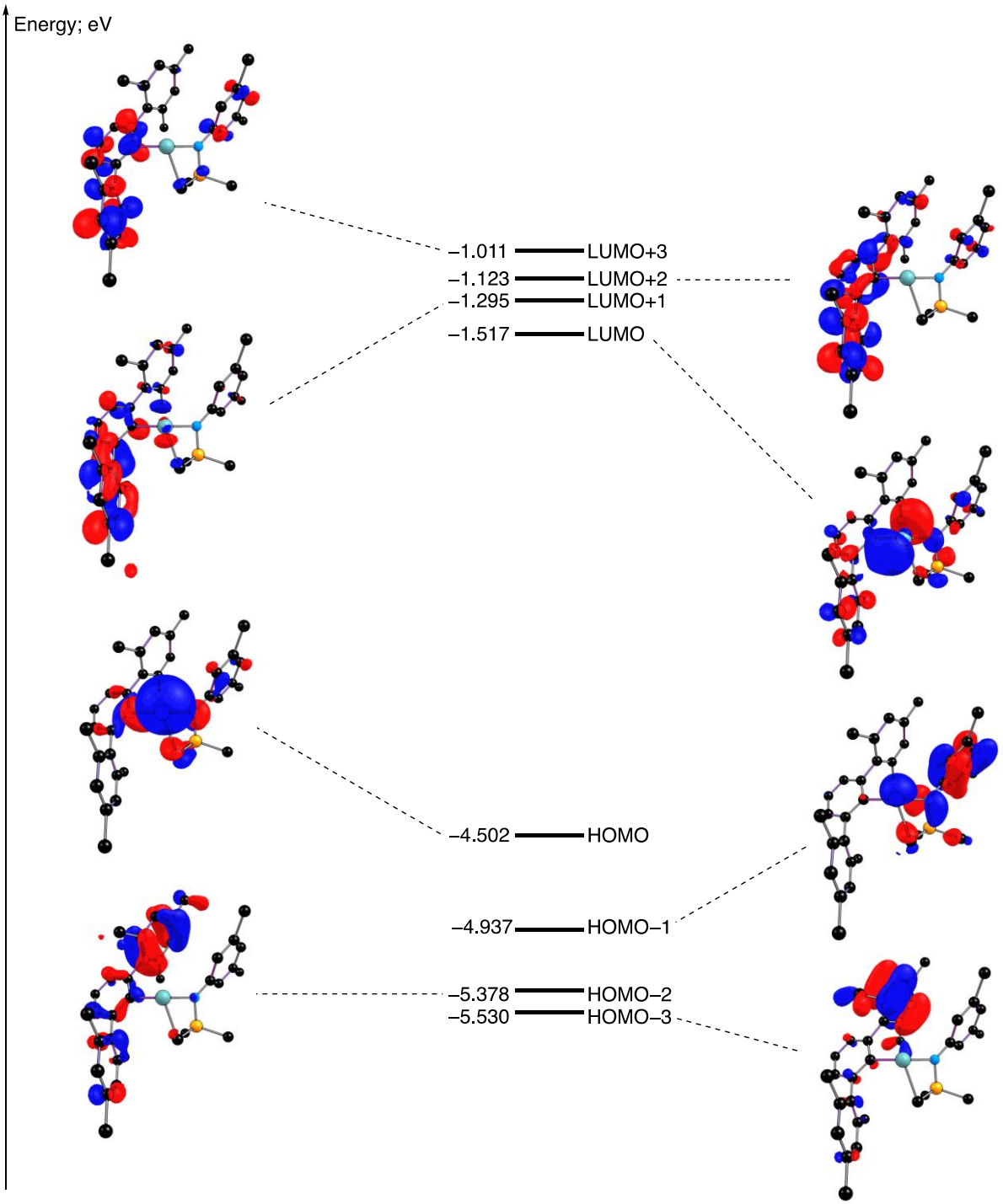


**Figure S85**. Molecular Orbital (BP86/def2-TZVP) diagram of **3b**.

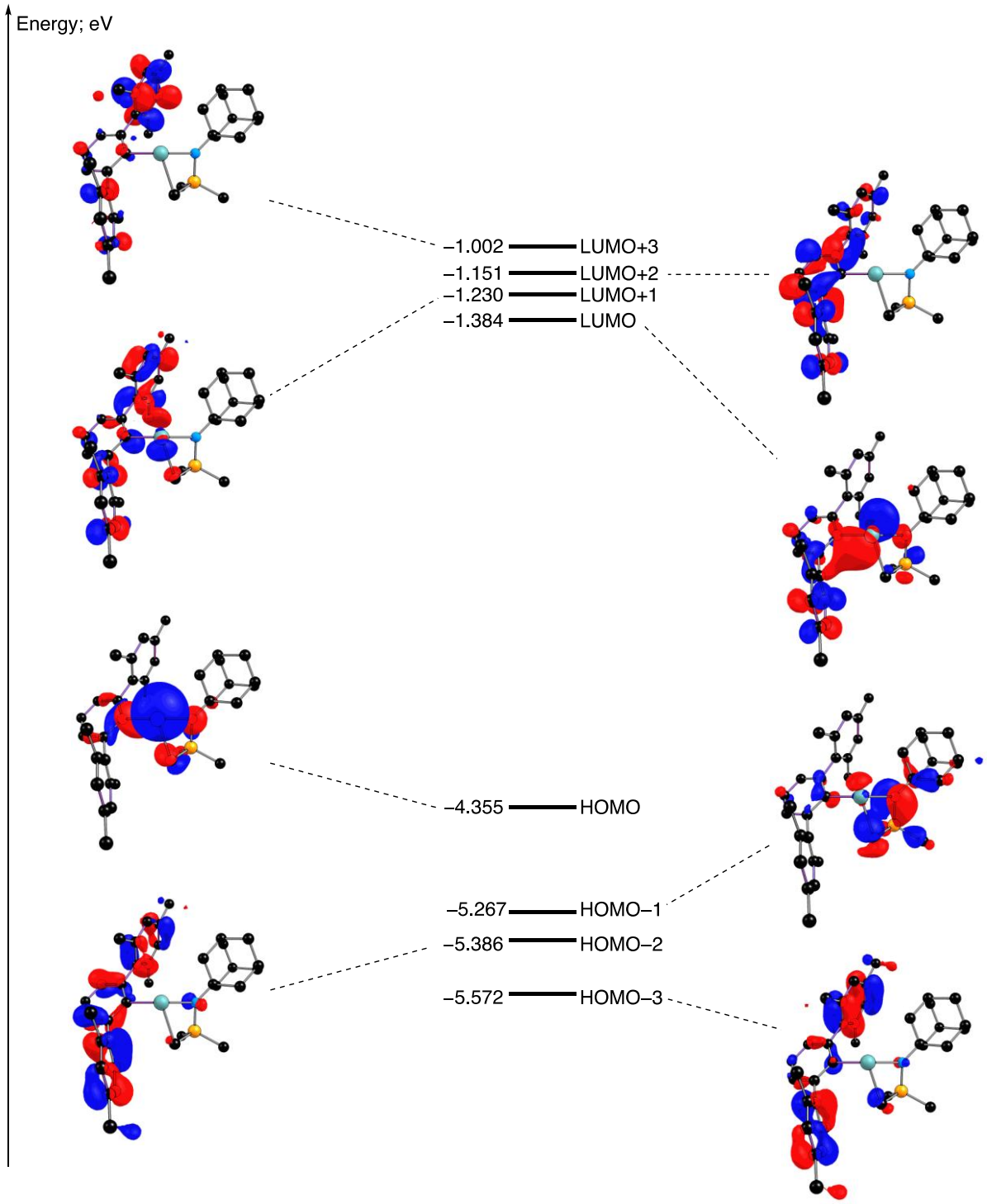


**Figure S86**. Molecular Orbital (BP86/def2-TZVP) diagram of **3c**.

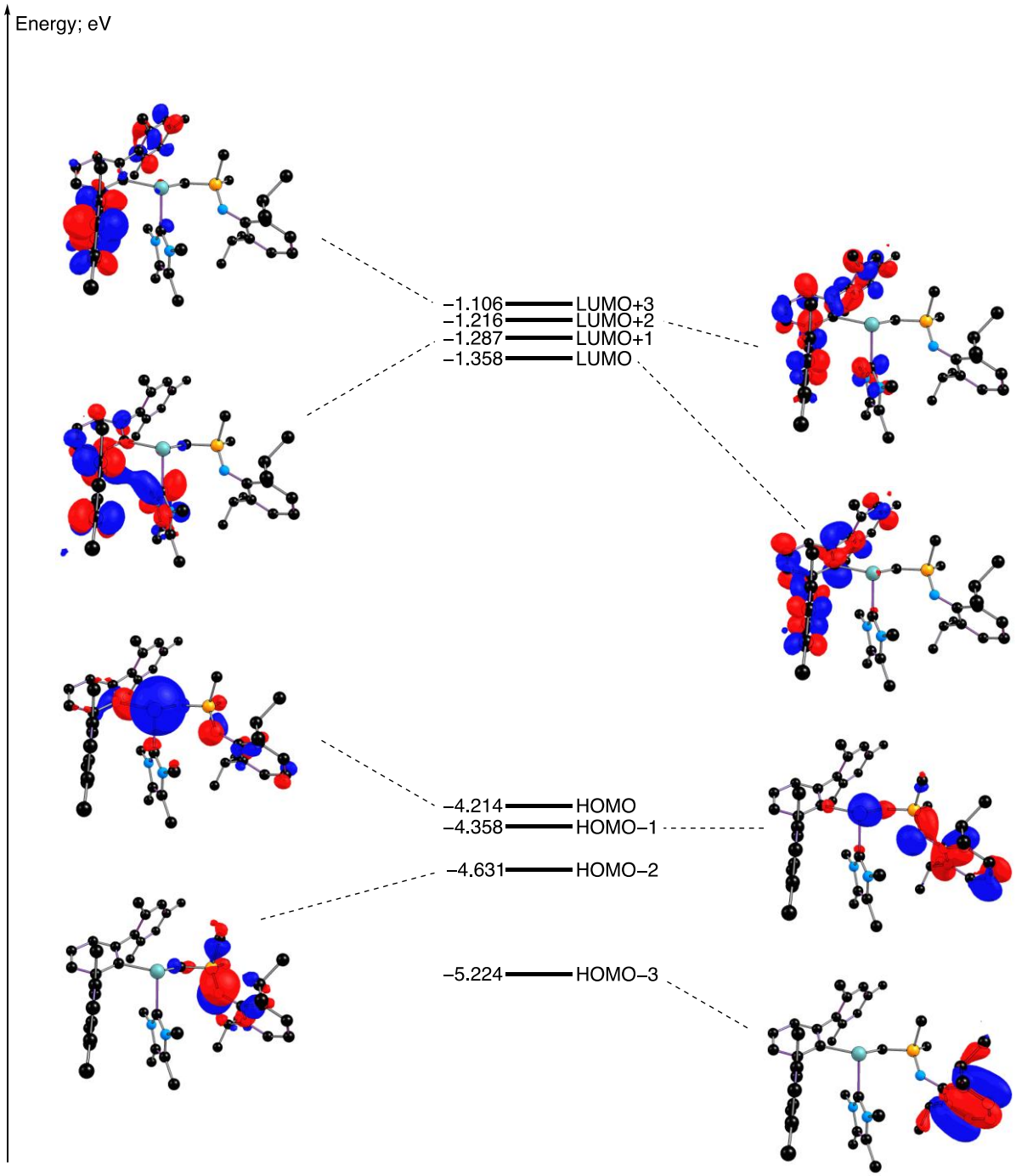


**Figure S87**. Molecular Orbital (BP86/def2-TZVP) diagram of **4a**.

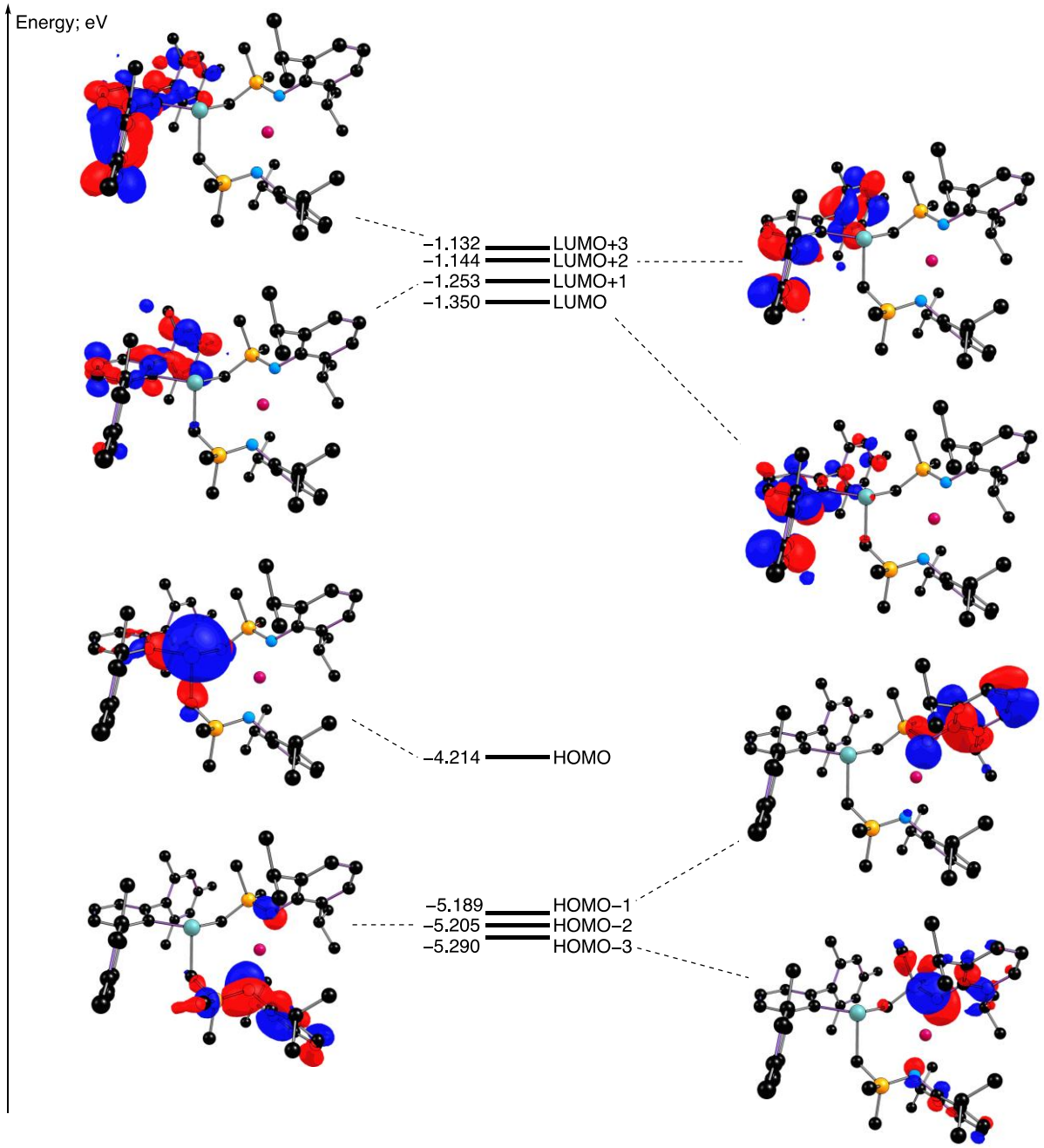


**Figure S88**. Molecular Orbital (BP86/def2-TZVP) diagram of **7**.

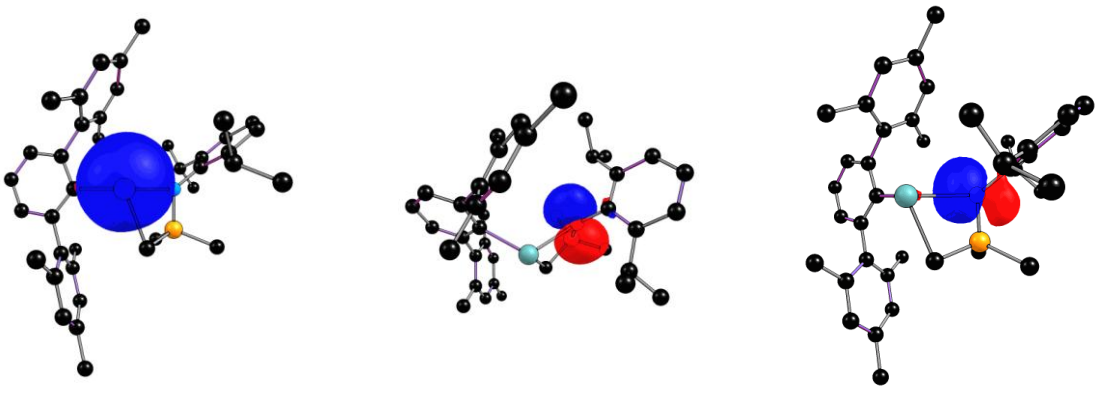

***Tin-centred lone pair (1.95 $e^-$) $s^{0.88}p^{0.12}$***



***Nitrogen-centred lone pair (1.77 $e^-$) p***



***Nitrogen-centred lone pair (1.73 $e^-$) $s^{0.35}p^{0.65}$***

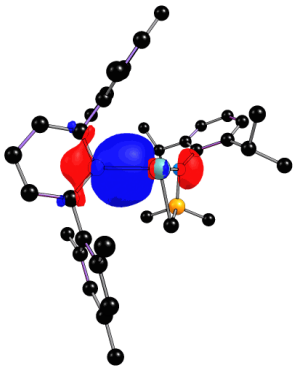

***Tin-Carbon bond (1.93 $e^-$) 22% Sn 78% C***

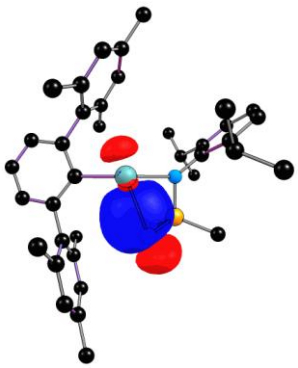

***Tin-Carbon bond (1.89 $e^-$) 17% Sn 83% C***

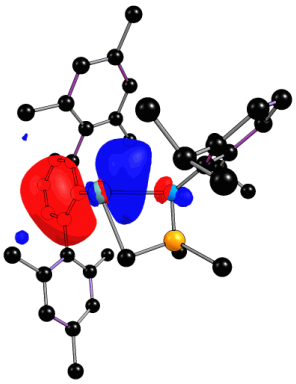

***Tin-centred lone vacant orbital (0.21 $e^-$) p***

**Figure S89**. Selected Natural Bond Orbitals (BP86/def2-TZVP) diagram of **3a**.

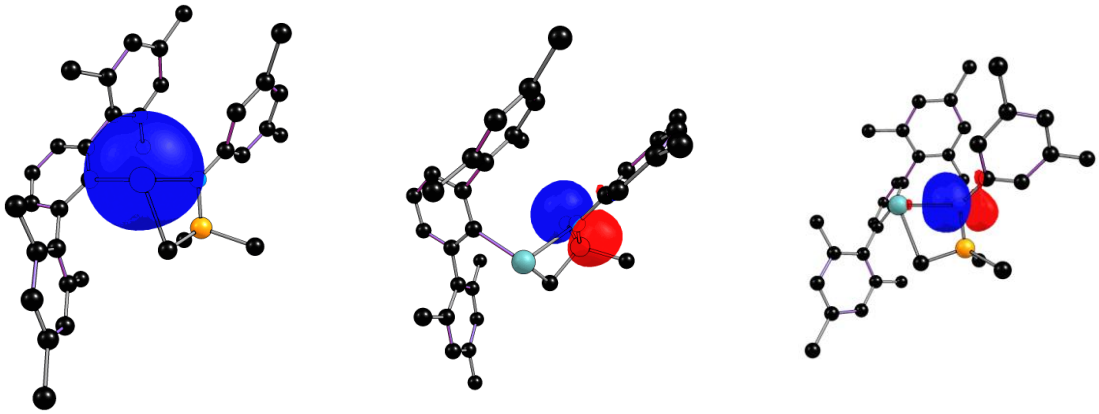

***Tin-centred lone pair***
***(1.96 $e^-$) $s^{0.85}p^{0.15}$***



***Nitrogen-centred lone pair***
***(1.71 $e^-$) $s^{0.06}p^{0.94}$***



***Nitrogen-centred lone pair***
***(1.73 $e^-$) $s^{0.28}p^{0.72}$***

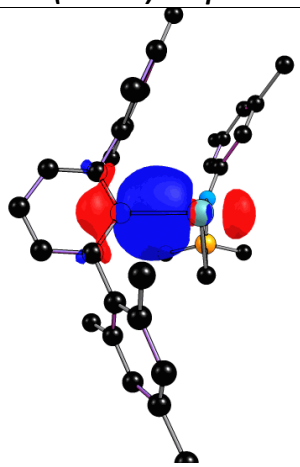

***Tin-Carbon bond***
***(1.93 $e^-$) 23% Sn 77% C***

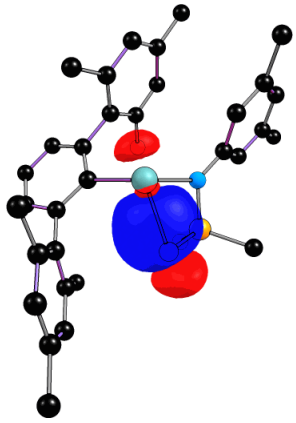

***Tin-Carbon bond***
***(1.89 $e^-$) 81% Sn 19% C***

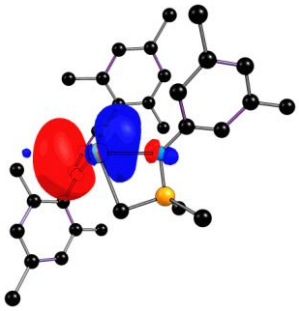

***Tin-centred lone vacant orbital (0.22 $e^-$) p***

**Figure S90**. Selected Natural Bond Orbitals (BP86/def2-TZVP) diagram of **3b**.

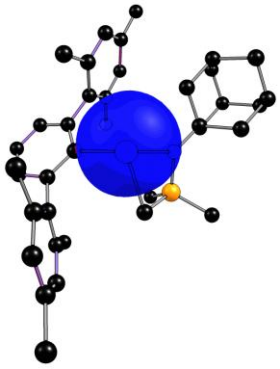

***Tin-centred lone pair***
***(1.96 $e^-$) $s^{0.86}p^{0.14}$***

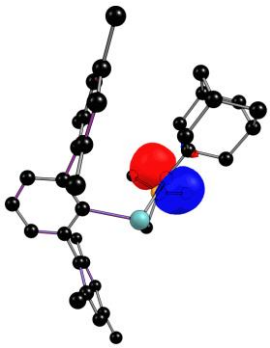

***Nitrogen-centred lone pair***
***(1.76 $e^-$) p***

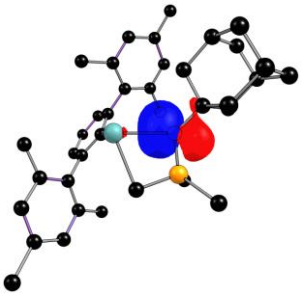

***Nitrogen-centred lone pair***
***(1.73 $e^-$) $s^{0.33}p^{0.67}$***

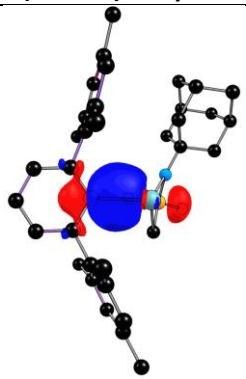

***Tin-Carbon bond***
***(1.93 $e^-$) 23% Sn 77% C***

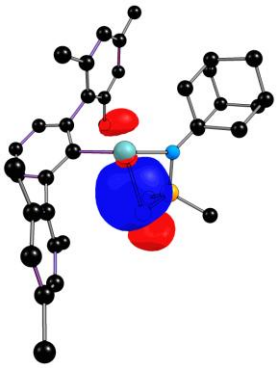

***Tin-Carbon bond***
***(1.89 $e^-$) 19% Sn 81% C***

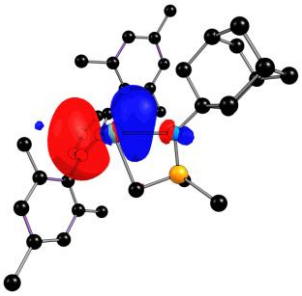

***Tin-centred lone vacant orbital (0.22 $e^-$) $s^{0.02}p^{0.98}$***

**Figure S91**. Selected Natural Bond Orbitals (BP86/def2-TZVP) diagram of **3c**.

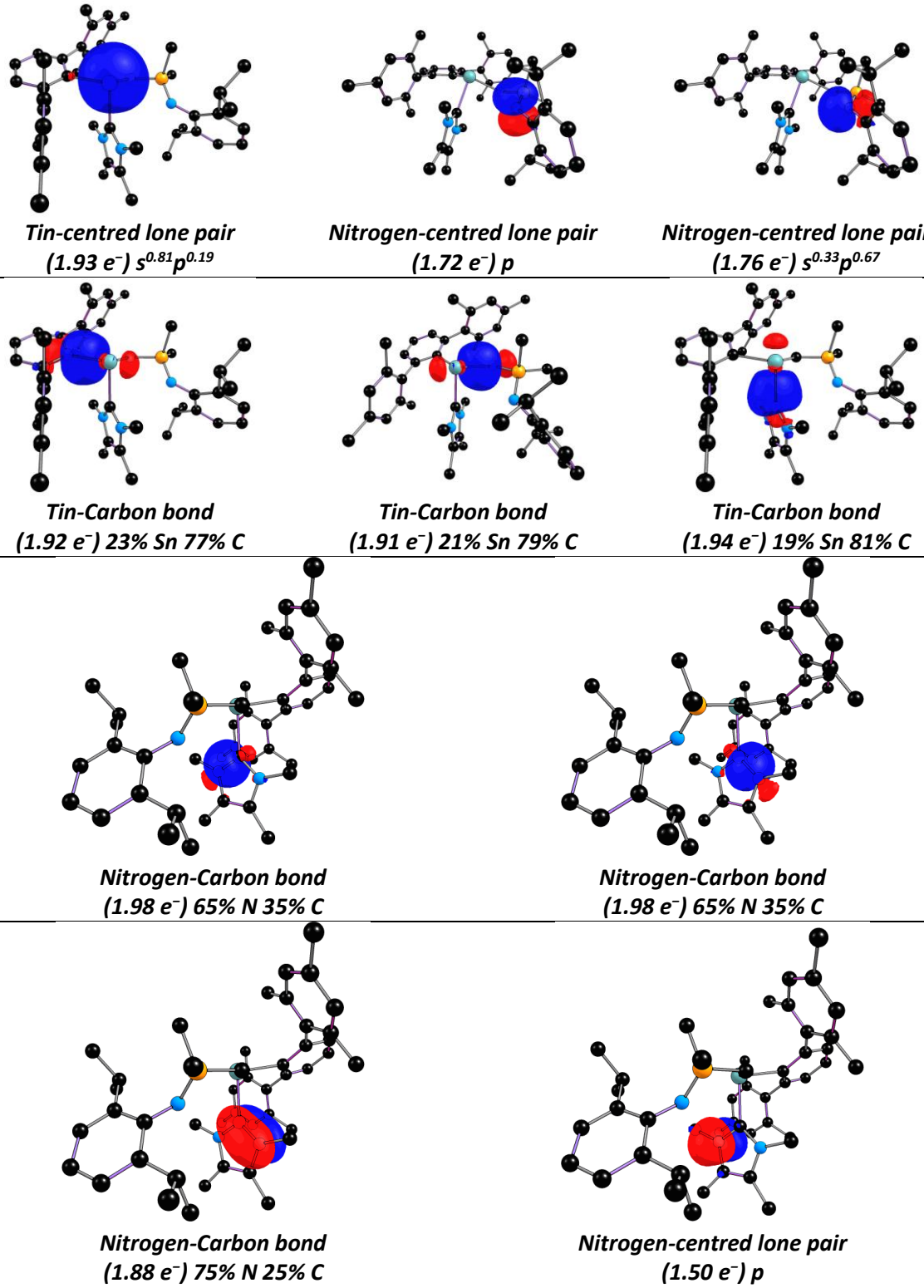


**Figure S92**. Selected Natural Bond Orbitals (BP86/def2-TZVP) diagram of **4a**.

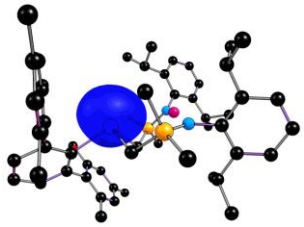

***Tin-centred lone pair***
***(1.91 $e^-$) $s^{0.81}p^{0.19}$***

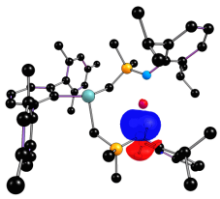

***Nitrogen-centred lone pair***
***(1.85 $e^-$) $s^{0.33}p^{0.66}$***

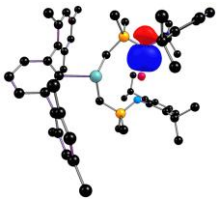

***Nitrogen-centred lone pair***
***(1.86 $e^-$) $s^{0.35}p^{0.65}$***

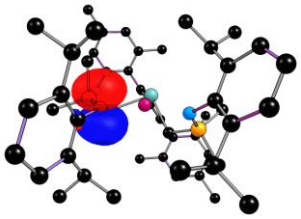

***Nitrogen-centred lone pair***
***(1.78 $e^-$) p***

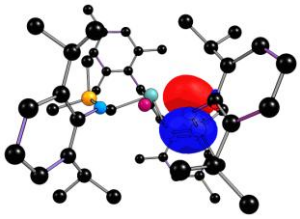

***Nitrogen-centred lone pair***
***(1.77 $e^-$) p***

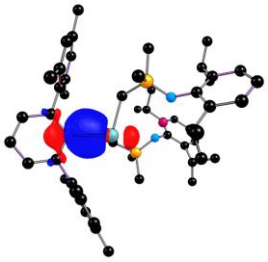

***Tin-Carbon bond***
***(1.93 $e^-$) 24% Sn 76% C***

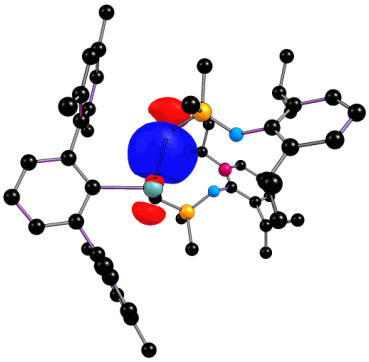

***Tin-Carbon bond***
***(1.92 $e^-$) 19% Sn 81% C***

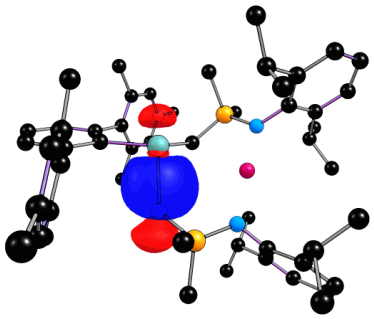

***Tin-Carbon bond***
***(1.91 $e^-$) 20% Sn 80% C***

**Figure S93**. Selected Natural Bond Orbitals (BP86/def2-TZVP) diagram of **7**.

## Energies and Frequencies for the DFT Optimised Geometries

**NH3**
SCF = -56.5089170006
H(0 K) = -56.475756
H(298 K) = -56.471943
G(298 K) = -56.494872
SCF+D3 = -56.5098942691
PCM SCF (Benzene) = -56.5111969594
BS2 (def2-tzvp) = -56.5836424941
Low Freq. = 1052.8240 $cm^{-1}$, 1615.0981 $cm^{-1}$

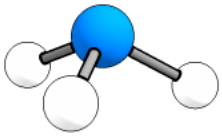

**1**
SCF = -2016.34775970
H(0 K) = -2015.724718
H(298 K) = -2015.678988
G(298 K) = -2015.805284
SCF+D3 = -2016.55620561
PCM SCF (Benzene) = -2016.34984705
BS2 (def2-tzvp) = -2017.87641272
Low Freq. = 11.5799 $cm^{-1}$, 19.7113 $cm^{-1}$

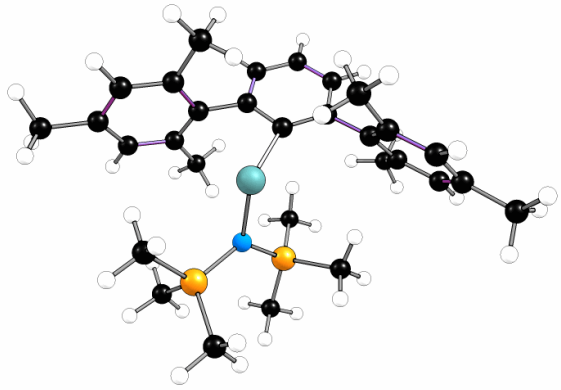

**HHMDS**
SCF = -873.580513276
H(0 K) = -873.350248
H(298 K) = -873.332018
G(298 K) = -873.394200
SCF+D3 = -873.627297014
PCM SCF (Benzene) = -873.581289692
BS2 (def2-tzvp) = -874.125928025
Low Freq. = 24.9284 $cm^{-1}$, 32.6687 $cm^{-1}$

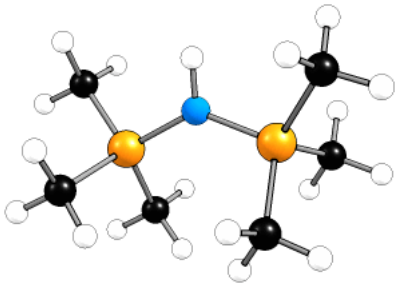

**2a**
SCF = -982.812371112
H(0 K) = -982.447201
H(298 K) = -982.424500
G(298 K) = -982.497792
SCF+D3 = -982.898709620
PCM SCF (Benzene) = -982.816130584
BS2 (def2-tzvp) = -983.635514935
Low Freq. = 12.5536$cm^{-1}$, 35.6827 $cm^{-1}$

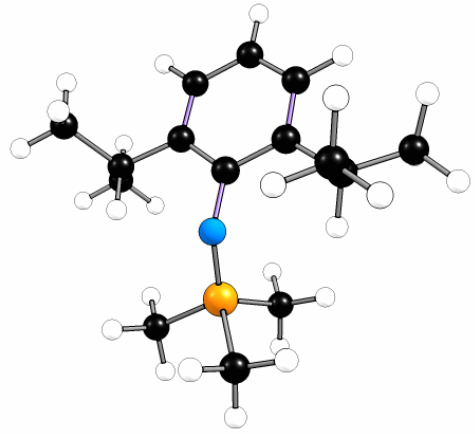

**2b**

SCF = -825.691800725
H(0 K) = -825.437052
H(298 K) = -825.419236
G(298 K) = -825.483158
SCF+D3 = -825.747744266
PCM SCF (Benzene) = -825.696717373
BS2 (def2-tzvp) = -826.348657288
Low Freq. = 19.1187 $cm^{-1}$, 28.5400 $cm^{-1}$

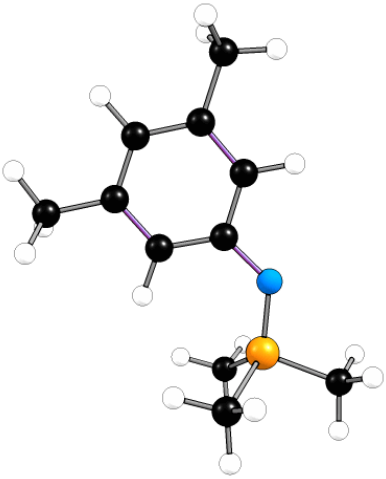

**2c**

SCF = -905.461143616
H(0 K) = -905.121522
H(298 K) = -905.104780
G(298 K) = -905.163472
SCF+D3 = -905.541445188
PCM SCF (Benzene) = -905.463506081
BS2 (def2-tzvp) = -906.194823599
Low Freq. = 25.1373 $cm^{-1}$, 57.5116 $cm^{-1}$

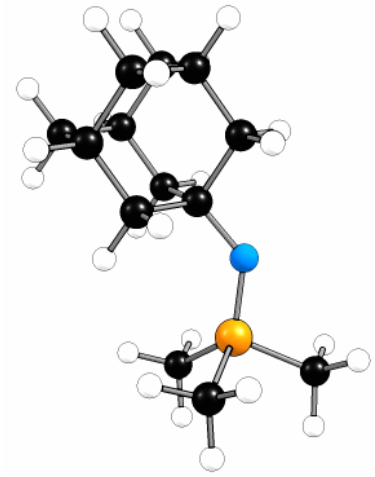

**TS1-3a**

SCF = -2999.10181772
H(0 K) = -2998.116954
H(298 K) = -2998.048760
G(298 K) = -2998.223988
SCF+D3 = -2999.43513561
PCM SCF (Benzene) = -2999.10599646
BS2 (def2-tzvp) = -3001.44546113
Low Freq. = -1425.5930 $cm^{-1}$, 9.9453 $cm^{-1}$

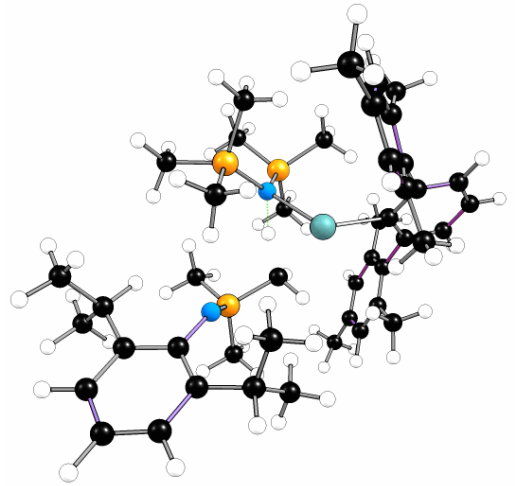

**3a**

SCF = -2125.59141191
H(0 K) = -2124.834322
H(298 K) = -2124.783982
G(298 K) = -2124.920267
SCF+D3 = -2125.83545169
PCM SCF (Benzene) = -2125.59518286
BS2 (def2-tzvp) = -2127.39614646
Low Freq. = 11.7302 $cm^{-1}$, 18.6694 $cm^{-1}$

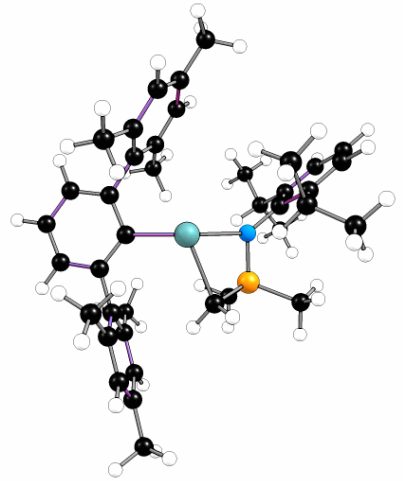

**TS1-3b**
SCF = -2842.01000546
H(0 K) = -2841.135197
H(298 K) = -2841.071922
G(298 K) = -2841.236625
SCF+D3 = -2842.31352108
PCM SCF (Benzene) = -2842.01324806
BS2 (def2-tzvp) = -2844.18468222
Low Freq. = -433.5398 $cm^{-1}$, 14.8287 $cm^{-1}$

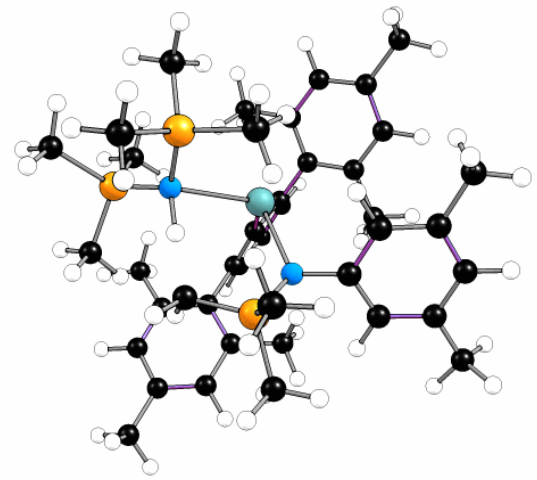

**TS1-3c**
SCF = -2921.77227932
H(0 K) = -2920.812996
H(298 K) = -2920.750603
G(298 K) = -2920.910490
SCF+D3 = -2922.10168759
PCM SCF (Benzene) = -2921.77533185
BS2 (def2-tzvp) = -2924.02315481
Low Freq.= -1256.9256 $cm^{-1}$, 12.8373 $cm^{-1}$

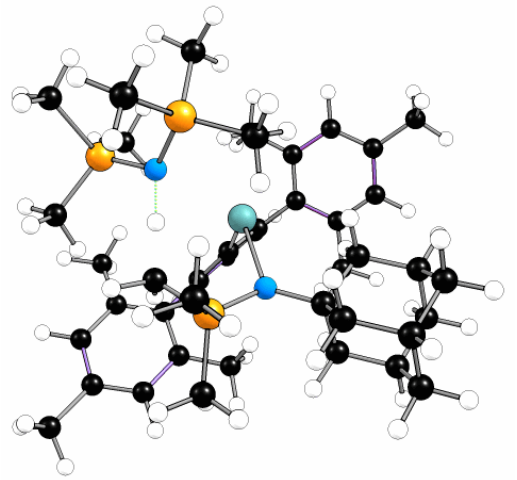

**3b**
SCF = -1968.48130383
H(0 K) = -1967.834530
H(298 K) = -1967.789000
G(298 K) = -1967.917330
SCF+D3 = -1968.69590466
PCM SCF (Benzene) = -1968.48580622
BS2 (def2-tzvp) = -1970.11899164
Low Freq. = 12.4990 $cm^{-1}$, 15.9098 $cm^{-1}$

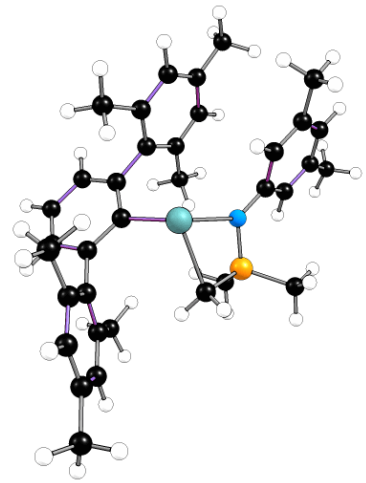

**3c**
SCF = -2048.24963551
H(0 K) = -2047.517790
H(298 K) = -2047.473264
G(298 K) = -2047.596869
SCF+D3 = -2048.48849945
PCM SCF (Benzene) = -2048.25305892
BS2 (def2-tzvp) = -2049.96381332
Low Freq. = 11.2760 $cm^{-1}$, 16.4489 $cm^{-1}$

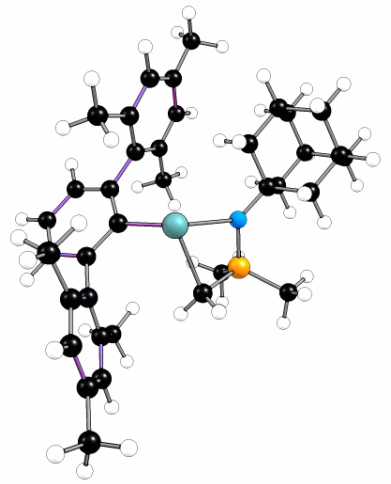

**A2a**
SCF = -2182.13704094
H(0 K) = -2181.343108
H(298 K) = -2181.290024
G(298 K) = -2181.435669
SCF+D3 = -2182.38371797
PCM SCF (Benzene) = -2182.14126558
BS2 (def2-tzvp) = -2184.00805341
Low Freq. = 7.5405 $cm^{-1}$, 9.8021 $cm^{-1}$

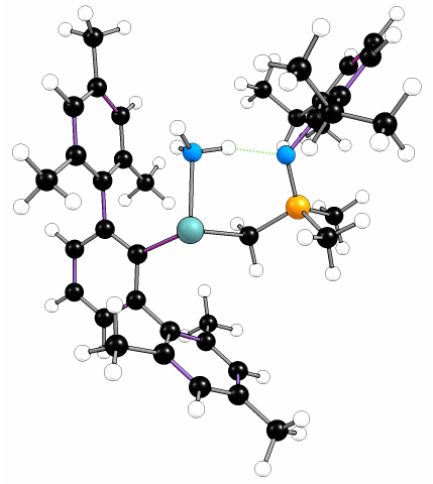

**TSA1a-Ba**
SCF = -2182.08869118
H(0 K) = -2181.296116
H(298 K) = -2181.243906
G(298 K) = -2181.381655
SCF+D3 = -2182.35537060
PCM SCF (Benzene) = -2182.09220259
BS2 (def2-tzvp) = -2183.95949666
Low Freq. = -114.5604 $cm^{-1}$, 20.8989 $cm^{-1}$

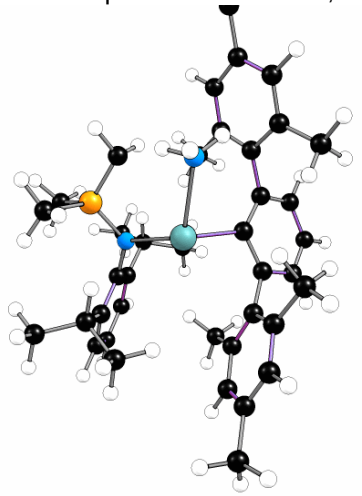

**A1a**
SCF = -2182.11361435
H(0 K) = -2181.320039
H(298 K) = -2181.266500
G(298 K) = -2181.409561
SCF+D3 = -2182.37029698
PCM SCF (Benzene) = -2182.11975182
BS2 (def2-tzvp) = -2183.98597229
Low Freq. = 13.4017 $cm^{-1}$, 18.4232 $cm^{-1}$

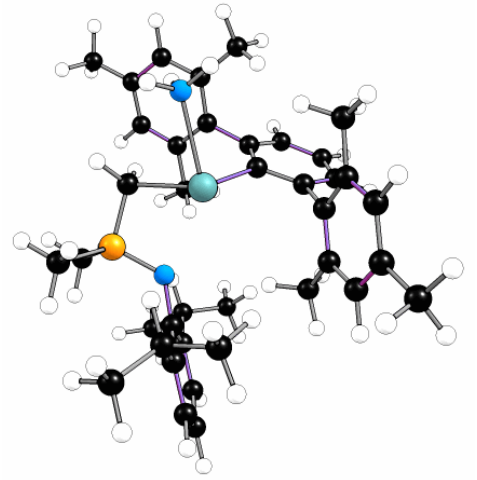

**Ba**
SCF = -2182.11448437
H(0 K) = -2181.321792
H(298 K) = -2181.268396
G(298 K) = -2181.410667
SCF+D3 = -2182.37756829
PCM SCF (Benzene) = -2182.11891916
BS2 (def2-tzvp) = -2183.98668980
Low Freq. = 14.2906 $cm^{-1}$, 17.1979 $cm^{-1}$

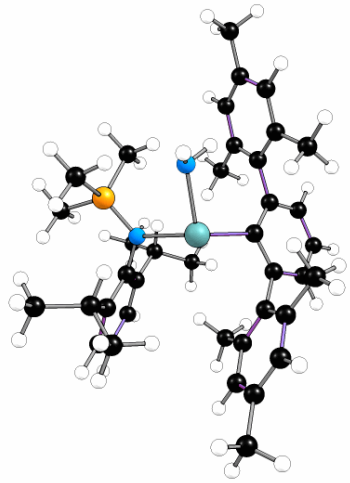

**C**
SCF = -1199.29899115
H(0 K) = -1198.873293
H(298 K) = -1198.842652
G(298 K) = -1198.937933
SCF+D3 = -1199.43321587
PCM SCF (Benzene) = -1199.30159514
BS2 (def2-tzvp) = -1200.35605919
Low Freq. = 18.3496 $cm^{-1}$, 21.5646 $cm^{-1}$

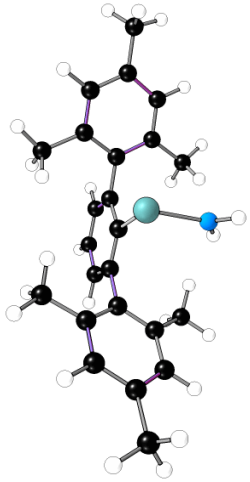

**A2b**
SCF = -2025.01815156
H(0 K) = -2024.334428
H(298 K) = -2024.286338
G(298 K) = -2024.422938
SCF+D3 = -2025.23114377
PCM SCF (Benzene) = -2025.02320243
BS2 (def2-tzvp) = -2026.72241752
Low Freq. = 6.1232 $cm^{-1}$, 10.7174 $cm^{-1}$

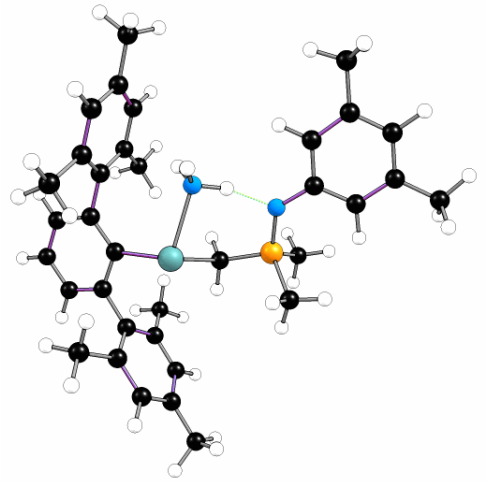

**5**
SCF = -2398.65310649
H(0 K) = -2397.797913
H(298 K) = -2397.737164
G(298 K) = -2397.902183
SCF+D3 = -2398.95454599
PCM SCF (Benzene) = -2398.65710114
BS2 (def2-tzvp) = -2400.75713263
Low Freq. = 8.6842 $cm^{-1}$, 12.3063 $cm^{-1}$

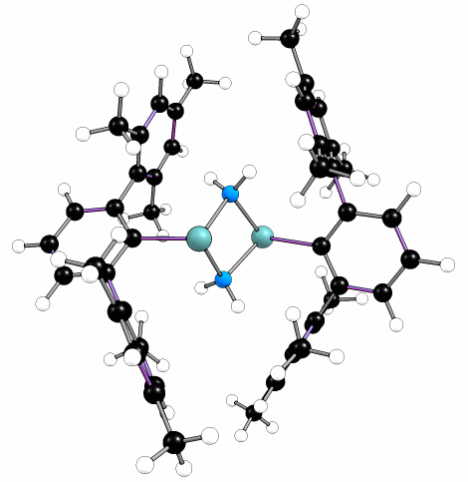

**A1b**
SCF = -2024.99862847
H(0 K) = -2024.315718
H(298 K) = -2024.266991
G(298 K) = -2024.402978
SCF+D3 = -2025.21938739
PCM SCF (Benzene) = -2025.00478565
BS2 (def2-tzvp) = -2026.70432140
Low Freq. = 12.6814 $cm^{-1}$, 15.0776 $cm^{-1}$

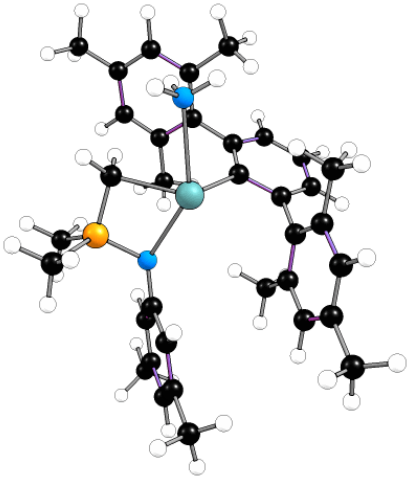

**TSA1b-Bb**
SCF = -2024.98009224
H(0 K) = -2024.297955
H(298 K) = -2024.250416
G(298 K) = -2024.382094
SCF+D3 = -2025.20582161
PCM SCF (Benzene) = -2024.98385929
BS2 (def2-tzvp) = -2026.68461604
Low Freq. = -108.5767cm-1, 15.7287cm-1

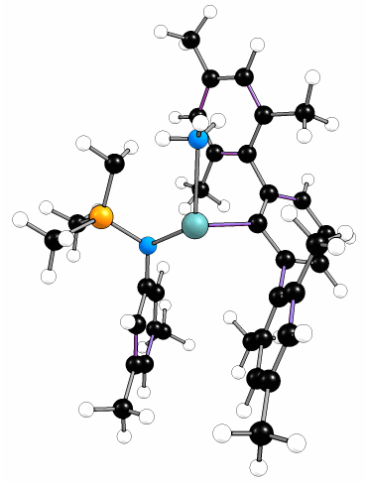

**Bb**
SCF = -2025.00053999
H(0 K) = -2024.318243
H(298 K) = -2024.269885
G(298 K) = -2024.404360
SCF+D3 = -2025.22356570
PCM SCF (Benzene) = -2025.00561704
BS2 (def2-tzvp) = -2026.70677007
Low Freq. = 15.5392 $cm^{-1}$, 19.3603 $cm^{-1}$

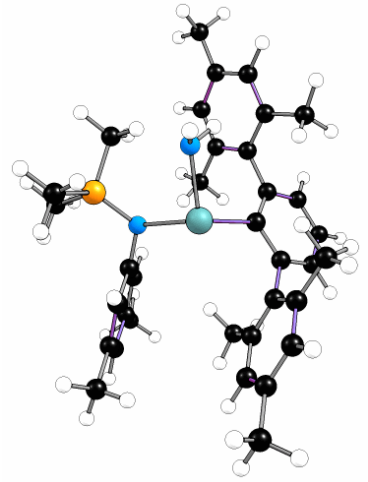

**4a**
SCF = -2508.77633974
H(0 K) = -2507.841374
H(298 K) = -2507.778637
G(298 K) = -2507.944051
BS2 (def2-tzvp) = -2510.99238832
Low Freq. = 8.4585cm-1, 11.1096cm-1

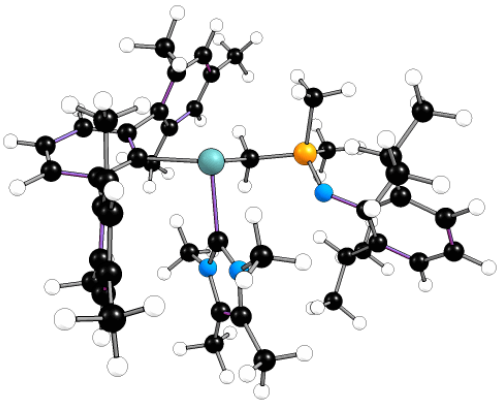

**6**
SCF = -3115.39801142
H(0 K) = -3114.283508
H(298 K) = -3114.209011
G(298 K) = -3114.398620
SCF+D3 = -3115.77024442
PCM SCF (Benzene) = -3115.40544354
BS2 (def2-tzvp) = -3118.02036569
Low Freq. = 8.4434 $cm^{-1}$, 14.5378 $cm^{-1}$

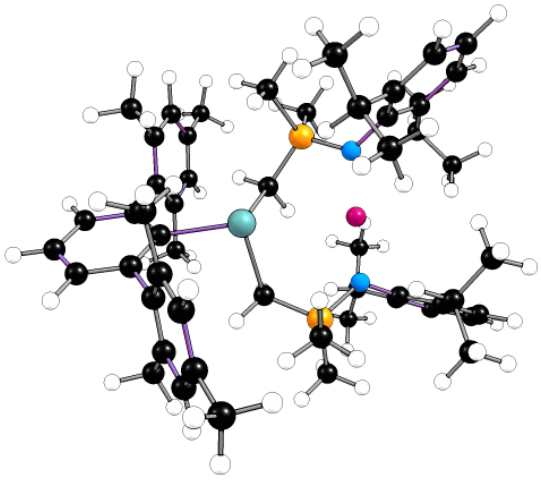

## References


[S1] M. Fischer, M. M. D. Roy, L. L. Wales, M. A. Ellwanger, A. Heilmann and S. Aldridge, Structural Snapshots in Reversible Phosphinidene Transfer: Synthetic, Structural, and Reaction Chemistry of a Sn=P Double Bond, *J. Am. Chem. Soc.*, 2022, **144**, 8908-8913.

[S2] a) N. Kuhn and T. Kratz, Synthesis of Imidazol-2-ylidenes by Reduction of Imidazole-2(3*H*)-thiones, *Synthesis,* 1993, 561-562; b) C. Barnett, M. L. Cole and J. B. Harper, Steric Properties of *N*-Heterocyclic Carbenes affect the Performance of Electronic Probes, *Eur. J. Inorg. Chem.*, 2021, **47**, 4954-4958.

[S3] S. K. Chen, W.-Q. Ma, Z.-B. Yan, F.-M. Zhang, S.-H. Wang, Y.-Q. Tu, X.-M. Zhang and J.-M. Tian, Organo-Cation Catalyzed Asymmetric Homo/Heterodialkylation of Bisoxindoles: Construction of Vicinal All-Carbon Quaternary Stereocenters and Total Synthesis of (-)-Chimonanthidine, *J. Am. Chem. Soc.*, 2018, *140*, 10099-10103.

[S4] a) Y. Liu, J. Du and L. Deng, Synthesis, Structure, and Reactivity of Low-Spin Cobalt(II) Imido Complexes $[(Me_3P)_3Co(Nar)]$, *Inorg. Chem.*, 2017, **56**, 8278-8286; b) K. E. Aldrich and A. L. Odom, A photochemical route to a square planar, ruthenium(IV)-bis(imide), *Chem. Commun.*, 2019, **55**, 4403-4406.

[S5] Y. M. Badiei, A. Krishnaswamy, M. M. Melzer and T. H. Warren, Transient Terminal Cu-Nitrene Intermediates from Discrete Dicopper Nitrenes, *J. Am. Chem. Soc.*, 2006, **128**, 15056-15057.

[S6] a) E. Kogut, H. L. Wiencko, L. Zhang, D. E. Cordeau and T. H. Warren, A Terminal Ni(III)-Imide with Diverse Reactivity Pathways, *J. Am. Chem. Soc.*, 2005, **127**, 11248-11249; b) T. F. C. Cruz, L. F. Veiros and P. T. Gomes, Cobalt(I) Complexes of 5-Aryl-2-iminopyrrolyl Ligands: Synthesis, Spin Isomerism, and Application in Catalytic Hydroboration, *Inorg. Chem.*, 2018, **57**, 14671-14685.

[S7] a) S. Bachmann, B. Gernert and D. Stalke, Solution structures of alkali metal cyclopentadienides in THF estimated by ECC-DOSY NMR-spectroscopy (incl. Software), *Chem. Commun.*, 2016, **52**, 12861-12864; b) S. Bachmann, R. Neufeld, M. Dzemski and D. Stalke, New External Calibration Curves (ECCs) for the Estimation of Molecular Weights in Various Common NMR Solvents, *Chem. Eur. J.*, 2016, **22**, 8462-8465.

[S8] Y. Peng, J.-D. Guo, B. D. Ellis, Z. Zhu, J. C. Fettinger, S. Nagase and P. P. Power, Reaction of Hydrogen or Ammonia with Unsaturated Germanium or Tin Molecules under Ambient Conditions: Oxidative Addition versus Arene Elimination, *J. Am. Chem. Soc.*, 2009, **131**, 16272-16282.

[S9] Bruker AXS Inc., *Bruker Apex CCD, SAINT v8.40B* (Ed.: Bruker AXS Inst. Inc.), WI, USA, Madison, 2019.

[S10] L. Krause, R. Herbst-Irmer, G. M. Sheldrick and D. Stalke, Comparison of silver and molybdenum microfocus X-ray sources for single-crystal structure determination, *J. Appl. Crystallogr.*, 2015, **48**, 3-10.

[S11] M. Sevvana, M. Ruf, I. Usón, G. M. Sheldrick and R. Herbst-Irmer, Non-merohedral twinning: from minerals to proteins, *Acta Crystallogr. D*, 2019, **75**, 1040-1050.

[S12] G. M. Sheldrick, Crystal structure refinement with *SHELXL*, *Acta Crystallogr. A*, 2015, **71**, 3-8.

[S13] G. M. Sheldrick, Crystal structure refinement with *SHELXL*, *Acta Crystallogr. C*, 2015, **71**, 3-8.

[S14] C. B. Hübschle, G. M. Sheldrick and B. Dittrich, *ShelXle*: a Qt graphical user interface for *SHELXL*, *J. Appl. Crystallogr.*, 2011, **44**, 1281-1284.

[S15] M. J. Frisch, G. W. Trucks, H. B. Schlegel, G. E. Scuseria, M. A. Robb, J. R. Cheeseman, G. Scalmani, V. Barone, G. A. Petersson, H. Nakatsuji, X. Li, M. Caricato, A. V. Marenich, J. Bloino, B. G. Janesko, R. Gomperts, B. Mennucci, H. P. Hratchian, J. V. Ortiz, A. F. Izmaylov, J. L. Sonnenberg, D. Williams-Young, F. Ding, F. Lipparini, F. Egidi, J. Goings, B. Peng, A. Petrone, T. Henderson, D. Ranasinghe, V. G. Zakrzewski, J. Gao, N. Rega, G. Zheng, W. Liang, M. Hada, M. Ehara, K. Toyota, R. Fukuda, J. Hasegawa, M. Ishida, T. Nakajima, Y. Honda, O. Kitao, H. Nakai, T. Vreven, K. Throssell, J. A. Montgomery, Jr., J. E. Peralta, F.

Ogliaro, M. J. Bearpark, J. J. Heyd, E. N. Brothers, K. N. Kudin, V. N. Staroverov, T. A. Keith, R. Kobayashi, J. Normand, K. Raghavachari, A. P. Rendell, J. C. Burant, S. S. Iyengar, J. Tomasi, M. Cossi, J. M. Millam, M. Klene, C. Adamo, R. Cammi, J. W. Ochterski, R. L. Martin, K. Morokuma, O. Farkas, J. B. Foresman and D. J. Fox, *Gaussian 16, Revision A.03*, Gaussian, Inc., Wallingford CT, 2016.
[S16] A. D. Becke, Density-functional exchange-energy approximation with correct asymptotic behavior, *Phys. Rev. A*, 1988, **38**, 3098-3100.
[S17] J. P. Perdew, Density-functional approximation for the correlation energy of the inhomogeneous electron gas, *Phys. Rev. B*, 1986, **33**, 8822-8824.
[S18] F. Weigend and R. Ahlrichs, Balanced basis sets of split valence, triple zeta valence and quadruple zeta valence quality for H to Rn: Design and assessment of accuracy, *Phys. Chem. Chem. Phys.*, 2005, **7**, 3297-3305.
[S19] S. Grimme, J. Antony, S. Ehrlich and H. Krieg, A consistent and accurate *ab initio* parametrization of density functional dispersion correction (DFT-D) for the 94 elements H-Pu, *J. Chem. Phys.*, 2010, **132**, 154104.
[S20] S. Grimme, S. Ehrlich and L. Goerigk, Effect of the damping function in dispersion corrected density functional theory, *J. Comp. Chem.*, 2011, **32**, 1456-1465.
[S21] NBO 7.0, E. D. Glendening, J. K. Badenhoop, A.E. Reed, J. E. Carpenter, J. A. Bohmann, C. M. Morales, P. Karafiloglou, C. R. Landis and F. Weinhold, *Theoretical Chemistry Institute, University of Wisconsin, Madison, WI,* 2018.